northumbria
UNIVERSITY
School of Engineering and Technology

Investigation of the Influence Coefficient Method for Balancing of Flexible Rotors Systems

Giuma Ramadan Hanish BSc (Eng.Hons)

This thesis is submitted in partial fulfilment of the requirements of the Northumbria University for the degree of Doctor of Philosophy

2005

Dedication

To my Mother, brothers, relatives, friends and to the memory of my brother Hesham, my sister Beshtia and my father.

Abstract

Several sophisticated procedures for balancing flexible rotors have been developed during the past two decades. For a variety of reasons, none of these methods has gained general acceptance by practicing balancing engineers. Some of these balancing techniques require a great deal of expertise from the operator. This thesis is dedicated to the research of flexible rotor balancing techniques, and aims to apply some advanced techniques to the field of high-speed rotor balancing. Significant progress in balancing methods for flexible rotors can be achieved by the improvement and optimization of existing balancing techniques.

Experimental tests were conducted to demonstrate the ability of the influence coefficient method to achieve precise balance of flexible rotors. Various practical aspects of flexible-rotor balancing were investigated. Tests were made on a laboratory quality test rig having a 3.6 m long rotor representing a High Pressure Turbine (H.P.T) (10.1 kg)(43.767 cm), a Low Pressure Turbine (L.P.T) (43.922 kg) (113.698 cm) and a Generator Rotor (G. Rotor) (71.611kg) (146.413 cm) and covering a speed range up to 6000 rpm. A specific data acquisition system has been developed for use in a high-speed rotor balance facility. Special measurement requirements for this facility include order-tracked vibration measurements and phase angle data. The data acquisition system utilizes dual high-speed computer systems to share the tasks of measurement data processing, and results display.

A study of balancing errors is systematically discussed in detail from the view point of increasing the balancing precision. The methods for controlling and reducing these errors are also discussed. Both the qualitative and quantitative analyses of balancing errors are performed as the guide to reduce the error and improve the balancing quality.

The thesis also presents the theoretical background and the techniques necessary to the procedure to balance the flexible rotor. A trim balancing method was developed to expand the implementation of flexible rotor balancing. A computer program has been written which generates influence coefficient from measured motions and goes on to predict the correction mass. The vibration has been measured at several locations and speeds and the results have been used to (a) ensure that the vibration levels were not excessive as the rotor speed increased and (b) to calculate the balance correction weights using the traditional influence coefficient method and a least squares influence coefficient method.

The procedure developed was verified using an experimental rotor rig. The successful application of the procedure to the balancing of this rotor demonstrates that balancing using Singular Value Decomposition, QR Factorization, and QR Factorization combined with SVD and new trim balancing method is not only a theoretical but also a practical possibility. The Moore-Penrose generalized inverse has been employed to solve the problem. The dynamic characteristics of the rotor rig, however, were somewhat limited and did not cover all the possibilities considered during the project. Therefore, a more complete numerical example was also successfully solved using the computer model of a rotor with characteristics similar to those of a real turbine by using a finite element software package called ANSYS.

Rotor unbalance and shaft misalignment are the two main sources of vibration in rotating machinery. The vibration caused by unbalance and misalignment may destroy critical parts of the machine, such as bearings, seals, gears and couplings. Experimental studies were performed on a system test apparatus to verify the correlation between shaft misalignment and rotor unbalance of multi-rotor multi-bearing systems. The rotor shaft displacements were measured under different misalignment and unbalance conditions. New equipment was installed using a laser alignment system and based upon vibration measurements of the operating machinery.

Balancing the rotors involves the selection of appropriate locations of the balancing planes. There are still some questions with regard to the practical selection of these balance planes. If the balancing planes are chosen incorrectly, the accuracy of the balancing condition will be affected. In this study, the desirability of using "optimum" locations for balance planes has been investigated by using some case studies. However in most machines, constraints exist which inhibit the use of the optimum locations, and a means to evaluate "non-ideal" locations is clearly necessary. At the same time, other "non-ideal" aspects of "real" balancing requirements must be recognized.

To provide the answer to the above question and to provide criteria for establishing ideal balance plane locations, an analysis was performed, which will give guidelines to the selection of balancing planes.

Table of contents

List of Figures

List of Tables

Acknowledgments

First and foremost, I would like to express my deepest gratitude to my thesis advisor, Dr Ken Leung for his invaluable guidance, advice and encouragement throughout my study. His support was always there when I needed it. I appreciate his idea for allowing me to create my own academic interest. Without his unlimited availability, endless patience, sound advice, and encouraging words, this thesis would surely not exist. I admire him as a teacher, as a leader and above all as a friend.

Most importantly, I would like to thank my family for standing behind me every step of the way and for always believing in me. They have understood about my absence at various gatherings. They have let me find my own way in life but never let me down when I needed them. They have always put my happiness before their own, and I can only hope that they have some idea of how much all of their love and support means to me.

My thanks also go to all my friends and relatives for their support and encouragement. I wish to express my profound thanks to Prof Santu Datta for his advice and help during the course of this work. Also, I would like to thank all technical, administrative and staff at the school of Engineering for their continuous support.

Last but not the least, I would like to acknowledge the engineering superintendent in Repsoil Oil Operation (Tripoli-Libya) Mr. Nuri Iseaid for his trust and belief in my ability.

Declaration

I hereby declare that:

During the period I have been registered for the degree of PhD, for which the thesis is submitted, I have not been a registered candidate for any other award of a University.

Furthermore, that I have attended relevant seminars within the University of Northumbria, and presented papers at several conferences and relevant meetings on the subject of vibration of rotating machinery.

Giuma R.Hanish

2005

List of symbols

(q)	The correction planes
(n)	The transducers to measure vibration
(h)	Represent the speeds
(m)	Opportunities to acquire data, such that $m = h * n$.
$S_1, S_2, ..., S_k$	The balancing speeds
$W_{n0}^h, W_{n1}^h, W_{n2}^h$	Initial vibration at each transducer and at each speed
Subscript n	n^{th} transducer
0	The original condition
Superscript h	Refers to the h^{th} speed
m_i,	j^{th} trial mass added for balancing
$r_1\ r_2$	Radius
$\phi_1 \cdot \phi_2$	Phase angle
$[X]$	Column vector of observed displacements for the unbalanced shaft
$[\alpha]$	The influence coefficient matrix
$[W]$	Unknown column vector of the effective rotor unbalance related to the corrections planes
α_{nj}^{k}	Influence coefficients relating the rotor response for the specified sensors and speeds to the balancing planes
$[\alpha]^{-1}$	Inverted influence coefficient matrix
$[\alpha]^T$	Conjugate transpose of influence coefficient matrix
$Y_i(x)$	Mode shapes

ϕ_i	Arbitrary parameters
$m(x)$	Mass distribution of the rotor
M_i	Generalized mass
$K_i\ i^{th}$	Mode generalized stiffness of the rotor
$m(x)$	Mass distribution of rotor
w_{in}	Critical speed.
$y(x)$	
Q	is an *m-by-n* orthogonal matrix
R	R is a *n-by-n* upper triangular
Q^T	Transpose of Q
R^{-1}	Inverted of R
USV	Singular value decomposition
U	Eigenvectors of $\alpha\alpha^T$.
V	The eigenvectors of $\alpha^T\alpha$.
S	is diagonal
$\sigma_{11}, \ldots\ldots \sigma_{nn}$	Diagonal elements of singular values
U^T	Transpose of U
V^T	Transpose of V
S^{-1}	Inverted of S
$\sigma_{\min}$ and $\sigma_{\max}$	The largest and smallest singular values.
$cond(\alpha)$	Condition number
α^+	Moore-Penrose pseudo-inverse or generalized matrix inverse.
$[V_R]$	Eigenvectors of R.
$[U_R]$	The eigenvectors of R.
$[U_R]^T$	Transpose of $[U_R]$
$[S_R]$	is diagonal of R

$[S_R]^{-1}$	Inverted of $[S_R]$
i	Square root of negative one
l	*Generally* used to indicate rotor length
m_i,	j^{th} added mass for balancing
x	Component of vibration vector along the X axis
α_{ij}	ij^{th} element of influence coefficient matrix
π	Standard constant 3.14159265
ρ	Mass density
Σ	Indicates mathematical summation series
ϕ	Leading phase angle
ω	Rotational frequency of rotor
ω_n	Undamped natural frequency

Additional nomenclature, which is not used consistently throughout the theses, is defined in the context in which it is used.

Chapter 1

INTRODUCTION

Nowadays in the industry, particularly where turbomachinery is used there is a trend to operate at increasing running speeds. In addition, to reduce manufacturing costs, there is a tendency to design new machines with more slender shafts so it is becoming increasingly important to ensure machine vibration is controlled within limits to ensure reliability.

Rotor balancing methods may be separated into two categories: rigid rotor balancing and flexible rotor balancing. These general titles refer to whether or not rotor flexibility was taken into account. That is, flexible rotor balancing procedures take into account rotor flexibility, while rigid rotor balancing procedures do not. Many flexible rotor balancing methods were suitable for balancing rigid rotors. However, rigid rotor balancing methods are, in general, not effective for balancing flexible rotors. A survey of the literature of flexible rotor balancing is presented in Chapter 3.

Several methods have been developed during the last fifty years for balancing flexible shafts, which have several flexural critical speeds within their range of service speeds. The methods of modal balancing and influence coefficient techniques have dominated much discussion and argument in recent years, but uncertainty still remains.

The basic consideration of the modal balancing method is that the unbalance response of a rotor can be expressed as a series of modal components, each one corresponding to a degree of freedom with characteristic natural frequency and mode shape. In a similar way, the unbalance forces may be expressed as a series of modal unbalances. Thus the deflection of the shaft is made up of contributions from the mode shapes of the system, the scale of each mode shape being affected by a suitable factor, which is a function of the corresponding modal unbalance. The advantage of this kind of analysis is that only a few modes affect the rotor response in its normal operating speed range.

Various procedures for the balancing of flexible rotors have been developed independently over the last fifty years; nevertheless, all the procedures share the same overall goal, namely the reduction of shaft vibration to acceptable levels. Influence coefficient methods were first developed in version limited to one and two balancing planes. These methods are based on a cause-effect philosophy, their only assumption being a direct proportion between the response of the rotor and the imbalance. The influence coefficient technique is to select correction masses to ensure that the shaft vibration is zero (or within specified tolerances) at a series of locations along the shaft for a series of steady shaft Speeds.

One common characteristic between the influence coefficient and the modal balancing methods is the large number of trial runs required before the correction masses can be defined. The influence coefficient method requires at least a trial run per balancing plane. Although similar numbers of additional runs were required every time the rotor was usually not able to travel through a natural frequency due to the resonance. The modal balancing method requires at least one trial run for each mode to be balanced, although additional runs might be required to determine the mode shapes and to reduce the influence of higher modes.

The influence coefficient approach has become more practical recently due to the introduction of newer types of sensors, electronic processing equipment and computers. Therefore, currently the influence coefficient method is a common approach to balancing flexible rotors. This present research involved further development of the influence coefficient method in order to reach an optimum procedure for rotor balancing. The influence coefficient method has the advantage of simplicity in application, which makes it suitable for a wide range of complex turbomachinery (e.g. helicopter shafts, multi-spool aircraft engines and ultracentrifuges), and computerization of the unbalance weight calculation. Its effectiveness is not influenced by the presence of damping in the system, or by vibratory motions of the locations at which readings were taken. It shares certain features of the other methods, i.e. the number of readings required to acquire the input data, and the accuracy with which these amplitude and phase readings must be made. Goodman (1964) developed a balancing procedure, which uses a least-squares technique to minimize

the (rms) residual amplitudes of vibration at selected locations on the rotor. A second application of the technique then uses weighted least squares to reduce the maximum residual vibration.

In recent years influence coefficient balancing has become the major technique used to develop computer aided balancing algorithms. However when the balance planes and speeds were chosen inadequately in balancing practice there may exist non-independent or nearly non-independent balance planes among the chosen balance planes. In this case the least squares algorithm can be used to obtain the correction masses which generally were considerably large and mutually counteracting. Darlow (1982) investigated the cause resulting in impractical correction masses in influence coefficient balancing and developed an algorithm to identify non- independent balance planes (which matrix column essentially cancel each other) and to eliminate the effect of this problem on computing correction masses.

Uncertainty is an unavoidable part of any measurement and it starts to matter when results are close to a specified limit. A proper evaluation of uncertainty is good professional practice and can provide valuable information about the quality and reliability of the result.

Singular value decomposition (SVD) was a useful method for understanding the structure of an ill-conditioned matrix, and it is a general method for linear decomposition techniques of a matrix into independent principal components of special case for square matrixes. With the singular value decomposition techniques used on the influence coefficient matrix, the nearly non-independent balance planes can be effectively identified. Additional information given by the SVD can be used to verify the reliability of influence coefficients and then select the optimal correction masses. By using this method the minimum number of balance planes, as well as minimum balance weights, can be found to balance a rotor in the most cost effective and accurate manner.

Rotor unbalance and shaft misalignment are the two main sources of vibration in rotating machinery such as a gas turbine. The vibration caused by unbalance and misalignment may destroy critical parts of the machine, such as bearings, seals and couplings.

Due to current trends in the design of rotating machinery towards higher speeds, manufacturers tend to produce machines, which operate closer to their lateral critical speeds than has previously been necessary. Consequently, the effect of the coupling upon the critical speeds and its misalignment on vibration amplitudes of such machines is becoming an increasingly important consideration for rotor-bearing systems.

Although shaft misalignment is a common fault in rotating machinery, the study of the effect of unbalanced rotor on shaft alignment is still inadequate. To the author's knowledge, no attempt has been made to study the correlation between the shaft-to-shaft alignment (internal alignment) and rotor unbalance

1.1 Objectives and Scope of The Project

The area of the research was associated with the rotor balancing particularly the influence coefficient method for balancing of flexible rotors. Previous investigators, in applying the principle of the influence coefficient method, used a reference run with no balance weights and a calibration or trial run with a balance weight or weight set attached to the rotor to generate the influence coefficients. Moreover, most previous work uses the basic principles of least square method. However, it was not sufficient to consider only the minimum of the sum-of-squares of the remaining vibration. Deficiencies in the correlation between the balancing planes and stability algorithm could also affect the outcome.

The aim of this project was to develop a new balancing procedure based on influence coefficient concepts. The method was able to deal with the balancing of rotors using mainly the information contained in the unbalance response of the rotor measured by the transducers.

The "trim" balancing run is defined by any correction balance run after the first attempted balance correction. Usually any mass adjustment due to the trim balancing mass amount

should be significantly less than the initial balance correction mass. The trim is usually a fine-tuning of the initial balance correction, because usually further reduction of the vibration level is necessary.

The SVD algorithm is added to the solution solver in order to analyze the influence coefficient matrix. Results from the SVD calculations can provide important information for determining the condition of the influence coefficient matrix so that non-independent balance planes can be identified. The influence coefficient matrix can be modified accordingly.

In order to correct the numerical instability of the influence coefficient matrix problems of previous research (see chapter 3), an investigation to improve the influence coefficient method for balancing flexible rotors was proposed using the SVD technique coupled with an influence coefficient method to determine the optimum balancing method for flexible rotors. A powerful computer algorithm was developed progressively to handle and improve the balancing method.

A new balancing method for the identification of rotor unbalance in rotating machines is presented. This method is based on the combined use of the QR factorization, singular value decomposition (SVD) technique, and the least square optimization technique. The SVD, QR factorization and the least square methods have been used individually in various balancing schemes, with some differences. The author is not aware that other investigators have combined these three methods previously. The present study suggests that it is advantageous to combine these three techniques for flexible rotor balancing.

1.2 Overview of The Thesis

The thesis has been organized in ten chapters and additional data has been included in seven appendices. **Chapter 1** has been dedicated to this introduction and a brief description of the remaining chapters and appendices follows.

In **Chapter 2:** brief theoretical backgrounds of some fundamental concepts of rotor dynamics are discussed in order to prepare the reader for future chapters.

The most important references found in the literature on flexible rotor balancing are analyzed in **Chapter 3**. Only relevant works from the thesis point of view have been included, although more material was read during the somewhat formidable task of reviewing the vast number of books, technical papers and reports generated on this subject. It was found however, that some authors were repetitive in the presentation of specific theoretical analyses and techniques and for the sake of shortness it was decided to include only the paper where the original ideas first appeared or those, which caused the biggest impact in the development of each area. The presentation of the literature review has been organized according to the different methods for rotor balancing and related analysis techniques.

Some fundamental theory on the main rotor balancing methods is presented in **Chapter 4**, attempting to give the necessary concepts required for the proper understanding of the remaining chapters of the thesis. The traditional solutions to the problem of rotor balancing are reviewed in Chapter 4, together with an analysis of their practical difficulties. The basic theory of the influence coefficient method is presented here with an improvement consisting of the use of trim balancing technique and the use of linear programming for the determination of the influence coefficients matrix.
Chapter 5 reviews the experimental system used in this study. The vibration amplitude and phase angle measurements instruments are covered in detail. Also the data acquisition system, used to handle the experimental tests data is viewed in detail as well. Laser alignment equipment used for the shaft-to-shaft alignment purpose is explained in this chapter.

Original work developed during this project is presented in chapters **6,7,8** and **9**. Chapter **6** contains the two different proposed methods. **Section one** deals with the measurement uncertainty in the rotor balancing, by using an experimental investigation in the accuracy of data taking, It is very important to stress, even at this early stage, the significance of this analysis because the whole process of balancing runs depends upon it. **Section two**, a new Trim Balancing Technique is presented and analyses the construction of the influence coefficient matrix for the trim balancing runs.

Chapter 7 covers a linear programming to solve an ill condition matrix of the influence coefficient method, using Least Square, QR Factorization, SVD and combination between QR Factorization and SVD.

Chapter **8** analyses a problem that has not even been identified, as such, before this project. This problem being related to the effectiveness of misaligned shafts into their balancing condition by using a system of multi-rotor multi-bearing.

Attempting to balance a rotor with trial runs requires the previous determination of the balancing planes of the rotor. Chapter **9** analyses different analytical methods used in practice for the determination of these planes, a Finite Element Method using ANSYS Package has been used in this theoretical study on the optimization of the balancing planes locations.

The particular discussion and contribution of this thesis to the state of the art of rotor balancing is analyzed in more depth in Chapters **10**. Chapter **10** also presents the conclusions of the project and proposes further research work on this area as itemized in chapter **11.** Some additional information is given in the appendices at the end of the thesis.

Appendix 1: ISO standards for Mechanical vibration and Rotor balancing, which had been considered through the thesis.
Appendix 2: Includes some glossary of terms used in this project.
Appendix 3: Summary of theoretical and numerical linear algebra.
Appendix 4: Influence coefficient Method for rotor balancing flow chart.
Appendix 5: Published papers or expected to published in the near future.
Appendix 6: Computer programmes written in Matlab to handle the data and analysis for the proposed tests.
Appendix 7: specifications of measurements instruments and DAQ card.
Appendix 8: Results tables for chapter 6,7 and 9.

Chapter 2

THEORETICAL BACKGROUND

2.1 Theoretical Background

In recent years the design of rotating machinery has moved towards reduced weight and increased operating speeds, with the purpose of increasing operating efficiency and therefore reducing the cost. However, these more efficient designs result in increased rotor flexibility and are, in general, more susceptible to a variety of undesirable rotordynamic phenomena. In particular, increased rotor flexibility substantially complicates rotor-balancing requirements.

The vibration of rotating shafts is a source of much trouble in the operation of a wide range of machinery. Large rotating systems require a regular schedule of rebalancing and alignment operations because of changing balance and alignment conditions. These conditions may change because of wear resulting from the handling of rough materials, due to the presence of materials which tend to stick to the rotor, a shift in position of the components of an assembled rotor and non-symmetric thermal stresses. Some of these factors could cause a rotor unbalance to change. Balancing problems could cripple industry, particularly on rotating machines such as compressors, steam and gas turbines and multi-stages pumps. In many cases, the solution to machine balancing can be simplified if the type of the rotor unbalance can be identified first. Essentially, there are four types of the rotor unbalance: static, couple, quasi-static, and dynamic. Each type of unbalance is identified by the relationship existing between the shaft centreline and the centre principal inertia axis, as illustrated in figure (2.1).

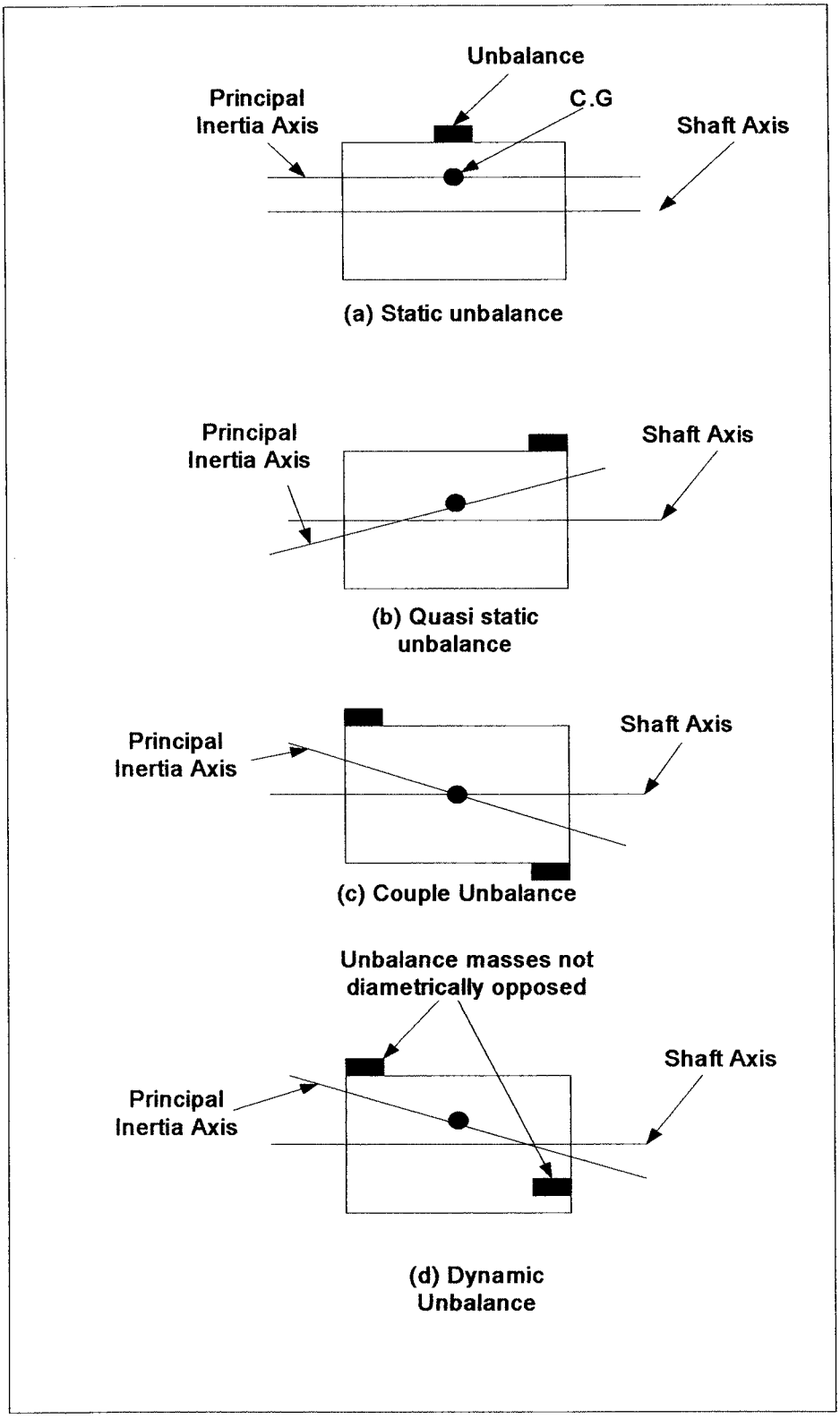

Figure 2.1 Rotor Balancing Types (Wowk 1995)

Different methods of balancing flexible rotors have been developed to determine the optimum balancing method for flexible rotors and minimum numbers of balance planes, as well as minimum balance weights Parkinson (1991). For example the methods of modal balancing and influence coefficient techniques have dominated much discussion and argument in recent years. In brief, the modal procedure is to balance successive modes of the rotor; one mode at a time with a set of masses specifically selected so as not to disturb the previously corrected lower modes.

The influence coefficient method requires no assumption other than linearity of the rotor system and the measuring system. The Unified Balancing Approach Darlow (1980) applies the empirical nature of influence coefficient balancing while taking advantage of the modal behaviour of the rotor and, thus, seeks to combine the best features of both modal and influence coefficient balancing. Further theories of the two main methods will be described in chapters 3 and 4.

2.2 Vibration Sources

All machinery with moving parts generates mechanical forces during normal operation. As the mechanical condition of the machine changes due to wear, changes in the operating environment e.g. load variations, so do these forces. Understanding machinery dynamics and how forces create unique vibration frequency components is the key to understanding vibration sources.

The vibration profile that results from motion was the result of a force imbalance. By definition, balance occurs in moving systems when all forces generated by, and acting on, the machine were in a state of equilibrium. In real-world applications, however, there is always some level of imbalance and all machines vibrate to some extent.

The machine vibration at rotation speed depends not only on the amount of rotor unbalance, but also on the existence and development stage of a number of possible defects as well as the deviations from the technical specifications in the following units: rotor, for example (shaft axis a number of connected rotors (shaft-to-shaft)), mechanical transmissions devices including, couplings, gears, belts and chains, electromagnetic

components of electric machines, bearing housings and machine supports including supporting foundations and the connections between the machine and the support components.

2.3 Vibration Problems in Rotating Machinery

Vibration in rotating machinery causes high levels of noise and wear, together with increased rotor bending stresses which lead to a lower machine fatigue life. Machine vibrations are themselves an indicator of the wellbeing of the machine, and can provide an early warning of the development of fault conditions. In fact most rotating machine health monitoring programmes include measurement of machine vibrations. The most common source of vibration is imbalance. All rotating machines have some residual imbalance because balancing procedures are imperfect, hence some vibrations are always present during operation. For this reason, designers estimate the accuracy of their balancing procedures and so are able to determine the likely levels of machine vibration before construction.

Any machine with rotating components is considered to be a rotating machine. The great majority of commercial machinery falls into this category. Rotating machines range in size from small gyroscopes weighing only a few kilograms to large rock tumblers weighing several tonnes. Other examples of rotating machines are household electric motors, internal combustion engines, gas turbine engines, steam turbines, electric generators, industrial compressors and power transmission systems.

With the increase in performance requirements of high speed rotating machinery in various fields such as gas turbines, process equipment and space applications, and the engineer is faced with the problem of designing a unit capable of smooth operation under various conditions of speed and load. In many of these applications the design operating range may be well above the rotor first critical speed. Under these circumstances, the problem of ensuring that a rotor-bearing system will perform with a stable, low-level amplitude of vibration is extremely difficult.

In the design of rotating machinery, performance considerations and rotordynamic considerations are often in conflict. The performance requirements lead to high shaft speeds and highly loaded rotating components. These features, however, tend to create rotordynamic problems.

In many rotor design applications such as compressors or turbines, the rotor experiences high vibrational amplitudes resulting in large forces being transmitted to the bearings and the support structure. These high vibrational responses may be due to several causes and may be roughly grouped under the headings synchronous and non-synchronous response. The forces and amplitudes for synchronous response are usually associated with unbalance forces in the rotor.

The unbalance may be the result of either the manufacturing process and/or the assembly of the components. Even if a rotor is well balanced initially, the balance degrades with use. Thermal gradients can cause the shaft to warp. Erosion of compressor and turbine blades can alter the balance of the rotor assembly. Therefore, in the design of the rotor-bearing system, provision should be made so that the increase of unbalance will not load the bearings excessively or cause large rotor amplitudes.

The main causes of vibrations in rotor-bearing systems can be summarized as follows:

- Absence of lubrication. Jarvis (1963).
- Bent shafts. Nicholas, Gunter, and Allaire (1976).
- Broken blades. Rao (1980).
- Cracked shafts. Nelson and Nataraj (1986).
- Damaged bearings. Hori and Uematsu (1980).
- Eccentricity. Timoshenko (1974).
- Misalignment. Hashemi (1983).
- Shaft whirl. Alford (1965).
- Shock loading due to step change in imbalance Lalanne (1983).
- Static or dynamic unbalance. Gash (1973).
- Thermally induced distortions in rotors. Hashemi (1984).

- Worn bearings. Parszewski, Kryniki and Kirby (1988).

The mass balancing of high-speed rotors is an integral part of the study and practice of rotordynamics. As is implied by the name, rotordynamics is concerned with the dynamics of rotating machinery.

Rotor vibration is generally classified according to the direction and frequency of the vibratory motion. The three possible directions of motion, as illustrated in Figure (2.2), are lateral, axial and torsional. Lateral motion involves a displacement from its central position, flexural deformation and/or rotation of the rotor's axis of rotation. In this context, rotation is about an axis intersecting and normal to the axis of rotation. Axial motion occurs parallel to the rotor's axis of rotation.

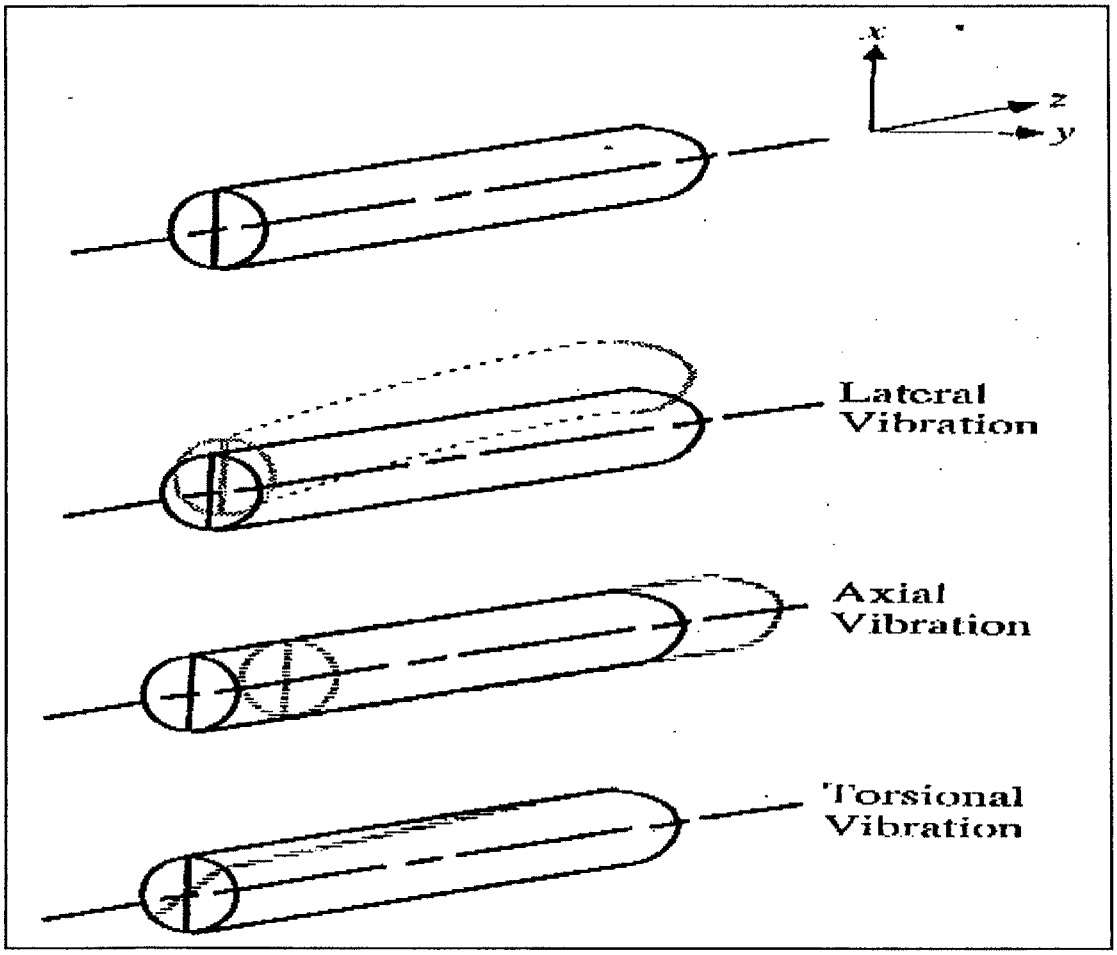

Figure 2. 2 Forms of Rotor Vibration Darlow (1989)

The presence of rotor mass imbalance, more commonly known as unbalance, is due to the eccentricity of the mass-centroidal axis of the rotor relative to its axis of rotation. In practice, this unbalance is generally a result of unavoidable imperfections in rotor manufacture and assembly. The term rotor balancing covers a broad range of procedures aimed at reducing rotor unbalance. The ultimate purpose of all rotor-balancing methods as summarized in figure 2.3, is to produce a smooth-running machine. This is achieved in practice not by removing all unbalance, but rather by applying compensating unbalances, or by removing mass by machining, which result in a smooth-running machine. Since rotor unbalance is generally distributed along the length of the rotor and compensating unbalances are applied at discrete axial locations, the complete elimination of unbalance is usually impossible, as well as unnecessary.

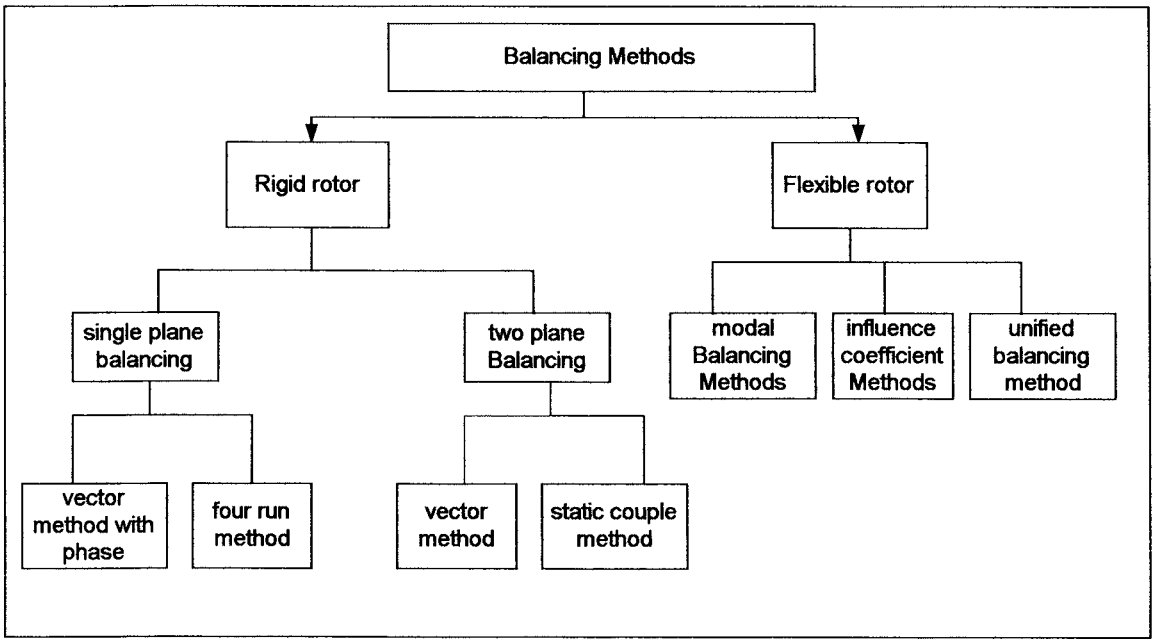

Figure 2. 3 Overview of The Rotor Balancing Methods Wowk (1995)

2.4 Rotor Design

From a rotordynamic standpoint, the successful design of a rotating machine involves:

- Avoiding critical speeds, if possible.
- Minimizing dynamic response at resonances if critical speeds must be traversed.

- Minimizing vibration and dynamic loads transmitted to machine structure, throughout the operating speed range.
- Avoiding rotor-to-casing rubs, while keeping clearances as tight as possible.
- Avoiding rotordynamic instability.

2.5 Shaft Alignment

Shaft alignment can deviate in several directions. There can be offset misalignment in the vertical and horizontal directions, angular misalignments in these directions, and any varied combination of these misalignment cases. Figure 2.4 shows parallel offset misalignment, in which the shafts of the two machines are on two separate but parallel centerlines. Figure 2.5 shows angular misalignment, in which the centerlines of the two shafts intersect at their coupling point, and are at an angle to each other. Figure 2.6 shows a general case of combined parallel and angular misalignment.

The degree to which these misalignments are to be corrected has a large impact on the amount of time needed to perform a precision alignment. Another type of misalignment not associated with couplings is bearing misalignment. The centerlines of two coupled shafts can be properly aligned, but the bearings on one side of the coupling may be misaligned. Bearings can be misaligned if they are not mounted in the same plane, if they are not normal to the shaft, or because of machine distortion due to soft foot, an uneven base, or thermal growth.

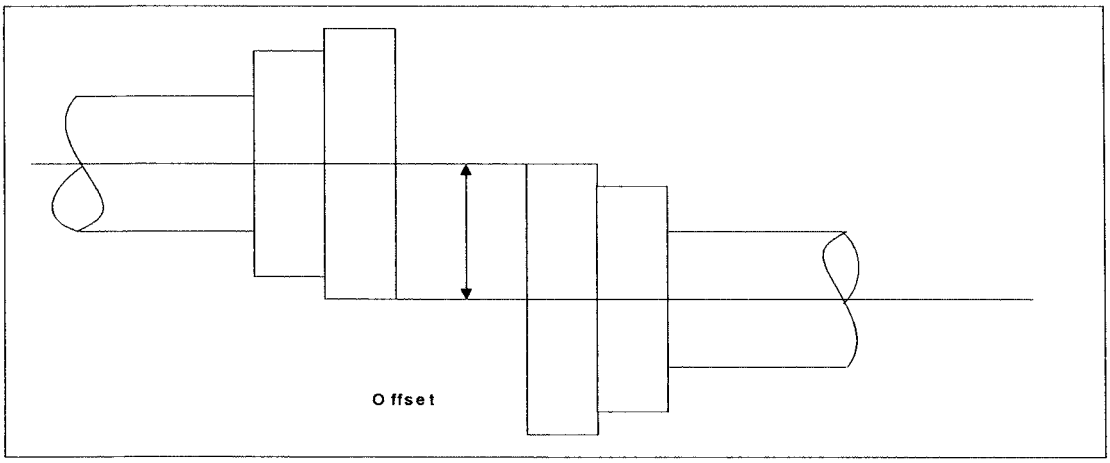

Figure 2. 4 Parallel Misalignments

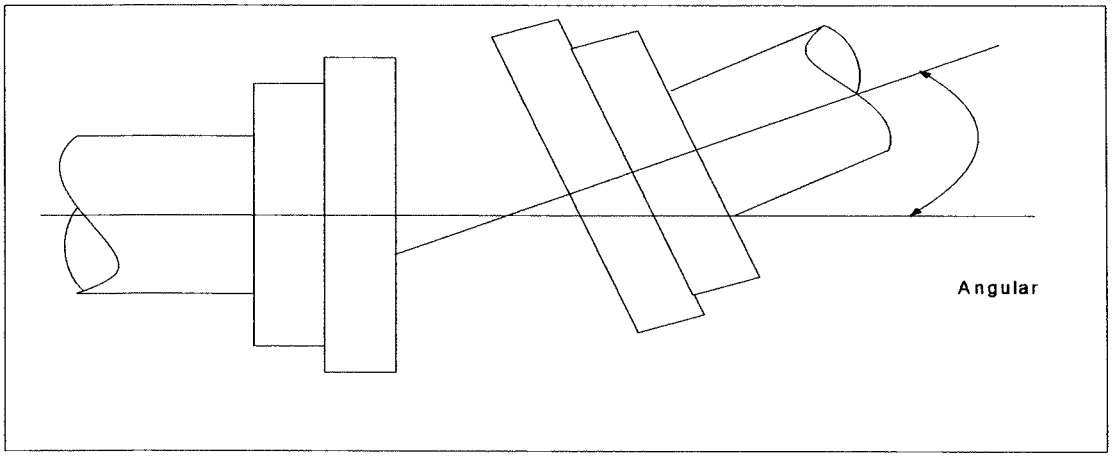

Figure 2. 5 Angular Misalignments

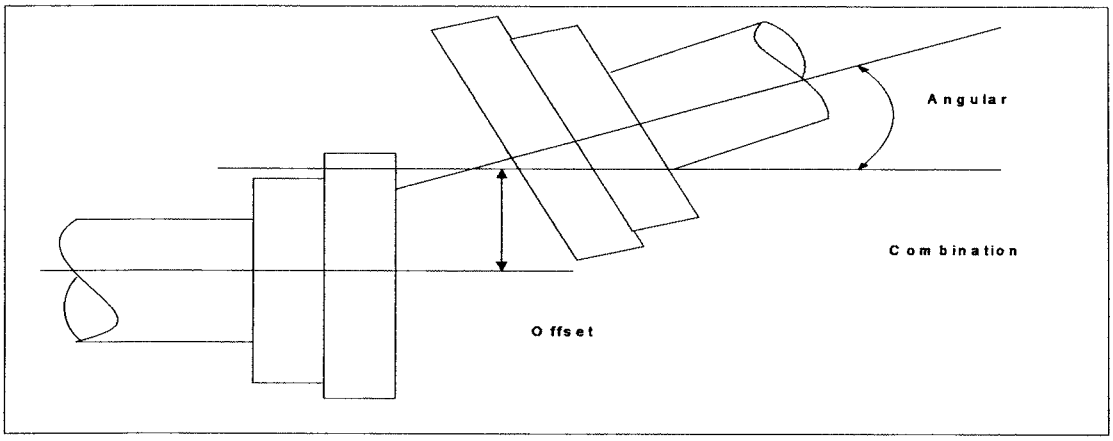

Figure 2.6 Parallel and Angular Misalignment

2.5.1 The Purpose of Alignment

Simply stated, the objective of shaft alignment is to increase the operating life period of rotating machinery, by minimizing the errors of assembly for joining components. Since the components that might fail are the bearings, seals, couplings and shafts, accurately aligned machinery will achieve the following results.

- Reduce the possibility of shaft failure.
- Moderate the power consumption.
- Reduce excessive axial and radial forces on the bearings to ensure longer bearing life and rotor stability under dynamic operating conditions.
- Minimize the amount of shaft bending from the point of power transmission in the coupling to the coupling end bearing.
- Minimize the amount of wear in the coupling components.
- Reduce mechanical seal failure.
- Maintain proper internal rotor clearances.
- Lower vibration levels in machine casings, bearing housings, and rotors.

2.6 Finite Element Method

The concept of finite element analysis (FEA) has been in use, in some form, for centuries. The simple idea is to replace a complex problem with a simpler one that represents the true solution to a desirable degree of accuracy. Serious use of FEA is not acceptable by the International standard organization (ISO's) when digital computers became available. With the increasing availability of computers in the 1980s and 1990s, the finite element method expanded rapidly. Nowadays, most structural design makes use of the finite element method, as it can significantly decrease the time and cost to market of a product.

2.6.1 Finite Element Method for Rotor Dynamics

Complex rotor systems have broad industrial applications, such as steam and gas turbines, turbogenerators, reciprocating and centrifugal compressors, internal combustion engines, and grinding and milling machines. Flexible rotating shafts are employed in those machines

for efficient power transmission, high-speed transportation, or cost-effective operation. The vibration of those flexible components is therefore a major concern in optimal design of complex rotor systems.

The vibration of flexible rotating shafts has been extensively studied in the past Dimentberg (1961), Eshleman (1978), Dimarogonas and Paipeties (1983), Lalanne and Ferraris (1990). Various numerical methods of analysis have been developed, including the direct stiffness method Enrich (1992), transfer matrix method Kramer (1993) and finite element methods (Kang, Shim and Lee 1992). Parallel to numerical methods, many researchers have also developed analytical techniques. The classical boundary value method is applied to study the natural frequencies and normal modes of rotating Timoshenko beams Zu and Han (1992). Transfer matrix analysis using distributed elements yields the steady state response of stepped flexible rotors Rao (1983), and a rotating Timoshenko beam carrying rigid thin disks Lee and Kang (1991).

Although the finite element method has been a standard structural analysis tool, analytical methods are always desirable because they deliver accurate results, which are numerically efficient and provide deep physical insight into the problem.

Although early dynamic models of rotor systems were formulated either analytically Dimentberg (1961) or using the transfer matrix approach Black (1974), the potential of the powerful finite element technique was recognized at a very early stage Ruhl and Booker (1972). Several finite element formulations using a uniform shaft element Nelson (1980), Chen and Ku (1991) or tapered shaft element Rouch and Rao (1979) were introduced to evaluate the modal characteristics of rotor-bearing systems. In a general finite element package, such as (ANSYS), not all these specializes element would be available. In this case, the Euler beam element will be used for the investigation.

2.7 Rotordynamics Preface to Choosing Balance Planes

Any typical rotor in principle has infinite number of planes containing unbalance. Since most rotors are somewhat asymmetrical in configuration, it is difficult to determine which of the planes contain the largest amounts of unbalance. The unbalance could be in any

plane or planes located along the axis of the rotor and it would be most difficult and time consuming to determine exactly which plane was in the wrong. Furthermore, it is not always possible to carry out mass corrections in just any plane. Therefore, the usual practice is to compromise by making mass corrections in the most convenient planes.

It is possible to make this compromise because, for a rigid rotor, any condition of unbalance can be compensated for by mass correction in any two balancing planes. This is true only if the rotor and shaft are rigid and do not bend or deflect due to the forces caused by the unbalance.

Flexible and quasi-flexible rotors exhibit dynamic response as they run through their bending critical speeds. The magnitude of the response is related to the unbalance present and the location of the unbalance. Balance masses need to be placed taking bending mode shapes into account. The effect of balance mass placement is dramatically more effective when masses can be placed in relation to the bending mode shape. Placement of masses in the body of the rotor has the added advantage that we are better able to keep balancing planes at the ends of the rotor open for trim balancing or future balance corrections on site.

Balancing of a flexible rotor requires elimination of rotor deformation so that other correction planes become necessary in addition to two correction planes. The number of additional correction planes necessary for eliminating deformation of a rotor is the same as the order of the critical speed Foiles, Allaire and Gunter (1998). That is, three correction planes are necessary for eliminating rotor deformation up to the first-order critical speed, and four correction planes are necessary for eliminating up to the second-order critical speed. This kind of correction is called multi-plane balancing of a flexible rotor.

Mathematically the existence of non-independent columns in a matrix means that a certain column can be obtained by the linear combination of other columns. In the influence coefficient balancing method each column in the matrix express the influence coefficients of a balance plane with respect to all measuring points. Therefore mathematical non-independent of columns is equal to the non-independent of balancing planes, so that the

physical meaning of non-independent of balance planes means that among that the selected balance planes a certain plane can be eliminated.

2.8 Non-independence of balance planes

The influence coefficient balancing methods has numerical difficulties when non-independent balancing planes are inadvertently used. This occurs as a result of the influence coefficient matrix being ill conditioned; because at least one of the columns of the matrix is nearly linearly dependent on the remaining columns.

It is possible to avoid this problem by evaluating the independence of the columns of the influence coefficient matrix. If this matrix is found to be ill conditioned, it is necessary to identify and eliminate the least independent of the balancing planes. This can be done by means of a Gram- Schmidt orthogonalization procedure for optimizing balancing plane selection Darlow (1980). The selection of balancing planes will be discussed in the following sections.

2.9 Trial-weight selection

The most considered problems in the starting of rotor balancing procedure regarding the balancing planes are;

- Where along the axis (plane selection)?
- Where along the radius and circumference (phase angle)?

The answers are usually the same place that the final correction mass is to be added. This, in effect, defines the plane where the correction masses will go. Some instrument manufacturers provide some guidance based upon their known electronic lag, but this cannot always be accurate because of foundation and stiffness variables of the system. If the trial mass is placed near the heavy spot, the vibration will get worse. If it is placed opposite the heavy spot, it will get better (depending on the size of the trial mass in relation to the true heavy spot). In the first case (near the heavy spot), the phase angle will not change much. In the second case (opposite the heavy spot), the phase angle will either not change much or flip 180°. In most cases, the amplitude and phase will both change. What is

most desired in the trial run is to get a phase change around 90° Wowk (1995), which will produce widely separated vectors and will result in the most accurate calculation

The trial mass should be sufficiently large to produce an amplitude change but not so large that it causes damage due to excessive vibration. A common criterion in popular use is to select a trial mass that produces a force of 10 percent of the rotor weight. Using this criterion, the additional dynamic load due to the trial mass should not exceed 10 percent of the static load. This is considered to be safe. Wowk (1995)

2.10 Errors Occurring During Correction (practical consideration)

In practice, errors during the correction of unbalance are unavoidable. This means that reduction of the initial unbalance according to the unbalance reduction ratio is not possible. The correction mass is usually not exactly accurate in its amount. Furthermore, its centre of gravity (C.G) position may not be defined precisely. The setting of the instrumentation is done with reference to an assumed value and, therefore, cannot generally be exact. Errors occur due to variations in:

- The trial and the correction masses,
- The position of the correction planes,
- The correction radius,
- The angular position of the correction masses.

Trial mass may be welded, or nuts and bolts can be used. If the machine has a balance wheel, masses will be installed there. Whatever permanent masses are used, they must be securely installed so they will not come loose when the machine is operated. If welding or bolting masses, it is important to take the masses of weld material or bolt into account.

The trial mass needs to be large enough to make a change in vibration levels but not so large as to cause damage to the machine being tested. The effect of the mass is proportional to the radius at which the mass is located and the square of the speed. It is best to start with a light mass and increase the mass as needed to have a measurable effect. But be certain the

trial mass will not come loose when the machine is run. Start with a small trial mass, and increase it if no effect in vibration level is observed.

Wowk (1995) recommended the following formula to select the trial mass;

$$W_t = 56{,}375\left(\frac{W_R}{N^2 * r}\right) \qquad (3.1)$$

Where

W_t = Trial mass, oz

W_R = Mass of the rotor, lb

N = Speed of the rotor rpm

r = Radius of trial mass, in

For the majority of machines the operate in the speed range of 1200 to 3600 rpm this formula (3.1) can be simplified to

$$W_t = 0.004\left(\frac{W_R}{r}\right)$$

In metric form, this equation is:

Trial mass (gram) = $30*(W_R$ (Kg)/ r (mm))/$(N)^2$

2.11 Shaft Alignment

Shaft misalignment occurs when the centrelines of rotation of two (or more) shafts are not in line with each other, or more precisely, it is the deviation of relative shaft position from a collinear axis of rotation when equipment is running at normal operating conditions Piotrowski, (1995).

Misalignment of machinery shafts causes reaction forces generated in the coupling, which affect the machines and are often a major cause of machinery vibration. Bloch (1976) identified the forces and moments developed by a misaligned gear coupling. Gibbons

(1976) showed that different types of misaligned couplings develop these forces and moments. Comparative values of these forces were presented. The effects that forces have upon the machines have been described in general terms.

Piotrowski (1986) provided information on the practical treatment of alignment methods and preparations. Acceptable amounts of misalignment must be modified to suit each individual drive train application. A general guideline for alignment tolerances is given. Sekhar and Prabhu (1995) presented the effects of coupling misalignment on turbomachinery vibrations. It was shown that the location of the coupling with respect to the bending mode shape had a strong influence on the level of vibration. An experimental investigation on the misalignment effect on cylindrical and three journal bearings was conducted by Prabhu (1997), which showed that an increase in angular misalignment had caused a change in the second harmonic of the vibration response. Simon (1992) predicted the behaviour of large turbo-machinery when subjected to imbalance and misalignment. The vibration excited by the coupling was computed numerically using assumed values for the reaction forces and moments at the coupling.

Chapter 3

REVIEW OF LITERATURE ON ROTOR BALANCING

3.1 Introduction

This chapter reviews the evolution of the balancing techniques. Emphasis has been given to publications where original ideas were first reported, or those papers, which achieved a widespread promotion of such ideas. Technical papers based on experimental work have also been summarized. Greater focus has been given to papers dealing with the influence coefficient balancing method.

The literature review is organized according to different balancing methods including; the influence coefficient methods, modal balancing, unified balancing, balancing using amplitude only, balancing using phase only and linear programming techniques, number of planes required to balance, redundant balance planes, and other topics. Some overlap could not be avoided due to the similarities between the different methods.

3.2 Rotor Balancing Review

Several review papers in the area of rotor balancing have been published over the past years for instance. Bishop and Parkinson (1972), Rieger (1973) and Parkinson (1991). Rieger (1986) in his book reviewed the state of the art on unbalance response and balancing of rigid and flexible rotors, also included a description of experimental work and a comparison between the different balancing methods.

One of the earliest general references to include a discussion of rotor balancing was that of Den Hartog in (1934), which highlighted various methods and machines used for rigid rotor balancing. A very simple single plane flexible rotor balancing procedure was also proposed by Den Hartog (1934).

Gosiewski (1985, 1987) presented his research on the automatic balancing of flexible rotors. A digital computer was used as the controller in his control scheme. Gosiewski's method is an extension of the influence coefficient method using the particular mass redistribution actuator proposed by Van De Vegte and Lake (1978). In this method, it is assumed that the influence coefficients for several spin-speed ranges are known beforehand and have been embedded into the computer's memory. Then, the position and magnitude of the correction masses are calculated based on the vibration measurement and the predetermined influence coefficient. Because the mass redistribution balancer can be adjusted during the rotating of the rotor, Gosiewski's method can handle the situation in which the system imbalance is time varying. Gosiewski also pointed out that operating the movable masses enables the influence coefficient matrix to be determined without stopping the rotor, but how this is done and how it affects the control scheme were not clearly stated.

Darlow (1989) reviewed the influence coefficient and modal balancing methods, as well as the unified balancing approach, previously proposed by himself together with Parkinson and Smalley.

Parkinson and McGuire (1995) summarized the developments in international standards. They considered in particular standards relating to balancing, especially flexible shafts, and acceptable vibration levels for rotating machinery. There is a collection of national and international standards in the field of balancing, which have been developed and up-dated over many years (see appendices 1).

3.3 Influence Coefficient Literature Review

Early research in rotor balance was first conducted by Thearle (1934) who presented a two plane semi-graphical balancing procedure based on a linear rotor system. This technique comprised a two-plane exact point balance; the balance computation included one speed and two vibration sensors. For many years, until computing devices progressed, a two-plane balance computation would be the practical limit for most field balancing. Baker (1939) suggested using groups of trial weights, which affect the vibration at only one bearing (at the one speed) at a time. Baker explored the use of this on machinery involving

both two and three bearings. With such a technique one could balance in more than two planes using essentially a single plane balance computation.

Unlike the modal balancing method, the influence coefficient method is an experimentally based method. This method assumes that the rotor response is proportional to the imbalance, and the effect of individual imbalances can be superimposed to give the final effect of a set of imbalances. It was originally proposed by Goodman (1964), refined by Lund and Tonneson (1972), and verified by Tessarzik and others (1972). Many least square estimation techniques (e.g., weighted least square estimation) can be used in this case because the number of vibration reading is more than the number of balancing planes. Some researchers Pilkey and Bailey. (1979,1983) have extended the least square estimation method to the constraint optimization method to control the possible range of the correction weight. The Unified Balancing Method tries to combine the modal and the influence coefficient balancing methods to get a better result with fewer trial runs. The theoretical basis, practical procedures, and experimental verifications of this method are described in detail in Darlow (1987).

Hopkirk (1940) formulated the two-plane balance using influence coefficients in the same manner as more modern treatments. Hopkirk used the influence coefficients transmission constants and used vector notation to denote these coefficients. Hopkirk presented an analytical solution in terms of vectors (complex valued quantities).

Most authors, who use an influence coefficient method, starting with Rathbone (1939) and Thearle (1934), have used a reference run with no balance weights and calibration or trial run with a trial weight or weight set attached to the rotor to generate the influence coefficients. For actual experimental rotor balancing, experimentally generated influence coefficients are preferred.

Church and Plunkett (1961) used a mobility method to generate influence coefficients without trial weights. Church and Plunkett excited the non-rotating shaft with a shaker, and they tested this theory on a very flexible shaft, whose first three resonances occurred at 550 rpm, 2000 rpm, and 4180 rpm, mounted in stiff ball bearings. However, this method did not produce reliable results and was difficult to applied to an actual machine, as is pointed out by Tonnesen (1974). This method would not be practical for field balancing.

Goodman (1964) substantially improved balancing technology when he introduced the least squares balancing procedure. This method uses data from multiple speeds and measurement locations, more measurements than balance planes, also it minimizes weighted sums of the squares of the residual vibration. This paper is discussed in detail, later in this chapter.

Rieger (1967) made an analytical study of the effectiveness of the influence coefficient method. Three practical rotor-bearing systems were examined: (a) rigid rotor in gas bearings; (b) supercritical flexible three-disk over hung rotor in fluid-film bearings; and (c) supercritical three-bearing rotor with one disk overhung in fluid-film bearings. The influence of measurement errors and correlation weight installation errors on the resulting balance was studied along with balance improvement with two, three and four balance planes. The number of bearing supports involved was shown to apply no influence on the quality of balance attainable. The effect of any bearing misalignment may affect the critical speed location and shaft bending stresses.

LeGrow (1971) presented a technique to generate the influence coefficients for an actual rotor using a computer model. The advantage in time and cost of such an approach could be substantial; however, this method could not balance the tested rotor sufficiently. A procedure for balancing flexible rotors was presented by LeGrow (1971), which was closely related to influence coefficient balancing. The author began with a brief discussion of the purpose of rotor balancing and complexities introduced by flexible rotors. LeGrow stated that the weighted least square influence coefficient procedure is not practical due to the number of runs and also requires a long time to balance a rotor.

Larson (1976) generated influence coefficients using a statistical technique. The imbalance runs corresponded to statistical trials and the influence coefficient assumed the role of the regression efficient. This approach allows one to average the data when constructing the influence coefficient matrix, and enables one to update the influence coefficients upon the addition of balance weights to a machine.

Drechslen (1976) suggested that the balancing may be accelerated by a consequential combination of experiments and data processing, which should yield balancing weights and improved influence coefficient matrix after each trial run. According to the author, even if the trial run has to be interrupted because of excessive vibration amplitudes, this method should yield balancing weights, which would reduce the amplitude of the explored speed range. Drechslen considered that this should help to reduce the number of interruptions necessary because of unsafe vibration levels in the higher critical speed and should contribute considerably to the acceleration of the balancing process. Drechslen also pointed out that the approximated influence coefficient matrix could either be calculated analytically or taken from a similar rotor. He considered the possibility of using more trial runs than linearly independent mass combinations for the calculation of the influence matrix. This can be done using a least-squares procedure, which minimizes the measuring errors. The least-squares procedure requires the inversion of a matrix whose determinant becomes zero. Drechslen proposed to use an initial approximation of the influence coefficient matrix to determine correction masses since the first trial run.

Badgley (1976) gave a description of the different techniques for multi-plane and multi-speed balancing by the influence coefficient method. Badgley included the known presentation of the influence coefficient theory and some comments related to the balancing process in practice. Badgley recognized that the higher cost involved in a field balancing is that of down time, so that shutting down a machine to re-balance the rotor is not a decision to be taken lightly. Badgley suggested that the optimal approach would be to determine the correction masses with the machine still running, and to shut down only long enough to install the balance masses. However, Badgley did not explain how these masses could be calculated without shutting the machine down. Another practical point raised by Badgley related to the stabilization of the operating conditions before recording the rotor vibration vectors. This stabilization may require several hours or even days for machines at high temperature. Badgely also experienced the errors inherent to the use of electronic instrumentation, suggesting using mean values of each parameter in order to increase the effectiveness in the determination of the correction masses.

Tessarzik, Badgley and Fleming (1976 b) published the third paper in a series of papers (1972, 1974) relating the results of an extended test program designed to evaluate the validity of the influence coefficient balancing method. In this paper, the authors discussed the results of a series of seven test cases involving the balancing of a test rig through four bending critical speeds. Of these four critical speeds, two were heavily damped by the journal bearings, and did not require balancing. The remaining critical speeds were lightly damped and required balancing to be negotiated. In general, the effectiveness of the balancing procedure did not vary. However, two exceptions were noted. Firstly, one attempt was made to balance the fourth critical speed without including any vibration data from the first critical speed. A distinct improvement was observed at the fourth critical speed, but only at the expense of the vibration level at the first critical speed. In all other cases involving balancing of the fourth critical speed, data from the first critical speed was included and no substantial increase in vibration level was observed at the first critical speed. Secondly, an attempt was made to balance the rotor using only data from accelerometers mounted on the bearing housings.

Consequently, the data from the accelerometers were reduced substantially, but the rotor vibration was actually increased and negotiation of even the first critical speed was not possible. This was interpreted as being due to a change in the rotor mode shape resulting in nodes being located at or very near to the bearings. The authors mentioned that this is a common danger incurred by using only bearing pedestal vibration data for balancing. These test results showed that the influence coefficient balancing procedure could be used for the balancing of a rotor for operation through more than one bending critical speed. In fact, balancing of a rotor through four bending critical speeds was demonstrated based on these encouraging results. The authors concluded the capability of this method for balancing a rotor through any number of flexural critical speeds.

Nakai and Miwa (1980) proposed a theoretical balancing technique using a method in which the residual vibration after balancing was minimized under such conditions that the amount of correction mass did not exceed a certain limit for each plane. Shiohata and Fujisawa (1980) presented a similar procedure in the same time. Woomner and Pilkey

(1981) used the same approach. These authors investigated the balancing by considering correction masses using a least-squares procedure modified by introducing a constrained coefficient into the performance function. The method was experimentally verified using a test rotor.

Tonnesen and Lund (1988) presented an investigation of experimental work to evaluate a supplementary method for balancing lightly damped rotors. The rotor, while running, is excited by an impact generator, and the response is measured at the bearings by transducers for displacement, force and acceleration. An FFT analyzer is employed to obtain frequency-dependent transfer functions from which the corresponding influence coefficients can be calculated. The results are compared with the values obtained from the conventional trial weight method, and they were also used in a successful balancing of the rotor.

Ling and Cao (1996) introduced frequency response functions, analyzing the relationships between the frequency response functions, influence coefficients and corresponding mathematical equations for high-speed rotor balancing. They also analyzed the relationships between the imbalance masses on the rotor and frequency response functions. The analysis was based on the modal balancing method and the equations related to the static and dynamic imbalance masses. The frequency response function was also obtained. Experiments on a high-speed rotor-balancing rig were performed to verify the theory, and the experimental data was in agreement with the analytical solutions.

Kang, Liu, and Sheen (1996) derived formulations to the influence coefficient matrices from motion equations for rotors. On the basis of their study, the influence coefficient approach can be verified from an analytical viewpoint. This study formulates an algorithm of plane separation based on the exact-point influence coefficient approach. From the analysis, a generalized procedure for multiplane separation for balancing a rigid rotor was provided by an inference from two-plane separation and then three-plane separation. A balancing machine to correct a large number of planes simultaneously or successively can utilize this process of multiplane separation.

3.4 Verification of The Influence Coefficient Method

With reference to the balancing of a two rotor, three-bearing turbine generator, Thearle (1934) described the application of an influence coefficient method. Groebel (1953) used practical influence coefficient methods to balance large generator rotors mode by mode. Den Hartog (1934) commented on the influence coefficient principle (for two-plane correction) in his book. It appeared that influence coefficient methods were used effectively for several decades before development of the computer.

An analytical study of the effectiveness of influence coefficient balancing was made by Rieger (1967), who examined three practical rotor-bearing systems: (a) rigid rotor in gas bearings, (b) a supercritical, flexible, three-disk overhung rotor in fluid-film bearings, and (c) a supercritical, flexible rotor with one disk overhung in three fluid-film bearings.

Tessarzik (1972) evaluated the effectiveness of the influence coefficient method with a flexible three-disk rotor operating through it's lowest bending critical speed. Tessarzik calculated the balance weights by a computerized influence coefficient procedure. The flexible rotor-bearing system used was designed to contribute negligible damping to the rotor whirl mode at the bending critical speed. Under such circumstances, large resonant amplitudes are expected unless the balancing procedure was effective. Tessarzik and Badgley, (1974) also developed a least-squares influence coefficient procedure along the lines proposed by Goodman (1964) to obtain a best balance for a rotor operating over a speed range containing several critical speeds.

Another interesting least-squares development has been reported by Little (1971), who used a linear programming technique to optimize the balance of rotors operating through several bending critical speeds.

Other publications relating to use of the influence coefficient method are Larsson (1976), Gu (1988), and Sanderson (1988). A further publication by Darlow (1989) compares the influence coefficient method with modal balancing, and describes a unified approach where the advantages of each are capitalized.

3.5 Goodman's 1964 Paper

In the early 1960's Goodman properly formalized the theory of the influence coefficient method. In 1964, Goodman described a mathematical procedure for the determination of correction masses using a least-squares minimization of the vibration readings. Due to the importance of this paper, it is discussed in more detail in this section. Goodman's procedure required the number of vibration readings to be larger or equal to the number of balancing planes. The influence coefficients were determined from the results of trial runs in which individual masses were attached to the balancing planes of the rotor. This produced an over-determined system of simultaneous equations that was solved minimizing the residual vibrations.

Goodman described in detail the empirical and analytical procedures for performing least squares influence coefficient balancing. Goodman began by citing the motivation for the development of the least squares method. This is followed by a brief description of the conventional procedure for field balancing (i.e. exact point influence coefficient balancing). The mathematical backgrounds for the least square and weighted least squares procedures are presented. The author stated that, in general, no more than three iterations are needed with the weighted least squares method to obtain sufficient convergence. The purpose of the weighted least squares method is to reduce the maximum predicted residual vibrations at the expense of the root mean square (rms) of these residuals. The first iteration of this procedure is identical to the least squares method. Goodman also stated that the most effective locations for the balancing planes might be determined either experimentally or analytically. Goodman concluded with some specific observations, concerning the application of a balancing procedure for this type. Goodman also stated that a systematic approach is necessary, which requires some reorientation on the part of balancing engineers. Also, the input to the procedure should be simple and quick so as not to discourage its use and ready access to the computer and quick turn around time were essential. The author ended the proposal by adding that the balancing method, as it was implemented, permits the use of specifically selected vibration readings for the calculation of correction masses while still calculating predicted residual vibration levels for all of the

vibration readings. Goodman was referring to graphical manipulations rather than physical manipulation of correction masses. In any case the advent of the high-speed digital computer has substantially altered this situation.

The author concluded with some general observations about practical field balancing problems, which are very important and are usually overlooked. He stated that while balancing procedures assume linear rotor behaviour, this is not always the case and under certain circumstances more than a single balancing process may be required possibly including a predetermination of influence coefficients. The importance of taking all balancing data under consistent operating conditions was stressed. The author considered some situations in which it may be advisable to either change the balancing plane locations or to increase the number of balance planes. Of particular interest is the case when one or more of the balancing planes were located at (or very near to) a vibration node and the case when the influence coefficient matrix was (nearly) singular.

3.6 Least Square Optimization/Linear Programming

Tessarzik, Badgley and Anderson (1972) presented the results of a series of tests designed to confirm the validity of the exact point speed influence coefficient method for balancing flexible rotors. This method was actually a particular case of general least square influence coefficient procedures for which the total number of vibration readings must be equal to the number of balancing planes. The authors described a test rig with a flexible shaft, supported by two tilting pad journal bearings with three heavy disks. Three balancing tests were conducted, each with a different initial unbalance configuration. In each of the tests the effectiveness of the exact point speed influence coefficient procedures for balancing flexible rotors was verified.

Lund and Tonnesen (1972) verified the accuracy of the least square influence coefficient method using a symmetric test rotor consisting of a shaft with four balancing planes. The shafts rotated in air lubricated journal bearings, which were mounted on flexible supports. After the initial balancing of the shaft, initial unbalance masses were attached to the disk of the rotor. Then, balanced by the least square method, the influence coefficient technique

using the same planes as those in which the initial unbalance masses, were attached. The accuracy of the method was evaluated by direct comparison between the calculated correction masses and the attached unbalance masses. Lund and Tonnesen also introduced the use of two trial runs per balancing plane shifting in each case the position of the trial mass by 180°. The authors justified the increase of the number of trial runs arguing that subsequent results of the experiments would not show any significant improvement. The multi plane multi speed influence coefficient balancing procedure was described in detail along with the results of a series of tests designed to evaluate this technique. This balancing procedure handles large quantities of vibration data through the use of a least square minimization algorithm. An extensive series of tests was described and the results of these tests evaluated. These tests involved the balancing of a flexible rotor through three critical speeds while varying sensor type, instruments, and balance speed and balance planes. In general the variation of the results from test-to-test was insignificant while the effectiveness of this influence coefficient balancing procedure was clearly and uniformly demonstrated. The authors concluded that this balancing procedure was valid and accurate and that for satisfactory balancing of the rotor, it was necessary to measure vibration amplitude and phase angle with an error not exceeding 3 - 4 %. In other words, the result of the balancing procedure is not likely to be adversely affected to a significant extent by reasonably small instrumentation errors.

Tessarzik and Badgley (1974) presented an extensive experimental investigation of which the first stage was reported in an earlier paper, Tessarzik and Badgley (1972). That first series of tests was concerned with the verification of the exact point-speed influence coefficient method for balancing of flexible rotors. A similar series of tests was described in this paper Tessarzik and Badgley (1974) in which the same test rig was used to verify and compare the exact point and least squares procedures for influence coefficient balancing. In addition, this second set of tests considered other configurations and more difficult balance conditions. Some theoretical advantages were suggested for each of these balancing procedures. The methods were, in general, equally effective for balancing the particular test rig and there was no noticeable difference in the results from the two procedures, however, for one specific test case, there was measurable differences. Two

disadvantages of influence coefficient balancing are discussed in this paper. The first of these concerns the large, impractical correction masses, which may be calculated when the balancing planes were not all linearly independent (particularly when two balancing planes were located close together). An influence coefficient orthogonalization procedure may be used to detect this condition. Subsequent elimination of the linearly dependent balancing planes will eliminate this problem.

Little and Pilkey (1976) described a linear programming method for the balancing that can place constraints on the magnitude of the balancing weights; however, this technique requires at least as many balance weights as measurements which was in general not possible. The first balance computation (analytical model) resulted in an unbounded solution when using 8 balance planes.

Tonnesen (1974) published the results of further experiments for the evaluation of the least squares influence coefficient method. Tonnesen used the same test rotor employed during the work reported by Lund and Tonnesen in (1972). Although in this case Tonnesen distributed the unbalance masses in more planes than there were correction planes available. Tonnesen also included the results of a balancing exercise with no damping in the system. The results of the experiments demonstrated a high accuracy in determining the correction masses required to compensate different unbalance configurations.

Bigret, Curami, Frigeri and Macchi (1977) described a modified influence coefficient balancing method adapted for use with an in-field computer for multi-speed, multi-plane balancing of a 235-MW turbomachine. This balancing method is the standard weighted least-squares influence coefficient method modified to use a generalized weighting of particular speeds or sensors. The in-field computer system used relied on manual input of vibration data by means of a Teletype. This balancing system was experimentally verified, with good success, as described in the paper.

Pilkey and Bailey (1979) corrected the deficiencies of the previous linear programming (Little and Pilkey (1976)) by using a different formulation for the problem. Pilkey and

Bailey separated their techniques into time-independent and time-dependent algorithms. The techniques investigated were the following:

- Linear Sum; Minimize the sum of all the computed residual measurements (absolute value of the residuals).
- Min-max; minimize the maximum residual measurement.
- Least Squares; Minimize the sum of the squares of all residual measurements including constraints on the magnitudes of the corrective balance weights. This leads to a quadratic program. The time-independent techniques only view the response with the shaft in its 0° position for balance weights placed on the X- and the Y-axes.

The methods studied by Pilkey and Bailey (1979) suggested a trend to improve the solution of balancing by more reliable numerical algorithm available at that time of the investigation. This trend goes on these algorithm improves and new algorithm

Darlow (1982) stated that the influence coefficient balancing calculations have certain numerical difficulties when non-independent balance planes were inadvertently used, resulting in impractical, artificially large, mutually counteracting correction masses being calculated. This occurred as a result of the influence coefficient matrix being ill-conditioned. Which means that at least one of the columns of the matrix was close to being linearly dependent on the remaining columns. Darlow presented a method to identify and eliminate the non-independent balance planes using a Gram-Schmidt orthogonalization procedure. Darlow defined a significance factor as a criterion to identify the non-independence of the balance plane. When the value of the significance factor is less than 0.2 this balance plane was considered as a non-independent plane and had to be eliminated. After the non-independent plane was eliminated, further calculation was still based on Goodman's method. Unfortunately, Dalow only gave example of the influence coefficient matrix studied. No details of his experimental rig could be found in the paper.

The present study carry on the trend that new numerical algorithm, such as QR and the SVD method, are tested for their suitability for rotor balancing.

Balda (1980) showed that the problem of balancing flexible rotors was a problem of minimax, the residual vibration, which in general was of a non-linear nature. It may be solved either by algorithms of mathematical programming or by special algorithms for non-linear minimax. There were cases for which the problem remains linear within particular iteration steps, which utilized the following methods: linear least-squares (LLSQ), linear and quadratic programming, and non-linear programming.

Drechslen (1980) presented a theory of flexible rotor balancing of the minimum number of balancing planes and the minimum amount of information necessary for successful rotor balancing. Drechslen considered that practical experience shows that a consistent consideration of extra balancing planes and extra information yields much better results and reduces the production time considerably. Drechslen also considered that the advanced averaging techniques on extra trial runs and extra balancing speeds yields a reliable influence coefficient matrix and can even be used to improve the right-hand side of the equation system. The extra planes can be used to minimize the magnitude of the balancing weights, thus indirectly improving the rotor performance at operating speed and over-speed considerably. In connection with these techniques all available information was considered. Even the total weight installed on the rotor with each trial run was an important feature, which can have an important influence on calculated balancing weights.

Darlow (1987) provided information on an important problem in balancing that results in ill-conditioning of the balance equations. When columns, corresponding to the balance planes, of the influence coefficient matrix form a linear (or nearly) dependent set of vectors very large correction weights can be computed. The majority of the effects of these weights cancel each other; this results from the ill-conditioning of the influence coefficient matrix. Darlow showed, with the aid of examples, that using fewer balance planes can solve the problem.

Krodkiewski (1994) presented a method for identifying both the plane and magnitude of the balance required to correct a system whose configuration and unbalance distribution may change whilst in operation. The method used a non-linear mathematical model of the

system and the measured vibration response both before and after the change in unbalance occurs. The non-linear model includes information about the bearings and supports. The model used measured data before and after the change in unbalance. The unbalance plane and magnitude are determined by trial-and-error until the algebraic equations that represent motion before and after the change in unbalance were solved.

Preciado, Bannister and Aguirre (1996) presented a general theory that makes use of multiple mass sets, which allow obtaining the influence matrix even when multiple trial mass sets were attached to the rotor during the trial runs. They also considered that the outlined method was suitable for application of least-squares minimization or for the weighting of vibration readings and balancing masses. Also they established a limitation in the traditional influence coefficient method, namely that the multiple mass set used in a trial run should not be a linear combination of previous sets already used for the configuration of the influence matrix. The first application example showed that the precision of the proposed method was equally as good as the precision of the traditional influence coefficient method. The significance lies in the fact that the two methods are equivalent.

Feng (1996) presented work, which was based on the influence coefficient method, which utilizes the unbalance response from vibration analysis software of rotor bearing foundation systems. Feng used least squares analysis to minimize the vibrations at the measurement locations at the balance speeds. Also an experiment on a flexible rotor bearing system showed, with an accurate model of the system, good balancing results achieved from just the response measurements of the unbalanced rotor. However, the results rely considerably on the adequacy of the rotor bearing system model and in general correction to the theoretical influence coefficients based on one trial run to achieve reliable balancing predictions.

Ding (1997) presented a further development of the one discussed by Krodkiewski (1994). When consideration was given to the possibility of identifying imbalance change at one plane, Ding's method allowed the identification of two planes where imbalance changes

take place. It also provided a basis for the formation of an algorithm for identifying multi-plane imbalance changes. The significance lay in the use of the relative journal bearing motion signals only. Ding obtained these signals by using the built-in transducers in the bearing housings. This was important for application and identification of a faulty unit of a turbogenerator set that has lost one or more of its blades. Ding used the computer simulation of a three-support rotor system to prove the method.

Foiles, Allaire and Gunter (2000) presented a theoretical basis for a min-max optimum method of balancing with more measurements than balance planes by using a set of experimentally determined influence coefficient matrix. Gunter, Allaire and Foiles published a companion paper entitled "Balancing of a 1150 MW Turbine Generator" (2000). The results applied to the example turbine generator show a significant improvement in balancing results by using the min-max approach rather than weighted least squares method.

3.7 Modal Balancing

The series of techniques that aim to balance a flexible rotor using its modal properties were grouped and known as the modal balancing method. In this technique, every vibration mode was corrected by attaching a set of masses to the rotor so that no effect was caused on previously balanced modes. This procedure requires the knowledge of the rotor mode shapes or feature functions.

Modal balancing procedures are characterized by the use of the modal nature of the rotor response. In this method, each mode is balanced with a set of masses specifically selected so as not to disturb previously balanced lower modes. There are two important assumptions: i) the damping of the rotor system is so small that it can be neglected; and ii) the mode shapes are planar and orthogonal. The first balancing technique similar to modal balancing was proposed by Grobel (1953). This method was refined in both theoretical and practical aspects by Bishop (1959), Bishop and Gladwell, (1959); Bishop and Parkinson, (1972). Many other researchers also published works on the modal balancing method, including Saito and Azurna (1984), and Meacham (1988). Their work resolved many

problems with the modal balancing method, such as i) how to balance the rotor system when the resonant modes are not separated enough; ii) how to balance the rotor system with residual bow: iii) how to deal with the residual vibration of higher modes: and iv) how to deal with the gravity sag. An excellent review of this method can be found in Darlow (1989). Most applications of modal balancing use analytical procedures for selecting correction masses. Therefore, an accurate dynamic model of the rotor system is required.

There were several procedures published in the literature for modal balancing of flexible rotors by Parkinson and his coworkers (1963). These procedures have received different names. All of them, however, were based on the assumption that the unbalance response of the rotor may be expressed as a series of modal contributions from the principal modes of vibration.

Balancing of a rotor to eliminate vibration as measured by a single sensor may not result in a minimum vibration level for the rotor as a whole, particularly when dealing with distorted or non- planar mode shapes. Difficulty may also occur as a result of the presence of vibration from other modes, which have not been previously balanced, although methods have been developed for dealing with this problem Parkinson (1991).

Parkinson and Bishop (1961) presented a general theoretical treatment of the vibration of rotating shafts supported on any number of bearings. This analysis considered uniform or non-uniform cross section, as well as flexible bearings. Parkinson and Bishop concluded that considering continuous shafts did not introduce anything new to the theory of shafts supported at their two ends, so that they should be balanced in the same way. The balancing procedure originally proposed by Bishop and Gladwell (1959) was based on the consideration of uniform shafts rotating in ideal bearings located at their ends. Subsequent efforts were focused in the elimination of the various restrictions considered in the original analysis. In this way, non-uniform shafts Gladwell and Bishop (1959a), flexible supports Gladwell and Bishop (1959b) and continuous shafts Parkinson and Bishop (1961) had later been considered. However, until that point in time no experimental results or practical applications had been reported. This probably reflected the practical difficulties

encountered when analysing the vibration characteristics of real systems, such as a large turbo alternator rotor, which are more complex than those predicted by theory for simpler systems.

Parkinson (1965) made another important contribution to the theory of modal balancing. In this paper he eliminated another restriction related to the bearing properties, which until that point of time had been considered symmetric in all theoretical analyses. He considered the motion of a symmetric shaft supported on asymmetric bearings and from the results of his analysis he proposed a modified balancing procedure that accounted for the differences in mode shapes of a pair of modes produced by the asymmetric characteristics of the bearings. His procedure considered balancing the rotor in two planes and he recommended using the principal planes of the bearings, although he neither justified this recommendation nor mentioned how these planes could be identified in practice. Furthermore, he considered the principal planes to be perpendicular to each other, which is not necessarily the case for real bearings.

In an attempt to solve one of such particular difficulties, Bishop and Parkinson (1963) analysed the problem of isolation of modes when the shaft has a gross component defect in an adjacent mode or when critical speeds are not widely spaced apart. Under these circumstances the rotor is said to have a mixed modal behaviour and the distortion of the extraneous modes cannot be neglected: therefore Bishop and Parkinson described a procedure based on the method of Kennedy and Pancu (1947) for isolating vibration modes. This procedure required the active participation of the analyst and determined a clear definition of the response in the vicinity of the resonances so that the position of the natural frequency defined by the maximum frequency spacing could be identified.

Parkinson, Jackson and Bishop reported in two papers (1963a and 1963b) the results of an experimental verification of the modal balancing method using thin shafts in laboratory conditions. The use of thin shafts showed the importance of initial bend as a source of forced vibration. The consideration of these components of the synchronous vibration required some additions to the original balancing theory and this was developed in the first

paper. The experimental apparatus and the results of the test program were described in the second paper, in which the authors concluded that the theory on the laboratory scale and that comparable test on large rotors would be justified.

Several researchers have published in the general area of modal balancing. For example Dimentberg (1961) and Federn (1964) published state-of-the-art reviews of modal balancing. Moore and Dodd (1964) discussed the practical applications of modal balancing to turbine-generator rotors. Actual experimental results were presented with a particular emphasis on rotors, which exhibited significant mixed mode behaviour.

Kellenberger (1967) proposed a significant modification to the modal balancing method. In this paper, Kellenberger analysed the balancing of flexible rotors with variable moments of inertia and variable mass distribution. Kellenberger established the equations for mass balancing separating the inertia forces from the unbalance forces. Furthermore, Kellenberger said that the nullification of the unbalance forces gives the condition for rigid rotor balancing and that the disappearance of the inertia forces contains an additional requirement for flexible balancing.

Lindley and Bishop (1963) discussed the application of modal balancing to large steam turbines in the range of 120-500 MW where the bearing stiffness is large compared to the shaft stiffness.

Bishop and Mahalingam (1966) discussed the results of a series of tests with a rotor of this type and extended the discussion of Parkinson (1965). Parkinson (1965) then proposed a technique for balancing such rotors, as an extension of modal balancing.

Parkinson (1976) reviewed the modal interpretation of the vibration of damped rotating shafts with the intention to remind the practical vibration engineer that no method of balancing is likely to be successful in an industrial context unless the shaft vibration is correctly interpreted. Parkinson defined the principal modes as those of a system vibrating freely in the absence of damping. Then Parkinson explained that these principal modes allow the use of principal co-ordinates, which means those complex systems, can be made

analogous with simple one-degree of freedom systems. Parkinson concluded that the description of planar response in modes is only valid for systems in which the damping can be reasonably approximated by mathematical expressions.

Kreuzinger-Janik and Lrretier (2000) produced the identification of the unbalanced distribution of flexible rotors, their method being based on the modal expansion of the frequency response functions. Basically, this expansion can be found either by a numerical calculation, which normally requires a model updating procedure for sufficient accuracy of the numerical model or by experimental results. In both cases, an appropriate modal testing technique was required for experimental modal analysis of the rotor. The results of an experimental modal analysis on a rotor were used to identify the unbalance distributions of rotors. The pre-tests have shown that there exist some non-linearities in the test rotor, which have been considered by a constant force level for all frequencies. They used a scanning laser vibrometer to detect the velocity, which gave them better accuracy of signal-to-noise ratios. The disadvantage of the proposed method is the necessity to expand the eigenvectors to non-excited locations, e.g. disc locations.

3.8 Combined Modal/Influence Coefficient

Parkinson (1991) published a review of the state of the art of rotor balancing. Parkinson compared the balancing methods, which were the influence coefficient technique, the modal balancing method and the modal balancing proceeded by rigid body balancing. In order to allow direct comparison of the three methods, the influence coefficient method was expressed in terms of the notation in the modal analysis. Parkinson's conclusion was that the influence coefficient method does not guarantee low residual vibration at the critical speeds, unless these critical speeds are selected as balancing speeds. Parkinson also mentioned the possibility of using the influence coefficient method with isolated modal components of vibration at the critical speeds.

Iwatsubo (1976) compared modal and influence coefficient balancing using numerical examples. Iwatsubo showed that influence coefficient balancing is more sensitive to

measurement error than was modal balancing. Iwatsubo indicated that a combined method would be preferable, but gave no details as to how this would be accomplished.

Tan and Wang (1993) developed a theory unifying the modal balancing and the influence coefficient methods. The unified theory was applied to the low-speed balancing of flexible rotors. It was shown that the modal and influence coefficient balancing techniques could be made equivalent by setting the initial unbalance deflections in both methods to zero. It was then proposed, as long as certain requirements are met, to balance a rotor at low-speeds (influence-coefficient method), whilst meeting the requirements of high speed (modal) balancing. That is, the rotor may be balanced for however many modes are required, without the need for it to run at or above its operating speed, which has obvious advantages for practical applications. It is important to recognize that the proposed method is distinct from low-speed rigid rotor balancing; it is an actual unification of the modal and influence coefficient techniques, applicable to flexible rotors at low speeds.

3.9 Unified Techniques

There have been several attempts to combine the influence coefficient and the modal balancing methods. Some authors have been able to recognize the similarity between these two methods. Other authors, however, treat them as separate parts in a balancing procedure.

Parkinson, Darlow, Smalley and Badgley (1980) presented the first of a series of papers related to the unification of the influence coefficient and the modal balancing methods. They described the independent use of the two methods to balance an experimental rotor with several critical speeds. They concluded that some similarities existed between the applications of both balancing procedures and proposed that the optimum method would involve a combination of the main features of these techniques Zorzi, Lee and Giordano (1984).

Chapter 4

Current Flexible Rotor Balancing Methods

4.1 Influence Coefficient Method

4.1.1 Introduction

The influence coefficient method aims to correct rotor unbalance by means of separate masses placed in predefined correction planes. Recording the changes of vibration amplitude due to the addition of trial masses, an influence coefficient matrix is assembled, this matrix represents the dynamic characteristics of the system. The influence coefficient method assumes a linear relation between the vibration response and the unbalance of a rotor. This linear relation defines the influence coefficients, which represent the vibration effect at some point on the shaft for a given speed, due to the addition of a unit mass in another or the same point along the rotor. A good review of this method can be found in Darlow (1982)

4.1.2 Basic principles of unbalance measurements

Consider a single disk first, a marker is usually used to measure the phase angle of the unbalance vibration. The displacement amplitude is commonly measured by a linear displacement transducer known as the proximity probe see figure 4.1

The original unbalance is measured first and the displacement of the rotor represented by rotating vector V_0. A known unbalance mass (known as trial mass) is then mounted on the disk see figure 4.2. The new vibration response of the rotor will be vector sum caused by the original unbalance and trial mass. ie,

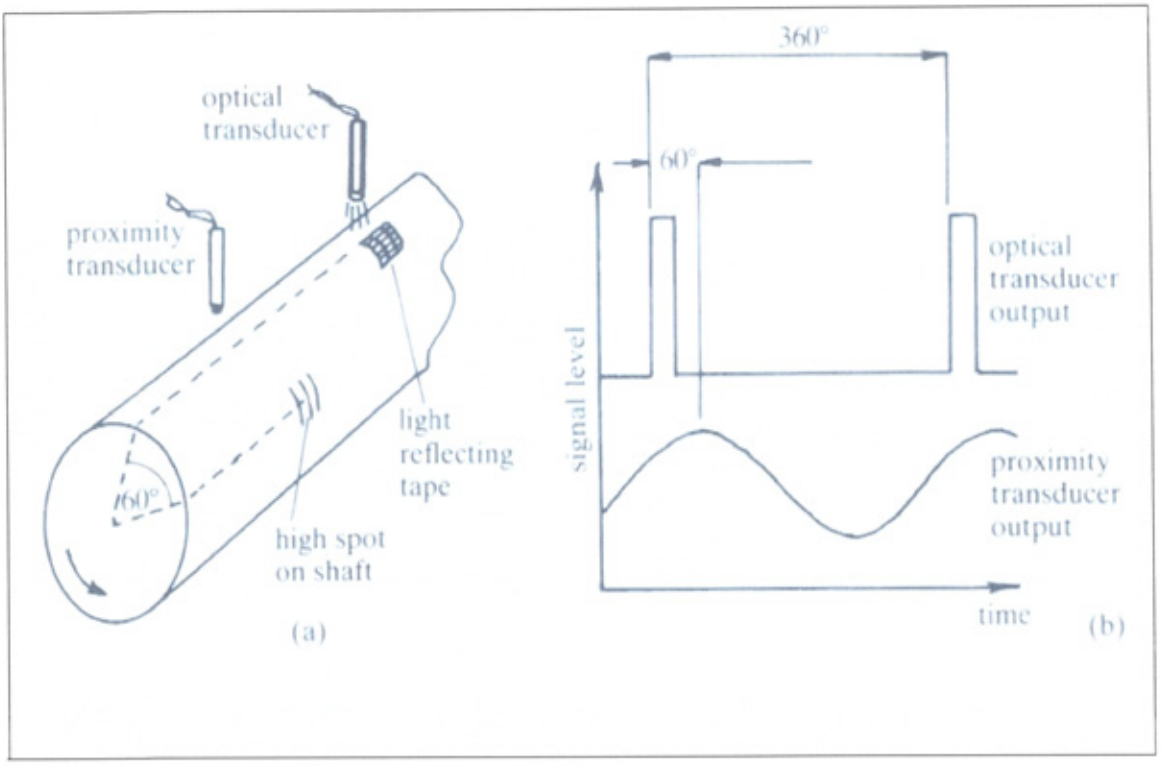

Figure 4.1 Phase Measurements (A) Shaft and Transducers (B) Transducers Output (Goodwin 1989)

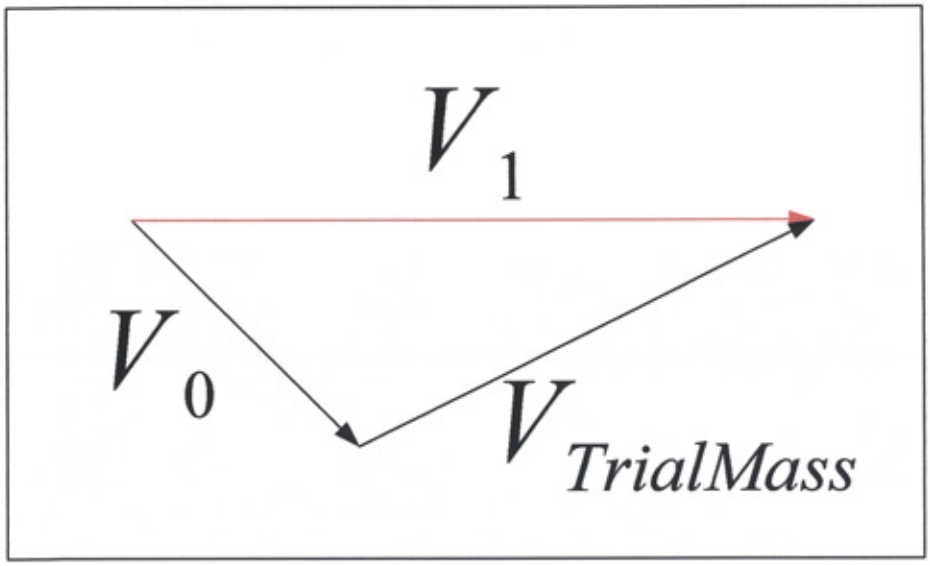

Figure 4.2 Victors Representation of Vibration Levels

$$V_1 = V_0 + V_T \tag{4.1.1}$$

$$V_T \ \alpha \ m_T * r_T \tag{4.1.2}$$

it can be proved that the correction balance mass calculated based on the vector equation,

$$M_C r_C = \left(\frac{m_T * r_T}{V_1 - V_0}\right) * (-V_0) \tag{4.1.3}$$

or

$$(-V_0) = (M_C r_C) * \left(\frac{V_1 - V_0}{m_T * r_T}\right) \tag{4.1.4}$$

$$M_C r_C = \left(\frac{V_1 - V_0}{m_T * r_T}\right)^{-1} * (-V_0)$$

$$M_C r_C = (\alpha)^{-1} * (-V_0) \tag{4.1.5}$$

With α known as the influence coefficient. The case can be extended to n balancing planes.

4.1.3 Procedure for Influence Coefficient Balancing

When applying the influence coefficient procedure, some prior knowledge of the dynamics of the rotor system is useful when choosing the location and number of balancing planes and sensors, choosing the balancing speeds, and estimating safe vibration limits. The balancing procedure began with taking uncorrected rotor data begins. Then, either one or two trial masses are installed in each balancing plane, one at a time, and trial mass data is taken. In general, the trial masses are removed. The influence coefficient matrix, one or more sets of correction masses and the corresponding expected residual vibration is then calculated. A set of correction masses is chosen and installed and check balance data is taken. In many cases, this is the end of the balancing procedure. However, if the check balance data is not satisfactory, or if vibration must be controlled at a higher speed, it is necessary to perform another balancing run and the procedure described above is repeated, which is called trim balancing see chapter 6.2 for more details.

4.1.4 Basic Steps of The Influence Coefficient Method

The influence coefficient balancing sequence is as follows:

1) Let (m) the correction planes, let (n) the transducers to measure vibration, and let (h) represent the speeds. There will then be (n) opportunities to acquire data, such that $m = h*n$. The balancing speeds are $h_1, h_2, \ldots, h_k$
2) An initial run is made to measure the initial vibration at each transducer and at each speed in the original condition. The vibration amplitude, and phase angle at each transducer are designated W_{n0}^h, where the subscript n refers to the nth transducer and 0 refers to the original condition. The superscript h refers to the hth speed.
3) A trial mass m_1 Attached to the rotor in measuring plane 1. Its radius is r_1 and phase angle is ϕ_1.
4) Run the rotor again and the vibration amplitude measured at each transducer (n) and at each speed (h). The results are obtained: W_{n1}^h
5) The trial mass from plane 1 is removed and a trial mass (the same trial weight or a different one) m_2 is attached in measuring plane 2. It has a radius of r_2 and phase angle location ϕ_2.
6) Run the rotor again and the vibration measured at each transducer (n) and at each speed (h). The measurements obtained are: W_{n2}^h
7) Repeat steps 5 and 6 for all of the correction planes available for $j = 3,4,\ldots,n$. The following measurements are obtained: W_{nj}^h

The basic equation for the influence coefficient method is

$$\alpha * W = X \tag{4.1.6}$$

Where $[X]$ is a column vector of observed displacements for the unbalanced shaft, $[\alpha]$ is the matrix of influence coefficients and $[W]$ is an unknown column vector of the effective rotor unbalance related to the corrections planes, to be determined from trial weight tests

4.1.5 Computation of The Influence Coefficients Matrix

α_{nj}^{k} are the influence coefficients relating the rotor response for the specified sensors and speeds to the balancing planes, with uppercase letters used for matrices and lower case letters used for vectors. The α_{nj}^{k} are determined empirically through the application of known trial masses in each of the balancing planes.

$$\alpha_{nj}^{k} = \frac{W_{nj}^{k} - W_{n0}^{k}}{m_j r_j} \tag{4.1.7}$$

Where $m_j r_j$ refers to the trial weight.

m_j is the mass and r_j, is the radius.

The Form of the traditional influence-coefficient matrix with elements can be expressed in matrix form, as follows:

$$\begin{bmatrix} \alpha_{11} & \alpha_{12} & \cdots & \alpha_{n1} \\ \alpha_{21} & \alpha_{22} & \cdots & \alpha_{2n} \\ \cdot & \cdot & \cdots & \cdot \\ \cdot & \cdot & \cdots & \cdot \\ \cdot & \cdot & \cdots & \cdot \\ \alpha_{m1} & \alpha_{m2} & \cdots & \alpha_{mn} \end{bmatrix} * \begin{bmatrix} W_1 \\ W_2 \\ \cdot \\ \cdot \\ \cdot \\ W_m \end{bmatrix} = \begin{bmatrix} -X_1 \\ -X_2 \\ \cdot \\ \cdot \\ \cdot \\ -X_m \end{bmatrix} \tag{4.1.8}$$

Where α_{ij} and X_i are constants, $i = 1,2 \ldots m$, $j = 1,2 \ldots n$

4.1.6 Calculation of Correction Masses

If $m = n$, (i.e. the number of correction planes equals to the number of measurement locations) the influence coefficient matrix is square and the residual vibration reduces, theoretically, to zero. In this case, the solution of equation (4.1.6) can be given by,

$$W = [\alpha]^{-1} * [X] \tag{4.1.8}$$

$$\begin{bmatrix} W_1 \\ W_2 \\ . \\ . \\ . \\ W_m \end{bmatrix} = \begin{bmatrix} \alpha_{11} & \alpha_{12} & . & . & . & \alpha_{n1} \\ \alpha_{21} & \alpha_{22} & . & . & . & \alpha_{2n} \\ . & . & . & . & . & . \\ . & . & . & . & . & . \\ . & . & . & . & . & . \\ \alpha_{m1} & \alpha_{m2} & . & . & . & \alpha_{mn} \end{bmatrix}^{-1} * \begin{bmatrix} -X_1 \\ -X_2 \\ . \\ . \\ . \\ -X_m \end{bmatrix} \tag{4.1.9}$$

in this case,the influence-coefficient matrix $[\alpha]$ must be inverted to $[\alpha]^{-1}$. To do this, the matrix must be square and nonsingular. This means that *m* must equal *n*, or the number of data points must equal the number of correction planes. If balancing done at a single speed *(h=1)*, m=*n*, and the number of transducers must equal the number of correction planes. If more data is acquired than is necessary, the data set is modified to make m=*n*, or the additional data is retained and a least squares is applied, usually to the speeds, to obtain an optimum balance.

If $m > n$, (i.e. there are more measuring locations than correction planes), the vibration errors may be reduced to a minimum and this is usually done by applying a least-squares solution whose general form is given by the following expression,

$$\begin{bmatrix} W_1 \\ W_2 \\ . \\ . \\ . \\ W_m \end{bmatrix} = \left(\left[\begin{bmatrix} \alpha_{11} & \alpha_{12} & . & . & . & \alpha_{n1} \\ \alpha_{21} & \alpha_{22} & . & . & . & \alpha_{2n} \\ . & . & . & . & . & . \\ . & . & . & . & . & . \\ . & . & . & . & . & . \\ \alpha_{m1} & \alpha_{m2} & . & . & . & \alpha_{mn} \end{bmatrix}^T * \begin{bmatrix} \alpha_{11} & \alpha_{12} & . & . & . & \alpha_{n1} \\ \alpha_{21} & \alpha_{22} & . & . & . & \alpha_{2n} \\ . & . & . & . & . & . \\ . & . & . & . & . & . \\ . & . & . & . & . & . \\ \alpha_{m1} & \alpha_{m2} & . & . & . & \alpha_{mn} \end{bmatrix} \right]^{-1} * \begin{bmatrix} \alpha_{11} & \alpha_{12} & . & . & . & \alpha_{n1} \\ \alpha_{21} & \alpha_{22} & . & . & . & \alpha_{2n} \\ . & . & . & . & . & . \\ . & . & . & . & . & . \\ . & . & . & . & . & . \\ \alpha_{m1} & \alpha_{m2} & . & . & . & \alpha_{mn} \end{bmatrix}^T * \begin{bmatrix} -X_1 \\ -X_2 \\ . \\ . \\ . \\ -X_m \end{bmatrix}$$

$$W = [\alpha^T * \alpha]^{-1} [\alpha]^T * [X] \tag{4.1.10}$$

Where $[\alpha]^T$ is the conjugate transpose of matrix $[\alpha]$. This method of solution may leave specific vibration readings higher than desired. That is the set of correction masses, which minimizes the sum of squares, or similarly the root mean square, of the residual vibration. The expected residual vibration can be calculated by substituting Equation (4.1.10), or the

numerical result of that equation, into Equation (4.1.6). While this least squares procedure provides for a minimization of the sum of the squares of the residual vibration amplitudes, it does not ensure that none of the individual residual vibration measurements remains large. In fact, it is not unusual for one or two of the vibration readings to retain quite large values, while the remainders are reduced substantially. If this situation is undesirable and it is preferred to minimize the maximum residual amplitude (i.e., the largest element of x), an iterative procedure may be used, which is developed by Goodman (1964). In general, this procedure tends to equalize the elements of x at the expense of the root mean square average of these elements.

4.1.7 Elimination of Non-Independent Balancing Planes

The unintentional use of non-independent balancing planes can result in singular, or near singular, influence coefficient matrices. Due to noise in the vibration data signals and the effect of other unbalanced modes, it is virtually impossible for the influence coefficient matrix to be exactly singular. However, this matrix can be near singular, in which case the data would not be rejected, but would often result in the calculation of fairly large correction masses, which essentially cancel each other.

The influence coefficient balancing calculations are prone to certain numerical difficulties when non-independent balancing planes are inadvertently used, resulting in impractical, counteracting correction masses being calculated. This occurs as a result of the influence coefficient matrix being ill conditioned. That is, at least one of the columns of the matrix is close to being linearly dependent on the remaining columns.

It is possible to anticipate and avoid this problem by evaluating the independence of the columns of the influence coefficient matrix. If this matrix is found to be ill conditioned, it is necessary to identify and eliminate the least independent of the balancing planes. This can be done by means of a Gram- Schmidt orthogonalization procedure for optimizing balancing plane selection. Darlow (1980).

From the mathematical theory when there exists non-independent columns in an influence coefficient matrix $[\alpha]$ the matrix is singular and the solution vector becomes infinite. When

there exists a nearly non-independent column in matrix $[\alpha]$, Equation (4.1.7) is ill conditioned. Moreover, the more the non-independence, the more serious the ill conditioning will be.

4.1.8 Principal Advantages Of Influence Coefficient Balancing

It is an entirely empirical procedure, which requires minimal prior knowledge of the dynamics of the rotor system.

- It is readily computerized and automated.
- It provides for least-squares minimization of data from any number of vibration sensors.
- Data manipulation techniques have been developed which compensate for measurement errors.
- It does not require a high degree of expertise.

4.2 The Modal Balancing Method

The modal balancing method is based on the orthogonal properties of rotor-bearing systems. The orthogonality principle states that the total kinetic or potential energies in a system where the corresponding sums have the kinetic or potential energies of each component vibration. This means that a rotor vibrating in one of its principal modes will not excite vibration in any other mode. So that, the orthogonality principle allows the use of correction masses such that only the energy contents in one mode is affected Goodwin (1989).

Further details of the application of the modal balancing method may be obtained from Moore and Dodd (1964), Lindley and Bishop (1963), and Bishop and Gladwell (1959). Noteworthy contributions have also been provided by Parkinson and Bishop (1965), Bishop and Mahalingham (1966) and Parkinson (1966). More reviews of the method have been given by Rieger (1982,1986), Rao (1983), and Kellenberger and Rihak (1988).

4.2.1 Modal Balancing Theory

For convenience, assume all the unbalance to be distributed in the y-x plane (ie, a 2D problem). This allows decoupling of y and z modes (ie, a 3D problem) and the discussion will be limited to only x-y plane Rao (1991). The deflected shape of the rotor at any speed can be expressed in modal series as

$$y(x) = \sum_{i=1,2,..} \phi_i Y_i(x) \tag{4.2.1}$$

Where $Y_i(x)$ are mode shapes and ϕ_i are arbitrary parameters. If $y(x)$ is measured at a given speed, ϕ_i can be determined by using the orthogonal principle as

$$\int_0^l y(x)m(x)Y_i(x)dx = \int_0^l \phi_i Y_i^2(x)m(x)dx = \phi_i M_i$$

or

$$\phi_i = \frac{1}{M_i}\int_0^l y(x)m(x)Y_i(x)dx \tag{4.2.2}$$

In the above $m(x)$ is mass distribution of the rotor and M_i is generalized mass in i^{th} mode. The mass eccentricity in the rotor is expressed in the modal series as follows:

$$a(x) = \sum_{i=1,2,..} \alpha_i Y_i(x) \tag{4.2.3}$$

Therefore, the unbalance distribution of the rotor (Figure. 4.3), can be expressed as

$$U(x) = \sum_{i=1,2,..} \lambda_i Y_i(x) \tag{4.2.4}$$

To determine α_i, in equation (4.2.3), we use the principle of virtual work (Virtual work is the work done by a real force acting through a virtual displacement or a virtual force acting through a real displacement). The virtual displacement of the rotor, at the given rotational speed is

$$\delta y = \sum \delta\phi Y_i(x) \tag{4.2.5}$$

The work done by the centrifugal forces during i^{th} mode virtual displacement is

$$W_{ce} = \int_0^l m(x)\omega^2[y(x)+a(x)]\delta\phi_i Y_i(x)dx \tag{4.2.6}$$

Using equations (4.2.1) and (.4.2.3) in the above, we get by using orthogonality principle, the following:

$$W_{ce} = \delta\phi_i M_i \omega^2(\phi_i + \alpha_i) \tag{4.2.7}$$

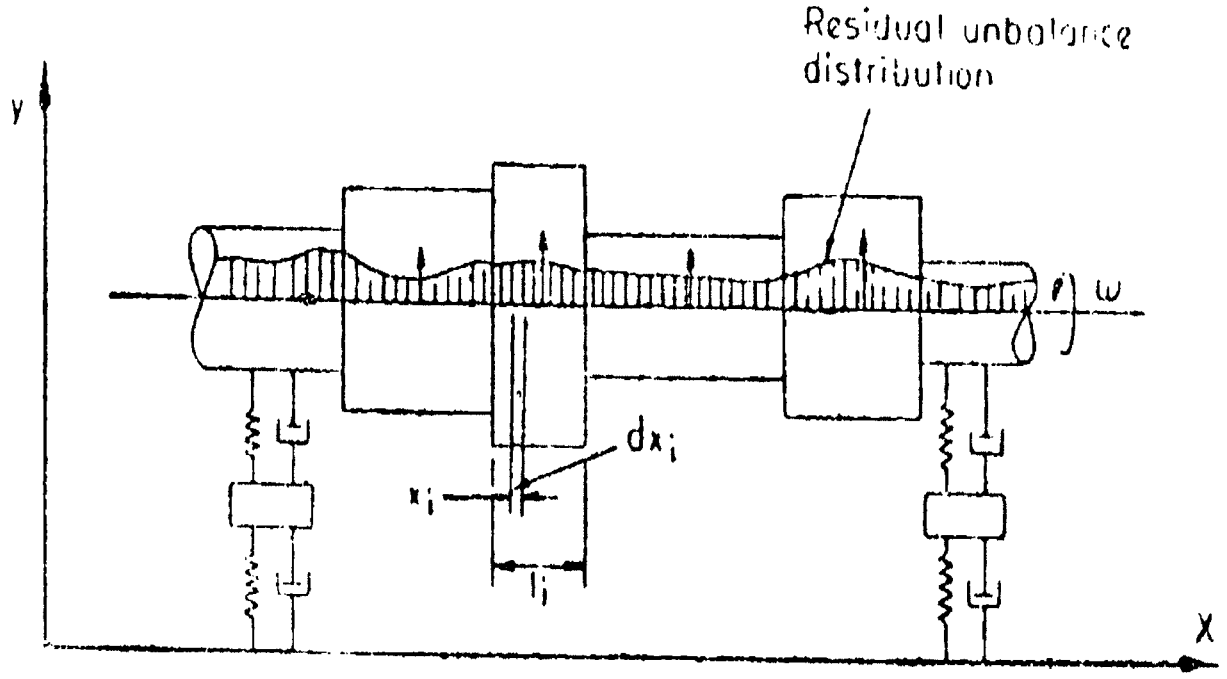

Figure 4.3 Distribution of Residual Unbalance In the Rotor Rao 1991

The strain energy stored in the shaft is

$$V = \int_0^l \frac{1}{2} EI(x)\left\{\sum \phi_i Y_i''(x)\right\}^2 dx = \frac{1}{2}\sum_{i=1,2,..} \phi_i^2 K_i \tag{4.2.8}$$

In equation (4.2.8), K_i is i^{th} mode-generalized stiffness of the rotor. work done by the elastic force in the virtual displacement of i^{th} mode is

$$W_{el} = -\frac{\partial V}{\partial \phi_i}\partial\phi_i = -\partial\phi_i \phi_i K_i \tag{4.2.9}$$

Since $\omega_{ce} + \omega_{el} = 0$, we get

$$\phi_i = \frac{\omega^2 M_i \alpha_i}{K_i - \omega^2 M_i} \tag{4.2.10}$$

From equation (4.2.10), we obtain

$$\alpha_i = \frac{1-\left(\omega^2/\omega_{in}^2\right)}{\left(\omega^2/\omega_{in}^2\right)}\phi_i \tag{4.2.11}$$

λ_i In the equation 4.2.4 can be evaluated by using orthogonalty principle

$$\lambda_i = \frac{1}{M_i}\int_0^l U(x)m(x)y_i(x)dx \tag{4.2.12}$$

In the above, $U(x)$ is evaluated from (Figure. 4.3), using $a(x)$ from equation (4.2.3) with the help of equations (4.2.11) and (4.2.2).

Let $p(x)$ be the balance distribution required in the i^{th} mode. We can express $p(x)$ in modal series as

$$p(x) = \sum_{i=1,2,} \beta_i Y_i(x) \tag{4.2.13}$$

Then

$$\beta_i = \frac{1}{M_i} \int_0^l p(x) m(x) Y_i(x) dx \tag{4.2.14}$$

For balance condition,

$$p(x) + U(x) = 0 \tag{4.2.15}$$

in the i^{th} mode,

$$\beta_i Y_i(x) + \lambda_i Y_i(x) = 0$$

i.e.,

$$\beta_i = -\lambda_i \tag{4.2.16}$$

from equations 4.2.12 and 4.2.14, we got

$$\int_0^l p(x) m(x) Y_i(x) dx = -\int_0^l U(x) m(x) Y_i(x) dx \tag{4.2.17}$$

If we choose to correct the unbalance by one mass w_c at radius a_c at plane x=c, and letting

$$U(x) \approx m(x) + a(x) \tag{4.2.18}$$

We get,

$$w_c a_c m(c) Y_i(c) = -\int_0^l m^2(x) a(x) Y_i(x) dx \tag{4.2.19}$$

Therefore

$$w_c = \frac{-\int_0^l m^2(x)a(x)Y_i(x)dx}{a_c m(c)Y_i(c)} \qquad (4.2.20)$$

Hence, to balance i^{th} mode, we need the following data:

$m(x)$ Mass distribution of rotor

w_{in} Critical speed.

$Y_i(x)$ Mode shape.

$y(x)$ Measured mode shape near critical speed

Then, we use equation (4.2.2) to determine ϕ_i equation (4.2.11) to determine α_i equation (4.2.3) to determine $a(x)$ and equation (4.2.20) to determine w_c.

In practice the theory described above becomes complicated and except for mass distribution $m(x)$, which can be well determined from the geometry of the rotor, the rest of the quantities cannot be accurately determined. The interaction between the two planes of bending during whirl also plays an important role.

A practical procedure to balance the rotor by modal correction, masses equal in number to the flexible mode shapes, (N), known as (N) plane method is as follows Bishop (1982).

Run the rotor to a safe speed approaching the first critical speed and record the bearing vibrations. Choose an appropriate location for the trial mass. For the first critical speed, this should be roughly in the middle for a symmetrical rotor in its axial distribution of mass. Record the readings at the same speed as in the previous run.

Using the above two readings, the correct mass and location can be determined using the equations described. With this correction mass, it should be possible to run the rotor through the first critical speed without considerable vibration.

Next, run the rotor to a safe speed approaching the second critical speed, if the operating speed is near second critical or above the second critical speed. Note the readings. Add a pair of trial masses 180° apart in two planes, without affecting the first mode. Note the readings at the same speed near the second critical. From the two readings we can determine the correction masses required.

Instead of N plane correction, Kellenberger (1972) suggests that the rotor should be corrected in (N + 2) planes, so as not to disturb the rigid body balance. Guidance for the location of trial masses, for a rotor with symmetric distribution of mass along its axis, is shown in Figure (4.4), for the rigid body modes and flexural modes

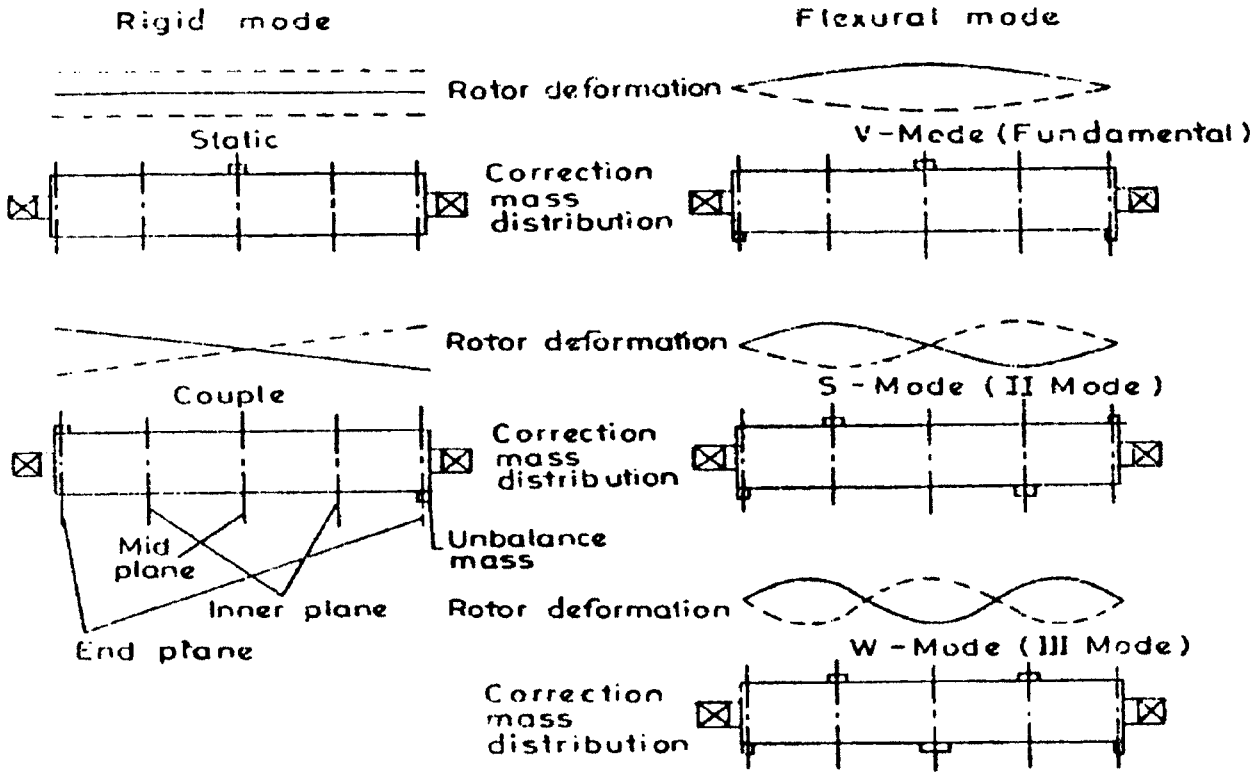

Figure 4.4 Rotor Mode Shape And Correction Masses Rao (1991)

4.2.2 Advantages and Limitations of Modal Balancing

Specific advantages and disadvantages may be identified with modal balancing, relative to the influence coefficient method. According to the requirements of a particular balancing situation, these advantages and disadvantages, as specified below take on different relative importance. The principal advantages of modal balancing are Darlow (1980):

- The number of sensitivity runs required at the highest balancing speed is minimized.
- Good sensitivity at the highest balancing speed can always be achieved.
- Balancing of a specific mode is provided and not affecting previously balanced modes.

Modal balancing does, of course, assume that the response of the rotor system is linear and that the vibration sensors are sufficiently accurate as also required by the influence coefficient method.

The principal disadvantages of modal balancing are Darlow (1989):

- The assumption of planar modes of vibration inherent in modal balancing may not be valid for systems with substantial damping or bearing cross coupling effects.
- For most (but not all) applications of modal balancing, accurate prior knowledge of the dynamics of the rotor system is required.
- Effective use requires a high degree of operator insight (i.e., requires a highly skilled operator).
- Balancing results are generally based on the vibration measured by only one or two sensors for a particular mode, which may not result in a uniformly well-balanced rotor.
- Modal balancing is usually not automated and is not easily used in production applications.

Chapter 5

EXPERIMENTAL SET-UP

5.1 Introduction

This Chapter is structured in various sections, which will cover the entire instrumentation and the equipment used in the entire research.

5.2 Methodology

A computer algorithm was developed to improve the balancing method. The computer algorithm was implemented for experimental verification, by using a high level technical language called Matlab.

The experiments involved balancing a rotor on a horizontal rig. The test rig had multi-rotors, which were supported by six hydrodynamic bearings. The test rig was designed specially for rotor dynamic studies, in particular for unbalance identification.

The rig was connected to a computer system via a data acquisition card in order to pick up transducer signals. The primary goal of this work was to design and apply a measurements and data acquisition system to provide the data required for the purpose of the current study Figures (5.1,5.2)

Figure 5.1 Over View of Rig And Its Foundation

5.3 The Experimental Rotor Rig

The experiment system was designed previously although no document had been written to describe the rig. In this study, the rig has been updated. The whole apparatus is mounted on rigid steel foundation as shown on Figure 5.1. The rig has a sump tank (3.40 m long, 0.44 m wide and 0.25 m high). It also has a protection cover of dimensions 3.60m long, 0.45m wide and 0.73 m high for safety reasons and also to prevent the lubricant liquid escaping from the sump tank. Details of the rig are described in this chapter for easy understanding and for completeness

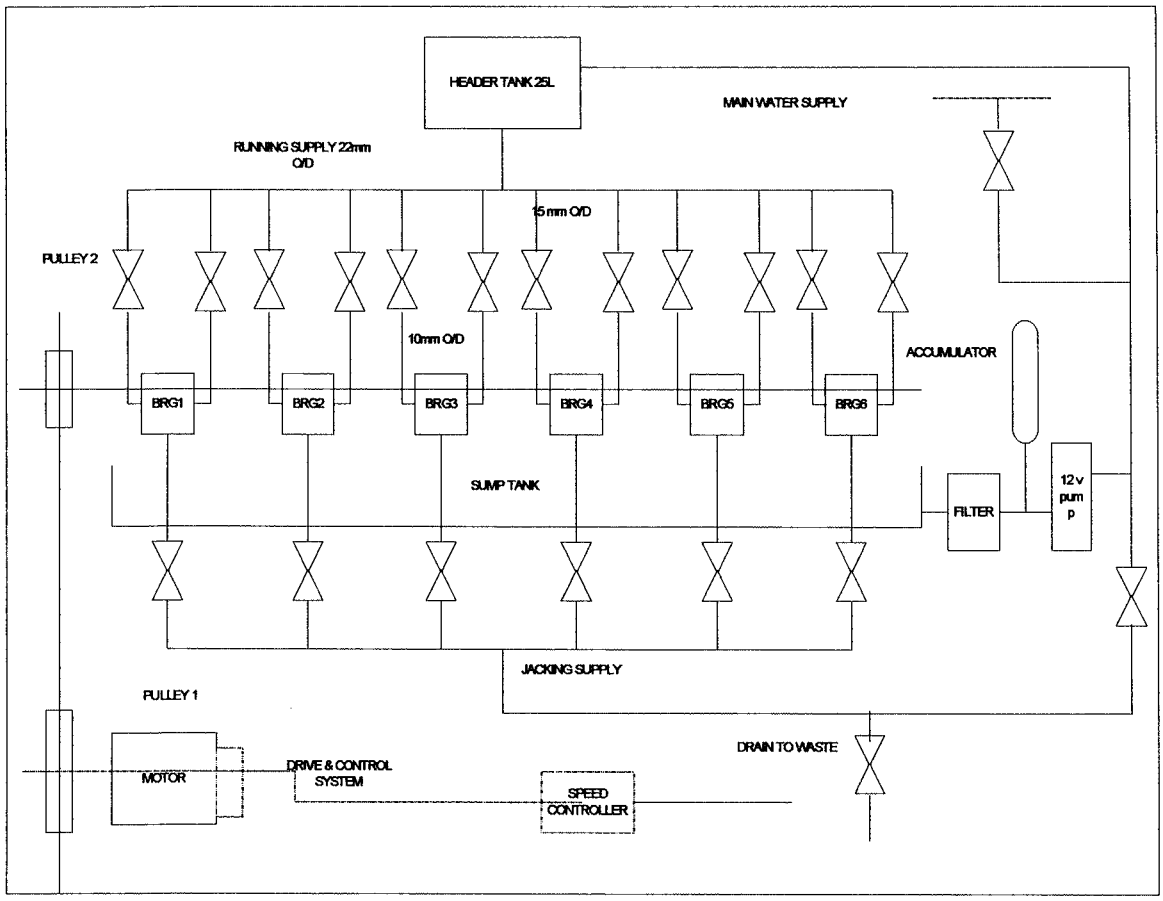

Figure 5.2 Overall View of The System

5.4 Rotor Design

The test rotor was designed to run up to speeds of 6000 rpm, which was above the first two critical speeds which are $\omega_{n1} = 1250 rpm$ and $\omega_{n2} = 2650 rpm$. The rotor consisted of the three sub-rotors as shown in Figure 5.3, which represent a high-pressure Turbine Rotor, a Low-pressure Turbine Rotor and a Generator Rotor.

12 radial holes were drilled 10mm deep also tapped to take 6mm screws in each balancing planes. In the High-pressure Turbine Rotor there are three balancing planes; for the Low-pressure Turbine Rotor five balancing planes and for Generator Rotor eight balancing planes. Details of the rotors are listed in Tables (5.1-5.3).

Figure 5.3 Overview of the three rotors

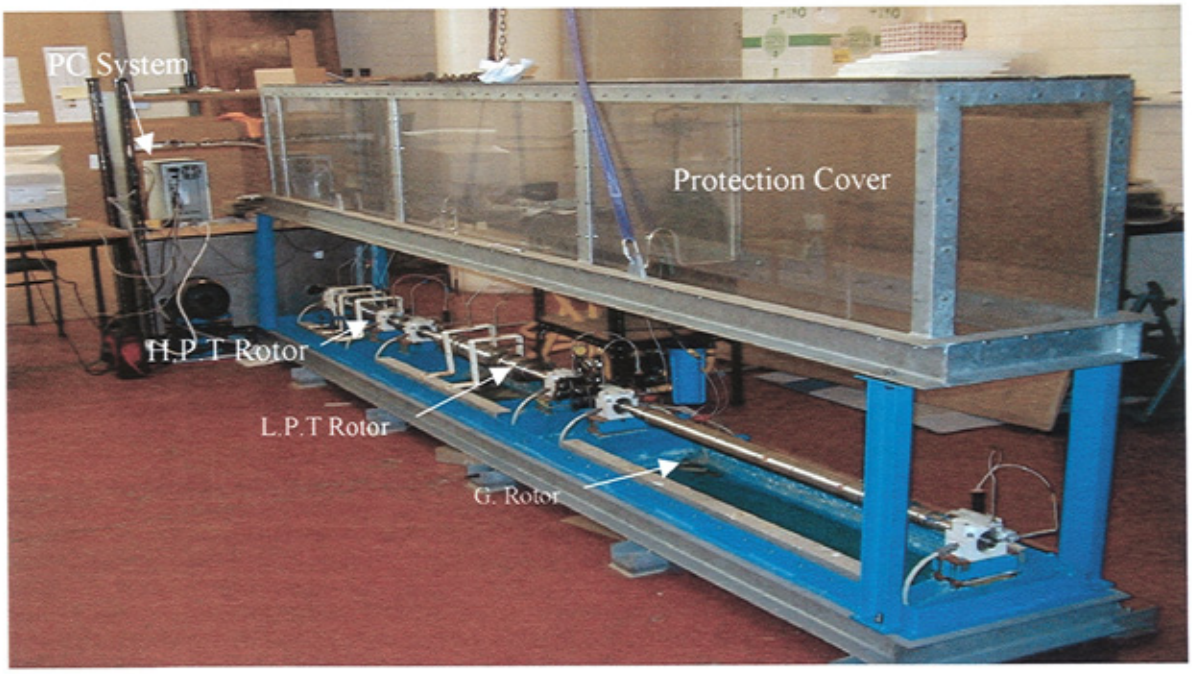

Figure 5.4 Overview of the Experimental System

H.P.T Rotor					
Section No.	**Length (mm)**	**Outside Diameter (mm)**	**Section No.**	**Length (mm)**	**Outside Diameter (mm)**
1	12.36	67.57	19	10	84
2	54.49	51.5	20	10	86
3	15.77	53.66	21	10	88
4	15.77	53.66	22	10	90
5	13.29	51.28	23	10	92
6	3.1	56.48	24	10	94
7	6.35	50.8	25	10	84
8	3.1	53.14	26	10	82
9	6.35	50.8	27	10	46.9
10	3.1	53.14	28	10	45.2
11	17.27	53.56	29	10	48.64
12	10	72	30	30.1	50.2
13	10	72	31	17.27	53.56
14	10	74	32	30.1	50.2
15	10	76	33	12.73	56.78
16	10	78	34	8.26	69.28
17	10	80	35	8.26	68.33
18	10	82	**Total length Weight**	**10.1 kg**	

Table 5.1 H.P.T rotor Dimensions

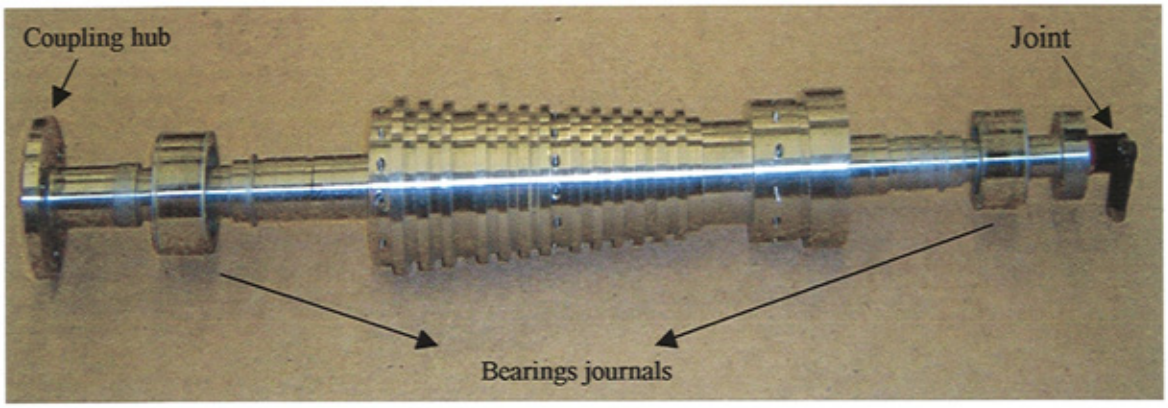

Figure 5.5 Overview of the H.P.T rotor

L.P.T Rotor					
Section No.	**Length (mm)**	**Outside Diameter (mm)**	**Section No.**	**Length (mm)**	**Outside Diameter (mm)**
1	10.59	71.18	26	19.5	79.5
2	77.86	28.79	27	11.21	82.15
3	26.8	30.42	28	10.71	86.45
4	32.85	24.05	29	6.31	88.97
5	18.17	29.9	30	7.25	89.98
6	5.09	31.25	31	12.71	84.99
7	15.12	32.13	32	9.57	86.55
8	5.09	31.25	33	21.14	79.5
9	15.12	32.13	34	23.14	73.82
10	31.65	34.74	35	16.85	94.5
11	16.34	66.16	36	33.44	63.75
12	27.44	55.55	37	27.59	94.5
13	42.26	97.57	38	54.44	59.23
14	54.44	59.23	39	42.26	97.57
15	27.59	94.5	40	27.44	55.55
16	33.44	63.75	41	16.34	66.16
17	16.85	94.5	42	31.65	34.74
18	23.14	73.82	43	15.12	32.13
19	21.14	94.5	44	5.09	31.25
20	9.57	86.55	45	15.12	32.13
21	12.71	84.99	46	5.09	31.25
22	7.25	89.98	47	18.17	29.9
23	6.31	88.97	48	32.85	24.05
24	10.71	86.45	49	26.8	30.42
25	11.21	82.15	50	77.86	28.79
			51	10.59	71.18
			Total length	**1136.98**	
			Weight	**33.822 kg**	

Table 5.2 Dimensions of the L.P.T rotor

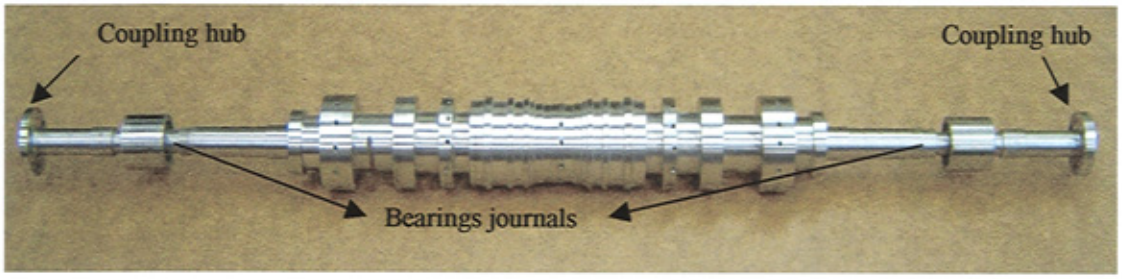

Figure 5.6 Overview of the L.P.T rotor

Generator Rotor		
Section No.	**Length (mm)**	**Outside Diameter (mm)**
1	16.82	71.41
2	61.58	41.47
3	99.35	26.8
4	10.62	31.54
5	37.58	26.69
6	28.7	33.80
7	32.04	46.02
8	16.73	41.2
9	51.32	54.26
10	55.97	56.55
11	750	58.54
12	16.73	41.2
13	32.04	46.02
14	28.7	33.80
15	37.58	26.69
16	10.62	31.54
17	99.35	26.8
18	61.58	41.47
19	16.82	71.41
Total length	**1464.13**	
Weight	**17.589 kg**	

Table 5.3 Dimensions of The G. rotor

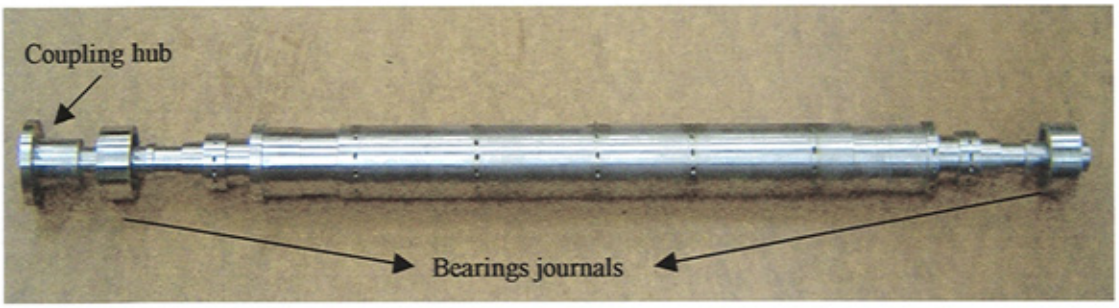

Figure 5.7 Overview of the G. rotor

5.5 Drive System

The test rig is driven by a 3-phase 'Brook Crompton',(3.0 kW) motor, which has an operation speed (rated speed) of 60 Hz (3600 rpm), with an ABB ACS 200 variable speed controller, see Figure (5.8). At the end of the motor there is a pulley to drive the shaft through a belt to step-up the speed with a ratio (i.e. gear ratio) equal to 4, which is adequate for the purpose of testing (6000 rpm). Both the rig pulley and the motor are mounted in a metal foundation. Figure (5.9) shows the over view of the driving system.

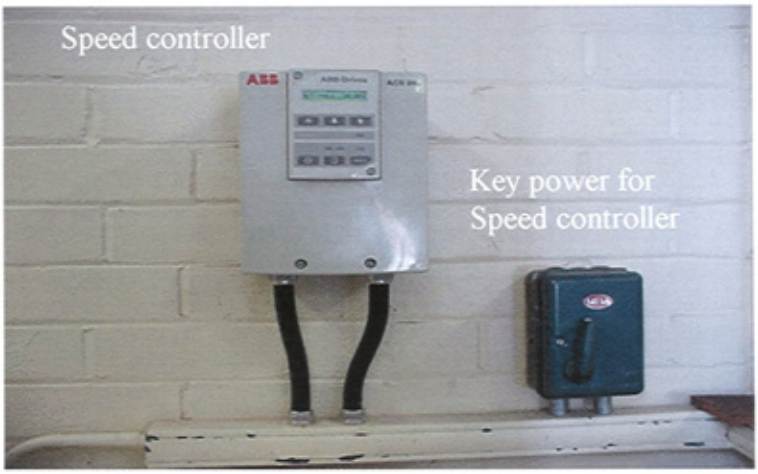

Figure 5.8 Speed Controller

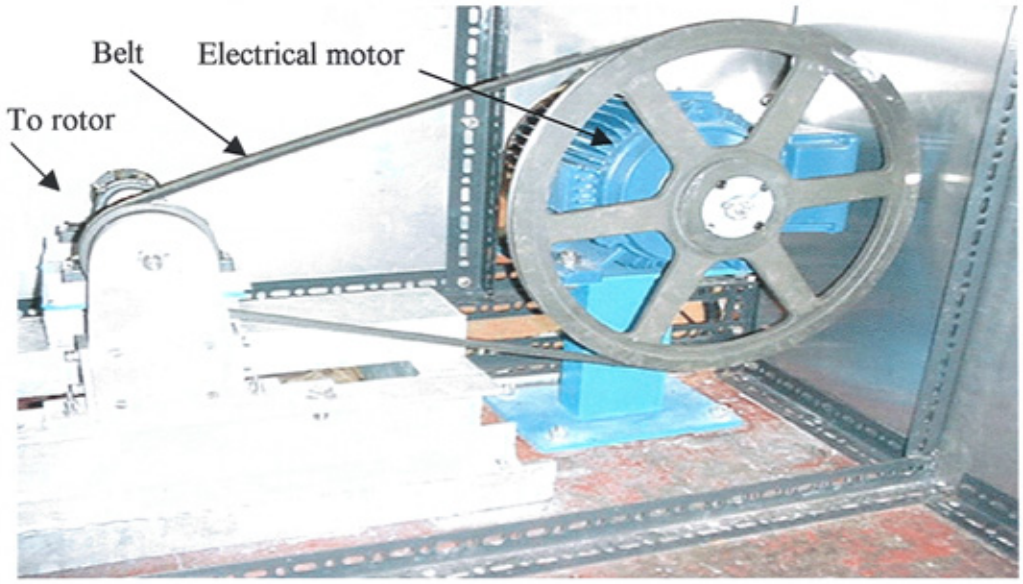

Figure 5.9 Driving System

5.6 Instrumentation and Other Equipment

Flexible couplings were used to connect the drive to the rotor to eliminate any motor induced vibrations. Water (domestic main bearings with pressure head of up to 34.5×10^5 N/m^2 (50 psi)) is used to lubricate the. The water is first passed through a filter to remove debris and then supplied to a header tank, which can accurately maintain the correct supply pressure. The height of the header tank can be adjusted from 0 mm to 850 mm (i.e 0-8339 N/m^2) above the level of the supply line to the bearings as showed in Figure (5.10). The typical pressure head used was 50 mm (i.e 4905 N/m^2). The flow to the bearings is through transparent piping. The transducers are operated by ABB supplier 27.5 volt for the transducers and 13.5 volt for the optical switch. The operating range of the displacement transducers is 0-1.25 mm with a resolution of 0.001 mm. The transducer was capable of measuring the amplitude of the bearing journals during the operation.

Figure 5.10 Lubrication Systems

5.7 Data Acquisition and Signal Processing

A new data acquisition system has been developed in this study. The system detailed above requires frequency-based measurements of the rotor response measured at selected locations along the rig. The transducer measurements are taken at each bearing in both the horizontal and vertical directions. These general-purpose Bently Nevada (3300 RAM) proximity transducer systems are advantageous for the present study due to their small size and low mass. In order to perform the signal processing required for the experiments, a reference signal is necessary. A colour mark sensor provided this reference. The signal from the marker allows the angular position of the rotor to be known relative to a selected location on the shaft. The rotation of a single mark on the rotor, which is detected by an optical switch, provided a once-per-revolution output pulse.

5.8 Data Acquisition

In many industrial applications the use of PC-based data acquisition (DAQ) systems is very desirable. The principal functions for the system to perform in this instance were to collect and store the data from the transducers and optical switch signals produced throughout this period, at a user-defined sample rate. With these specifications in mind, a National Instruments PCI-6024 PC-based DAQ card, together with the corresponding signal connection board and cabling are chosen, see Figures (5.11,5.12). This high-performance (DAQ) card has 16 single-ended or 8 differential analogue input channels (16 single-ended used in this case) (see appendix 7), with 12-bits resolution and a maximum collective sampling rate of 4096 Hz. Software-selectable gain permitted input voltage ranges of between -10V and +10 V. single-ended mode allows for all of the channels to reference the same ground.

The DAQ system was integrated into a Pentium III 550 M PC, with 128 MB of RAM and 7.0 GB of hard-disk space via a 68-pin male SCI-II type cable connection. The DAQ driver software (NI-DAQ) supplied with the card had to be used. All of the functions required to operate the card were contained in the NI-DAQ, including routines for analogue input, data acquisition and analogue output. There was a choice of programming languages that could

be used to create the application using the NI-DAQ function, in this case Matlab 5.3 was chosen. It was necessary for all of the transducer and optical switch data to be stored to the hard disk on the PC for record keeping purpose.

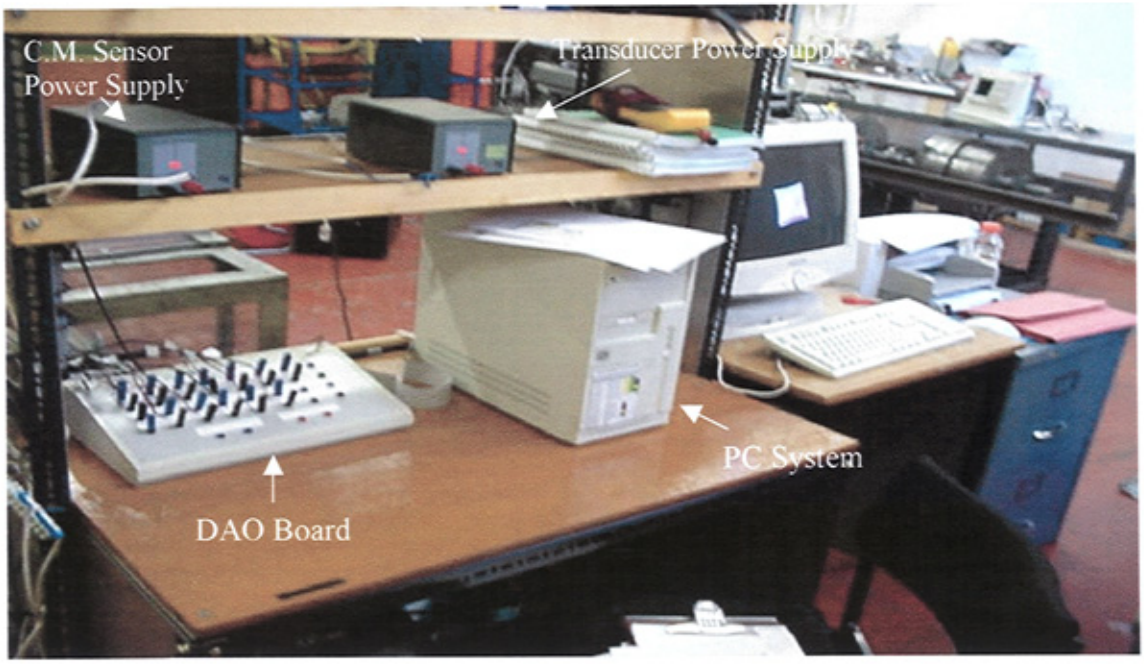

Figure 5.11 Experimental Computer System Facilities

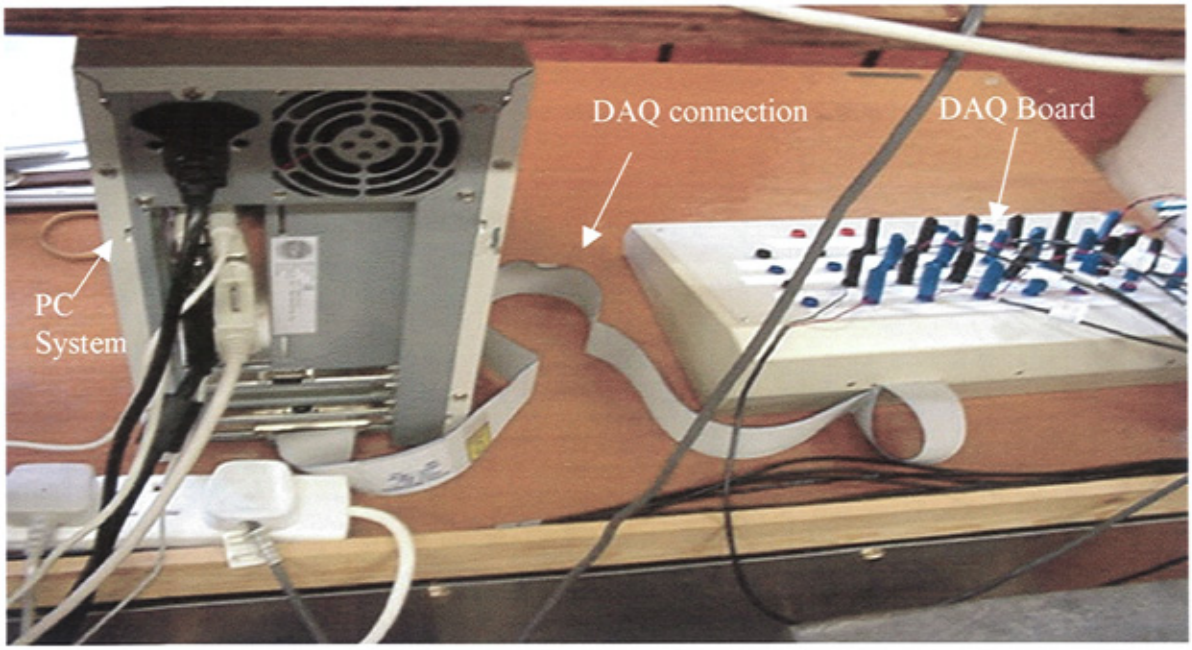

Figure 5.12 DAQ Board and its Connection To the computer system

5.9 Vibration Amplitude Measurements

The relative displacement between the shaft and test bearing was measured with eddy-current displacement probes. Bently Nevada 3300 RAM proximity transducers type as shown in Figure (5.13), all the transducers are calibrated and the results achieved were almost identical to the results supplied by the manufacture. Measurements were taken at all bearings in both the horizontal and vertical directions. The performance of these transducers was found sufficient for this application. These transducers were mounted using stainless steel trade screws allowing the transducers to be removed when necessary. In this case, the gain was set so that the maximum reading did not exceed ± 10 V, which was the upper limit of the input voltage into the data acquisition system. Figure (5.14) shows the power supply for the transducers. The specifications of the probes are shown in appendix 7.

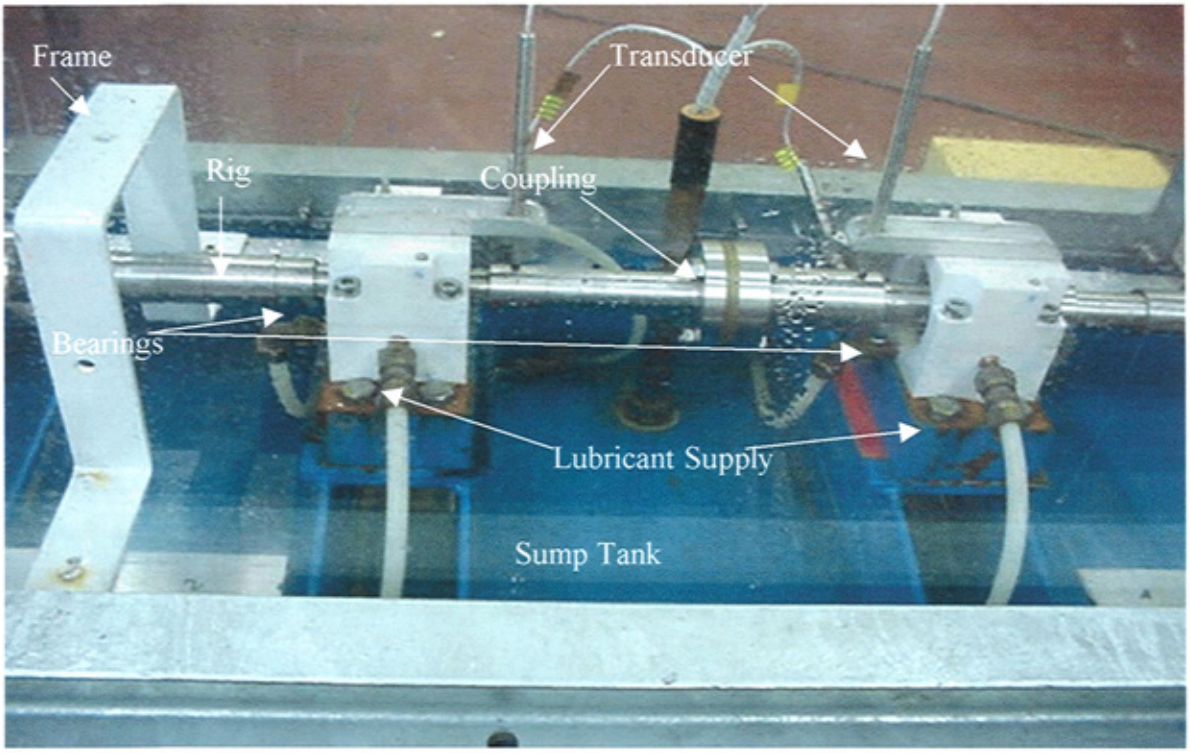

Figure 5.13 Rotors Connections

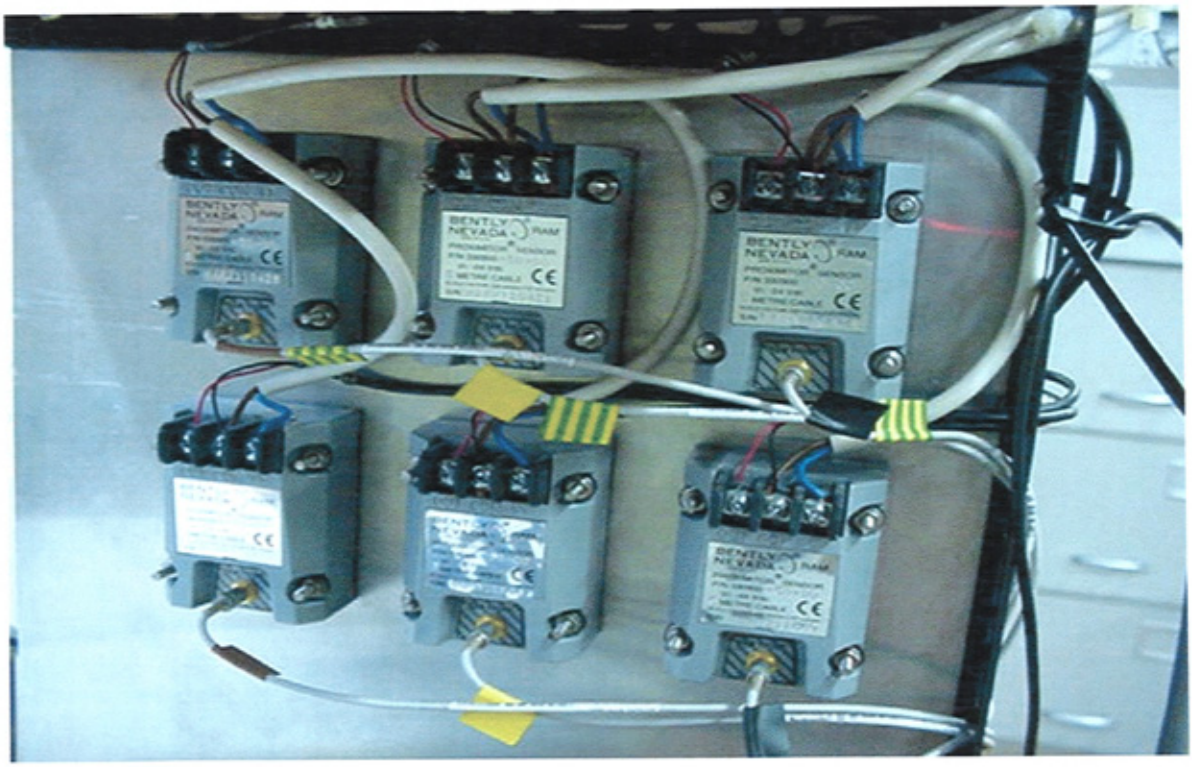

Figure 5.14 Transducers Power Supply

5.10 Phase Angle Instrument

In order to perform the signal processing required for these experiments, a reference signal was necessary. This reference signal see Figure (5.15), is provided by a "Colour Mark Sensor" signal, which allows the angular position of the rotor to be known relative to a selected location on the shaft. The OMRON E3M-VG Colour Mark Sensor (an optical switch) (see specification shown in appendix 7) was powered by a 13.5V supply, and provided an output pulse of almost 9V upon the passing of the edge of the mark, returning to 0V once the mark had passed the sensor. In this way, the optical switch sensors provided a once-per-revolution pulse. The sensor had a detecting distance of 2.0 mm.

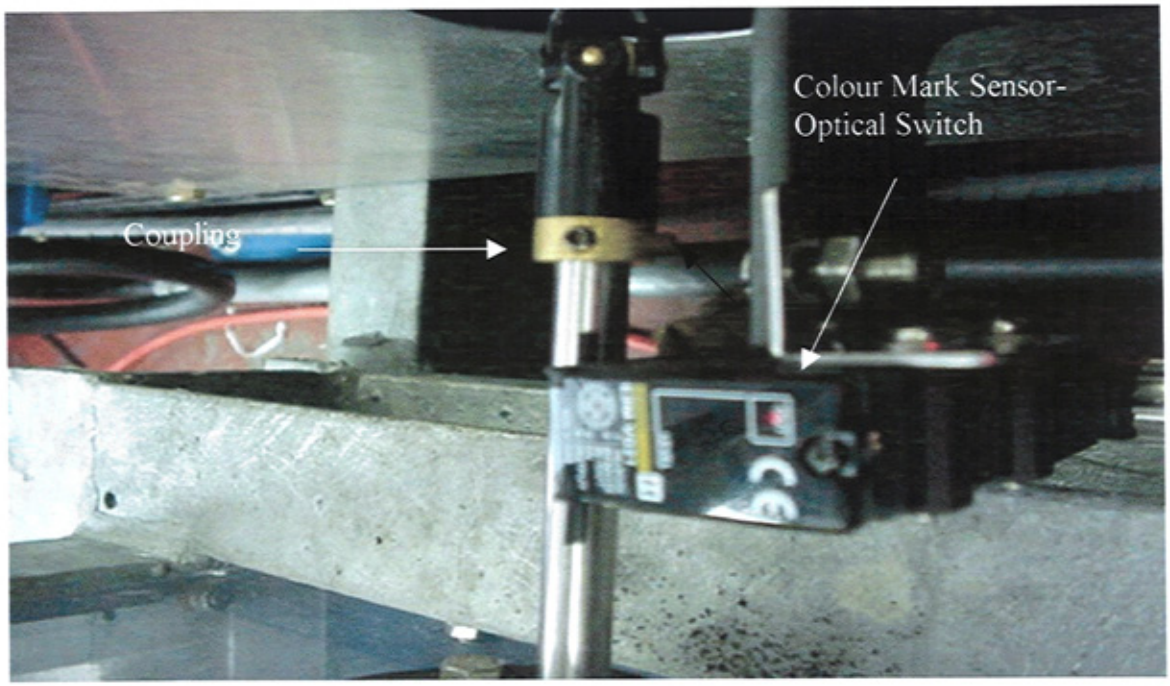

Figure 5.15 Colour Mark Sensor

5.11 Trial and Balance Weights

Most balancing procedures require a trial mass to be installed into the rotor to measure how the rotor will respond to this weight. This weight induced a different balance condition with an accompanying change in the vibration level and/or phase angle. This change, once introduced into balance calculations, dictated how much weight would be required to be added and the radial location for the correction mass placement. If the vibration levels were not acceptable after a trial/correction mass was placed on the rotor, a further weight called a 'trim' weight can be installed. Sometimes this weight will be required to be located at a slightly different location than the previous weight. Trial, balance, and trim weights may be made from any material. Common materials were bolts, washers, or C-clamps. Some machines would require imagination to devise an attachment method. Other machines, such as turbomachinery, had balance weight holes provided which may require some machine disassembly to access them. All weights, regardless of material or attachment method, must be held rigidly in place. This may be accomplished by e.g. welding. Relying on a bolt and nut with split washer should not be considered. If a bolt and nut configuration was used the bolt should have its threads staked to prevent the nut from shifting. A SC-300 SOLEX

digital weighting scale with capacity of 600 X 0.1g (1.2 X 0.0002lb) was used to measure the trial and correction masses.

5.12 System Development

Mechanically and instrumentally improvement on the finished experimental system comprised;

- Drilling more holes in the shaft, (16 planes with a hole 30° around the shaft).
- Fixing an optical switch (phase angle instrument) in the couplings.
- Fabricating a moveable frame, which allowed the author to measure the vibration amplitude at any position on the shaft.
- Modification the optical switch diagrams in the connection circuit figure 5.16. In order to work with the 13.5V power supply, the improvement was made by adding a 2-X-2.2 Ohm resistance connected in series.

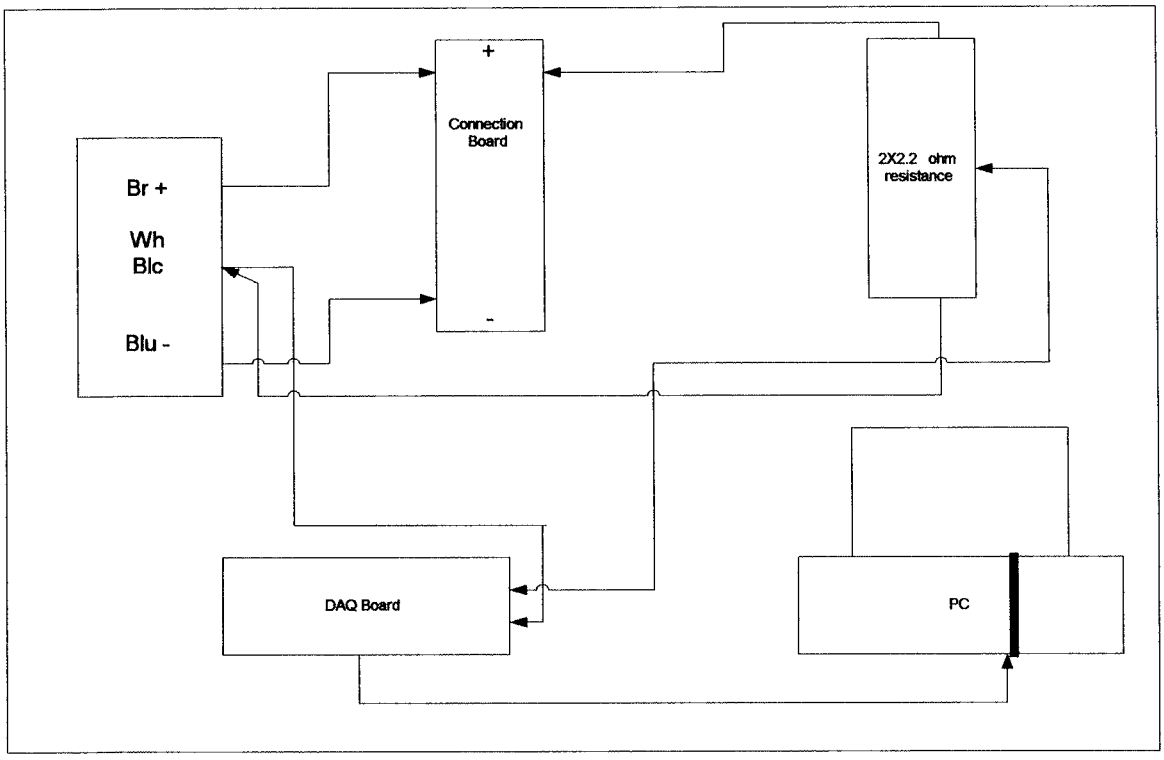

Figure 5.16 Colour Mark Sensor Modified Connection Board

5.13 Shaft Alignment Equipment

An OPTALIGN PLUS laser equipment figure 5.17 was used to measure the shaft-to-shaft alignment (bearing centreline), with the OPTALIGN PLUS PC DISPLAY software running. The optional OPTALIGN PLUS Commander program allows the user to set-up alignment jobs in advance, permanently archive measurement files, and create adaptable customized alignment reports for fulfillment of ISO quality standards, all with the convenience of Microsoft Windows on any standard PC. The alignment readings obtained can be seen and stored on the OPTALIGN PLUS laser system for reporting results. The connections of the alignment equipment to the system (HPT ⇔LPT) rotors are shown in Figures (5.18,5.19).

Figure 5.17 OPTALIGN PLUS Hand Calculator

5.13.1 The Advantage of OPTALIGN PLUS Laser Shaft Alignment

- Take alignment readings with only simple keys (OPTALIGN PLUS manual)
- Patented one-beam technology saves setup time & effort
- The industry's smallest sensors fit into tight spaces
- Patented EZ-Sweep measurement technique eliminates backlash problems

- Only one cable to connect without tangling
- Tolerance Check smiley shows
- Alignment condition at a glance
- Automated reporting
- Via direct printer connection
- Non-volatile memory stores alignment jobs, accepts advance setups from a PC.
- The hand calculator Figure (5.17) specification and the list of the standard package are shown in appendix 7.

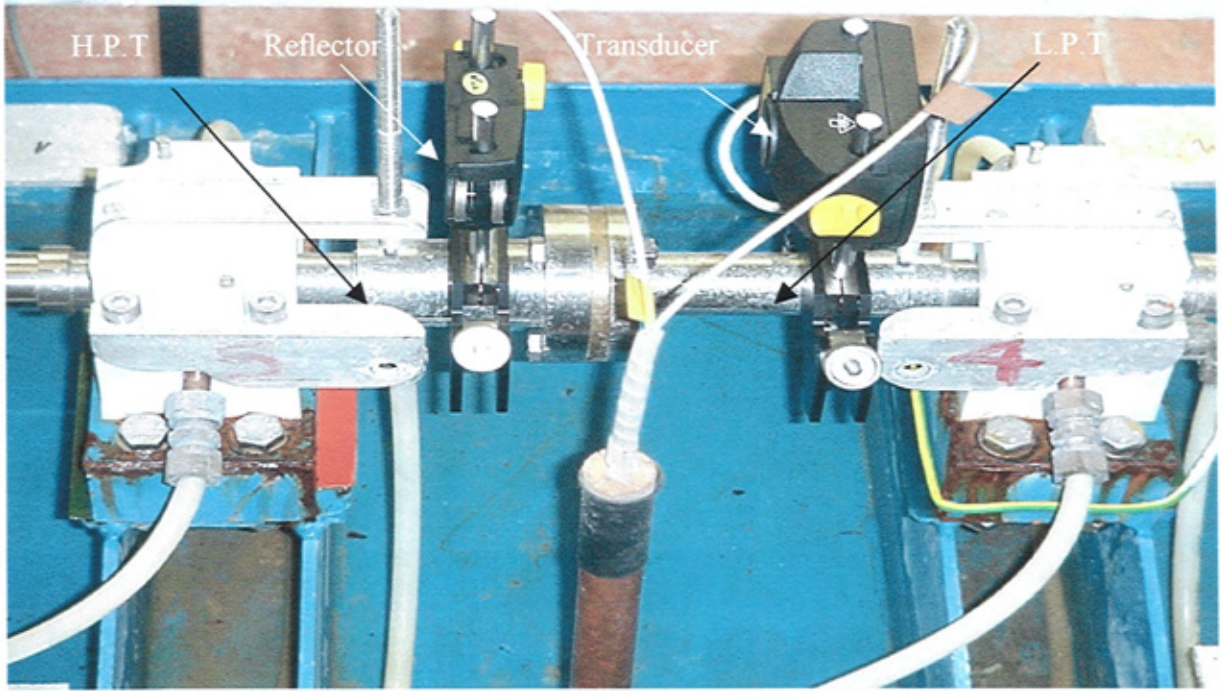

Figure 5.18 Laser Alignment Equipment Connected To The System

Figure 5.19 Overview of Laser Alignment Equipment Connotation

CHAPTER 6

INVESTIGATION OF THE MODIFIED BALANCING METHODS AND RESULTS

This chapter is divided into two sections. Section one contains the experimental investigation of the measurement errors and uncertainty and section two discusses the experimental investigation of the improvement of the trim balancing technique.

6.1 The Effect of Measurement Uncertainty on Rotor Balancing

6.1.1 Introduction

In the past few decades, the fast development of measuring technology, and particularly the use of measuring transducers and electrical data acquisition, have led to the means of measuring being highly refined. Nowadays, measurement instruments and data processing techniques are being improved very quickly because of the rapid development of computers. Most modern measurement instruments include data processing programs

Balancing of rotors has been discussed in a number of papers and the balancing techniques of flexible rotors have been almost established in the international standard (ISO 11342). On the other hand, the balancing techniques of flexible rotors which are used in the high speed rotating machines have been theoretically proposed by Bishop & Gladwell and (1959) By using these techniques, the unbalance force can be theoretically established. These techniques, however, are limited in practice because of measurement errors, thus the rotor must be balanced with the trial and error method. It is important to clear up the cause of the discrepancy and to balance the rotor easily within a specified allowance in a short time.

A measurement result is complete only when accompanied by a quantitative statement of its uncertainty. The uncertainty is required in order to decide if the result is adequate for its intended purpose and to determine if it is consistent with other similar results. Even the very best measurement methodologies for the most very well behaved metrics will exhibit

errors. Thus the primary objective of this work is to provide a methodology of the measurement accuracy of the experimental work carried in this research. The experimental researchers who develop or use such measurement methodologies, however, should attempt to:

- Minimize their uncertainties/errors
- Understand and document sources of uncertainty/error
- Quantify the amounts of uncertainty/error.

6.1.2 Accuracy, Errors and Uncertainty in Rotor Balancing Measurement

The uncertainty is an estimate of likely limits of the experimental error. It is sometimes referred to as the measurement accuracy. But accuracy is a measure of error, not uncertainty. Accuracy refers to the difference between a result and the true value.

Many different measurements were used to characterize measurement error, often making it difficult to determine which interpretation should be associated with the uncertainty.

There is no such thing as a perfect measurement. Each measurement contains a degree of uncertainty due to the limits of instruments and the people using them. The accuracy of the measurement refers to how close the measured value is to the true or accepted value

One important distinction between accuracy and precision is that accuracy can be determined by only one measurement, whilst precision can only be determined with multiple measurements. Precision refers to how close together a group of measurements actually are to each other. Precision has nothing to do with the true or accepted value of a measurement, so it is quite possible to be very precise and at the same time totally inaccurate. In many cases, when precision is high and accuracy is low, the fault can lie with the instrument.

In general, errors are viewed to have two components, a random and a systematic component. Random errors are considered to arise from unpredictable variations of influence effects and factors, which affect the measurement process, producing fluctuations in between repeated measurements in the results. Random errors cannot be compensated

for but only treated statistically. By increasing the number of repetitions, the average effect of random errors approaches zero or, more formally stated, their expectation or expected value is zero.

6.1.3 Measurement of Vibration Parameters

In order to calculate the masses and phase angles for mounting of balancing weights with high accuracy, it is necessary to measure the exact values of vibration parameters. The vibration sensor should be attached either with a magnetic coupling or threaded coupling. Before the vibration sensor is attached, it is necessary to prepare the sensor mounting surface. It is recommended to fix the vibration sensor on the same place every time when the machine is being balanced. For this reason the measurement points must be marked.

When using displacement sensors for measuring rotor deflection, the proper choice of the axial location of the sensors is very important. If the sensors are all located near rotor deflection nodes (zero displacement) the rotor may appear to be well balanced when in fact it is not. Thus, in general, proper selection and location of vibration sensors is critical to successful and efficient rotor balancing

6.1.4 Reasons of Measurements Inaccuracy

The vibration parameter measurements are one of the main sources of mistakes that prevent efficient balancing. The following mistakes are the most frequent ones:

- Incorrect vibration transducer attachment;
- The presence of vibration signals have approximately the same frequency from sources other than the unbalance signal;
- The influence of vibration background noise.
- The absence of a signal from the pulse reference (colour mark)
- The signal from the pulse reference is unstable.
- The vibration transducer is loosely attachment of or the place poorly prepared.

- The measurement point (for example, the measurement might be made in axial direction instead of the radial one) has been wrongly selected

6.1.5 Vibration amplitude measurements instrument

Proximity transducers were used to measure the vibration amplitude of the shaft. Measurements were taken at all bearings in both the horizontal and vertical directions and along the rotor, as can be seen in Figures 6.1. The advantage of the transducers was their small size and low mass. The performance of these devices was easily capable of measuring the type of vibration produced by this application. The method of mounting these transducers by using stainless steel thread screws within the voltage range of interest, allowed the transducers to be removed when necessary. In this case, the desired voltage range to be achieved was set so that the maximum reading did not exceed 10 V, this was the upper limit of the input voltage into the data acquisition system.

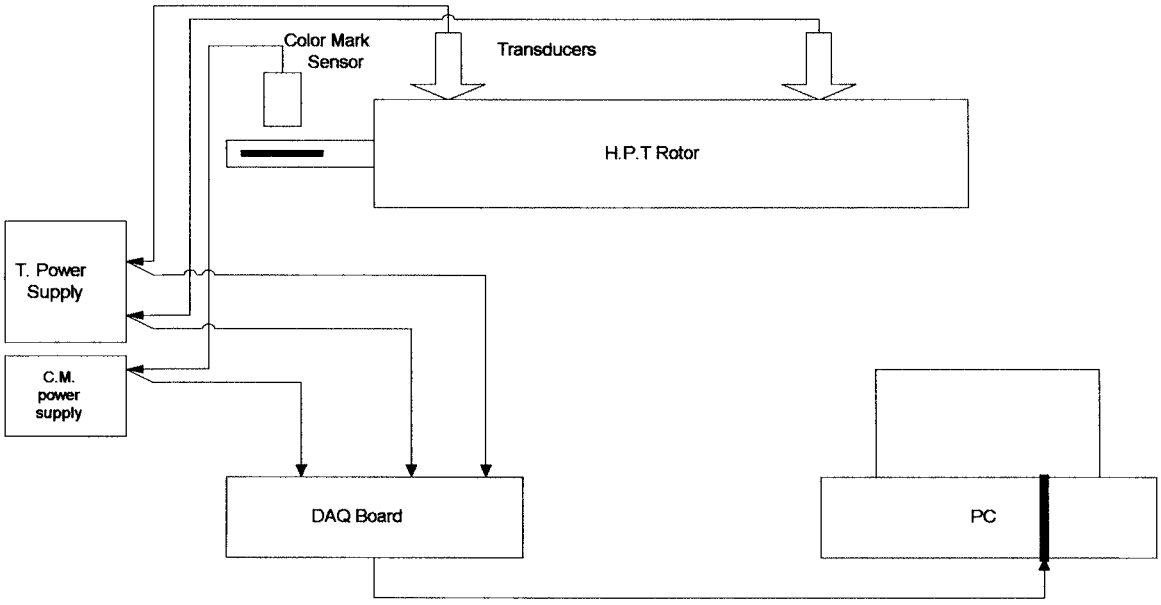

Figure 6.1 Schematic diagram of the experimental test procedure for 2 plane balancing

6.1.6 Phase Angle Reading Instrument

To measure the phase angle of vibration amplitudes, it is necessary to have a pulse reference colour mark transducer device that gives an electric pulse corresponding to a certain position of a rotating machine part. A reference mark should be placed on a rotating machine part to fix its position. The reference mark must be available for the transducer when the system is in operation.

In order to perform the signal processing required for the work of rotor balancing experiments, a reference signal was necessary. This reference signal, often called the optical switch signal, allows the angular position of the rotor to be known relative to a fixed reference. A colour mark sensor with a contrast mark was used as a pulse reference. It is attached to a rotating part of the machine.

Colour Mark Sensor (an optical switch) as shown on Figure 5.15 was powered by a13.5V supply, and provided an output pulse of almost 9 V upon the passing of the edge of the mark, returning to 0 V once the mark had passed the sensor. In this way, the optical switch sensors provided a once-per-revolution pulse. The sensor had a detecting distance of 2.0 mm. This ensured a consistent measurement of shaft rotation, which was important for balancing purposes so that the unbalance phase angle could be easily measured from the horizontal (0°) position

6.1.7 Classification of Error Sources

Errors must be treated differently if they arise from consistent and repeatable sources (like an offset in calibration) or if they arise from random fluctuations in the measurements. The former are called "systematic" or "bias" errors, and the latter "random" errors. In concept it is easy to differentiate these errors by the following test: Random errors are reduced when an experiment is repeated many times and the results averaged together, while systematic errors remain the same.

6.1.8 Experimental Results

The results tables below (tables 6.1-6.6) show the mean value and the standard deviation of the vibration amplitude and their phase angle relationship, the data obtained by using DAQ and transmitted to a computer program written in Matlab, which has the ability to calculate the average and the standard deviation via an existing command.

As you can see from Figure (6.2) the data has been taken in different locations along the multi rotor system (HP, LP Turbine rotors and Generator rotor). 12 proximity transducers with resolution of 0.001 mm (measurement points) were located to measure the vibration amplitude and an Omran colour mark switch with resolution of 3° was used to measure the phase angle. The data taken 15 times for each transducer then move on to the next transducer till the last measurement point and this procedure was repeated 5 times.

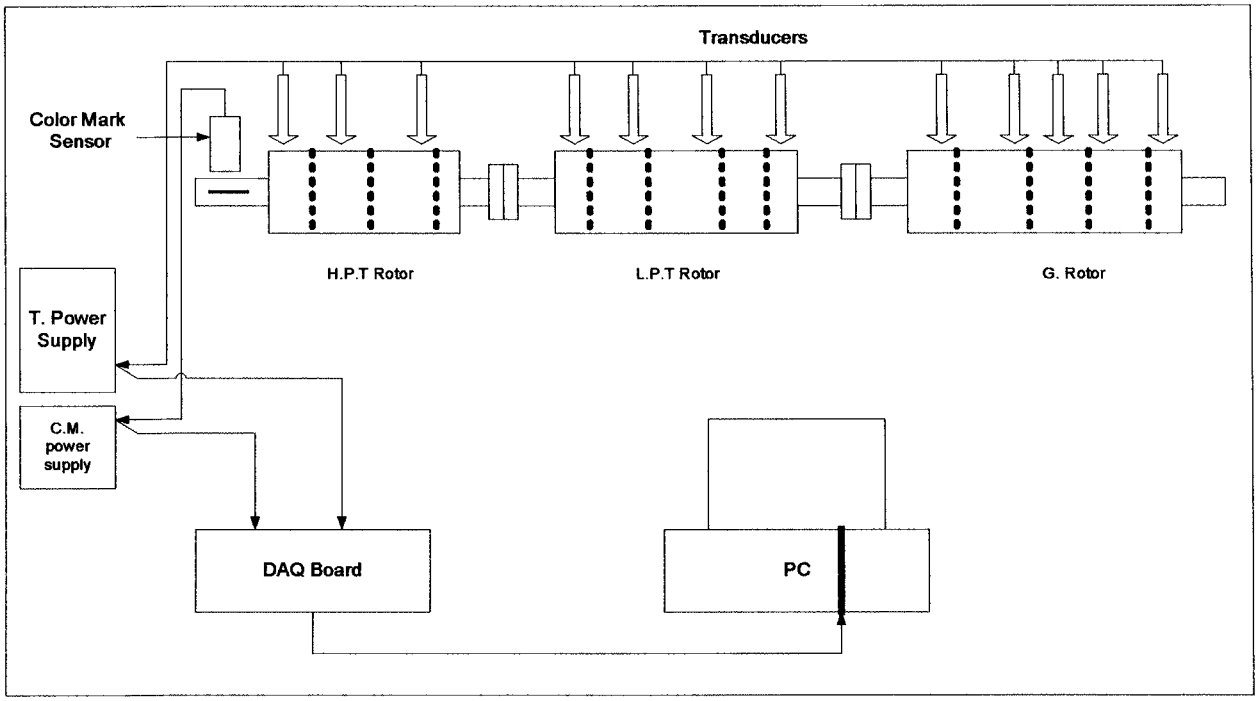

Figure 6.2 Schematic diagram of the experimental test procedure for multi plane balancing

- **Mean value and standard deviation of the vibration amplitude of, 12 measurements points, and taking 15 measurements at each point, for 5 iteration with rotor speed of 1500 rpm**

Mean value of the vibration amplitude (mm) of 12 measurements points, and taking 15 measurements at each point, for 5 iteration with rotor speed of 1500rpm												
Iterations	**MP1**	**MP2**	**MP3**	**MP4**	**MP5**	**MP6**	**MP7**	**MP8**	**MP9**	**MP10**	**MP11**	**MP12**
1	0.407	0.197	0.210	0.467	0.352	0.618	3.597	0.879	0.780	1.054	1.965	0.644
2	0.405	0.198	0.216	0.465	0.350	0.616	3.584	0.879	0.799	1.054	1.952	0.629
3	0.406	0.198	0.216	0.463	0.350	0.616	3.586	0.877	0.799	1.053	1.955	0.633
4	0.425	0.187	0.198	0.472	0.331	0.591	3.593	0.891	0.777	1.055	1.965	0.630
5	0.418	0.180	0.197	0.476	0.337	0.597	3.570	0.890	0.778	1.055	1.962	0.639

Table 6.1 Mean value of the vibration amplitude reading

Standard deviation of the vibration amplitude of 12 measurements points, and taking 15 measurements at each point, for 5 iteration with rotor speed of 1500rpm												
Iterations	**MP1**	**MP2**	**MP3**	**MP4**	**MP5**	**MP6**	**MP7**	**MP8**	**MP9**	**MP10**	**MP11**	**MP12**
1	0.004	0.005	0.004	0.004	0.004	0.009	0.015	0.007	0.004	0.004	0.008	0.005
2	0.005	0.005	0.004	0.004	0.004	0.011	0.014	0.005	0.004	0.004	0.009	0.007
3	0.005	0.005	0.004	0.004	0.004	0.012	0.009	0.005	0.004	0.002	0.011	0.005
4	0.006	0.005	0.004	0.004	0.004	0.009	0.013	0.006	0.003	0.003	0.013	0.008
5	0.006	0.004	0.004	0.004	0.004	0.009	0.014	0.005	0.003	0.002	0.011	0.008

Table 6.2 Standard deviation of the vibration amplitude reading

- **Mean value and standard deviation of the phase angle of 5 scans, 12 measurements points, and taking 15 measurements at each point, with rotor speed of 1500 rpm**

Mean value of the phase angle (degree) of 12 measurements points, and taking 15 measurements at each point, for 5 scans with rotor speed of 1500rpm												
Iteration	**MP1**	**MP2**	**MP3**	**MP4**	**MP5**	**MP6**	**MP7**	**MP8**	**MP9**	**MP10**	**MP11**	**MP12**
1	30.274	25.959	124.318	307.504	326.252	345.473	14.394	3.392	316.253	110.867	95.351	157.640
2	31.294	24.018	124.760	306.431	324.856	344.610	14.644	3.811	313.776	111.571	95.200	157.404
3	31.294	25.084	124.760	305.764	324.789	344.610	14.644	3.408	313.776	111.571	95.200	157.404
4	30.153	25.605	125.138	305.679	324.784	344.282	14.325	4.128	313.789	110.713	94.639	156.943
5	30.483	25.798	123.673	305.622	324.873	346.038	14.383	3.933	313.831	110.340	95.995	156.056

Table 6.3 Mean value of the phase angle reading

Standard deviation of the phase angle (degree) of 12 measurements points, and taking 15 measurements at each point, for 5 iteration with rotor speed of 1500rpm												
Iterations	**MP1**	**MP2**	**MP3**	**MP4**	**MP5**	**MP6**	**MP7**	**MP8**	**MP9**	**MP10**	**MP11**	**MP12**
1	2.471	2.196	3.107	2.057	2.137	2.631	2.654	1.259	1.908	1.94	2.908	2.33
2	3.467	1.287	3.184	1.982	3.11	2.974	2.582	1.191	3.108	1.67	3.071	2.278
3	3.467	2.211	3.184	2.057	3.134	2.974	2.588	1.187	3.108	1.67	3.071	2.278
4	3.208	2.202	3.098	2.045	3.272	2.881	2.582	1.262	2.992	1.642	2.068	2.263
5	3.277	2.331	3.13	1.919	3.068	2.868	2.579	1.242	2.972	0.929	2.69	1.915

Table 6.4 Standard deviation of the phase angle reading

6.1.9 Data of Measurement Uncertainty on Rotor Balancing

The experimental set up for this test is shown in Figure (6.2). As we can be seen from the results (see data table 6.5), which were taken on the High Pressure Turbine rotor H.P.T, see Figure (6.3), the traditional Influence Coefficient method was used to verify the effectiveness of the measurement uncertainty on rotor balancing. Seven scans were taken in the three runs (initial, trial mass 1,trial mass 2). As we can see from the above tables that the vibration amplitude and the phase angle at each location a long the multi-rotor system was stable, and the reason of taking more the required averaging number the measurements was to ensure the stability of the system. The methods of calculation carried for this test can be found in details in section 6.2.2.1.

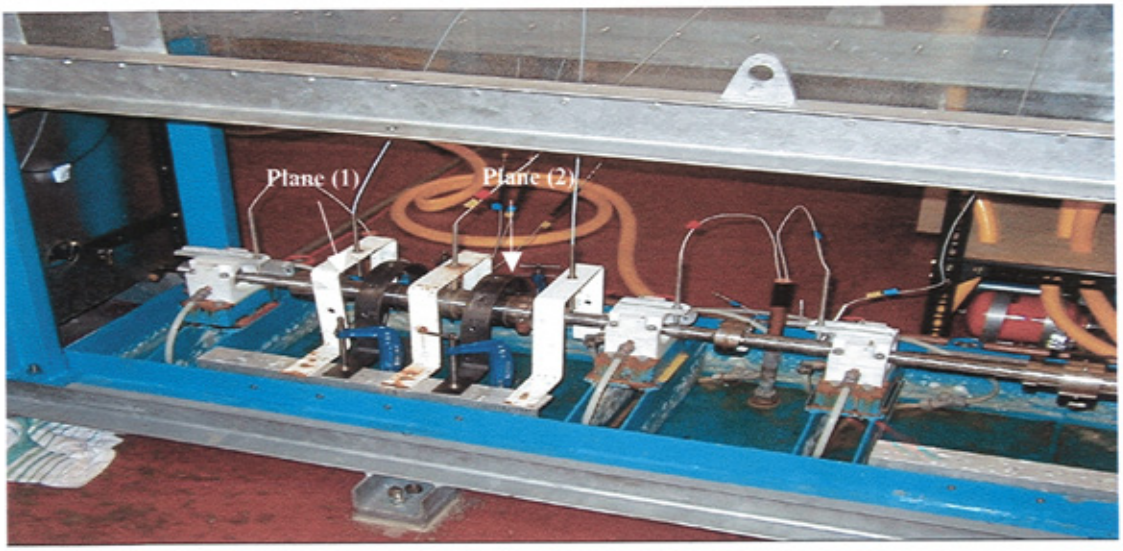

Figure 6.3 H.P.T rotors

Run	Trial Mass	Vibration amplitude (mm)/ Phase angle (degree) (plane 1) Radius 29.3mm						
		Scan1	Scan2	Scan3	Scan4	Scan5	Scan6	Scan7
Initial run (0)		0.19@ 155.42	0.18@ 152.76	0.18@ 173.32	0.19@ 160.59	0.19@ 157.45	0.17@ 167.14	0.18@ 161.66
Trial mass runs 1	33@ 60°	0.19@ 89.63	0.18@ 66.17	0.15@ 65.33	0.15@ 68.82	0.15@ 86.34	0.15@ 81.33	0.14@ 76.48
Trial mass runs 2	33@ 60°	0.15@ 86.00	0.15@ 92.25	0.13@ 79.85	0.15@ 88.67	0.14@ 92.98	0.14@ 99.07	0.14@ 84.00

Run	Trial Mass	Vibration amplitude (mm)/ Phase angle (degree) (plane 2) Radius 37.05mm						
		Scan 1	Scan 2	Scan 3	Scan 4	Scan 5	Scan 6	Scan 7
Initial run		0.23@ 227.15	0.24@ 276.00	0.23@ 204.00	0.22@ 286.93	0.23@ 229.33	0.24@ 221.02	0.23@ 233.33
Trial mass runs 1	33@ 60°	0.21@ 130.18	0.19@ 282.95	0.18@ 241.33	0.19@ 131.51	0.19@ 128.85	0.18@ 127.52	0.18@ 126.66
Trial mass runs 2	33@ 60°	0.17@ 304.41	0.18@ 283.23	0.18@ 133.33	0.19@ 136.82	0.19@ 298.43	0.18@ 278.96	0.18@ 264.98

Table 6.5 test Data of (HPT rotor)

Tests Cases	Mean value of Initial Vibration amplitude Plane (1)	Calculated Correction mass Plane (1)	Actual Correction mass added Plane (1)	Mean value of Residual vibration Plane (1)	Theoretical expected Residual vibration Plane (1)	Correction mass difference % Plane (1)	Vibration reduction % Plane (1)
Results of Scan (1)	0.19@ 155.42	18.41@175.77	18.6@180	0.12@ 132.15	0.121	-1.03	63.16
Results of Scan (2)	0.18@ 152.76	19.19@171.57	19.5@180	0.13@ 44.86	0.102	-1.62	72.22
Results of Scan (3)	0.18@ 173.32	15.08@164.76	15.3@150	0.10@ 333.00	0.112	-1.46	55.56
Results of Scan (4)	0.19@ 160.59	17.25@174.72	17.6@180	0.11@ 122.33	0.112	-2.03	57.89
Results of Scan (5)	0.19@ 157.45	15.65@179.07	15.3@180	0.10@ 111.25	0.098	2.24	52.63
Results of Scan (6)	0.17@ 167.14	13.93@ 173.54	14.1@ 180	0.09@ 24.99	0.091	-1.22	52.94
Results of Scan (7)	0.18@161.66	19.40@175.02	19.5@180	0.12@278.12	0.121	-0.52	66.67
Mean value	0.18@161.19	16.99@173.49	17.2@180	0.09@320.00	0.091	-1.24	50.00

Tests Cases	Mean value of Initial Vibration amplitude Plane (2)	Calculated Correction mass Plane (2)	Actual Correction mass added Plane (2)	Mean value of Residual vibration Plane (2)	Theoretical expected Residual vibration Plane (2)	Correction mass difference % Plane (2)	Vibration reduction % Plane (2)
Results of Scan (1)	0.23@ 227.15	43.57@33.87	43.2@30	0.16@ 120.53	0.159	0.85	69.57
Results of Scan (2)	0.24@ 276.00	43.82@32.23	43.7@30	0. 18@350.63	0.18	0.27	75.00
Results of Scan (3)	0.23@ 204.00	40.42@34.43	40.3@30	0.13@ 116.23	0.13	0.3	56.52
Results of Scan (4)	0.22@ 286.93	43.64@32.85	43.7@30	0.18@ 117.33	0.18	-0.14	81.82
Results of Scan (5)	0.23@ 229.33	42.59@33.86	42.4@30	0.14@ 44.00	0.139	0.45	60.87
Results of Scan (6)	0.24@ 221.02	40.94@32.48	40.4@30	0.13@ 66.37	0.128	1.32	54.17
Results of Scan (7)	0.23@233.33	42.92@35.72	42.4@30	0.14@83.99	0.138	1.21	60.87
Mean value	0.23@239.68	42.56@ 33.63	42.4@30	0.14@99.12	0.139	0.38	60.87

Table 6.6 Results of the test (HPT rotor)

6.1.10 Results Discussion of The Effect of Measurement Uncertainty on Rotor Balancing

The results tables (6.1-6.4) show the mean value of the vibration amplitude and their phase angle relation. The data were obtained by using DAQ and transmitted to a computer program written in matlab, which has the ability to calculate the average and the standard deviation via an existing command.

As you can see from Figure (6.2) the data has been taken in different locations along the multi rotor system (HP, LP Turbine rotors and Generator rotor). 12 proximity transducers were located to measure the vibration amplitude and an Omron colour mark switch was used to measure the phase angle.

Several tests have been done in order to ensure that the phase angle and the vibration amplitude (see section 6.1.9) readings are acceptable in comparison with the resolution and the standard deviation of the phase measurement instrument (colour mark sensor). The results of the tests shows the stability of the system, which can be seen from the reading, obtained for the vibration amplitude and the phase angle, if we pick up one case of averaging data, for instance the transducer in the first position from the driving system. The mean value of the vibration amplitude was between 0.405 mm and 0.4425 mm, and the standard deviation of this case was between 0.004 and 0.006. Likewise the mean value of the angle measurement for the same case was between 30.153° and 31.294° and the standard deviation was between 2.471° and 3.467°.

6.1.10.1 Data of Measurement Uncertainty on Rotor Balancing

The experimental set up for this test is shown in the schematic diagram sees Figure (6.1). As we can see from the results (tables 6.5 and 6.6), for the High Pressure Turbine rotor H.P.T, the traditional influence coefficient method was used to verify the effectiveness of the measurement uncertainty on rotor balancing. Seven scans were taken in the three runs (initial, trial mass 1,trial mass 2).

The results of 2 plane, 2 measurements locations and 7 scans data taken (table 6.6) shows that there are Random "errors" caused by a number of unpredictable and unknown

variations. Sources come from the correction mass added to the system, which is slightly different than the calculated masses. In addition the phase angle is not the same recommended position see table 6.6.

Also table 6.6 shows the percentage of improvement in terms of residual vibration amplitude. We can see that when we take the average reading the results improve, as it was 50% in plane 1 and 39.13% in plane 2, which is a good improvement to the system. In the results table also we worked out the difference between the recommended correction masses and their locations with the actual masses added to the system. The author made every effect to achieve the right correction mass, but it was difficult to add the calculated correction mass in the right phase as well, that was because of the mechanical design of the rig.

The amount of the correction masses is different in every scan result, also from the mean value of the scans. We can see the vibration amplitude and the phase angle reading are within the resolution of the equipment used in this test. In the stage of balancing, the values of the machine sensitivity to the attached masses play a significant role. Two types of mistakes can be determined on this stage:

- The trial mass was very small. In this case the calculations were made on the basis of the values that may result entirely from measurement errors. The result of the calculation was unpredictable. The accuracy of the calculation in this case was also low and it was impractical to expect good efficiency of this step of balancing.
- A too sensitive pulse reference will react to changes as additional marks and such reaction can be a random one, which means that the transducer will produce no definitive impulse with each revolution. A user can be tempted to use a transducer with a long distance capability close to the marked surface. It should be noted that this can significantly increase the number of noise signals from the phase angle reader and it may be necessary to install the transducer far from the mark to eliminate the noise signals. In practice, such a transducer is often impractical to attach in its previous position after removal for mass installation.

6.2 New Proposed Technique For Flexible Rotor Trim Balancing

6.2.1 Introduction

The "trim" balancing run is defined as any correction balance run after the first attempted balance correction. Usually any mass adjustment due to the trim balancing mass amount should be significantly less than the initial balance correction mass. The trim is usually a fine-tuning of the initial balance correction, because further reduction of the vibration level is usually necessary (Wowk 1995).

This part of the chapter presents a new balancing method for trim balancing mass calculation. This method is based on the combined use of the original influence coefficient matrix and the new data obtained after adding the correction mass to the system.

6.2.2 New Trim Balancing Calculations

The influence coefficient method aims to correct rotor unbalance by means of separate masses placed in predefined correction planes. Recording the changes of vibration due to the addition of trial masses, an influence coefficient matrix is assembled. This matrix represents the dynamic characteristics of the system. The influence coefficient method assumes a linear relation between the vibration response and the unbalance of a rotor. This linear relation defines the influence coefficients, which represent the vibration effect at some point on the shaft for a given speed, due to the addition of a unit mass in another or the same point along the rotor.

Three methods (A, B, C) have been tested in this study. Their procedures are described in the following sections. Computer programs were developed based on this procedure and the programs were able to handle data acquisition and balancing calculations. The program can be applied to 2,3,4 balancing planes. The two-plane rotor balancing method is described in details as an example is shown below;

The first stage of the balancing will include the following procedure:

Run **0:** vibration for rotor measurements without trial mass (initial run)

The measured initial vibration amplitudes of two planes are labeled as: x_{01} & x_{02}

Run **1**: rotor vibration is measured with trial mass m_1 inserted at plane 1

The vibration amplitude of two planes in trial mass m_1 run are labeled as: x_{11} & x_{12}

Where; x_{11} is for run 1 and plane 1

x_{12} is for run 1 and plane 2

Run **2** with trial mass m_2 inserted at plane 2

The vibration amplitude of two planes in trial mass two m_2 run are labeled as: x_{21} & x_{22}

Where x_{21} is for run 2 and plane 1

x_{22} is for run 2 and plane 2

After adding the calculated correction masses we obtain the amplitude of two planes u_{11} & u_{12}

The independent calculation for the traditional influence coefficient at the first stage as follows;

$$\alpha * W = X \qquad \text{(Equation 6.2.1)}$$

Where $[X]$ is a column vector of (observed vibration displacements) for the unbalanced shaft, $[\alpha]$ is the matrix of influence coefficients and $[W]$ is a column vector which includes the correction mass of the rotor.

6.2.2.1 Method A

The form of the traditional influence coefficient matrix with elements for two planes balancing, as an example, can be expressed in matrix form, as follows:

$$\begin{bmatrix} \alpha_{11} & \alpha_{12} \\ \alpha_{21} & \alpha_{22} \end{bmatrix} * \begin{bmatrix} W1 \\ W2 \end{bmatrix} = \begin{bmatrix} -x_{01} \\ -x_{02} \end{bmatrix}$$ From equation 6.2.1

$$\begin{bmatrix} W1 \\ W2 \end{bmatrix} = \begin{bmatrix} \alpha_{11} & \alpha_{12} \\ \alpha_{21} & \alpha_{22} \end{bmatrix}^{-1} * \begin{bmatrix} -x_{01} \\ -x_{02} \end{bmatrix}$$ (Equation 6.2.2)

Where:

$$\alpha_{11} = x_{11} - x_{01} / m_1$$

$$\alpha_{12} = x_{12} - x_{01} / m_2$$

$$\alpha_{21} = x_{21} - x_{02} / m_1$$

$$\alpha_{22} = x_{22} - x_{02} / m_2$$

In method A, equation 6.2.2 is repeated for every balancing stage.

6.2.2.2 Method B

Independent calculation uses the new vibration which is obtained after adding the correction mass. In this method the trim balancing run is considered as a reference run (run 0 data), and then the new influence coefficient matrix is constructed and the right hand side matrix based on this new data, as you can see from the equation 6.2.3 below

$$\begin{bmatrix} \beta_{11} & \beta_{12} \\ \beta_{21} & \beta_{22} \end{bmatrix} * \begin{bmatrix} W1 \\ W2 \end{bmatrix} = \begin{bmatrix} -u_{11} \\ -u_{12} \end{bmatrix}$$

$$\begin{bmatrix} W1 \\ W2 \end{bmatrix} = \begin{bmatrix} \beta_{11} & \beta_{12} \\ \beta_{21} & \beta_{22} \end{bmatrix}^{-1} * \begin{bmatrix} -u_{11} \\ -u_{12} \end{bmatrix} \qquad \text{(Equation 6.2.3)}$$

Where:

$$\beta_{11} = x_{11} - u_{11} / m_1$$

$$\beta_{12} = x_{12} - u_{11} / m_2$$

$$\beta_{21} = x_{21} - u_{12} / m_1$$

$$\beta_{22} = x_{22} - u_{12} / m_2$$

Method B was presented by Wowk (1995), for rigid rotor only. But in this paper a flexible rotor has been considered as well as a rigid rotor.

6.2.2.3 Method C

In this method the trim balancing run considered as reference run (run 0 data), but the construction of the new influence coefficient matrix has not changed and uses the same influence coefficient matrix of method A because in fact all the elements of the Matrix in method A are built upon the ordinal run data (run 0). The right hand side matrix is based on this new data, as you can see from the equation 6.2.4 below.

$$\begin{bmatrix} \alpha_{11} & \alpha_{12} \\ \alpha_{21} & \alpha_{22} \end{bmatrix} * \begin{bmatrix} W1 \\ W2 \end{bmatrix} = \begin{bmatrix} -u_{11} \\ -u_{12} \end{bmatrix}$$

$$\begin{bmatrix} W1 \\ W2 \end{bmatrix} = \begin{bmatrix} \alpha_{11} & \alpha_{12} \\ \alpha_{21} & \alpha_{22} \end{bmatrix}^{-1} * \begin{bmatrix} -u_{11} \\ -u_{12} \end{bmatrix} \qquad \text{(Equation 6.2.4)}$$

Where:

$$\alpha_{11} = x_{11} - x_{01} / m_1$$

$$\alpha_{12} = x_{12} - x_{01} / m_2$$

$$\alpha_{21} = x_{21} - x_{02} / m_1$$

$$\alpha_{22} = x_{22} - x_{02} / m_2$$

The new trim balancing calculation method (C) involves replacing the 'original plus trial' vector with the new data vector of those results obtained after the correction mass has been added to the rotor. Then the trim balancing calculation is performed. In essence, the correction mass is being treated like a trial mass run data. So the results of the trim balancing calculation (the correction mass and phase angle) are applied as new correction mass plus the original correction mass.

The new correction mass is located relative to the last correction mass, and it is assumed that the last correction mass is removed as the new correction mass is added. This trim process can be repeated, many times, but if the trim has to be repeated many times then we should consider if another cause of the vibration is at work, or possibly that the balance condition has been taken to the best possible level with the equipment available.

The new proposed method (C) indicates that the new trim balancing vibration amplitude data, assumed as the original vibration only for the right hand side matrix, at the same time the original influence coefficient (method A) will stay the same because the elements of method A matrix are based on the initial run data.

6.2.3 Validation of the new trim balancing approach and computer program.

The validation of method C were used to balance the H.P & I.P turbine rotors using 2, 3 and 4 planes balancing and the traditional influence coefficient method (mentioned as method A in this thesis) and the least square influence coefficient procedure. The purpose of the test program was to evaluate the accuracy of the calculated influence coefficients matrix. A second purpose was to compare between the different ways of formatting the influence coefficients matrix, after adding the correction masses into the rotor. The test

measurements were taken at speeds below the critical speed in some cases and above in others.

After adding on the correction masses, the rotor was again run up to speed to check the residual vibration amplitude level. It was found that the vibration level had been reduced in most 2, 3 and 4 planes balancing tests

A number of test cases (see table 6.7) have been carried out to demonstrate the new trim balancing procedure and after reviewing the data the two plane calculations were performed. The previous trial masses were removed and new calculated correction masses were added to the rotor. Then, new data was collected as trim data. Trim calculations were then performed.

Tables A8.1-A8.3 are the obtained data and the calculated results achieved on the high-pressure turbine rotor. The test was applied by using the traditional Influence Coefficient Method in the first balancing stage, which use two balancing planes, two measurement locations (Proximity Transducers) and one speed, then methods B&C are used in the further runs (trim balancing runs).

6.2.4 List of tests

Table 6.7 shows the number of test cases that have been studied to demonstrate the relation between Method B and the proposed method C. The tests are divided into 2 sections based on HPT & LPT rotors. Figure 6.4 shows the schematic diagram of HPT experimental set up

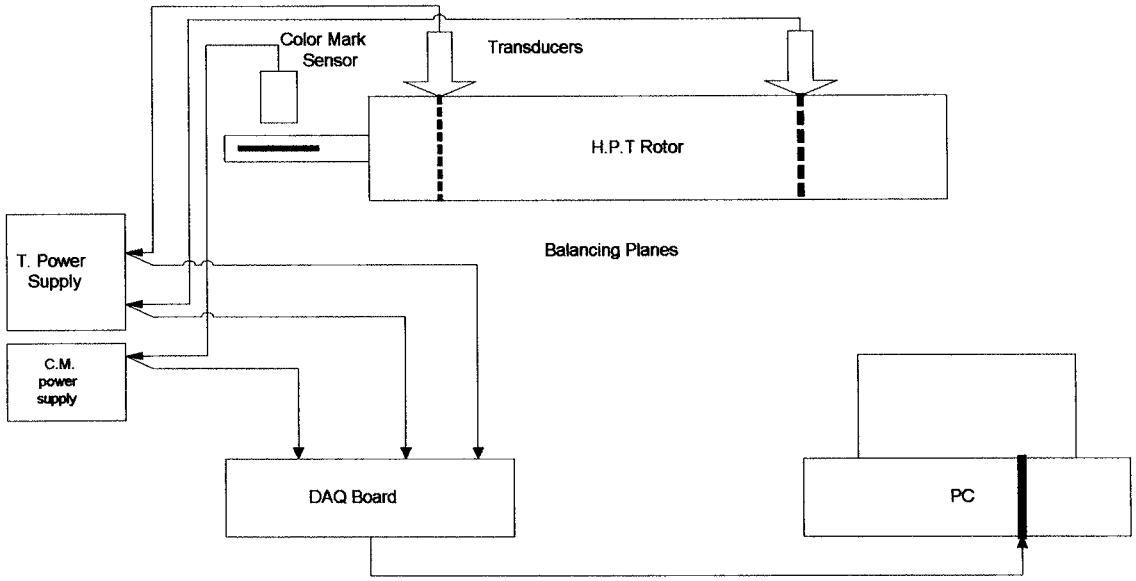

Figure 6.4 schematic diagram of HPT rotor test set up

HPT rotor (Traditional Influence Coefficient)		
Number of Balancing planes	Number of measurements points	RPM
2	2	1080 rpm
2	2	3000 rpm
2	2	3500 rpm
3	3	1080 rpm
3	3	3000 rpm
3	3	3500 rpm
LPT rotor (Traditional Influence Coefficient)		
2	2	1080 rpm
2	2	3000 rpm
2	2	3500 rpm
3	3	1080 rpm
3	3	3000 rpm
3	3	3500 rpm
4	4	1080 rpm
4	4	3000 rpm
4	4	3500 rpm
HPT rotor (Influence Coefficient Least Square Method)		
2	2	3 speeds (1080, 3000, 3500 rpm).
3	3	3 speeds (1080, 3000, 3500 rpm).
LPT rotor (Influence Coefficient Least Square Method)		
2	2	3 speeds (1080, 3000, 3500 rpm).
3	3	3 speeds (1080, 3000, 3500 rpm).
4	4	3 speeds (1080, 3000, 3500 rpm).

Table 6.7 Experimental procedure tests for method B&C

6.2.5 Results Tables For Trim Balancing Technique

In this section, data and results tables, which demonstrate the tests, held on HPT and LPT rotors, by using different planes and calculation methods.

6.2.5.1 Test results of the 2 plane balancing HPT rotor (as an example)

Tables 6.8,6.9 and 6.10 illustrate the data and results of two planes balancing on HPT rotor, tables 6.9 and 6.10 show the results of trim balancing 1&2, as we can see the correction masses are calculated by two different methods.

Test results for the 2 plane balancing of HPT rotor (10.1 Kg)(1080 rpm)							
Run	T. Mass	Vibration amplitude (mm)		Phase angle (deg)		Correction masses/phase	
		Plane (1) Radius29.3mm	Plane (2) Radius37.05mm	Plane (1) Radius29.3mm	Plane (2) Radius37.05mm	Plane (1) Radius29.3mm	Plane (2) Radius37.05mm
0		0.651	0.394	10.285	252.692	58.160@ -100.009	66.136@ -64.615
1	26.8@60	0.827	0.224	74.226	182.168		
2	26.8@60	0.866	0.589	345.714	148.030		

Table 6.8 Data and results of initial balancing test

Trim balancing run (1) results for the 2 plane balancing of HPT rotor (10.1 Kg)(1080 rpm)										
							METHOD (B)		*METHOD (C)*	
Run	C. Mass		Vibration amplitude (mm)		Phase angle (deg)		Correction masses/phase		Correction masses/phase	
	Plane (1)	Plane (2)	Plane (1)	Plane (2)	Plane (1)	Plane (2)	Plane (1)	Plane (2)	Plane (1)	Plane (2)
1	59.1@ -120.000	65.6@-60.000	0.112	0.110	13.382	11.955	35.906@ 46.959	17.625@ -102.623	30.201@ 42.128	13.665@ 10.325

Table 6.9 Data and results of trim balancing (run 1)

Trim balancing run (2) results for the 2 plane balancing of HPT rotor (10.1 Kg)(1080 rpm)										
Run	C. Mass + T.Mass 1		*METHOD B*		*METHOD C*		*METHOD B*		*METHOD C*	
			Vibration amplitude /Phase angle		Vibration amplitude /Phase angle		Correction masses/phase		Correction masses/phase	
	Plane (1)	Plane (2)	Plane (1)	Plane (2)	Plane (1)	Plane (2)	Plane (1)	Plane (2)	Plane (1)	Plane (2)
2	31.3@ 30.000	14.9@- 30.000	0.110@ 9.298	0.112@ 30.666	0.115@ 46.558	0.112@ 58.687	32.00@ 28.203	13.11@ 53.005	29.680@ 302.586	16.220@ 268.006

Table 6.10 Data and results of trim balancing (run 2)

Table A8.1-A8.3 show the data and results of tests held on HPT and LPT rotors, by using different planes (2,3&4), and using least square method (more measurement locations than balancing planes) and using different calculation methods (B&C).

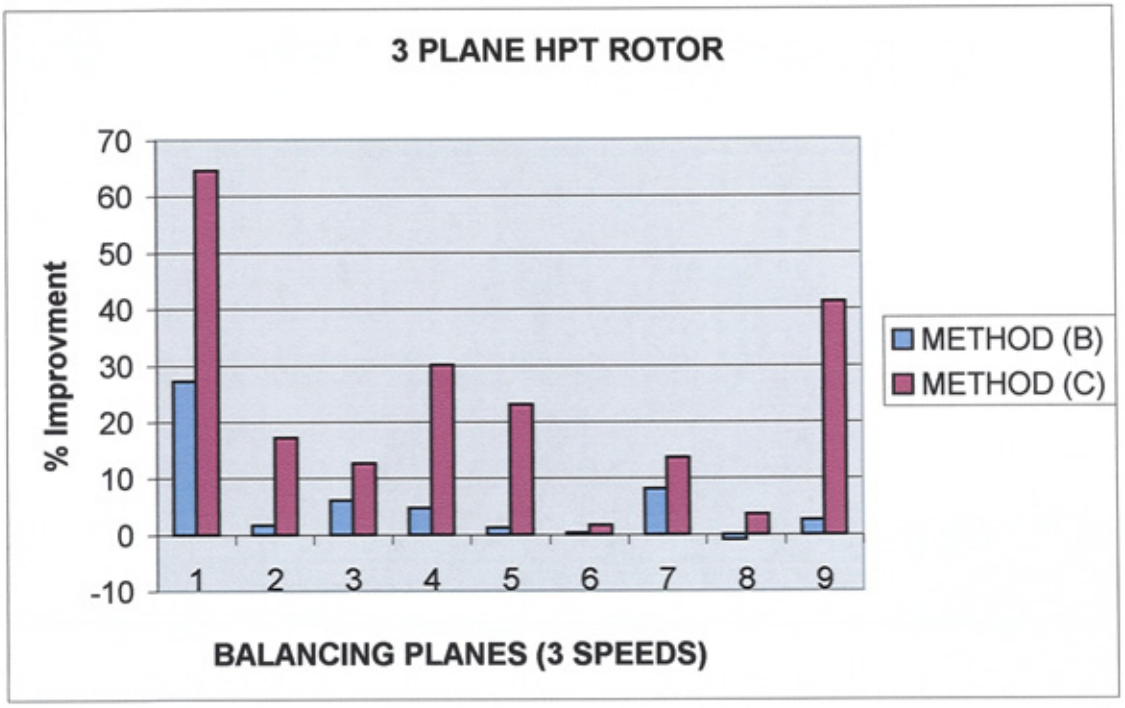

Figure 6.5 Methods B&C improvement comparison for 3 planes balancing of HPT rotor

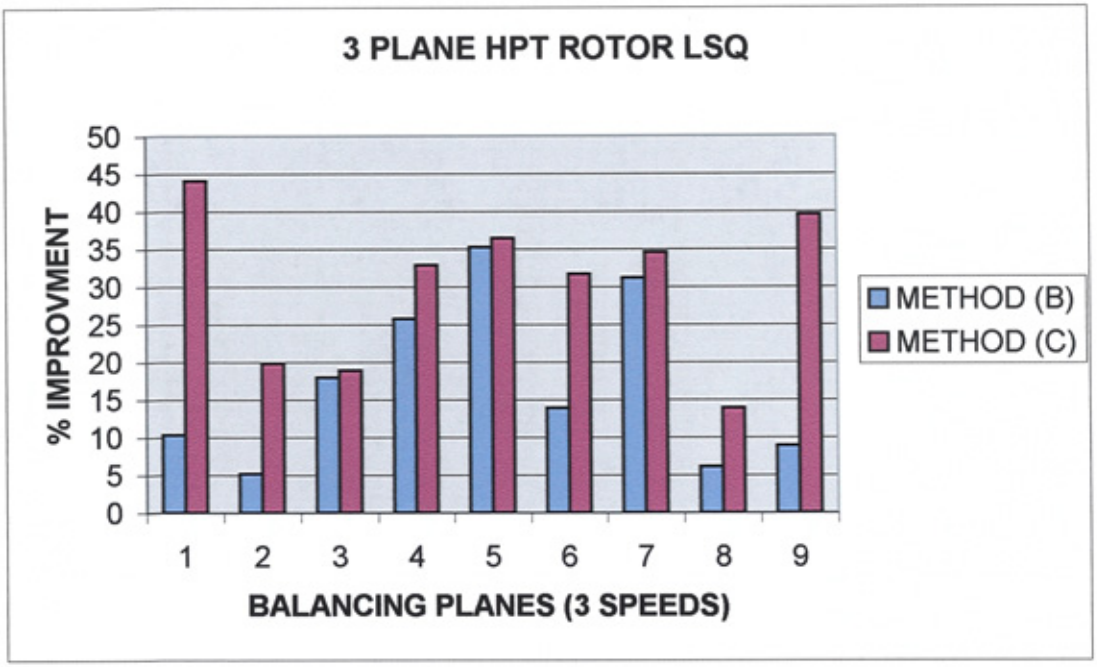

Figure 6.6 Methods B&C improvement comparison for multi speeds, 3 planes balancing of HPT rotor

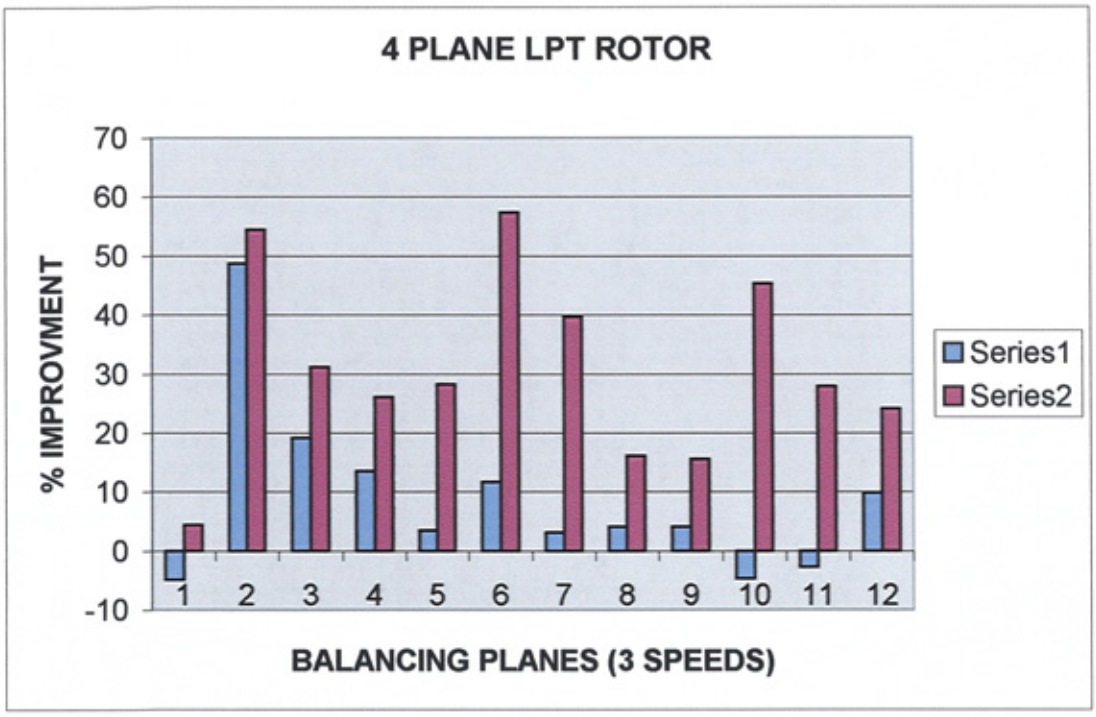

Figure 6.7 Methods B&C improvement comparison for 4 planes balancing of LPT rotor

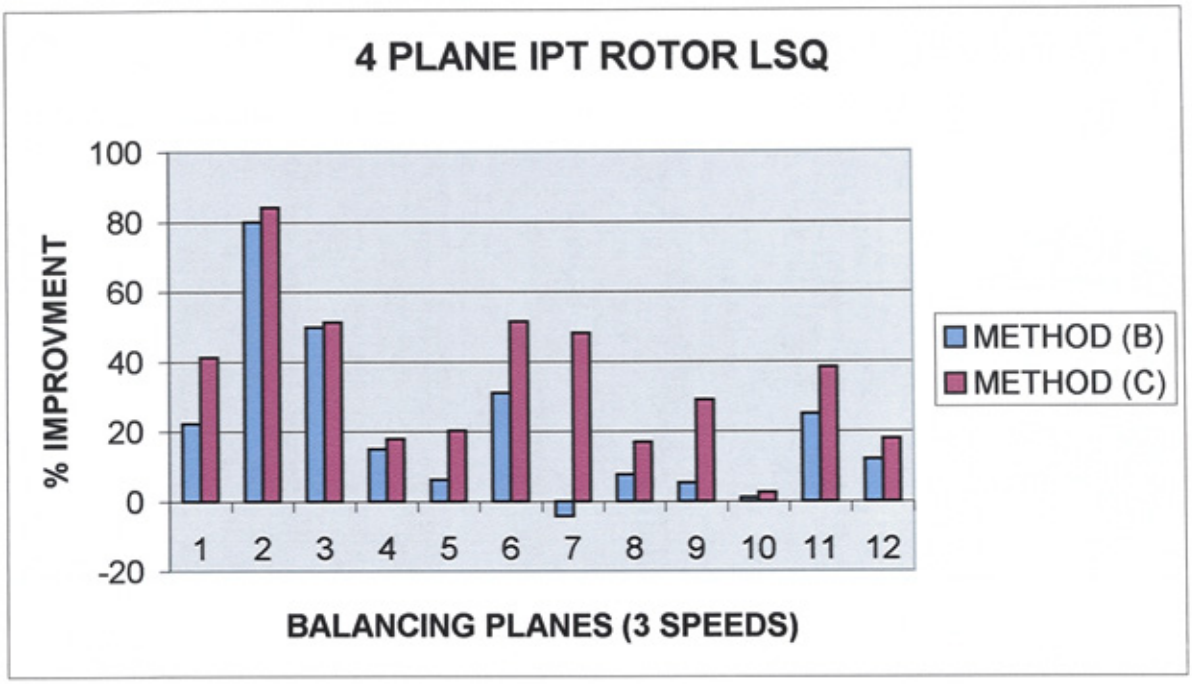

Figure 6.8 Methods B&C improvement comparison for multi speeds, 4 planes balancing of LPT rotor

6.2.6 Results Discussion of a new proposal for rotor balancing using trim-balance techniques

As we can see from the table the results obtained are acceptable, comparing the initial vibration amplitude level with that obtained one after finishing the balancing procedure and adding the correction masses residual vibration. Regarding the measurement uncertainty the results are still very reasonable. For example the initial vibration on plane 1 was 0.6511mm and after balancing became 0.1129mm, which means that, the vibration level on the rotor was cut up to 80%. Moreover in the other case the improvement was fluctuated as you can see in figures 6.8-6.8.

The outcome results obtained from the trim balancing runs are not very accurate, because the exact calculated correction mass was not inserted. This also was the case in happen to the phase angle of the correction mass, the holes or in other words the points around the balancing plane were drilled each 30°, for instance in the case 1 (HPT rotor 1080 rpm) (see schematic diagram in Figure 6.1). The results in tables 6.8-6.10 show that the

calculated correction mass and phase angle were 58.160g@-100.009 deg for plane 1 and 66.1368g@ -64.615deg for plane 2, and the actual mass, which added to the rotor, was 59.1g @ 120 deg and 65.6g@-60 deg for plan 1 & 2 respectively. As you can see there is a difference between the calculated and actual correction mass/phase angle, which will affect the results of the first iteration in trim balancing runs.

6.2.7 Conclusion of the tests results

Table (A8.3) shows the cases of improvement to the system after adding the correction mass calculated by method B and C added to the system respectively. The improvement results were different from case to case and also from plane to plane. Generally speaking the results show that the percentage improvement of method C almost gives a positive outcome compared with Method B.

CHAPTER 7

NEW BALANCING PROCEDURES BASED ON MODIFIED QR AND SVD TECHNIQUES WITH LEAST SQUARE OPTIMIZATION

7.1 Introduction

Most rotor balancing techniques today utilize exact point (speed) or least squares balancing methods. An exact point balance solves for as many corrective balance weights as vibration measurements that are utilized and it has a unique solution. Least squares balancing involve using more measurements than balance planes available and is determined by minimizing the 2norm of the final balancing response vector. Weighting functions are sometimes used to improve the method when results are not satisfactory. Often least squares balancing and other methods of balancing produce a state of balance where a few locations along the rotor have vibrations, which are rather high, compared to the remaining locations. In other cases, the method may indicate that large balance weights are needed to balance rather small residual vibrations.

In order to find the correction masses for unbalanced rotating machinery, several balancing techniques have been developed Foiles (1998). Each method has advantages and disadvantages in application. In this study, the influence coefficients techniques, combining with Least squares, QR, and SVD methods are used to make the best estimation of correction masses according to acceptable level of residual vibrations.

Goodman improved balancing technology in 1964 when he introduced the least squares balancing procedure. This method used data from multiple speeds and measurement locations, more measurements than balance planes, to minimize weighted sums of the squares of the residual vibration. The technique was to minimize the maximum residual vibration through an iteration of the weighting used for the least squares optimization.

Experimental results using a least-squares approach have been given by Lund and Tonneson (1972), which verify the effectiveness of this method. A further development has

been given by Little (1976) in which linear programming was used to optimize the balance of rotors operating through several bending critical speeds. These authors achieved smooth shaft operation using Influence coefficient balancing after having previously tried several other flexible rotor-balancing methods.

Darlow (1980) provided information on an important problem in balancing that results in ill conditioning of the balance equations of the influence coefficient matrix. When columns, corresponding to the balance planes, form a linear (or nearly) dependent set of vectors very large correction weights can be computed. The majority of the effects of these weights cancel each other; this results from the ill conditioning of the influence coefficient matrix. Darlow reduced the non-independent balance planes using a Gram-Schmidt orthogonaliztion procedure. Darlow defined an important factor as a standard to identify the non: independence of the balance plane. When the value of the factor is less than 0.2 this balance plane is considered as a non-independent plane and has to be eliminated. After the non-independent plane has been reduced further calculation for the correction mass still uses Goodman 's method. Darlow explained the procedure of calculating the significant factor as follows;

This significant factor must be, by definition, real-valued, non-negative and no larger than one, and it is a criteria used to evaluate independence of the vectors, as described below.

To summarize the procedure, after e_1 is calculated from

$$e_1 = \frac{u_1}{\|u_1\|} \tag{7.1}$$

Where the superscript bar represents the ith basis vector and $\|u_i\|$ represents the Euclidean norm u_i. Clearly, the vector with the largest Euclidean norm is always retained, the following sequence of calculations is performed for u_i

1. The orthogonal portion of u_i, is computed from

$$v_i = u_i - \sum_{j=1}^{l} \left(e_j^{'} * u_i\right) * e_j \tag{7.2}$$

Where l basis vectors have thus far been determined $(l \le i-1)$.

2. The significance factor for u_i, is computed from

$$S_{fi} = \frac{\|v_i\|}{\|u\|} \tag{7.3}$$

3. *If* S_{fi} *is* not less than the specified amount, the next basis vector *is* computed from

$$e_{l+1} = \frac{v_i}{\|v_i\|} \tag{7.4}$$

If S_{fi} *is* less than the specified amount, then u_i is eliminated. In either case, the above procedure is then repeated for the next u_i, until it has been completed for u_m.

The correction mass calculation is then performed using the remaining columns of the influence coefficient matrix. With the exception of the significance factors and Euclidean norms, all values used in this procedure are complex.

7.2 Accuracy of Solutions and an Ill-Conditioned Matrix

In the last four decades, many different algorithms for solving linear systems of equations have been developed and implemented. Any of these matrix solvers has certain advantages and negative aspects as well. For example, fast algorithms are often more memory consuming or less robust than slower algorithms. Therefore, it is not easy to select an optimal algorithm for a given matrix method.

We call a square matrix $[\alpha]$ ill conditioned if it is invertible but can become singular (non-invertible) if some of its entries are changed ever so slightly. The condition number of $[\alpha]$ is a measure of how ill conditioned $[\alpha]$ is and the bigger the condition number is the more ill conditioned $[\alpha]$is. Well-conditioned matrices have condition numbers close to 1. Solving linear systems whose coefficient matrices are ill conditioned is tricky because even

a small change in the data (e.g., the right-hand side vector) can lead to radically different answers.

The accuracy of the final results is mainly influenced by;

- The model accuracy,
- The accuracy of the matrix method,
- The accuracy of the matrix solver,

The examples shown in appendix 3 have dramatically different solutions because the coefficient matrix $[\alpha]$ is ill conditioned. A system of equations is said to be ill conditioned if a relatively small change in the elements of the coefficient matrix $[\alpha]$or $[x]$causes a relatively large change in the solution. Conversely a system of equations is said to be well conditioned if a relatively small change in the elements of the coefficient matrix $[\alpha]$ or $[x]$causes a relatively small change in the solution. Clearly we require a measure of the condition of a system of equations.

The rank of a matrix can be more effectively determined from the SVD of a matrix since its rank is equal to the number of its non-zero singular values. In practice, rather than counting the non-zero singular values, MATLAB determines from the SVD by counting the number of singular values greater than some tolerance value. This is a more realistic approach to determining rank than counting any non-value.

Although most least square problems solution based on the QR decomposition or normal equations are cheaper and more commonly used, the SVD is employed in a variety of applications, from least squares problems to solving systems of linear equations. Each of these applications exploits key properties of the SVD its relation to the rank of a matrix and its ability to approximate matrices of a given rank. Many fundamental aspects of linear algebra rely on determining the rank of a matrix, making the SVD an important and widely used technique.

7.3 Methods Based On The QR Factorization Of Least Square Problem

Orthogonal matrix triangularization (*QR* decomposition) reduces a real (*m,n*) matrix $[\alpha]$ with $m \geq n$ and full rank to a much simpler form. If $[\alpha]$ is *m-by-n* with linearly independent columns , then $[\alpha]$ can be factorized as

$$\alpha = Q * R \tag{7.5}$$

where Q is an *m-by-n* orthogonal matrix and R is a *n-by-n* upper triangular. In some cases, the normal equation for least square problems can be ill conditioned, that is small error in the calculation of the entries of $\alpha^T * \alpha$ can some times cause relativly large errors in the solutions Gilbert Strang (1988). In these cases, the least square solutions can be often computed more relibly through a QR factorization of $[\alpha]$, where,

$$\Rightarrow W = R^{-1} * Q^T * X \tag{7.6}$$

Therefore the solution W of the least square problem is given by solving the linear system of equations $W = \alpha^{-1} * X$ and the QR decomposition of $[\alpha]$.

$$Q^T * Q = I = \begin{bmatrix} 1 & 0 & . & . & . & 0 \\ 0 & 1 & . & . & . & 0 \\ . & . & . & . & . & . \\ . & . & . & . & . & . \\ . & . & . & . & . & . \\ 0 & 0 & . & . & . & 1 \end{bmatrix}$$

Where $Q^T = [q_{ij}]^T = [q_{ji}]$ is the transpose Q

So that the solution of the system can then be solved in the form of

$$\alpha * W = X$$
$$\Rightarrow Q * R * W = X$$
$$\Rightarrow (Q^T * Q) * R * W = Q^T * X$$
$$\Rightarrow R * W = Q^T * X$$

Hence

$$W = \left(R^T * Q^T * Q * R\right)^{-1} R^T * Q^T * X$$

$$= \left(R^T * R\right)^{-1} R^T * Q^T * X$$

$$= R^{-1} * Q^T * X \qquad (7.7)$$

7.4 Singular Value Decomposition

Using the singular value decomposition SVD of a matrix in computations, rather than the original matrix, has the advantage of being more robust to numerical error. Additionally, the SVD exposes the geometric structure of a matrix, an important aspect of many matrix calculations. $[\alpha]$ Matrix can be described as a transformation from one vector space to another. The components of the SVD quantify the resulting change between the underlying geometry of those vector spaces.

The Singular Value Decomposition (SVD) is a widely used technique to decompose a matrix into several component matrices, exposing many of the useful and interesting properties of the original matrix. Using the SVD, we can determine the rank of matrix, quantify the sensitivity of a linear system to numerical error, or obtain an optimal lower-rank approximation to the matrix. Our interest in the SVD, from the point of view of learning dynamical systems, is its ability to split a vector space into lower-dimensional subspaces Howard Anton (1993).

In many practical systems however, the author found that either Lay David (1997);

I. The matrix is ill-conditioned and many of the singular values are very small.

II. The matrix is singular and thus singular values with positions that exceed the known rank are meaningless, although for the reasons given above, these may not be identically zero.

More commonly, the matrix $[\alpha]$ will be rectangular containing more or less unknowns than equations and the inverse will not exist. In the case of more known than unknowns, a least squares solution technique is often employed.

The inversion of a highly ill-conditioned matrix has positive and negative components with large magnitudes. In a system with no errors, these components are delicately balanced to nearly cancel each other out to obtain the solution vector $[x]$. However, errors exist in the data and design matrix, which result in the data being unable to clearly distinguish between two or more of the unknowns, tipping the balance.

The singular value decomposition (SVD) is a powerful technique in many matrix computations and analyses. It is employed in a variety of applications, from least squares problems to solving systems of linear equations. Each of these applications exploits the close relation of the SVD to the rank of a matrix and its ability to approximate matrices of a given rank.

An *m-by-n* of matrix $[\alpha]$ can be factorized into:

$$\alpha = USV^T \tag{7.8}$$

Where U is orthogonal *m-by-m* matrix and the columns of the U are the eigenvectors of $\alpha\alpha^T$. Likewise, V is orthogonal *n-by-n* matrix and the columns of the V are the eigenvectors of $\alpha^T\alpha$. The matrix S is diagonal and it is the same size as $[\alpha]$. Its diagonal elements, called sigma, $\sigma_{11},.....,\sigma_{nn}$ are the square roots of the nonzero eigenvalues of both $\alpha\alpha^T$ and $\alpha^T\alpha$. They are the ***singular values*** of matrix $[\alpha]$.

The Singular Value Decomposition (SVD) rewrites the coefficient matrix to three matrices including two orthogonal matrices U, V and a diagonal matrix S i.e., $\alpha = USV^T$. Here,

$$U^T U = VV^T = I = \begin{bmatrix} 1 & 0 & . & . & . & 0 \\ 0 & 1 & . & . & . & 0 \\ . & . & . & . & . & . \\ . & . & . & . & . & . \\ . & . & . & . & . & . \\ 0 & 0 & . & . & . & 1 \end{bmatrix}$$

Where $U^T = [u_{ij}]^T = [u_{ij}], V^T = [v_{ij}]^T = [v_{ij}]$ are the transpose matrices of U and V respectively and S is a diagonal matrix

$$S = \begin{bmatrix} \sigma_{11} & 0 & . & . & . & 0 \\ 0 & \sigma_{22} & . & . & . & 0 \\ . & . & . & . & . & . \\ . & . & . & . & . & . \\ . & . & . & . & . & . \\ 0 & 0 & . & . & . & \sigma_{nn} \end{bmatrix}$$

The coefficient matrices of the system can then be moved to the right hand side of the equal sign.

$$\begin{aligned} &\alpha * W = X \\ &\Rightarrow U * S * V^T * W = X \\ &\Rightarrow (U^T * U) * S * V^T * W = U^T * X \\ &\Rightarrow (S^{-1} * S) * V^T * W = S^{-1} * U^T * X \\ &\Rightarrow (V * V^T) * W = V * S^{-1} * U^T * X \end{aligned}$$

$$W = V * S^{-1} * U^T * X \tag{7.9}$$

Where $S^{-1} = \begin{bmatrix} \sigma_{11} & 0 & . & . & . & 0 \\ 0 & \sigma_{22} & . & . & . & 0 \\ . & . & . & . & . & . \\ . & . & . & . & . & . \\ . & . & . & . & . & . \\ 0 & 0 & . & . & . & \sigma_{nn} \end{bmatrix}^{-1} = \begin{bmatrix} 1/\sigma_{11} & 0 & . & . & . & 0 \\ 0 & 1/\sigma_{22} & . & . & . & 0 \\ . & . & . & . & . & . \\ . & . & . & . & . & . \\ . & . & . & . & . & . \\ 0 & 0 & . & . & . & 1/\sigma_{nn} \end{bmatrix}$$

Another use of the SVD provides a measure, called a condition number, which is related to the measure of linear independence between the column vectors of the matrix. The condition number (with respect to the Euclidean norm) of a matrix $[\alpha]$ is

$$cond(\alpha) = \frac{\sigma_{max}}{\sigma_{min}} \tag{7.10}$$

Where σ_{min} and σ_{max} are the largest and smallest singular values of $[\alpha]$. If $[\alpha]$ is rank deficient, then $\sigma_i = 0$ and we consider $cond(\alpha) = \infty$. Using the condition number, we can quantify the independence of the columns of $[\alpha]$. Note that $cond(\alpha) \geq 1$. If $cond(\alpha)$is close to 1, then the columns of $[\alpha]$ are very independent. When the condition number is large, the columns of $[\alpha]$ are nearly dependent.

As we will see in the next section, the notion of a condition number becomes important in solving linear systems, where $cond(\alpha)$ in some sense measures the sensitivity of the system to noise in the data.

7.4.1 Pseudoinversion By Means of SVD

If a complex matrix $[\alpha]$ is ill-conditioned then the solution of the system

$$\alpha * W = X$$

Is not unique. In such a case the system can be solved by using the pseudoinverse of the matrix $[\alpha]$ (least square approach), which is defined as:

$$\alpha^{+} = (\alpha^{T} * \alpha)^{-1} * \alpha^{T} \tag{7.11}$$

By means of the SVD of $[\alpha]$, its pseudoinversion can be calculated in two steps. During the first step, the SVD of $[\alpha]$ is performed for each frequency line and Eq. (7.11) by means of Eq. (7.6) to:

$$\alpha^{+} = \left([V]^{T}\right)^{-1} * [S]^{-1} * [U]^{T} \tag{7.12}$$

Taking into account that matrices U and V are unitary by definition, it can be obtained:

$$\alpha^{+} = [V] * [S]^{-1} * [U]^{T} \tag{7.13}$$

Consequently, the inversion of the matrix $[\alpha]$ has been reduced to the inversion of a diagonal matrix, which is easily performed. For singular matrices, the meaningless singular values are excluded from the inversion process by introducing regularization in the form of the Moore-Penrose pseudo-inverse or generalized matrix inverse. Golub and Van Loan (1989). Nobel and Daneil (1988).

For ill-conditioned matrices, inclusion of the small singular values in the inversion will lead to problems in obtaining a stable solution. This is because the small singular values are associated with the most ill-posed measurements in the vector $[X]$. As these measurements are inevitably corrupted by noise, the corresponding large reciprocal values in S^{-1} will tend to amplify the noise. It is therefore likely that some regularization of the small singular values will be necessary for ill-conditioned matrices John Mathews and Kurtis Fink (1999).

7.5 QR Decomposition together with Singular Value Decomposition

Both the QR and the SVD algorithms are improvements of the traditional least square method of the matrix $[\alpha]$ is ill conditioned. Therefore, attempts have been made in this study to combine the good features of the QR algorithm and the SVD algorithm. In this case, if,

$$\alpha = Q * R$$

and

$$R = U_R S_R V_R^{T}$$

Then, the correction masses can be estimated, as follows,

$$[W] = [V_R]\,[S_R]^{-1}[U_R]^T[Q]^T[X] \tag{7.14}$$

7.6 Unresolved Issues in Balancing

Normally, balance requirements are stated in terms of a maximum response value at any available measurement point. With exact point methods, this is difficult to achieve with some rotors, sometimes requiring many balance runs with success being highly dependent upon the skill and experience of the individual performing the balance. A major improvement in balancing was introduced by Goodman (1964) with least squares balancing, which allowed balancing to be done with fewer balance weight distributions than measurements. Usually this is employed as a relatively simple minimization of the 2-norm of the final vibration called least squares error balancing. But often least squares balancing will leave a small number of measurement points with high vibrations relative to the rest of the vibration levels.

7.7 SVD Algorithm For Influence Coefficient Balancing

Another frequent complaint in balancing involves the calculation of large balance weights by least squares methods when the rotor unbalance is not large. Sometimes these calculated weights exceed the capacity of balance planes or cannot be applied for other reasons. This problem occurs when the influence coefficient matrix is ill conditioned. Some of the columns of the influence coefficient matrix are or nearly are linearly dependent. The least squares method is not well adapted to solve this problem. Pilkey and Bailey (1979) addressed the min-max balance method using a linear programming approach, separating their technique into time independent and time dependent algorithms. The linear programming method allows the magnitude of the balance weights to be constrained, but the method has not come into extensive industrial practice.

The procedure for computing correction masses, using the (SVD) algorithm, would then be,

$$[W] = [V]\,[S]^{-1}[U]^T[X] \tag{7.15}$$

The behaviour of a complex matrix during its direct inversion can be determined by means of its rank. If the matrix is not of full rank (i.e. its rows (or columns) are not independent), then the matrix will be singular (or nearly singular). Consequently, its direct inversion either cannot be calculated or will have possible errors.

Therefore, it is of major importance to be able to estimate the rank of the matrix. This can be achieved easily by means of SVD. There are (U) and (V) matrices which have all their rows independent as they are unitary by definition. What is remaining is the matrix of the singular values (S). So it is obvious that the rank of the matrix under consideration is equal to the rank of singular values matrix. But the rank of (S) can be easily obtained, since it only consists of diagonal elements and therefore its rank can be retrieved by omitting the singular values which are equal to zero or are very small compared to the non-zero ones.

For most problems using the *m-by-n* influence coefficient matrix, the number of balancing planes (n columns) is smaller than that of measurements (i.e. m rows). For convenience it is reasonable to assume $m \geq n$. This was traditionally handled by Goodman's procedure (1964). The presence of dependent balancing planes would cause the $[\alpha]$ matrix to be ill conditioned. In this case, the (SVD) algorithm provides a better alternative to $[\alpha]^T$ and provides a more reliable estimation of the correction masses while equation 7.7 would have failed.

For the problems of influence coefficient balancing the number of the chosen balance planes and that of the total vibration readings (including vibration measurement points and balance speeds) are n and m respectively. Otherwise influence coefficient consists of magnitude and phase angle' so the influence coefficient matrix $[\alpha]$ is *m-by-n* complex matrix. Here the vector $[X]$ represents the initial unbalance vibration. According to Goodman's procedure, the correction mass can be solved by

$$[W] = \left(\alpha * \alpha^T\right)^{-1} * \alpha^T * X \tag{7.16}$$

In order to identify the existence of non-independent or near non-independent balance planes and avoid possibly resulting in impractical correction masses solved by equation

(7.12), the singular value decomposition of the matrix is used to compute correction masses for influence coefficient balancing. The major procedure of computing correction masses for influence coefficient balancing is outlined as follows:

$$[W]=[U]\,[S]^{-1}[V]^{T}[X] \tag{7.17}$$

It should be mentioned, when equation (7.17) is well conditioned, the correction masses solved by equation (7.17) are consistent with that solved by equation (7.16). However, when some singular values in equation (7.17) are small relative to the uncertainty in elements of $[\alpha]$, it can be considered that there exist non-independent or nearly non-independent balance planes. In this case, the best approximating matrix α^{T} of influence coefficient matrix should substitute $[\alpha]$, then, the correction masses can be solved from (7.17).

For influence coefficient balancing it is almost impossible to give a threshold value that is used to determine whether there exist or not non-independent balance planes since it is difficult to obtain the uncertainty in influence coefficient for various balancing cases. However the important function of the SVD algorithm for influence coefficient balancing is according to the information obtained in orthogonal decomposition of unbalance vibration and correction mass.

7.8 Investigation of The Validation of The Proposed Method

The materials presented in this series of tests are to investigate the new methods of balancing flexible rotors to compute the correction masses for influence coefficient balancing.

The outlined methods involve the least square optimization, QR factorization, singular value decomposition (SVD) and the QR combined with SVD.

7.8.1 Validation and Comparison of Methods

The effectiveness of the methods described has been examined and validated by using case studies (HPT rotor, LPT rotor G rotor). The method tested in the study is as follows,

The basic equation for the influence coefficient method

$$\alpha * W = X \tag{7.18}$$

Where $[X]$is a column vector of observed displacements for the unbalanced shaft, $[\alpha]$ is the matrix of influence coefficients and $[W]$ is an unknown column vector of the effective rotor unbalance related to the corrections planes, to be determined from trial weight tests

$$\alpha_{ij} = \frac{X_{ij} - X_i}{m_j}$$

X_{ij} represents the dynamic motions at location i due to a trial mass force at j.

m_j is the unbalance introduced at location j

In the traditional influence coefficient method, Eq. 7.18 can be expressed in matrix form, as follows,

$$\begin{bmatrix} \alpha_{11} & \alpha_{12} & . & . & . & \alpha_{n1} \\ \alpha_{21} & \alpha_{22} & . & . & . & \alpha_{2n} \\ . & . & . & . & . & . \\ . & . & . & . & . & . \\ . & . & . & . & . & . \\ \alpha_{m11} & \alpha_{m21} & . & . & . & \alpha_{mn} \end{bmatrix} * \begin{bmatrix} W_1 \\ W_2 \\ . \\ . \\ . \\ W_m \end{bmatrix} = \begin{bmatrix} -X_1 \\ -X_2 \\ . \\ . \\ . \\ -X_m \end{bmatrix}$$

Where α_{ij} and X_i are constants, $i = 1,2...m$, $j=1,2...\ n$

- **Standard matrix inversion**

$$(W) = \alpha^{-1} * X$$

- **Standard least square method**

$$(W) = (\alpha^T * \alpha)^{-1} \alpha^T * X$$

- **QR Decomposition with Least Square**

$$W = R^{-1} * Q^T * X$$

- **Singular Value Decomposition**

$$[W] = [V]\,[S]^{-1}[U]^T[X]$$

- **QR Decomposition together with Singular Value Decomposition**

$$[W] = [V_R]\,[S_R]^{-1}[U_R]^T[Q]^T[X]$$

7.8.2 Test Procedures

The above-mentioned method has been applied on the system, which consisted of three rotors (HPT rotor, LPT rotor G rotor).

Firstly the three rotors are balanced, see results tables see A8.4,A8.10 and A8.18, then a known mass was introduced to the system for each rig, in order to find out whether the proposed balancing methods will identify the unbalance masses which had been added to the rotors.

Due to the stability of the experimental system (HPT, LPT and G rotors) we used in the above experimental results, the results achieved shows no different between all methods

(normal solution, least square, QR factorization and SVD) used to calculate the final correction masses.

In the next subsection in this chapter, the author will try some artificial data to demonstrate the proposed methods and the use of plane elimination by using the influence coefficient matrix rank.

7.9 Theoretical (artificial data) demonstrating a new technique based on modified QR and SVD techniques with least square optimization ($A*x=b$)

7.9.1 Introduction

It would be nice if we could get exact solutions to numerical problems. But, the reality is that because problems are continuous while computer calculation is discrete, this is not generally possible.

Stability tells us what is possible (or what we can expect) when solving a problem. i.e., it tells us what it means to get the "right answer" even if this is not the exact answer.

In terms of linear algebra, we want to "solve" an overdetermined system of equations; i.e., $A*x=b$ where A has more rows than columns.

The idea of a least-squares solution is to find the x that minimizes the 2-norm of the residual $r=b-A*x$.

7.9.2 Stability of Least-Squares Algorithms

There are various ways to solve least-squares problems, including the normal equations, QR, and the SVD. We now compare these methods and show that the use of normal equations is generally unstable

Householder, Householder with column pivoting, and SVD produce answers of roughly the same quality. However some least-squares problems will not have full rank. i.e., rank(A) < m, possibly with m < n, so the system of equations is underdetermined. Such problems do not have a unique solution!

Typically the "solution" is specified as the one with minimum norm.

A further complication is that the correct solution depends on rank (A) and determining the rank of a matrix in the face of rounding errors is never a trivial task.
Rank-deficient least-squares problems are fundamentally different to full-rank least-squares problems.

7.9.3 Theoretical (artificial data) Results Discussion

Table A8.27 illustrates the properties and solutions of the examples (see section A8.3). According to the results achieved the elimination of the matrix by using the rank seems to give a better and stable solution.

7.9.3.1 Comparison of Algorithms

1. Solving the normal equations is the cheapest, roughly by a factor of 2. However, we will see that it is much less well conditioned than the other two methods i.e., there can be instabilities (accumulation of roundoff errors)
2. QR is cheaper than SVD when $m \approx n$. It is the method of choice as long as A is not too close to being rank deficient.
3. SVD costs about as much as QR when $m \geq n$ (which is often the case!). It is also the method of choice if A is close to being rank deficient (all data are not independent).

• When $m \leq n$ or $m = n$ and the equations are degenerate or singular.
Degeneracy happens when the equations are not linearly independent. The determinant of a square matrix is zero if and only if it's singular. The number of linearly independent equations is called the rank of **A**. If the rank is less than the size, the matrix is said to be not of **full rank**. Because of this, there is a set of nonzero vectors that produce zero output. These vectors can be added to any solution, and it's still a solution. Therefore the solution is not unique.

The space spanned by the set of vectors that produce zero is called the nullity of A. We would like to know a single solution and the characterize the nullity of **A**.

• When $m = n$ and A is of full rank. We would like to find the unique solution x in a way that is accurate. In some cases the matrix **A** can be nearly singular. In such cases it can be impossible to compute the solution (even though it exists) because of numerical errors. By using a modern computers and integrated by modern programmes such as matlab a few seconds are enough to solve the problem.

• When $m \geq n$, the system is over determined. In this case we would like to find the best compromise solution. Often, the best solution is defined in the sense of least squares.
That is, minimize:

$(A*x-b)^2$

There are many ways to do this. One way is to convert the equations into another linear $n*n$ problem that solves this least squares. This is

$A^T*A*x=A^T*b$

These are called the normal equations of the initial problem. The solution is

$$x=\left(A^T*A\right)^{-1}*A^T*b$$

The matrix $\left(A^T*A\right)^{-1}*A^T$ is called the psuedoinverse. Notice, sometimes $\left(A^T*A\right)^{-1}$ can be solved with a method for well-posed linear systems, but can be singular or nearly so. Therefore, the normal equations for overconstrained systems should be used with caution.

• In some cases we would like to solve

$A*x=b$

for many different b 's

SVD is even more robust and reliable than Householder, but substantially more expensive. In fact, the only fully stable method for solving rank deficient least-squares problems is via SVD, with QR with partial pivoting being almost always stable in practice.

7.10 Results Discussion of a new balancing procedure for flexible rotors based on modified QR and SVD techniques with least square optimization

In this part the QR factorization and singular value decomposition have been introduced to the computation of correction masses for influence coefficient balancing. The singular value of influence coefficient matrix can provide important information for determining the condition of influence coefficient matrix so that non-independent or nearly non-independent balance planes can be effectively identified with the SVD algorithm. By using the SVD algorithm the correction masses for influence coefficient balancing are resolved into several mutually orthogonal components. Therefore, the most adequate correction masses can be selected according the contribution of each correction mass component to reducing unbalance vibration. The purpose of the following tests were to examine the validation of the combination of least square, QR factorization, singular value decomposition (SVD) and the QR combined with SVD (LSQ+QR+SVD)

7.10.1 High Pressure Turbine Rotor

The initial balancing results (table A8.4) were achieved for the HPT rotor by using traditional Influence Coefficient Method (two plane, two measurements locations and one speed).

Tables A8.5-A8.9 show the results of tests held on High Pressure Turbine Rotor by using (3 plane balancing, 5 measurements locations and 4 operation speeds 840,1080,2040,3000 rpm). The known masses added to the system were 50.1 @0° (plane 1), 36.1 g @0° (plane 2). According to the results tables the introduced masses are added in plane 1&3

7.10.2 Low Pressure Turbine Rotor

The initial balancing results (table A8.10) were achieved for the LPT rotor by using traditional Influence Coefficient Method (two plane, two measurements locations and one speed).

Tables A8.11-A8.17 shows the results of tests held on L.P.T rotor by using (4 plane balancing, 5 measurements locations and 4 operation speeds 1500,2040,3000,3600 rpm, the known Masses added to the system were 86.7 @0 (plane 1), 96.3 g @0 (plane 2). According to the results tables the introduced masses are added in plane 1&4

7.10.3 Generator Rotor

The initial balancing results (table A8.18) achieved for the G rotor by using traditional Influence Coefficient Method (two plane, two measurements locations and one speed).

Tables A8.19-A8.26 shows the results of tests held on Generator rotor by using (4 plane balancing, 5 measurements locations and 4 operation speeds 2040,3000,3500,4000 rpm, the known Masses added to the system were 96.4 @0° (plane 1), 91.3 g @0° (plane 2) According to the results tables the introduced masses are added in plane 1&4

7.11 Experimental and Theoretical (artificial data) Results Conclusion

Section A8.3 illustrates the properties and solutions of some theoretical examples (artificial data). According to the results achieved the elimination of the matrix by using the rank seems to give a better and stable solution, also for the summarized results in table A8.27

SVD is even more robust and reliable than Householder, but substantially more expensive. In fact, the only fully stable method for solving rank deficient least-squares problems is via SVD, with QR with partial pivoting being almost always stable in practice.

First of all the system is well balanced comparing the vibration amplitude level before and after balancing procedure. Unfortunately, the results of the proposed method did not show magnificent results as shown in the results table, but some results are quite close to the amount of the introduced masses can be seen in the results tables (targeted amount). Also from the results as you can notice the Least Square method, SVD, and the QR factorization combined with SVD are giving the same amount of results for the three types of rotors and also for all kind of speeds in this particular tests

With the improvements of computer programs (MATLAB) technology and faster complicated mathematical operations, it is recommended to use the proposed methods to answer the influence coefficient matrix to assure the stability and accuracy of the amount of the correction masses and their phase angle, which will assure smooth operation run to the system. Subsequently, we recommend using the SVD method because it can give the right answer whether the matrix well/ill conditioned as we can see from the artificial data taken from different references.

SVD is even more robust and reliable than Householder, but substantially more expensive. In fact, the only fully stable method for solving rank deficient least-squares problems is via SVD, with QR with partial pivoting being almost always stable in practice.

The results achieved in the experimental tests, which held on H.P, L.P, and generator rotors as indicated in the tables shown in appendix 8. The underlined methods have given the same answer for all methods used for calculating the correction masses, which means that the influence coefficient matrices for the all the tests were not rank deficient and were conditioned, but at the same time an example, by using artificial data showed that normal equation, least square and QR decomposition based methods fails if $[\alpha]$ was rank deficient. However since the normal least square method (Goodman's procedure) is the fast way to solve the least square problem. It is the method of choice when the matrix is well – conditioned.

Chapter 8

SHAFT-TO-SHAFT ALIGNMENT

8.1 Introduction

Over the past twenty years, the level of awareness concerning the importance of accurate and precise shaft alignment has increased dramatically. Therefore shaft alignment seems to have become a more important task when installing and maintaining machinery

In today's competitive economic climate rotating machines are driven at higher speeds and placed under more demanding load conditions, whilst modern machine design tends towards lighter weight construction. Such factors render machines more vulnerable to the consequences of misalignment and underwrite the need for effective alignment methods to be applied to the system.

True flexible couplings can withstand substantial misalignment, but these couplings may transfer misalignment forces into other machine components such as mechanical seals, bearings and shafts that are not designed to withstand these excessive misalignment forces.

It is generally agreed that proper alignment is critical to the life of the machine and coupling wear, bearing failures, bent rotors, plus bearing housing damage are all common results of poor alignment Eisenmann (1998). We also know that loads on mechanical parts, such as bearings, seals, and couplings, decrease with improved alignment.

This research determines experimentally, the effect of shaft alignment to balanced rotors. Previous studies (Piotrowski (1986), Prabhu (1997), Simon (1992)) have indicated that there seems to be a correlation between machine misalignment, and machine vibration. It has long been known that machines that were not in good alignment vibrated at characteristic frequencies, but direct research on balancing have been rare.

8.2 Definitions of Shaft Misalignment

Shaft misalignment can be divided into two components: offset misalignment, and angular misalignment. As can be seen in Figures 2.4,2.5 (chapter 2) and as these names suggest, offset (or parallel) misalignment occurs when the centerlines of two shafts are parallel but do not meet at the power transfer point, and angular misalignment occurs when the centerline of two shafts intersect at the power transfer point but are not parallel. Often misalignment in actual machinery exhibits a combination of both types of misalignment Figures 2.6. (Piotrowski, 1995).

8.3 The Objective Of Accurate Alignment

In simple terms, the objective of shaft alignment is to increase the operating life of rotating machinery. To achieve this goal, machinery components that are most likely to fail must operate within their design limits. Since the components that are most likely to fail are the bearings, seals, coupling, and shafts, accurately aligned machinery must achieve the following results:

- Reduce excessive axial and radial forces on the bearings to ensure longer bearing life and rotor stability under dynamic operating conditions.
- Minimize the amount of shaft bending from the point of power transmission in the coupling to the coupling end bearing.
- Minimize the amount of wear in the coupling components.
- Maintain proper internal rotor clearances.
- Eliminate the possibility of shaft failure from cyclic fatigue.
- Lower vibration levels in machine casings, bearing housings, and rotors

8.4 Alignment Methods In Comparison

There are a number of different methods whereby acceptable rotating machine alignment can be achieved. These range from an inexpensive straight edge to the more sophisticated and inevitably more expensive laser systems. We can condense these methods into three basic categories:

- Eyesight - straightedge and feeler gauges
- Dial indicators - mechanical displacement gauges
- Laser alignment systems

Each category of course has a number of options contained within it. We can, however, generally review the benefits and limitations of each method, as follows:

The straightedge has been used quite often for alignment figure 8.1, because it's cheap and simple. However, since the resolution of the human eye is limited and will vary from person to person, alignment accuracy is correspondingly limited. The corrective values for machine feet are usually estimated according to the experience of the alignment engineer, who must know the particular machine involved quite well. The result of this type of alignment is repeated until the machine is more or less aligned, and even then, the accuracy of results usually leaves much to be desired.

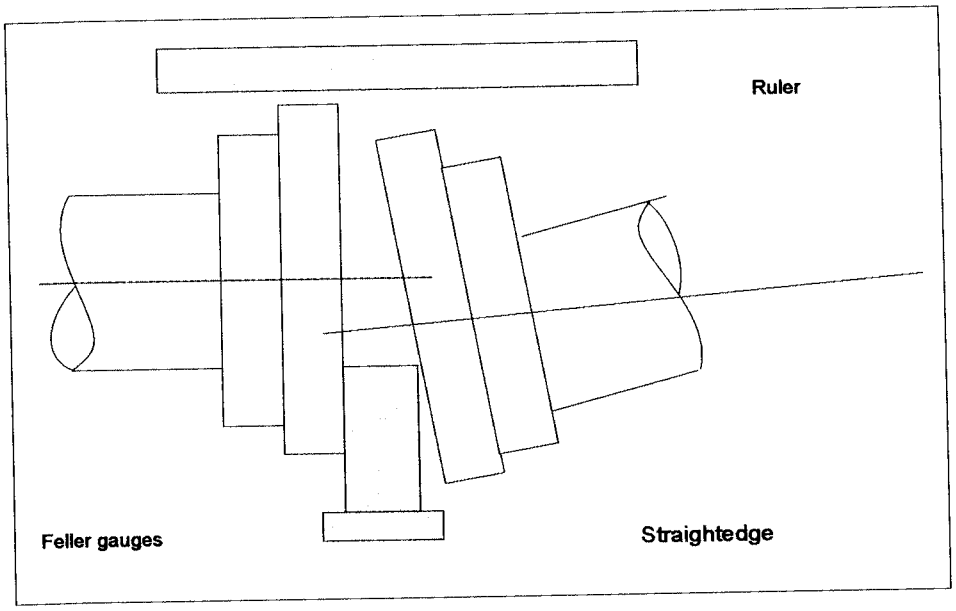

Figure 8.1 Straightedge methods

Dial gauges represent a considerable advancement over the straightedge, as measuring accuracy of 1/100mm, (ten times that of straightedges) may be obtained - provided that the operator has the necessary training and experience to mount the hardware and carry out the procedures properly. In practice, however, alignment accuracy with dial indicators often

ends up being compromised due to operator errors or failure to make adequate compensation for the mechanical fixturing required for mounting the dial indicators Piotrowski (1995).

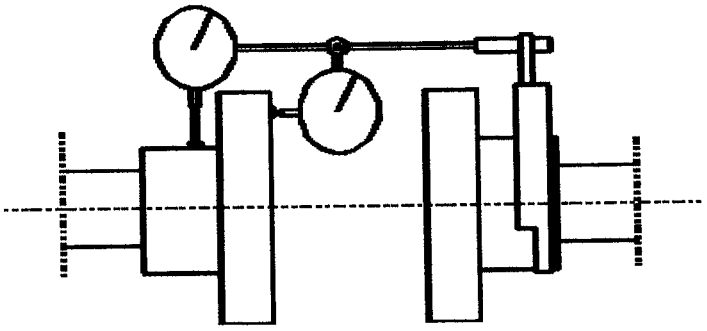

Figure 8.2 Face-Rim Method (world pump July 2001)

8.4.1 Examples of errors:

Indicator bracket sag: should always be measured before actual alignment readings are taken. (World pump July 2001)

Internal friction: sometimes the gauge must be tapped in order for the indicator needle to settle on its final value. (World pump July 2001)

1/100mm resolution: up to 0.005mm rounding error may occur with each reading - for a total of up to 0.04mm error in values used for result calculations. This may easily be compounded several times by the time coupling or machine foot results are obtained. (World pump July 2001)

Reading errors: simple human errors that occur all too often when dials must be read under cramped poorly lit conditions and severe time constraints. These are often compounded by having to read dials upside down or front-to-back (using a mirror) at the various shaft rotation positions required for alignment measurement. (World pump July 2001)

Axial shaft play: can affect face readings taken to measure angularity unless two axially mounted gauges are used. (World pump July 2001)

8.5 Laser Alignment

Recent advances in laser alignment technology have made it possible to align the machines, within very tight tolerances. A good laser alignment system should have an accuracy of shaft alignment conditions at least 0.00254 mm [prufteknik manual]. Detection of misalignment has been made simple, but achieving the alignment condition is still a time consuming effort. Often, several iterations are required to reach the desired alignment

8.5.1 Laser Alignment Equipment Mounting

An example of a laser system is shown in Figures 8.3,8.4. The detector is a biaxial, analog photoelectric semiconductor position detector with a resolution of 1 micron. The linearization characteristics of each laser detector are unique and are stored in the systems computer.

The laser transmitter is attached to the shaft of the driving machine and the reflector is attached to the shaft of the machine to be moved. The prism reflects the beam in a plane parallel to that in which it receives the beam. The computer receives its input data directly from the detector through a connecting cable and calculates the alignment correction values for the feet of the machine to be moved. In properly installed equipment, there are no outside forces or strains on the bearings or shafts. A laser alignment system eliminates the effects of irregular shaft or coupling surfaces, eccentricity, bent shafts, etc. Unlike conventional methods using dials gauges where a spanner bar is used, there is no sag in the laser beam. The effects of vibration on the alignment process are insignificant, as the laser beam travels at the speed of light.

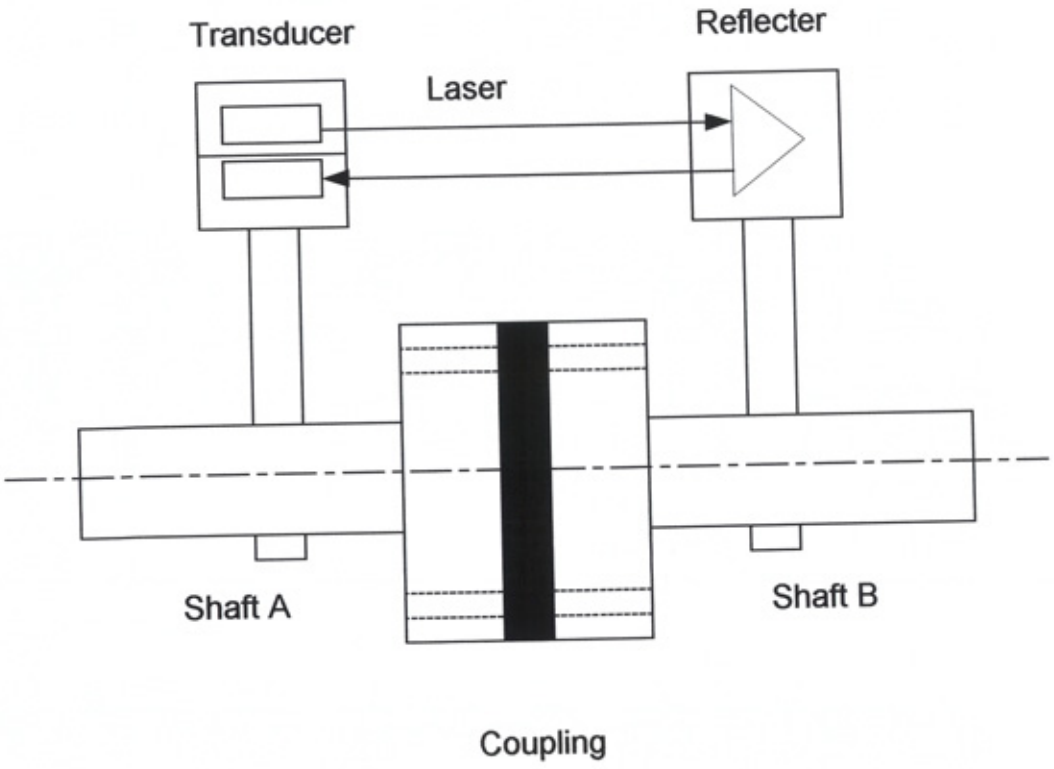

Figure 8.3 sketch of Laser alignment set up

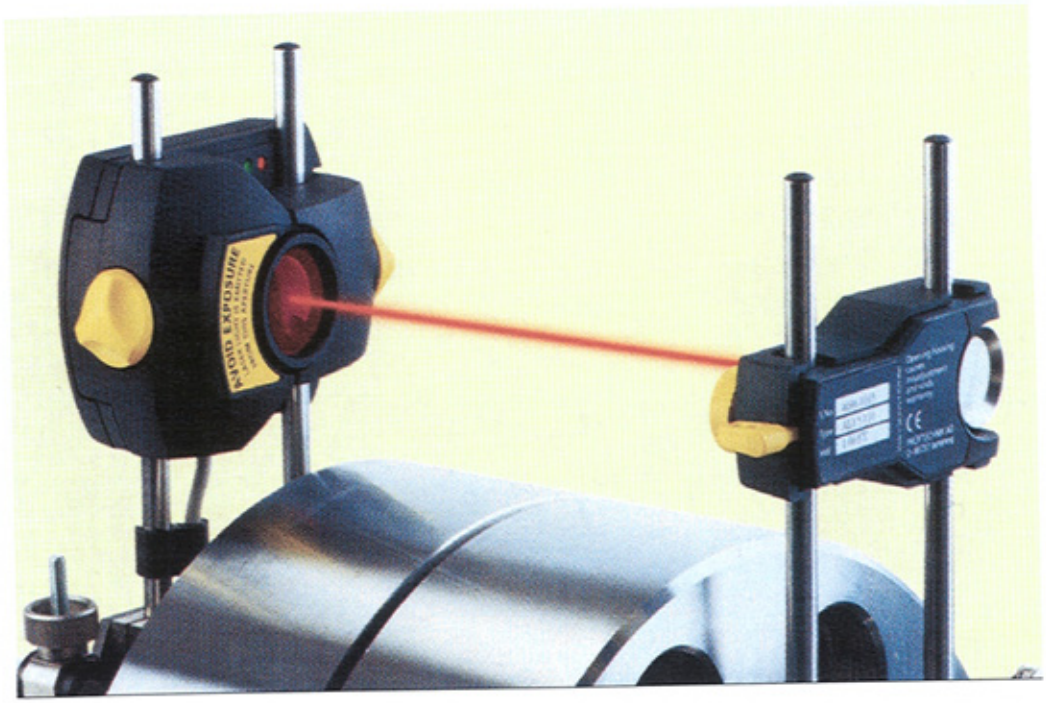

Figure 8.4 Laser alignment set up (pruftechnik manual)

8.5.2 summary of some of the benefits of laser alignment

- Precision alignment with no manual data input or interpretation
- Graphic display of alignment results at coupling and machine feet
- No mechanical fixtures bracket sag
- No need to disassemble the coupling
- Accurate and repeatable results across a wide range of engineering skills
- No need to take readings at predetermined locations or clock positions
- Data storage and print out of results for report generation
- Traceable calibration of system accuracy.

8.5.3 Disadvantage of Using Laser Alignment

Alignment accuracy affected by ambient light and airborne particles.

8.6 Implementing Alignment Standards

Based on the manufacture's data of the alignment equipment (Pruftechnik), used in this study, Table 8.1 shows the accuracy achievable based upon many years of experience in supplying laser systems to industry. These standards are a good guide to upper and lower limits that will improve plant-operating condition.

Misalignment can be classified into four grades, as follows,

1. Unsafe: the degree of misalignment is outside the tolerance limit.

2. Poor: the degree of misalignment is inside the tolerance limit but outside the recommended limit.

3. Acceptable: the degree of misalignment is in the recommended range for operating.

4. Excellent: the degree of misalignment is close to perfect alignment.

A tolerance chart is shown in table 8.1 that will help in establishing a goal for doing the alignment.

Suggested Shaft Alignment Tolerances					
	PRM	Metric (mm)		Inch (mils)	
Soft foot	Any	0.06 mm		2.0 mils	
Offset		Acceptable	Excellent	Acceptable	Excellent
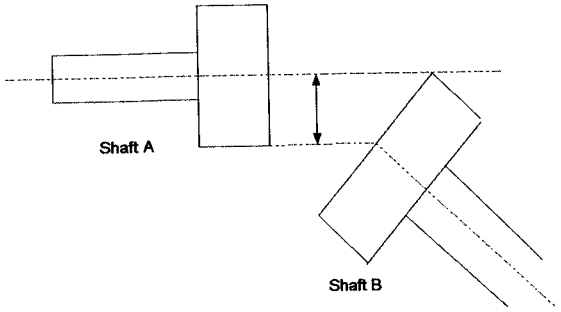	600			9.0	5.0
	750	0.19	0.09		
	900			6.0	3.0
	1200			4.0	2.5
	1500	0.09	0.06		
	1800			3.0	2.0
	3000	0.06	0.03		
	3600			1.5	1.0
	6000	0.03	0.02		
	7200			1.0	0.5
Angularity	600			15.0	10.0
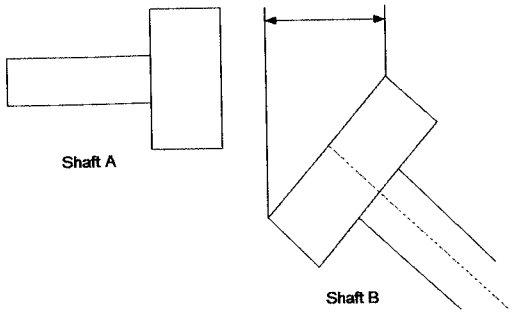	750	0.13	0.09		
	900			10.0	7.0
	1200			8.0	5.0
	1500	0.07	0.05		
	1800			5.0	3.0
	3000	0.04	0.03		
	3600			3.0	2.0
	6000	0.03	0.02		
	7200			2.0	1.0

Table 8.1 Alignment tolerances according to RPM (Pruftechnik company manual)

8.7 Procedure for Experimental Investigation

The following sections describe the procedures applied to the experimental investigation.

Shims are inserted into the system (underneath the bearing pedestals), in order to introduce a misaligned state to the system and consequently increase the vibration amplitude. The shims have a thickness of 0.3 mm

8.7.1 Shaft alignment equipment

An OPTALIGN PLUS was used to measure the shaft-to-shaft alignment, with the OPTALIGN PLUS PC DISPLAY software running. The alignment readings obtained can be seen and stored on the OPTALIGN PLUS laser system for reporting and results.

The connection of the alignment equipment to the system High Pressure Turbine (HPT) and Low Pressure turbine (LPT) (HPT ⇔LPT) rotors are shown in Figures 8.5 and 8.6. The most important requirement for any shaft alignment system is repeatability of the readings. This is evaluated with a 360 deg repeatability test. (The symbol ⇔ means the shaft connection)

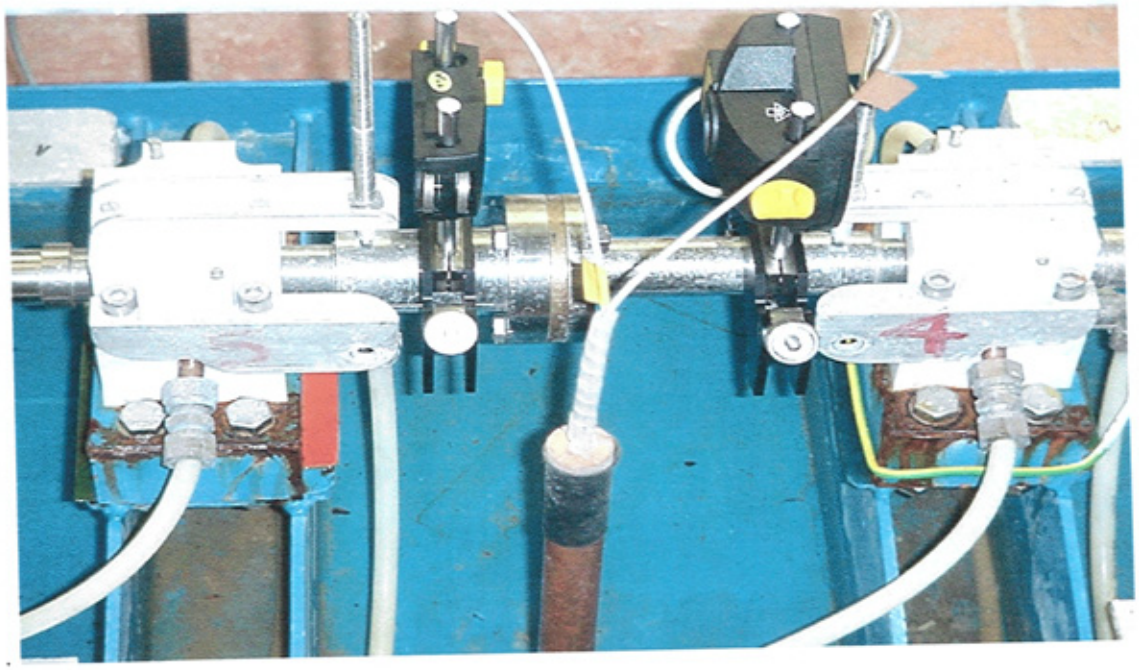

Figure 8.5 laser alignment equipment connected to the system

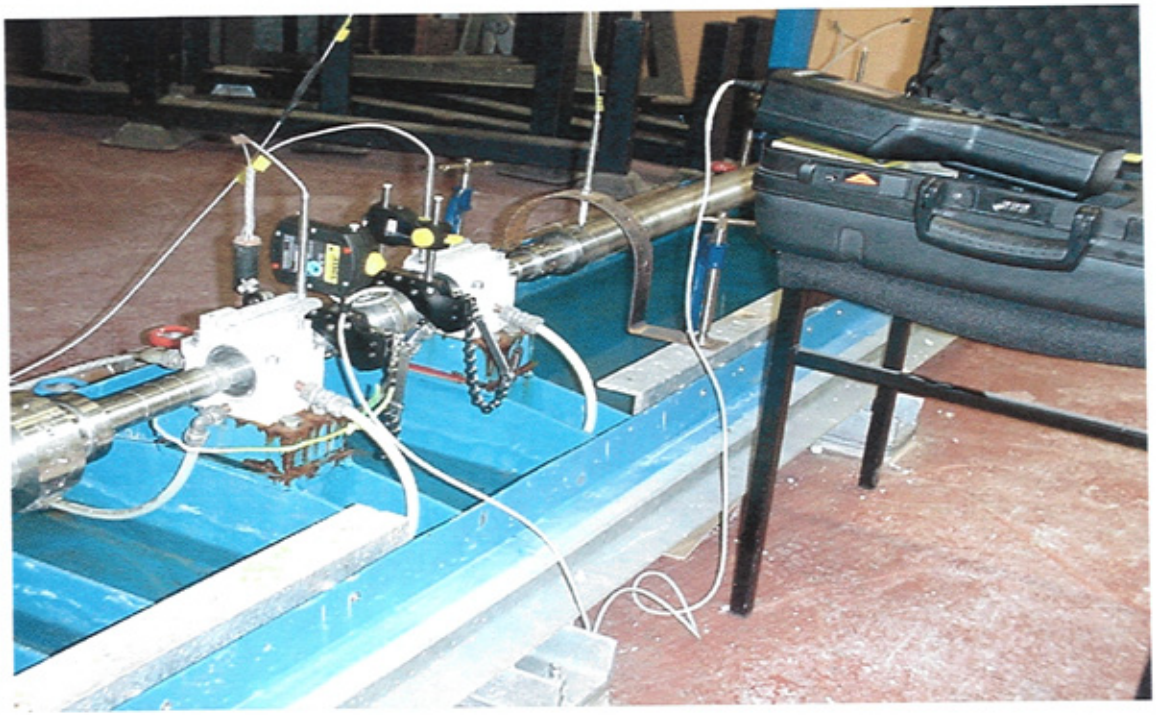

Figure 8.6 over view for the laser alignment equipment connection

8.8 Tests Procedures

All changes in alignment were made to the system (multi shaft-multi bearings). Misalignment conditions were varied in the following order for **HPT⇔ LPT rotors** and **HPT+ *LPT Rotors*⇔G Rotor:**

- ❖ Offset misalignment
- ❖ Angular misalignment
- ❖ Combination of offset and angular misalignment

The High-pressure turbine and Low-pressure turbine Rotors coupling has a 65mm diameter figure 8.7, whereas the Low-pressure turbine and generator Rotors has a 70mm diameter figure 8.8.

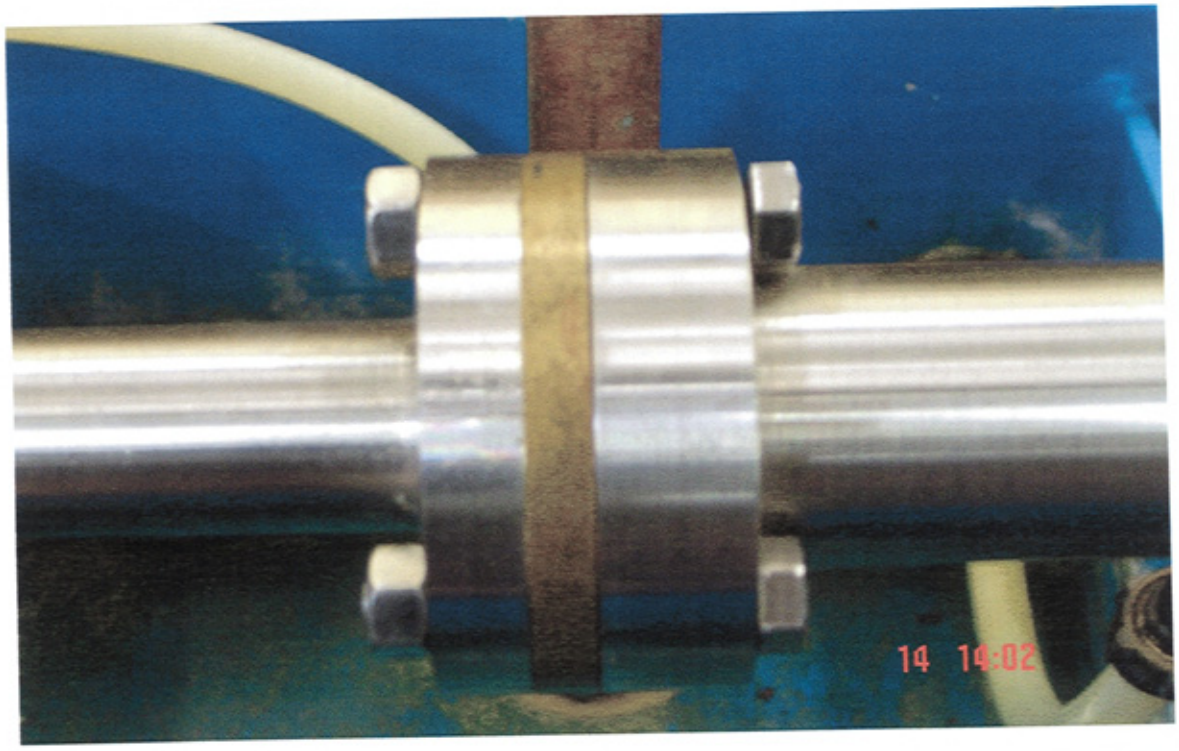

Figure 8.7 HPT rotor and LPT rotor rigid coupling

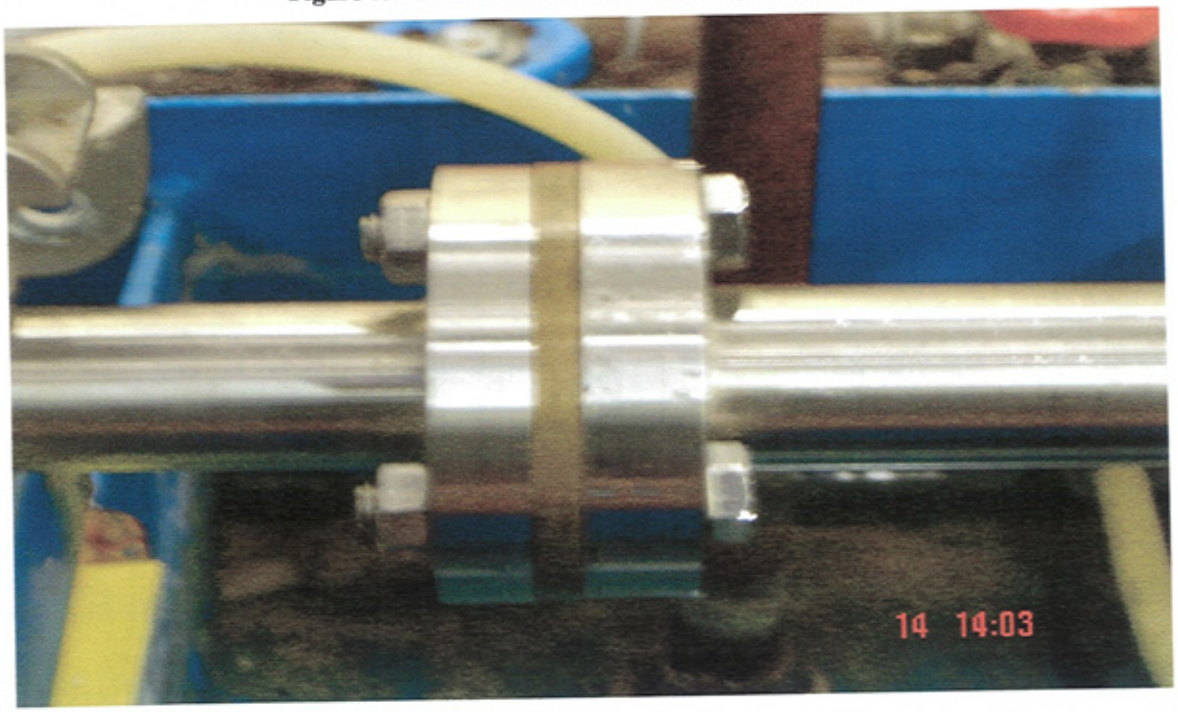

Figure 8.8 LPT rotor and G rotor rigid coupling

8.8.1 Initial Data

Align and Balance the HPT⇔ LPT Rotors in order to make sure that the system is well aligned and balanced, which was the purpose of the first set of the tests.

8.8.2 Effect of Misalignment Shafts on Balanced Rotors

After ensuring that the system is well balanced, the desired test requires the introduction of misalignment to the system HPT⇔ LPT Rotors. The sequence of the test was as mentioned by adding 2X0.3 mm shim to the bearing baseplates, in order to achieve parallel, angular and angular & parallel misalign shafts. The HPT rotor was the fixed part, to which the laser transducer was attached and the LPT Rotor was the moving part, to which the reflector was attached.

- Introduce offset misalignment to the system, and then record the alignment measurements
- Introduce Angular misalignment to the system, and then record the alignment measurements
- Introduce Offset & Angular misalignment to the system, and then record the alignment measurements

8.8.3 Effect of unbalanced rotors on aligned shafts

After finishing the previous listed tasks, we would investigate the effect of unbalanced rotors on aligned shafts, so that, the system was well aligned again, and then an unbalance masses was added to the system, in order to have an imbalanced system.

- Introduce known mass to the system (just to keep the system in unbalance state), and then check the alignment

8.9 Alignments and Balancing Results

Using OPTALIGN PLUS for the misalignment experiments to collect data. For all cases, the data was transferred to the OPTALIGN PLUS software then analyzed to determine the

change in the expected coupling condition with respect to the misalignment condition. The balancing data was analysed by using a Matlab program written by the author.

8.9.1 HP connected to LP Rotors Tests Results

8.9.1.1 Initial Alignment

Figure 8.9 is a diagram plotted from the prufftecknik software provided with the equipment used in these tests. Table 8.2 shows the set up dimensions of H.P.T rotor connected to L.P.T Rotor. The rotors are connected via rigid coupling and the test speed was 3000 rpm.

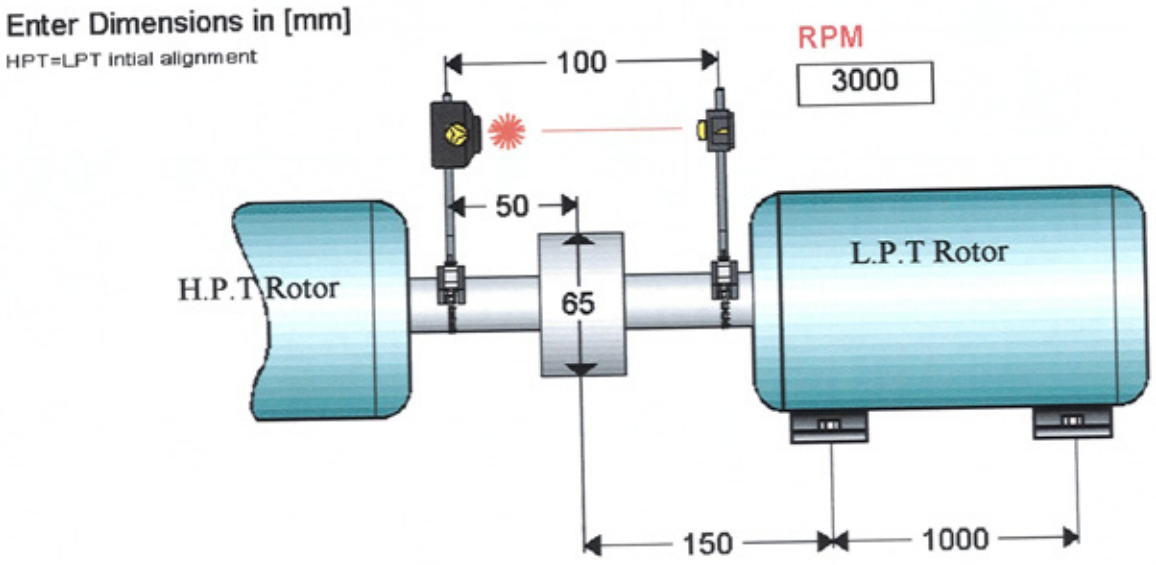

Figure 8.9 HPT& LPT connection dimensions (diagram plotted from the prufftecknik software provided with equipment used in these tests)

Rotors Dimensions		
Coupling diameter	65	mm
Rotational speed	3000	rpm
Transducer to coupling	50	mm
Transducer to reflector	100	mm
Coupling to left foot, Right rotor	150	mm
Coupling to right foot, Right rotor	1000	mm

Table 8.2 shaft alignment dimensions

The purpose of the test was to ensure that the system was well aligned. Figure 8.10 is the diagram plotted from the prufftecknik software, which showing the test results. Table 8.3 shows the amount of angular, offset misalignment and soft foot. For example as you can see from the table the amount of the Vertical Angular Misalignment was -0.01 mm which means that a 0.01 mm shim was required to be added. (A minus results means adding shims and a plus results means removing shims)

Note that, the "smiling" or "sad" faces indicate whether the displayed alignment condition fell within tolerances or not, for the RPM involved

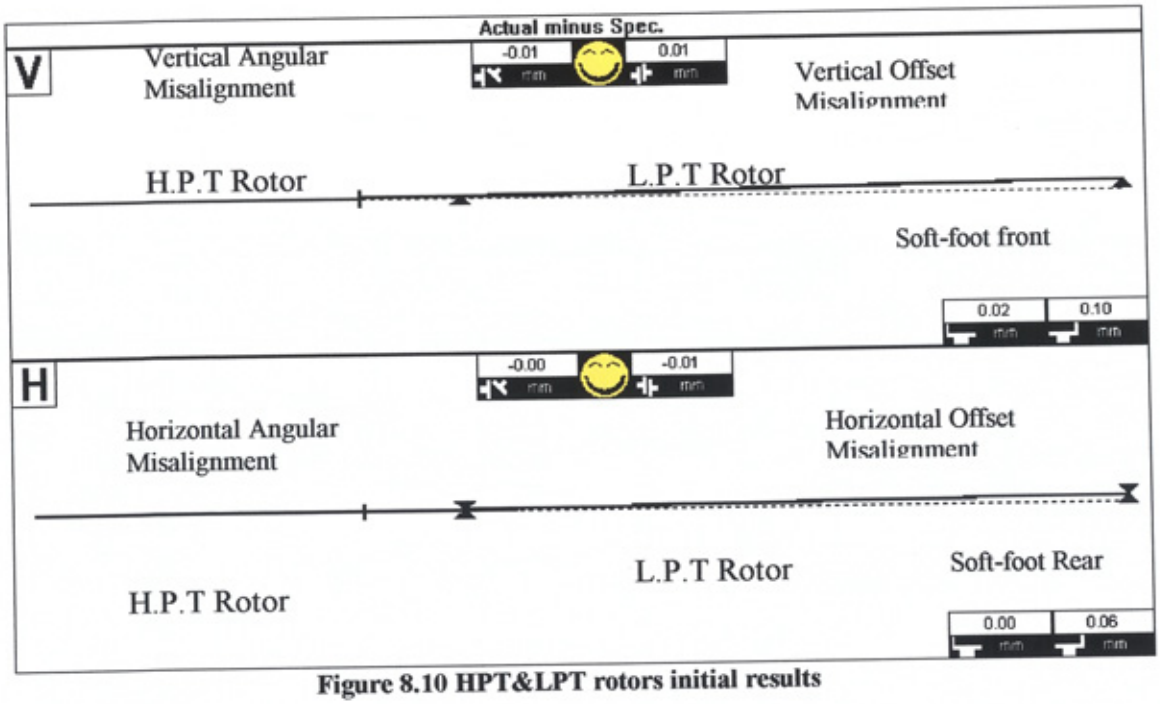

Figure 8.10 HPT&LPT rotors initial results

Measurements Mode	Misalignment results
Vertical Angular Misalignment	-0.01 mm
Vertical Offset Misalignment	0.01 mm
Horizontal Angular Misalignment	-0.00 mm
Horizontal Offset Misalignment	-0.01 mm
Soft-Foot correction values L.P.T Rotor	
Left foot front	-0.02 mm
Right foot front	-0.10 mm
Left foot rear	-0.00 mm
Right foot rear	-0.06 mm

Table 8.3 results tables of initial alignment

8.9.1.2 Results of the balancing HPT & LPT rotors after alignment

The purpose of the test is to ensure that the system is well balanced. Table 8.4 shows the measurements of vibration amplitude and phase angle, also the amount of correction mass required to balance the system.

Results of the balancing HPT & LPT rotors after alignment									
Run	T. Mass	Vibration amplitude (mm)				Phase angle (deg)			
		Plane (1) 29.3mm	Plane (2) 37.05mm	Plane (3) 48.6mm	Plane (4) 48.6mm	Plane (1) 29.3mm	Plane (2) 37.05mm	Plane (3) 48.6mm	Plane (4) 48.6mm
0	33.5@60°	0.2882	0.2198	0.5006	0.7424	238.6667	200.5904	221.5385	205.9615
1		0.1490	0.2076	0.6960	0.8718	233.1818	199.5455	257.1429	235.8621
2		0.3126	0.2608	0.3516	0.6203	240.0000	201.9188	183.1579	202.9956
3		0.3175	0.2344	0.4420	0.4689	121.5584	140.7407	321.4286	344.0000
4		0.2955	0.1954	0.4103	0.7131	238.0645	205.3012	154.9180	164.4444
Vibration after balancing		0.1032	0.1152	0.2743	0.4352	205.1286	244.5154	311.3657	186.5243

Correction masses/phase			
Plane (1) 29.3mm	Plane (2) 37.05mm	Plane (3) 48.6mm	Plane (4) 48.6mm
23.7290 @18.5524	27.1793 @104.6661	25.8600 @79.0162	47.4090 @48.5887

Table 8.4 data and results of initial balancing

8.9.1.3 Parallel Misalignment

2X0.3(mm) were added to the system to ensure that the system was in a parallel misaligned state. Table 8.5 shows the amount of angular, offset misalignment and soft foot. For example as you can see from the table the amount of the Vertical offset Misalignment was 0.09 mm which means that the system is in a misalignment condition. Table 8.6 shows the amount of vibration amplitude and phase angle when the system in the misalignmed condition. As we can see from the results the amount of the vibration amplitude near the coupling (plane 2 &3) is higher than the other positions.

Measurements Mode	Misalignment results
Vertical Angular Misalignment	0.02 mm
Vertical Offset Misalignment	0.09 mm
Horizontal Angular Misalignment	-0.05 mm
Horizontal Offset Misalignment	-0.11 mm
Soft-Foot correction values L.P.T Rotor	
Left foot front	-0.05 mm
Right foot front	0.26 mm
Left foot rear	-0.01 mm
Right foot rear	-0.79 mm

Table 8.5 results of parallel misalignment

Vibration amplitude (mm)				Phase angle (deg)			
Plane (1) 29.3mm	Plane (2) 37.05mm	Plane (3) 48.6mm	Plane (4) 48.6mm	Plane (1) 29.3mm	Plane (2) 37.05mm	Plane (3) 48.6mm	Plane (4) 48.6mm
1.2796	3.5995	3.797	1.3623	345.2459	352.6230	217.2131	117.23469

Table 8.6 Data of Vibration amplitude and phase angle for HPT & LPT rotors after introducing parallel misalignment

8.9.1.4 Angular Misalignment

2X0.3(mm) were added to the system to ensure that the system was in angular misaligned state. Table 8.7 shows the amount of angular, offset misalignment and soft foot. For example as you can see from the table the amount of the Horizontal Angular Misalignment was -0.04 mm, which means that, the system is in misalignment condition. Table 8.8 shows the vibration amplitude and phase angle when the system in the misaligned condition. As

we can see from the results the amount of the vibration amplitude near the coupling (plane 2 &3) is also higher than the other positions.

Measurements Mode	Misalignment results
Vertical Angular Misalignment	0.02 mm
Vertical Offset Misalignment	0.04 mm
Horizontal Angular Misalignment	-0.04 mm
Horizontal Offset Misalignment	-0.03 mm
Soft-Foot correction values L.P.T Rotor	
Left foot front	0.01 mm
Right foot front	0.35 mm
Left foot rear	-0.05 mm
Right foot rear	-0.61 mm

Table 8.7 results of angular misalignment

Vibration amplitude (mm)				Phase angle (deg)			
Plane (1) 29.3mm	Plane (2) 37.05mm	Plane (3) 48.6mm	Plane (4) 48.6mm	Plane (1) 29.3mm	Plane (2) 37.05mm	Plane (3) 48.6mm	Plane (4) 48.6mm
1.0720	3.4428	3.801	1.9634	90.0548	96.9796	156.3934	317.2551

Table 8.8 Data of Vibration amplitude and phase angle for HPT & LPT rotors after introducing angular misalignment

8.9.1.5 Parallel and Angular Misalignment

2X0.3(mm) were added to the system vertically and horizontally to ensure that the system is in offset and angular misaligned state. Table 8.9 shows the amount of angular, offset misalignment and soft foot. For example as you can see from the table the amount of the Horizontal Angular Misalignment was -0.03 mm and, Vertical Offset Misalignment was -0.09 mm, which means that, the system is in a misaligned condition. Table 8.10 shows the vibration amplitude and phase angle when the system is in the misaligned condition. As we can see from the results the vibration amplitude near the coupling (plane 2 &3) is also higher than the other positions.

Measurements Mode	Misalignment results
Vertical Angular Misalignment	0.02 mm
Vertical Offset Misalignment	0.09 mm
Horizontal Angular Misalignment	-0.03 mm
Horizontal Offset Misalignment	-0.04 mm
Soft-Foot correction values L.P.T Rotor	
Left foot front	-0.04 mm
Right foot front	0.31 mm
Left foot rear	-0.03 mm
Right foot rear	-0.47 mm

Table 8.9 results of parallel and angular misalignment

Vibration amplitude (mm)				Phase angle (deg)			
Plane (1) 29.3mm	Plane (2) 37.05mm	Plane (3) 48.6mm	Plane (4) 48.6mm	Plane (1) 29.3mm	Plane (2) 37.05mm	Plane (3) 48.6mm	Plane (4) 48.6mm
1.5092	3.5238	3.6093	1.9585	98.4490	133.6935	346.7213	120.9836

Table 8.10 Data of Vibration amplitude and phase angle for HPT & LPT rotors after introducing parallel and angular misalignment

8.9.1.6 After Finishing The Tests (HP connected to LP Rotors)

The purpose of this test is to ensure that the system is in a well-aligned state. Table 8.11 shows the amount of angular, offset misalignment and soft foot. For example as you can see from the table the amount of the Horizontal Angular Misalignment was -0.01 mm and, Vertical Offset Misalignment was 0.00 mm, which means that, the system is in good condition. Table 8.12 shows the data and results of the balancing test. The balancing test was also to keep the rotors in a well balanced state. The vibration amplitude and phase angle when the system was in aligned condition are acceptable.

Measurements Mode	Misalignment results
Vertical Angular Misalignment	-0.00 mm
Vertical Offset Misalignment	0.00 mm
Horizontal Angular Misalignment	-0.01 mm
Horizontal Offset Misalignment	-0.00 mm
Soft-Foot correction values L.P.T Rotor	
Left foot front	-0.00 mm
Right foot front	0.00 mm
Left foot rear	-0.03 mm
Right foot rear	-0.23 mm

Table 8.11 results after finishing the tests

Results of the balancing HPT & LPT rotors after been alignment									
Run	T. Mass	Vibration amplitude (mm)				Phase angle (deg)			
		Plane (1)	Plane (2) 37.05mm	Plane (3) 48.6mm	Plane (4) 48.6mm	Plane (1) 29.3mm	Plane (2) 37.05mm	Plane (3) 48.6mm	Plane (4) 48.6mm
0		0.4490	0.3876	0.6960	0.8718	50.7383	31.5207	46.3366	221.5385
1	33.8@60°	0.3126	0.5608	0.5516	0.6203	233.1818	199.5455	257.1429	128.8621
2		1.3504	1.2845	1.0574	1.4090	240.0000	201.9188	183.1579	202.9956
3		1.5311	1.3040	1.0647	1.3895	73.0070	48.6598	326.5979	120.0000
4		1.3284	1.1575	0.9499	1.2943	238.0645	205.3012	282.0619	334.2857
Vibration after balancing		0.2435	0.1851	0.3658	0.3320	63.1351	288.6923	299.2354	285.2514

Results of the balancing HPT & LPT rotors after been alignment			
Correction masses/phase			
Plane (1) 29.3mm	Plane (2) 37.05mm	Plane (3) 48.6mm	Plane (4) 48.6mm
14.8176@ 43.1780	30.1105 @ -128.6921	54.7733 @ -128.4081	29.1208 @ -83.9798

Table 8.12 Balancing data and results after finishing the tests

8.9.1.7 Alignment Results After Adding Known Mass to The System

Known masses were added to the system to ensure that the system was in an unbalanced state. Table 8.13 shows the vibration amplitude and phase angle along the rotors. The vibration levels have increased significantly comparing them with the initial balanced results. The system run until reach the steady state condition which typically was between 2-3 minutes to measure the shaft misalignment.

Table 8.14 shows the amount of angular, offset misalignment and soft foot. For example as you can see from the table the amount of the Horizontal Angular Misalignment was -0.03 mm and, Vertical Offset Misalignment was 0.09 mm, which means that, if the system is in unbalance condition, the alignment state of the system has to be checked, as in this case the alignment results show that the system needs to be aligned.

Vibration amplitude (mm)				Phase angle (deg)			
Plane (1) 29.3mm	Plane (2) 37.05mm	Plane (3) 48.6mm	Plane (4) 48.6mm	Plane (1) 29.3mm	Plane (2) 37.05mm	Plane (3) 48.6mm	Plane (4) 48.6mm
1.8359	3.8021	3.66983	2.4866	237.2185	232.1633	194.7395	231.6832

Table 8.13 Data of Vibration amplitude and phase angle for HPT & LPT rotors after introducing unbalance mass

Measurements Mode	Misalignment results
Vertical Angular Misalignment	0.02 mm
Vertical Offset Misalignment	0.09 mm
Horizontal Angular Misalignment	-0.03 mm
Horizontal Offset Misalignment	-0.03 mm
Soft-Foot correction values L.P.T Rotor	
Left foot front	0.04 mm
Right foot front	-0.32 mm
Left foot rear	0.03 mm
Right foot rear	0.47 mm

Table 8.14 results of alignment after adding known mass to the system

8.9.2 LP and G Rotors Alignment Tests Results

Figure 8.16 is a diagram plotted from the prufftecknik software provided with equipment used in these tests. Table 8.15 shows the set up dimensions of H.P.T rotor connected to L.P.T Rotor and G. rotor. The rotors are connected via rigid couplings and the test speed was 3000 rpm.

8.9.2.1 Initial Alignment

The purpose of the test was to ensure that the system was well aligned. Table 8.16 shows the amount of angular, offset misalignment and soft foot. For example as you can see from

the table the amount of the Vertical Angular Misalignment was -0.01 mm, which means that, the system was well aligned.

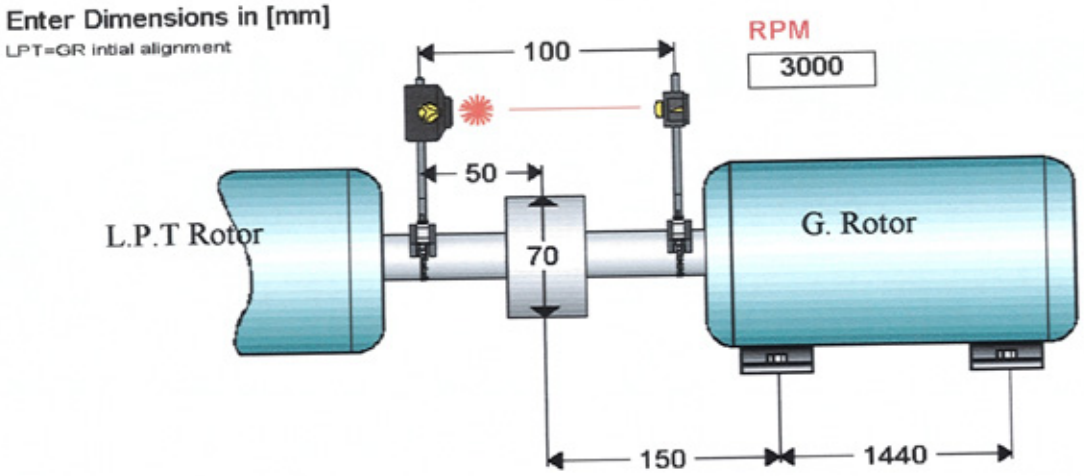

Figure 8.11 LPT & G. Rotor connection dimensions

Rotors Dimensions		
Coupling diameter	70	mm
Rotational speed	3000	rpm
Transducer to coupling	50	mm
Transducer to reflector	100	mm
Coupling to left foot, Right rotor	150	mm
Coupling to right foot, Right rotor	1440	mm

Table 8.15 LPT & G. Rotor connection dimensions

Measurements Mode	Misalignment results
Vertical Angular Misalignment	-0.01 mm
Vertical Offset Misalignment	-0.01 mm
Horizontal Angular Misalignment	-0.00 mm
Horizontal Offset Misalignment	0.00 mm
Soft-Foot correction values L.P.T Rotor	
Left foot front	-0.01 mm
Right foot front	-0.15 mm
Left foot rear	-0.01 mm
Right foot rear	-0.10 mm

Table 8.16 results of initial alignment test

8.9.2.2 Balancing After Alignment Results (LP⇔G Rotors)

The purpose of the test was to ensure that the system was well balanced. Table 8.17 shows the measurements of vibration amplitude and phase angle, also the amount of correction mass required to balance the system.

Results of the balancing LPT & G rotors after been alignment									
Run	T. Mass	Vibration amplitude (mm)				Phase angle (deg)			
		Plane (1) 29.3mm	Plane (2) 37.05mm	Plane (3) 48.6mm	Plane (4) 48.6mm	Plane (1) 29.3mm	Plane (2) 37.05mm	Plane (3) 48.6mm	Plane (4) 48.6mm
0		0.4490	0.3876	0.6960	0.8718	50.7383	31.5207	46.3366	221.5385
1	33.6@60°	0.3126	0.5608	0.5516	0.6203	233.1818	199.5455	257.1429	128.8621
2		1.3504	1.2845	1.0574	1.4090	240.0000	201.9188	183.1579	202.9956
3		1.5311	1.3040	1.0647	1.3895	73.0070	48.6598	326.5979	120.0000
4		1.3284	1.1575	0.9499	1.2943	238.0645	205.3012	282.0619	334.2857
Vibration after balancing		0.2936	0.3010	0.4016	0.5294	66.7254	93.3258	263.9830	19.2158

Correction masses/phase			
Plane (1) 29.3mm	Plane (2) 37.05mm	Plane (3) 48.6mm	Plane (4) 48.6mm
54.4492@ 43.1780	29.9323@ -128.6921	28.9484@ -128.4081	14.7299@ -83.9798

Table 8.17 Results of the balancing LPT & G rotors after been alignment

8.9.2.3 Parallel Misalignment

2X0.3(mm) shims were added to the system to ensure that the system was in a parallel misaligned state. Table 8.18 shows the amount of angular, offset misalignment and soft foot. For example as you can see from the table the amount of the vertical offset Misalignment was 0.16 mm which means that the system is in a misaligned condition. Table 8.19 shows the vibration amplitude and phase angle when the system was in a misaligned condition. As we can see from the results of the vibration amplitude near the coupling (plane 2 &3) is higher than the other positions.

Measurements Mode	Misalignment results
Vertical Angular Misalignment	-0.03 mm
Vertical Offset Misalignment	0.16 mm
Horizontal Angular Misalignment	-0.02 mm
Horizontal Offset Misalignment	-0.08 mm
Soft-Foot correction values L.P.T Rotor	
Left foot front	-0.22 mm
Right foot front	-0.80 mm
Left foot rear	0.04 mm
Right foot rear	0.36 mm

Table 8.18 results of parallel alignment test

Vibration amplitude (mm)				Phase angle (deg)			
Plane (1) 29.3mm	Plane (2) 37.05mm	Plane (3) 48.6mm	Plane (4) 48.6mm	Plane (1) 29.3mm	Plane (2) 37.05mm	Plane (3) 48.6mm	Plane (4) 48.6mm
1.2527	1.5385	1.2918	1.2821	-70.3367	154.4842	128.9162	-63.1481

Table 8.19 Data of Vibration amplitude and phase angle for LPT & G rotors after introducing parallel misalignment

8.9.2.4 Angular Misalignment

2X0.3(mm) shims were added to the system to ensure that the system was in an angular misaligned state. Table 8.20 shows the amount of angular, offset misalignment and soft foot. For example as you can see from the table the amount of the Horizontal Angular Misalignment was 0.06 mm, which means that, the system was in a misaligned condition. Table 8.21 shows the vibration amplitude and phase angle when the system was in a misaligned condition. As we can see from the results of the vibration amplitude near the coupling (plane 2 &3) was also higher than the other positions.

Measurements Mode	Misalignment results
Vertical Angular Misalignment	-0.04 mm
Vertical Offset Misalignment	0.31 mm
Horizontal Angular Misalignment	0.06 mm
Horizontal Offset Misalignment	0.24 mm
Soft-Foot correction values L.P.T Rotor	
Left foot front	-0.40 mm
Right foot front	-1.28 mm
Left foot rear	-0.12 mm
Right foot rear	1.03 mm

Table 8.20 results of angular misalignment test

Vibration amplitude (mm)				Phase angle (deg)			
Plane (1) 29.3mm	Plane (2) 37.05mm	Plane (3) 48.6mm	Plane (4) 48.6mm	Plane (1) 29.3mm	Plane (2) 37.05mm	Plane (3) 48.6mm	Plane (4) 48.6mm
1.2845	1.5726	1.2552	1.1868	135.5100	-114.9675	164.8802	-106.4642

Table 8.21 Data of Vibration amplitude and phase angle for LPT & G rotors after introducing angular misalignment

8.9.2.5 Parallel And Angular Misalignment

2X0.3(mm) shims were added to the system vertically and horizontally to ensure that the system was in offset and angular misaligned state. Table 8.22 shows the amount of angular, offset misalignment and soft foot. For example as you can see from the table the amount of the Horizontal Angular Misalignment was 0.05 mm and, Vertical Offset Misalignment was -0.08 mm, which means that, the system was in a misaligned condition. Table 8.23 shows the vibration amplitude and phase angle when the system was in a misaligned condition. As we can see from the results of the vibration amplitude near the coupling (plane 2 &3) is also higher than the other positions.

Measurements Mode	Misalignment results
Vertical Angular Misalignment	0.01 mm
Vertical Offset Misalignment	0.08 mm
Horizontal Angular Misalignment	0.05 mm
Horizontal Offset Misalignment	0.12 mm
Soft-Foot correction values L.P.T Rotor	
Left foot front	-0.05 mm
Right foot front	0.26 mm
Left foot rear	-0.01 mm
Right foot rear	0.97 mm

Table 8.22 Results of parallel and angular alignment test

Vibration amplitude (mm)				Phase angle (deg)			
Plane (1) 29.3mm	Plane (2) 37.05mm	Plane (3) 48.6mm	Plane (4) 48.6mm	Plane (1) 29.3mm	Plane (2) 37.05mm	Plane (3) 48.6mm	Plane (4) 48.6mm
1.7753	2.3004	2.0343	1.5238	157.7852	149.0467	229.8205	-158.0583

Table 8.23 Data of Vibration amplitude and phase angle for LPT & G rotors after introducing parallel and angular misalignment.

8.9.2.6 After Finishing The Tests (LP and G Rotors)

The purpose of this test was to ensure that the system was in a well-aligned state. Table 8.24 shows the amount of angular, offset misalignment and soft foot. For example as you can see from the table the amount of the Horizontal Angular Misalignment was 0.01 mm and, Vertical Offset Misalignment was 0.01 mm, which means that, the system was in good condition. Table 8.25 shows the data and results of balancing test. The balancing test was also to keep the rotors in a well balanced state. The vibration amplitude and phase angle when the system in alignment condition was satisfactory.

Measurements Mode	Misalignment results
Vertical Angular Misalignment	0.00 mm
Vertical Offset Misalignment	0.01 mm
Horizontal Angular Misalignment	0.01 mm
Horizontal Offset Misalignment	0.01 mm
Soft-Foot correction values L.P.T Rotor	
Left foot front	-0.00 mm
Right foot front	0.07 mm
Left foot rear	0.01 mm
Right foot rear	0.17 mm

Table 8.24 results after finishing the tests

Results of the balancing LPT & G rotors after been alignment									
Run	T. Mass	Vibration amplitude (mm)				Phase angle (deg)			
		Plane (1) 48.6mm	Plane (2) 48.6mm	Plane (3) 29.7mm	Plane (4) 29.7mm	Plane (1) 48.6mm	Plane (2) 48.6mm	Plane (3) 29.7mm	Plane (4) 29.7mm
0		0.3996	0.3993	0.8401	0.6471	63.5323	61.4226	68.2463	42.3495
1	378@60°	0.5226	0.8217	0.3528	0.7399	71.1096	28.2610	165.7873	168.4674
2		1.0104	1.8852	1.6068	0.6496	218.0644	215.3324	192.0619	214.2057
3		1.5311	1.3040	1.0647	1.3895	140.0000	201.9188	183.1579	202.9956
4		1.3284	1.1575	0.9499	1.2943	167.6253	314.9951	256.3057	169.1229
Vibration after balancing		0.2001	0.1919	0.6018	0.3861	318.0218	133.1582	218.6923	112.1584

Results of the balancing LPT & G rotors after been alignment			
Correction masses/phase			
Plane (1)	Plane (2)	Plane (3)	Plane (4)
54.9429@ -118.9075	16.2971@ 154.3664	28.1887@ 7.2293	14.5772@ 114.4449

Table 8.25 Balancing results after finishing the tests

8.9.2.7 Alignment Results After Adding Known Mass To The System

Known masses were added to the system to ensure that the system was in an unbalanced state. Table 8.26 shows the vibration amplitude and phase angle along the rotors. As we can notice the vibration level is increased compared to the initial balanced results. The system

run until reach the steady state condition which typically was between 2-3 minutes to measure the shaft misalignment.

Table 8.27 shows the amount of angular, offset misalignment and soft foot. For example as you can see from the table the amount of the Horizontal Angular Misalignment was -0.02 mm and, Vertical Offset Misalignment was 0.16 mm, which means that, if the system is in unbalance condition. The alignment state of the system has to be checked, as in this case the alignment results show that the system need to be aligned.

Vibration amplitude (mm)				Phase angle (deg)			
Plane (1) 29.3mm	Plane (2) 37.05mm	Plane (3) 48.6mm	Plane (4) 48.6mm	Plane (1) 29.3mm	Plane (2) 37.05mm	Plane (3) 48.6mm	Plane (4) 48.6mm
2.0654	2.6951	2.6348	1.8852	193.7101	-222.0224	259.4478	172.3491

Table 8.26 Data of Vibration amplitude and phase angle for LPT & G rotors after introducing known mass to the system

Measurements Mode	Misalignment results
Vertical Angular Misalignment	-0.03 mm
Vertical Offset Misalignment	0.16 mm
Horizontal Angular Misalignment	-0.02 mm
Horizontal Offset Misalignment	-0.08 mm
Soft-Foot correction values L.P.T Rotor	
Left foot front	0.04 mm
Right foot front	-0.47 mm
Left foot rear	0.03 mm
Right foot rear	0.66 mm

Table 8.27 results of alignment test after adding known mass to the system

Vibration amplitude (mm)/ Phase angle (deg)				
Vibration amplitudes Data after the conduced Cases	**Balancing Plane (1) Radius 29.3mm**	**Balancing Plane (2) Radius 37.05mm**	**Balancing Plane (3) Radius 48.6mm**	**Balancing Plane (4) Radius 48.6mm**
Initial balancing	0.103@ 205.128	0.115@ 244.515	0.274@ 311.365	0.435@ 186.524
Introducing parallel Misalignment	1.279@ 345.245	3.797@ 352.623	3.599@ 217.213	1.362@ 117.234
Introducing angular Misalignment	1.072@ 90.054	3.442@ 96.979	3.801@ 156.393	1.963@ 317.255
Introducing Parallel & angular Misalignment	1.509@ 98.449	3.523@ 133.693	3.609@ 346.721	1.958@ 120.983
Balancing the system	0.243@ 63.135	0.185@ 288.692	0.365@ 299.235	0.332@ 285.251
Known mass to the system	1.835@ 237.218	3.802@ 232.163	3.669@ 194.739	2.486@ 231.683

Table 8.28 Summarised results of vibration amplitude after alignment tests

8.10 Results LP⇔G Rotors Alignment Tests Results with different misalignment and multi measurement points.

Several cases of misalignment were applied to the HPT rotor connected with LP⇔G Rotors see figure (8.11). The aim of the second set of tests was to investigate the effectiveness of the misaligned shafts on their balancing condition. To do this test we have to make sure that the system is well aligned and balanced, which was the purpose of the first set of the tests. The desired test requires the introduction of misalignment to the system HPT⇔ LPT Rotors, the sequence of the test was as mentioned on the previous part by adding a 2X0.3 mm shim to the bearing baseplate, in order to achieve parallel, angular and angular & parallel misalign shafts. The HPT rotor was the fixed part, to which the laser transducer was attached and the LPT Rotor was the moving part, which the reflector was attached figure (8.12).

Table 8.29 shows the amount of offset misalignment and Vibration Amplitude before and after offset alignment tests (mm) at six different locations along the rotors. Table 8.30 shows the amount of angular misalignment and Vibration Amplitude before and after offset alignment tests (mm) at six different locations along the rotors.

Figure 8.13 indicates the relation between Angular misalignment and vibration amplitude before and after angular alignment tests (mm) at six different locations along the rotors, also Figure 8.14 shows the relation between offset misalignment and vibration amplitude before and after angular alignment tests.

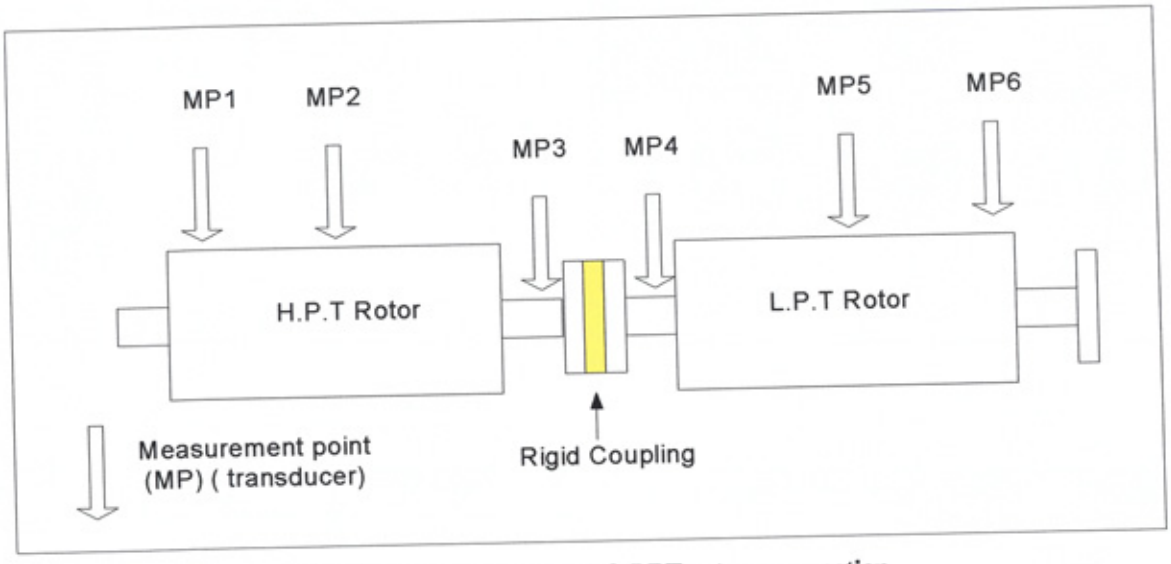

Figure 8.12 sketch of HPT & LPT rotors connection

Offset Misalignment (mm)	Vibration Amplitude before and after offset alignment tests (mm)											
	MP1		MP2		MP3		MP4		MP5		MP6	
	Before	After	Before	After	Before	After	Before	After	Before	After	Before	After
0.01	0.384	0.701	0.366	0.925	0.55	1.123	0.594	1.322	0.399	1.4	0.300	1.653
0.03	0.456	0.9	0.458	0.964	0.752	1.545	0.778	1.63	0.486	1.765	0.408	1.876
0.09	0.605	1.279	0.786	1.123	0.896	2.499	0.869	2.697	0.583	2.748	0.586	2.162
0.1	0.716	1.235	0.885	1.295	0.832	2.482	0.968	2.815	0.598	2.968	0.692	2.312
0.12	0.991	1.365	0.98	1.423	0.983	2.523	0.999	2.831	0.796	2.985	0.771	2.699

Table 8.29 Data of Vibration amplitude before and after offset misalignment

Angular Misalignment (mm)	Vibration Amplitude before and after offset alignment tests (mm)											
	MP1		MP2		MP3		MP4		MP5		MP6	
	Before	After	Before	After	Before	After	Before	After	Before	After	Before	After
0.01	0.384	0.860	0.366	0.622	0.55	0.951	0.594	1.194	0.399	1.050	0.300	0.935
0.03	0.456	0.972	0.458	0.720	0.752	1.798	0.778	1.880	0.486	1.849	0.408	1.535
0.09	0.605	1.072	0.786	1.004	0.896	2.442	0.869	2.601	0.583	2.000	0.586	1.963
0.1	0.716	1.135	0.885	1.235	0.832	2.696	0.968	2.778	0.598	2.356	0.692	2.213
0.12	0.991	1.523	0.98	1.325	0.983	3.238	0.999	3.199	0.796	2.887	0.771	2.301

Table 8.30 Data of Vibration amplitude before and after angular misalignment

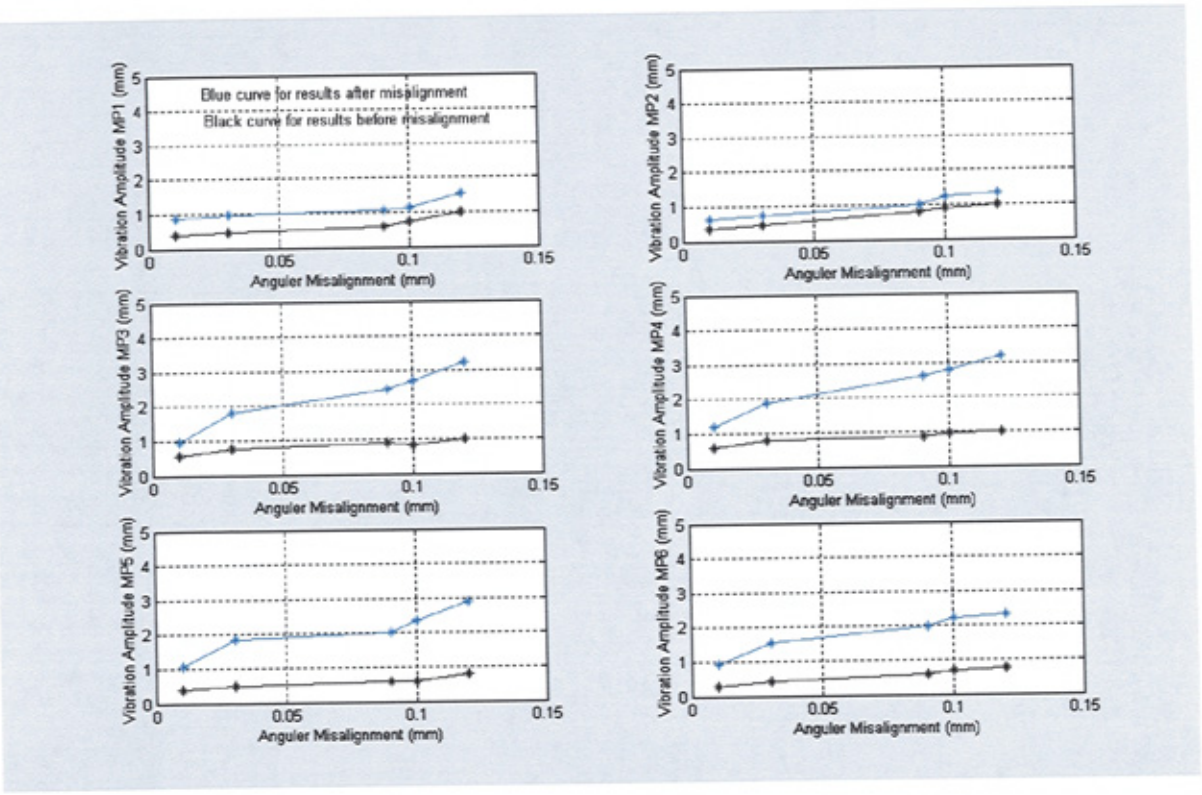

Figure 8.13 Angular misalignment Vs vibration amplitude

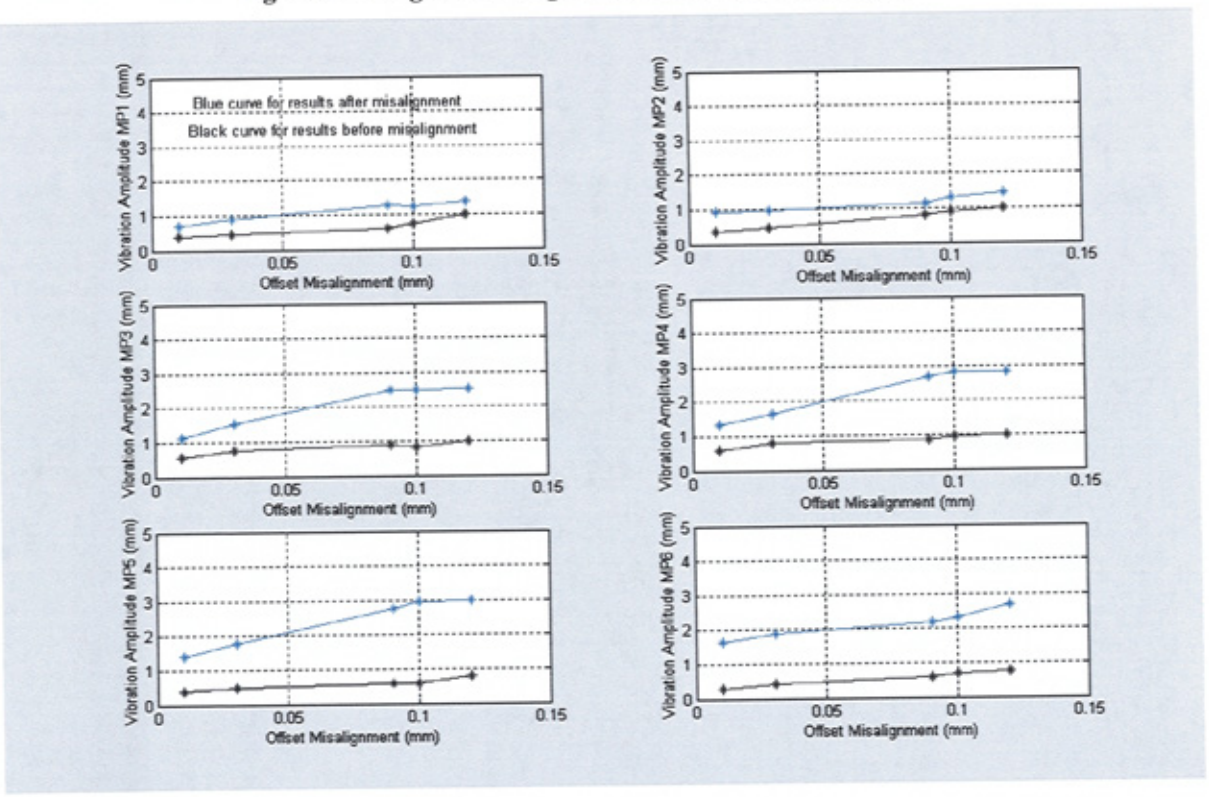

Figure 8.14 offset misalignment Vs vibration amplitude

8.11 Results Discussion of the Experimental Investigation into The Behavior of Misaligned Shafts on Balanced Rotors

All changes in alignment were made to the system (multi shaft-multi bearings). Misalignment conditions were varied in the following order for **HPT⇔ LPT rotors** and **HPT+ *LPT Rotors*⇔G Rotor:**

- ❖ Offset misalignment
- ❖ Angular misalignment
- ❖ Combination of offset and angular misalignment

Using OPTALIGN PLUS for the misalignment experiments to collect data. For all cases, the data was transferred to the OPTALIGN PLUS software then analyzed to determine the change in the misalignment condition. The balancing data was taken by using a Matlab program written by the author to handle and analyse the balancing data.

The alignment and balancing results obtained from both before and after any unbalance and misalignment were made can be seen in data and the results tables (see section 8.10). These alignment readings were stored on the OptAlign Plus laser hardware for future reporting and results. The balancing data was also saved in the experimental computer system.

The aim of the second set of tests was to investigate the effect of the misaligned shafts on their balance condition. To do this test we had to make sure that the system is well aligned and balanced, which was the purpose of the first set of the tests. The desired test requires the introduction of misalignment to the system HPT⇔ LPT Rotors, the sequence of the test was as mentioned on the previous part by adding a 2X0.3 mm shim to the bearing baseplate, in order to achieve parallel, angular and angular & parallel misalign shafts. The HPT rotor was the fixed part, which the laser transducer was attached and the LPT Rotor was the moving part, which the reflector was attached.

The dynamic effect of the hydrodynamic bearing was neglected, because the rotor unbalance was assumed to be the major force affect the system (Leung 1988).

From the second tests (section 8.9.2), it is very clear that the corrections and modifications made to this system had a direct effect on the system vibration amplitude. For instance if we have a look at the results of the vibration amplitude after introducing parallel (offset) misalignment, this was increased sharply from 0.1032mm to 1.2796mm, 0.1152mm to 3.5995mm, 0.2743mm to 3.797mm, 0.4352mm to 1.3623mm at measurement locations respectively.

The third part of the tests held on the HPT⇔ LPT rotors were to study the effect of unbalanced rotors on the aligned shafts. The procedure was achieved by aligning and balancing the HPT⇔ LPT rotors then introduces a known mass to the rotor in order to establish an unbalanced system. The rotor was rotated and the vibration amplitude was measured to make sure that the system was in an unbalance condition. The next step was to test the alignment to see whether the unbalance mass had changed the system alignment condition. The results in this particular test showed that the alignment condition of the system was getting worse after the shafts became unbalanced. It is believed that this change in the vibration amplitude was due to either a rotating unbalance of the system or some sort of structural movement of the base or foundation. Likewise, when we applied the same test on the LPT⇔ Generator rotor connecting the HPT& LPT to become the fixed part and the G rotor as moving part. The vibration of the system changed following the change in the alignment and balancing condition.

We also notice that in the results form of vibration shown in the tables (see section 8.10) that the largest vibration occurred at the bearing closest to the coupling. Therefore there was a high probability that an alignment error exists.

Initially, the system was aligned and balanced. The vibration amplitude data obtained after every misalignment type introduced to the shafts showed a dramatic increase in the vibration response. After this series of tests the system was balanced again. Then a

known mass was added to the system as an unbalance mass, in order to produce an unbalance system. The shafts were aligned again and the vibration data achieved after that showed that the unbalanced rotors had affected their aligned condition.

The conclusions of the tests in this study are shown in table 8.28. As we can see the vibration response indicates that shaft misalignment does have a significant affect on the vibration amplitudes of the system. For instance, the results showed that planes 2 and 3 had higher vibration amplitudes (3.5995mm, 3.7971mm) respectively at all types of misalignment, because these planes are closer to the coupling, generally speaking. As the experimental results prove the vibration amplitude is increased after we introduced the misalignment to the system (Parallel, angular and Parallel, & angular misalignments) and gave similar results.

Additional tests were held to demonstrate the relation between misalignment shafts and the rotor vibration (see tables 8.29 and 8.30 also figures 8.13 and 8.14), the results show that the vibration data, which was collected after adding the parallel misalignment to the system, became higher than the original vibration data.

To sum up the conclusion from the above tests, there is a relationship between misaligned rotors and unbalanced rotors, which is increasing the misalignment produces higher vibration amplitude. Moreover these results also show that the misaligned shaft has an effect on the balanced rotors, similarly to the unbalanced rotors on aligned shafts. So the vibration data, which was collected after adding the parallel misalignment to the system, became higher than the original vibration data.

Chapter 9

FINITE ELEMENT MODELLING

9.1 Introduction

Rotating machines are becoming increasingly precise and higher speed due to the progress of technology. These machines therefore require much higher operational efficiency and stable behavior under far more severe conditions. The primary factors that degrade the performance of machines operating at a high speed are vibration and accompanying problems such as discomfort, noise and fatigue.

The selection of balancing planes was discussed by Church and Plunkett (1961). In their conclusion the authors state that, the number of balancing masses and measurements points that should be used for any flexible shaft balancing is not optional but equal to the number of critical speeds below the maximum balancing speed.

There is still concern with regard to the practical application of this balance plane optimization procedure. Specifically, these questions concern the effect on real rotor balancing test data, a refinement of the acceptable level of the significance factor and whether this acceptable level should be related to the order of the influence coefficient matrix. These questions can and will be answered as practical experience is gained with this and similar procedures.

Various methods for vibration analysis of rotor-bearing systems have been developed during the past few decades. These methods may be divided into two major classes according to the modeling procedure involved. The first method was the finite element method (FEM) in which a rotor bearing system is approximated by a finite degree of freedom system whose motions are described by ordinary differential equations Nelson and Mcvaugh (1976), Glasgow and Nelson 1980, and Gmlir and Rodrigues (1991). The second is the analytical method in which the rotor-bearing system is treated as a distributed parameter system whose motions are described by partial differential equations Kang, Shim and Lee (1992). With the recent development of computer hardware and software, the

discretization method has become a popular method for the analysis of vibrations since it can be easily applied to complex rotor-bearing systems.

The finite element method is used to build a discrete model of the rotor bearing system. The deflection of the whole system is combined by the integrity of the dynamic variables and unbalance forces. On numeric solutions, the analysis and calculations are done by the influence coefficient method from a model built using the commercial finite element software "ANSYS".

The chance of using non-independent balancing planes can lead to a singular or near singular influence coefficient matrix .Due to noise in the vibration data, it is almost impossible to have an influence coefficient matrix which is singular, but this matrix can be near singular for example having a very small determinant which can often results in calculation of large correction masses, which will need to be eliminated (cancel each other, i.e. eliminate the redundant balancing planes) (see chapter 7 where some artificial data was used to demonstrate the elimination of planes).

9.2 Tests conducted on the optimization of balancing planes

A number of test cases have been studied to demonstrate the relation between the amount of trial masses locations and the balancing planes. The tests were divided into 5 sections based on a simple uniform rotor and High-pressure turbine rotor with real data. The lists below are tests conducted of theoretical calculation leading to optimization of locations of balancing planes;

1. The effect of small trial mass, which is (10%, 20%) of the mass of the rotor (simple uniform rotor).
2. The effect of the rotor stiffness (simple uniform rotor).
3. The effect of different locations of planes (e.g. when adding the correction mass in a different plane to the trial mass plane) (simple uniform rotor).
4. Implement the method into HPT rotor.

9.3 Results

9.3.1 Bench mark test

In order to verify the accuracy of finite element modeling by ANSYS for the rotor-bearing system in this chapter, a pin-pin rotor model Figure (9.1) was built, and the results compared between the software package analysis (ANSYS) and theoretical calculation. It was found that both results agreed in terms of the values of the natural frequencies and deflection force as seen from the result tables (9.1-9.4) for 2D & 3D(20,12,7,5) Elements pin-pin rotors model.

The properties of the model were;

Density (rho) =7905 Kg/m^3.

Young's Modulus (E) =196 Gpa.

Length of the beam (L) =1 m.

Diameter of the beam (d) =0.05 m.

Moment of inertia (I) =pi*d^4/64.

Area (A) =pi*d^2/4 m^2

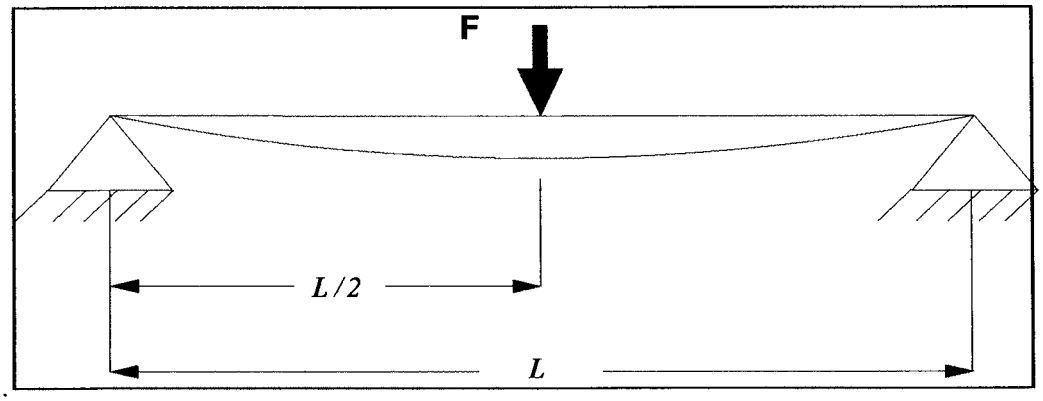

Figure 9.1 pin-pin rotors

Force(Newton)	Analytical	2D ANSYS	3D ANSYS	
	Maximum Deflection (m)	Maximum Deflection Y Direction Due to F_y(m)	Maximum Deflection Y Direction Due to F_y(m)	Maximum Deflection Z Direction Due to F_z(m)
100	0.34646e-004	0.346e-004	0.346e-004	0.346e-004
200	0.9292e-004	0.692e-004	0.692e-004	0.692e-004
300	1.0394e-004	1.04e-004	1.04e-004	1.04e-004
400	1.3858e-004	1.38e-004	1.38e-004	1.38e-004
500	1.7323e-004	1.73e-004	1.73e-004	1.73e-004

Table 9.1 Results of 2D & 3D-20 Elements pin-pin rotors model

Force (Newton)	Analytical	2D ANSYS (12 Elements)	2D ANSYS (7 Elements)	2D ANSYS (5 Elements)
	Maximum Deflection(m)	Maximum Deflection Y Direction Due to F_y(m)	Maximum Deflection Y Direction Due to F_y(m)	Maximum Deflection Y Direction Due to F_y(m)
100	0.34646e-004	0.343e-004	0.346e-004	0.346e-004
200	0.9292e-004	0.685e-004	0.693e-004	0.693e-004
300	1.0394e-004	1.03e-004	1.04e-004	1.04e-004
400	1.3858e-004	1.37e-004	1.39e-004	1.39e-004
500	1.7323e-004	1.71e-004	1.73e-004	1.73e-004

Table 9.2 Results of 2D (12,7 and 5) Elements pin-pin rotors model

9.3.2 Results of adding small trial mass (10%, 20%) of the rotor mass

Figure 9.2 shows a schematic diagram of a pin-pin rotor model showing the balancing planes locations where the unbalance and trial masses have been added, Table 9.3 shows the amount of unbalance mass which was calculated by using normal solution, QR and SVD methods, trial mass, the actual mass added to the system and the results of correction masses.

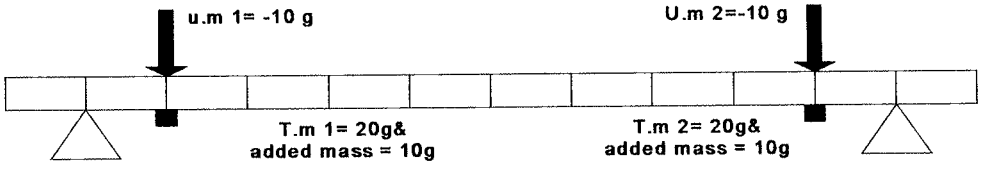

Figure 9.2 schematic diagram of Pin-Pin Rotor show the location of U. mass (10g) & T. mass

Young's Modulus	Unbalance Mass (gram)	Trial Mass (gram)	Correction Mass (gram)	
210E9	10	20	10.0000	10.0000
210E9	15	30	15.0000	15.0000
210E9	20	40	20.0000	20.0000

Table 9.3 Results of using small trial mass

9.3.3 Results of The effect of the rotor stiffness

9.3.3.1 Case (1) change the rotor stiffness and u.mass =150

Figure 9.3 shows a schematic diagram of a pin-pin rotor model showing the balancing planes locations where the unbalance and trial masses have been added. Table 9.4 shows the results of using different Young's modulus and small unbalance.

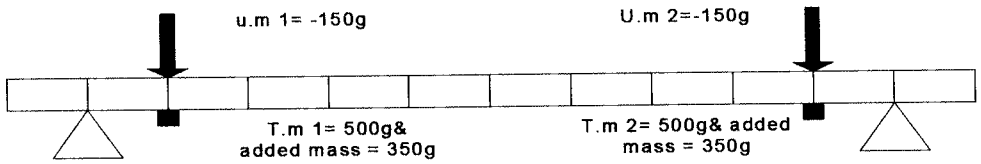

Figure 9.3 schematic diagram of Pin-Pin Rotor show the location of U. mass (150g) & T. mass

Young's Modulus	Unbalance Mass (gram)	Trial Mass (gram)	Correction Mass (gram)	
210E7	150	500	149.9993	149.9993
210E8	150	500	149.9993	149.9993
210E9	150	500	149.9993	149.9993
210E10	150	500	149.9993	149.9993
210E11	150	500	149.9993	149.9993

Table 9.4 Results of using different young modulus and small Trial mass

9.3.3.2 Case (2) change the rotor stiffness and u.mass =300

Figure 9.4 shows a schematic diagram of a pin-pin rotor model showing the balancing planes locations where the unbalance and trial masses have been added. Table 9.5 shows the results of using different Young's modulus and large unbalance.

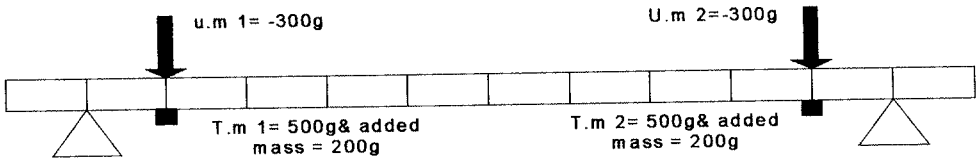

Figure 9.4 schematic diagram of Pin-Pin Rotor show the location of U. mass (300g) & T. mass

Young Modules	Unbalance Mass	Trial Mass	Correction Mass	
210E7	300	500	300.066	300.066
210E8	300	500	300.066	300.066
210E9	300	500	300.066	300.066
210E10	300	500	300.066	300.066
210E11	300	500	300.066	300.066

Table 9.5 Results of using different young modulus and big Trial mass

9.3.4 The effect of changing the balancing planes locations (e.g. adding the correction mass in a different plane of the trial mass plane).

Figure 9.5 and 9.6 shows a schematic diagram of a pin-pin rotor model showing the balancing planes and trial masses locations. Figure 9.7 shows the data and results at each node when 12, 14 correction masses were added.

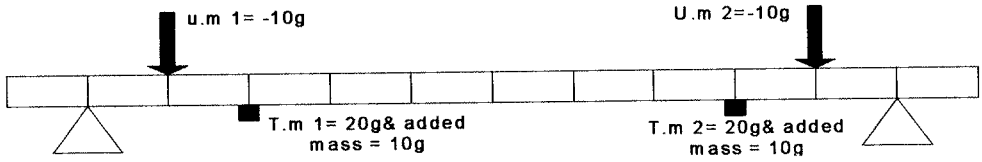

Figure 9.5 schematic diagram of Pin-Pin Rotor show the location (1) of U. mass & T. mass

- **E=210E9 & T.Mass=20 % U.M=10 not same plane (4&8)**

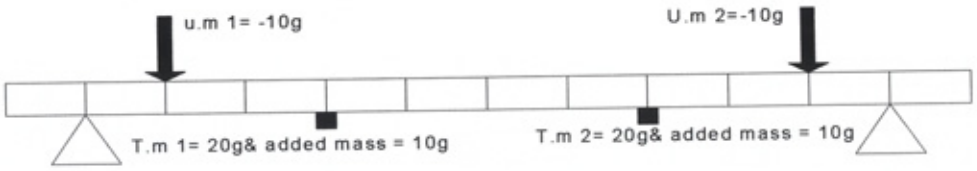

Figure 9.6 schematic diagram of Pin-Pin Rotor show the location (2) of U. mass & T. mass

- **E=210E9 & T.Mass=20 % U.M=10 not same plane (5&7)**

Node	10 U.Mass	12 C.Mass	14 C.Mass
1	0	0	0
2	-6.10E-07	5.82E-07	7.32E-07
3	-1.14E-06	1.14E-06	1.43E-06
4	-1.53E-06	1.64E-06	2.04E-06
5	-1.76E-06	2.00E-06	2.47E-06
6	-1.84E-06	2.12E-06	2.62E-06
7	-1.76E-06	2.00E-06	2.47E-06
8	-1.53E-06	1.64E-06	2.04E-06
9	-1.14E-06	1.14E-06	1.43E-06
10	-6.10E-07	5.82E-07	7.32E-07
11	0	0	0
Correction Masses	⇒	**12.9412 (P1)** **12.9412 (P2)**	**14.5681 (P1)** **14.5681(P2)**

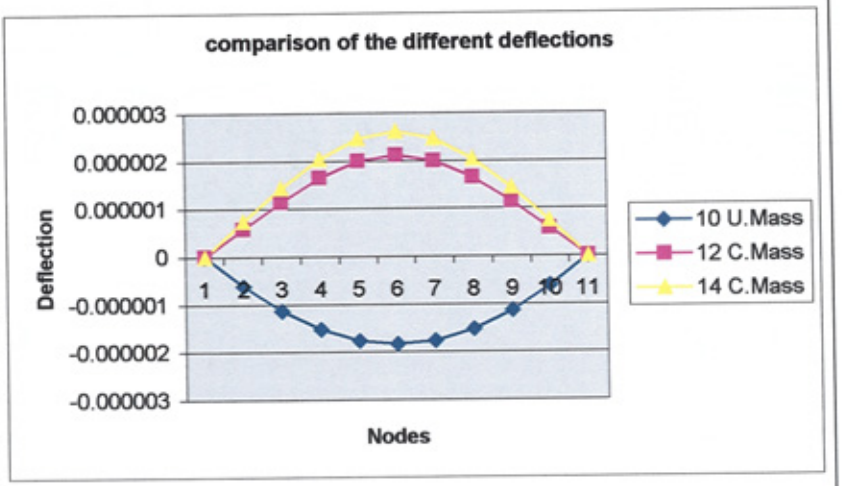

Figure 9.7 results of small trial masses

9.3.5 rotor balancing planes eliminations

The influence coefficient procedure is based on the assumptions of rotor linearity and the position of rotor unbalance. The influence coefficient balancing methods has numerical difficulties when non-independent balancing planes are inadvertently used. This occurs as a result of the influence coefficient matrix being ill conditioned, because at least one of the

columns of the matrix is nearly linearly dependent on the remaining columns. It is possible to avoid this problem by eliminating the dependence of the columns of the influence coefficient matrix. If this matrix is found to be ill conditioned, it is necessary to identify and eliminate the least independent of the balancing planes. The list of the tests conducted is;

Set 1 (held on symmetrical rotor)

2 planes balancing with different significant factors

Set 2 (held on symmetrical rotor)

6 planes balancing with different significant factors

Set 3 (held on High pressure turbine rotor)

2 planes balancing with different significant factors

Set 4 (held on High pressure turbine rotor)

7 planes balancing with different significant factors

9.3.5.1 Numerical Examples

Four sets of cases were used to demonstrate the balancing plane optimization procedure. The data used for these test cases are actual test data by using ANSYS software. For sets 1&2 of these test cases the data was intentionally arranged to provide a matrix columns order after elimination resulting a well-conditioned influence coefficient matrix. The influence coefficient matrices for the test cases are rectangular, with seven rows and six columns for case 3 (symmetrical rotor) and seven columns and eight rows for case4 (H.P.T rotor figure 9.). The correction masses shown below were calculated using the standard least-squares solution, QR factorization, SVD.

9.4 Results of the numerical examples

Several tests were held to demonstrate the proposed method, which is the elimination of some of the balancing planes. The cases were applied on a symmetrical rotor and the high pressure turbine rotor (H.P.T).

9.4.1 Set 1 (2 plane H.P.T rotor significant factor =0.01)

This case was applied to the rotor by using two plane balancing (influence coefficient procedure), and two unbalance masses of (100 g) were added to the rotor at the balancing planes. Also in this test several other significant factors were applied. We found that all the results gave similar values, so it was decided to present only one case of the significant factor (0.01)

The influence coefficient matrix $[a]$ for the test

$$1.0e\text{-}008 * \begin{bmatrix} 0.2888 & 0.1975 \\ 0.1975 & 0.2911 \end{bmatrix}$$

Matrix condition number =5.2746

Results of the correction masses

Least square solution = QR solution = SVD solution $= \begin{bmatrix} 99.9856 \\ 100.0109 \end{bmatrix}$

Influence coefficient matrix Columns Significant factor $= [1.0000 \quad 0.3660]$

The $[a]$ matrix after Column elimination $=1.0e\text{-}008 * \begin{bmatrix} 0.2888 & 0.1975 \\ 0.1975 & 0.2911 \end{bmatrix}$

Results of the correction mass after elimination the influence coefficient matrix columns.

Least square solution = QR solution = SVD solution $= \begin{bmatrix} 99.9856 \\ 100.0109 \end{bmatrix}$

Elimination by using rank

New Matrix columns order $= [2 \quad 1]$

Results of the correction masses calculated by different method **(Least square, QR and SVD)** after elimination the influence coefficient matrix columns of the new ordered matrix using QR pivoting.

Least square solution = QR solution = SVD solution $= \begin{bmatrix} 100.0109 \\ 99.9856 \end{bmatrix}$

9.4.2 Set 2 (2 plane symmetrical rotor Tolerance = 0.01)

This case was applied on the symmetrical rotor by using two planes balancing (influence coefficient procedure), and two unbalance masses of 100 g added to the rotor at the balancing planes. Also in this test several other significant factors were applied. We found that all the results were giving the similar results, so we decided to present only one case of the significant factor (0.01)

The influence coefficient matrix $[a]$ **for the test**

$$1.0e\text{-}007 * \begin{bmatrix} 0.4913 & 0.4299 \\ 0.4299 & 0.7676 \end{bmatrix}$$

Matrix condition number=6.0756

Results of the correction masses

Least square solution = QR solution = SVD solution $= \begin{bmatrix} 100.0060 \\ 99.9949 \end{bmatrix}$

Influence coefficient matrix Columns Significant factor $= [1.0000 \quad 0.3349]$

The $[a]$ **matrix after Column elimination** $= 1.0e\text{-}007 * \begin{bmatrix} 0.4913 & 0.4299 \\ 0.4299 & 0.7676 \end{bmatrix}$

Results of the correction mass after elimination the influence coefficient matrix columns.

Least square solution = QR solution = SVD solution $= \begin{bmatrix} 100.0060 \\ 99.9949 \end{bmatrix}$

Elimination by using rank

New Matrix columns order $= [2 \quad 1]$

Results of the correction masses calculated by different method **(Least square, QR and SVD)** after elimination the influence coefficient matrix columns of the new ordered matrix using QR pivoting.

Least square solution = QR solution = SVD solution $= \begin{bmatrix} 99.9949 \\ 100.0060 \end{bmatrix}$

9.4.3 Set 3 (6) plane symmetrical rotor

This case was applied on the symmetrical rotor by using six planes balancing (influence coefficient procedure), and two unbalance masses of 100 g were added to the rotor at the balancing planes (planes 1&6). Also in this test several other significant factor were applied, and we found that some of the results were giving the similar results, so that we decided to present only one case of the significant factor (0.01,0.02,0.1)

The influence coefficient matrix $[a]$ for the test

$$1.0e\text{-}006 * \begin{bmatrix} 0.0491 & 0.0699 & 0.0813 & 0.0780 & 0.0678 & 0.0430 \\ 0.0466 & 0.0697 & 0.0840 & 0.0816 & 0.0714 & 0.0455 \\ 0.0532 & 0.0819 & 0.1045 & 0.1034 & 0.0916 & 0.0589 \\ 0.0520 & 0.0816 & 0.1105 & 0.1151 & 0.1055 & 0.0697 \\ 0.0452 & 0.0714 & 0.0987 & 0.1055 & 0.1003 & 0.0686 \\ 0.0430 & 0.0682 & 0.0959 & 0.1045 & 0.1029 & 0.0768 \end{bmatrix}$$

Matrix Rank= 6

Matrix condition number= 2.0294e+003

Results of the correction masses using QR pivoting.

Least square solution = QR solution = SVD solution $= 1.0e+003 * \begin{bmatrix} -2.3830 \\ 2.2716 \\ -0.1210 \\ -1.4665 \\ 2.1753 \\ -1.2964 \end{bmatrix}$

9.4.3.1 Case 1 elimination by using significant factor (0.01)

Influence coefficient matrix columns significant factor =

$$[1.0000 \quad 0.0374 \quad 0.0216 \quad 0.0082 \quad 0.0071 \quad 0.0106]$$

Matrix Columns order after elimination = $[1 \quad 2 \quad 3 \quad 6]$

The $[a]$ matrix after Column elimination

$$1.0e\text{-}006 * \begin{bmatrix} 0.0491 & 0.0699 & 0.0813 & 0.0430 \\ 0.0466 & 0.0697 & 0.0840 & 0.0455 \\ 0.0532 & 0.0819 & 0.1045 & 0.0589 \\ 0.0520 & 0.0816 & 0.1105 & 0.0697 \\ 0.0452 & 0.0714 & 0.0987 & 0.0686 \\ 0.0430 & 0.0682 & 0.0959 & 0.0768 \end{bmatrix}$$

Matrix condition number = 471.2122

Results of the correction mass after elimination the influence coefficient matrix columns.

Least square solution = QR solution = SVD solution = $1.0e+003 * \begin{bmatrix} -1.4705 \\ 0.9262 \\ 0.3560 \\ -0.2803 \end{bmatrix}$

Elimination by using rank (QR)

New Matrix columns order = $[4 \quad 2 \quad 6 \quad 1 \quad 5 \quad 3]$

Results of the correction mass after elimination the influence coefficient matrix columns of the new ordered matrix using QR pivoting.

Least square solution = QR solution = SVD solution = 1.0e+003 * $\begin{bmatrix} -1.4665 \\ 2.2716 \\ -1.2964 \\ -2.3830 \\ 2.1753 \\ -0.1210 \end{bmatrix}$

Influence coefficient matrix columns significant factor

= [1.0000 0.1106 0.0534 0.0130 0.0035 0.0018]

Matrix Columns order after elimination = [1 2 3 4]

The $[a]$ matrix after Column elimination =

1.0e-006 * $\begin{bmatrix} 0.0780 & 0.0699 & 0.0430 & 0.0491 \\ 0.0816 & 0.0697 & 0.0455 & 0.0466 \\ 0.1034 & 0.0819 & 0.0589 & 0.0532 \\ 0.1151 & 0.0816 & 0.0697 & 0.0520 \\ 0.1055 & 0.0714 & 0.0686 & 0.0452 \\ 0.1045 & 0.0682 & 0.0768 & 0.0430 \end{bmatrix}$

Matrix condition number = 328.8743

Results of the correction masses calculated by different method **(Least square, QR and SVD)** after elimination the influence coefficient matrix columns of the new ordered matrix using QR pivoting.

Least square solution = QR solution = SVD solution = 1.0e+003 * $\begin{bmatrix} 0.2956 \\ 1.0930 \\ -0.3652 \\ -1.5127 \end{bmatrix}$

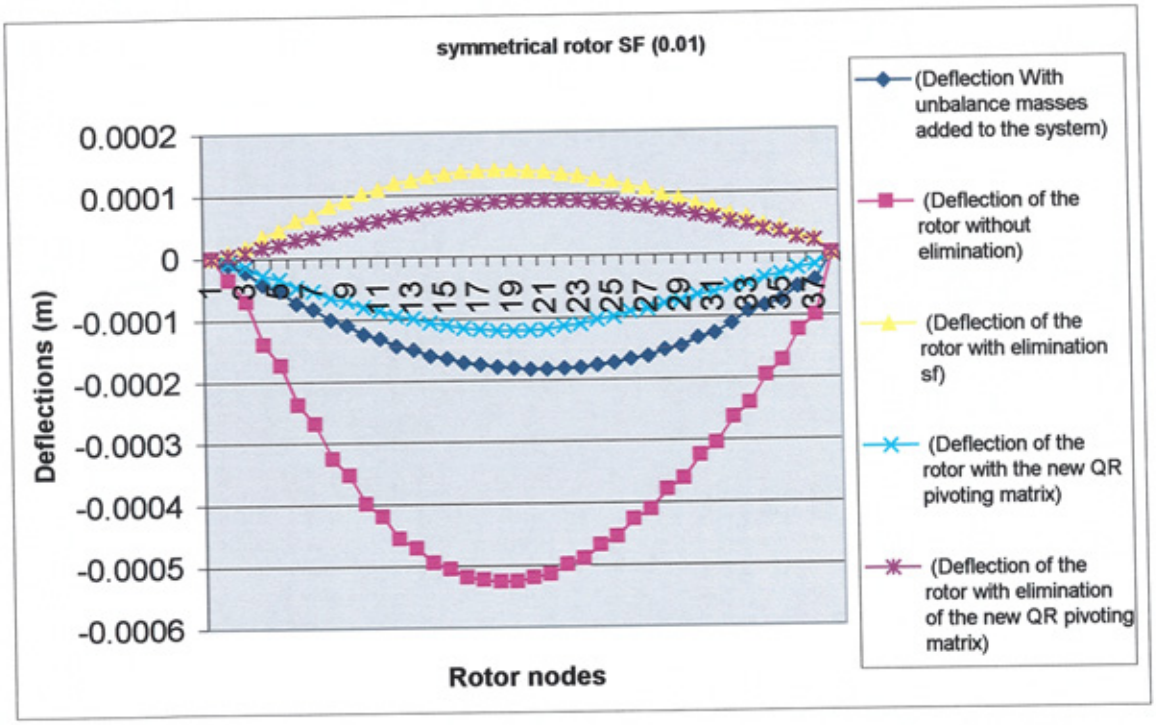

Figure 9.8 Results of symmetrical rotor after adding correction masses with S_f (0.01)

9.4.3.2 Case 2 elimination by using significant factor (0.02)

Influence coefficient matrix columns significant factor =
$[1.0000 \quad 0.0374 \quad 0.0216 \quad 0.0082 \quad 0.0071 \quad 0.0106]$

Matrix Columns order after elimination = $[1 \quad 2 \quad 3]$

The $[a]$ matrix after Column elimination = 1.0e-006 *

$$\begin{bmatrix} 0.0491 & 0.0699 & 0.0813 \\ 0.0466 & 0.0697 & 0.0840 \\ 0.0532 & 0.0819 & 0.1045 \\ 0.0520 & 0.0816 & 0.1105 \\ 0.0452 & 0.0714 & 0.0987 \\ 0.0430 & 0.0682 & 0.0959 \end{bmatrix}$$

Matrix condition number =320.0884

Results of the correction masses calculated by a different method **(Least square, QR and SVD)** after elimination of the influence coefficient matrix columns of the new ordered matrix using QR pivoting.

Least square solution = QR solution = SVD solution = 1.0e+003 * $\begin{bmatrix} -2.7105 \\ 2.6102 \\ -0.4928 \end{bmatrix}$

New Matrix columns order = [4 2 6 1 5 3]

Results of the correction masses calculated by different method **(Least square, QR and SVD)** after elimination of the influence coefficient matrix columns of the new ordered matrix using QR pivoting.

Least square solution = QR solution = SVD solution = 1.0e+003 * $\begin{bmatrix} -1.4665 \\ 2.2716 \\ -1.2964 \\ -2.3830 \\ 2.1753 \\ -0.1210 \end{bmatrix}$

Influence coefficient matrix Columns Significant factor

= [1.0000 0.1106 0.0534 0.0130 0.0035 0.0018]

Matrix Columns order after elimination = [1 2 3]

The $[a]$ matrix after Column elimination = 1.0e-006 * $\begin{bmatrix} 0.0780 & 0.0699 & 0.0430 \\ 0.0816 & 0.0697 & 0.0455 \\ 0.1034 & 0.0819 & 0.0589 \\ 0.1151 & 0.0816 & 0.0697 \\ 0.1055 & 0.0714 & 0.0686 \\ 0.1045 & 0.0682 & 0.0768 \end{bmatrix}$

Matrix condition number = 70.0338

Results of the correction masses calculated by a different method **(Least square, QR and SVD)** after elimination of the influence coefficient matrix columns of the new ordered matrix using QR pivoting.

Least square solution = QR solution = SVD solution = $\begin{bmatrix} 737.9302 \\ -323.6241 \\ -559.6382 \end{bmatrix}$

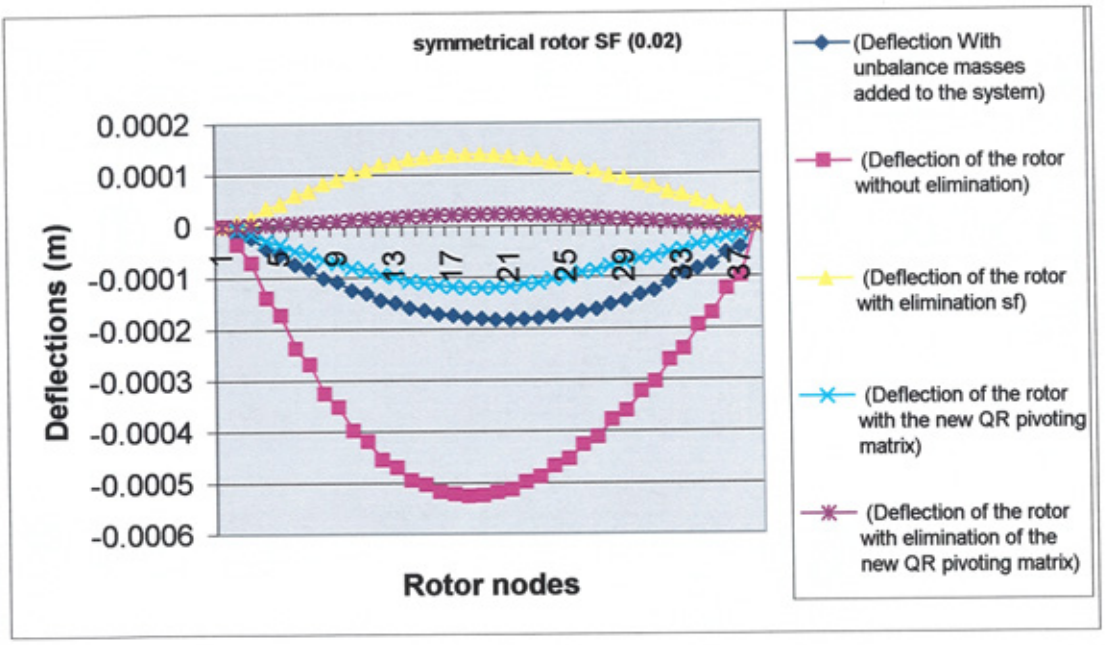

Figure 9.9 Results of symmetrical rotor after adding correction masses with S_f (0.02)

9.4.3.3 Case 2 elimination by using significant factor (0.1)

Influence coefficient matrix Columns Significant factor

$= \begin{bmatrix} 1.0000 & 0.0374 & 0.0216 & 0.0082 & 0.0071 & 0.0106 \end{bmatrix}$

The $[a]$ **matrix after Column elimination** = 1.0e-007 * $\begin{bmatrix} 0.4913 \\ 0.4657 \\ 0.5322 \\ 0.5201 \\ 0.4523 \\ 0.4299 \end{bmatrix}$

Matrix condition number = 58.4423

Results of the correction masses calculated by a different method **(Least square, QR and SVD)** after elimination of the influence coefficient matrix columns of the new ordered matrix using QR pivoting.

Least square solution = QR solution = SVD solution = 305.0215

Elimination by using rank (QR)

New Matrix columns order = [4 2 6 1 5]

Results of the correction masses calculated by a different method **(Least square, QR and SVD)** after elimination of the influence coefficient matrix columns of the new ordered matrix using QR pivoting.

Least square solution = QR solution = SVD solution = 1.0e+003 *

$$\begin{bmatrix} -1.4665 \\ 2.2716 \\ -1.2964 \\ -2.3830 \\ 2.1753 \\ -0.1210 \end{bmatrix}$$

Influence coefficient matrix Columns Significant factor =

[1.0000 0.1106 0.0534 0.0130 0.0035 0.0018]

Matrix Columns order after elimination = [1 2]

The $[a]$ matrix after Column elimination = 1.0e-006 *

$$\begin{bmatrix} 0.0780 & 0.0699 \\ 0.0816 & 0.0697 \\ 0.1034 & 0.0819 \\ 0.1151 & 0.0816 \\ 0.1055 & 0.0714 \\ 0.1045 & 0.0682 \end{bmatrix}$$

Matrix condition number = 18.8034

Results of the correction masses calculated by a different method **(Least square, QR and SVD)** after elimination of the influence coefficient matrix columns of the new ordered matrix using QR pivoting.

Least square solution = QR solution = SVD solution = $\begin{bmatrix} 117.3121 \\ 44.4290 \end{bmatrix}$

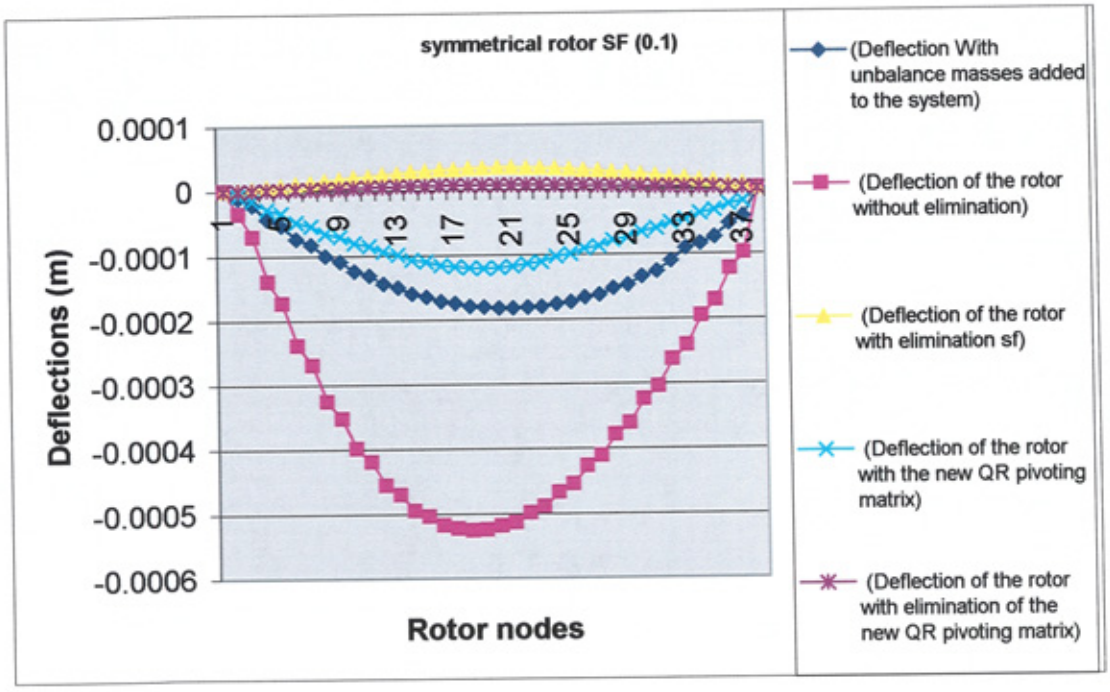

Figure 9.10 Results of symmetrical rotor after adding correction masses with S_f (0.1)

9.4.2 Implementation of the method into HPT rotor

Figure 9.11 shows a diagram of a High-pressure turbine rotor. Table 9.6 shows the geometric data of the HPT rotor. Figure 9.12 shows a schematic diagram of HPT rotor model showing the balancing planes and trial masses locations

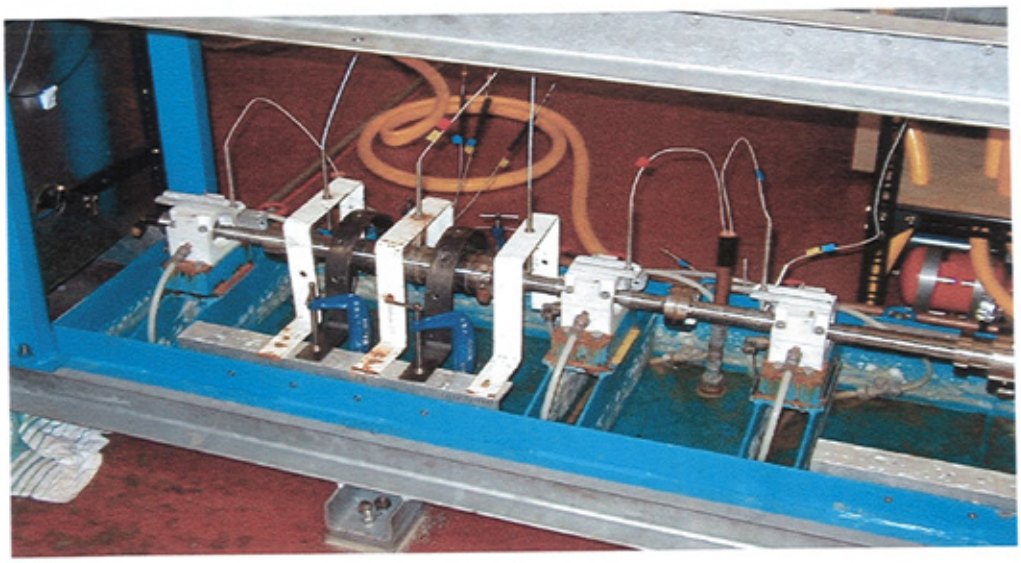

Figure 9.11 HPT rotor

H.P.T Rotor						
Sec No.	Length (mm)	O.D (mm)	Area	Izz=Iyy	Mass/Len	Ixx
1	12.36	67.57	3.59E+00	1023261.396	2.80E+04	2.05E+06
2	54.49	25.75	5.21E-01	21581.41161	4.06E+03	4.32E+04
3	15.77	26.83	5.65E-01	25436.28047	4.41E+03	5.09E+04
4	15.77	26.83	5.65E-01	25436.28047	4.41E+03	5.09E+04
5	13.29	25.64	5.16E-01	21214.99812	4.03E+03	4.24E+04
6	3.1	28.24	6.26E-01	31219.76889	4.89E+03	6.24E+04
7	6.35	25.4	5.07E-01	20431.7601	3.95E+03	4.09E+04
8	3.1	26.57	5.54E-01	24464.54438	4.32E+03	4.89E+04
9	6.35	25.4	5.07E-01	20431.7601	3.95E+03	4.09E+04
10	3.1	26.57	5.54E-01	24464.54438	4.32E+03	4.89E+04
11	17.27	26.78	5.63E-01	25247.1991	4.39E+03	5.05E+04
12	10	35	9.62E-01	73661.92969	7.50E+03	1.47E+05
13	10	36	1.02E+00	82448.1504	7.94E+03	1.65E+05
14	10	37	1.08E+00	91997.87809	8.39E+03	1.84E+05
15	10	38	1.13E+00	102354.1134	8.85E+03	2.05E+05
16	10	39	1.19E+00	113561.0351	9.32E+03	2.27E+05
17	10	40	1.26E+00	125664	9.80E+03	2.51E+05
18	10	41	1.32E+00	138709.5431	1.03E+04	2.77E+05
19	10	42	1.39E+00	152745.3774	1.08E+04	3.05E+05
20	10	43	1.45E+00	167820.3941	1.13E+04	3.36E+05
21	10	44	1.52E+00	183984.6624	1.19E+04	3.68E+05
22	10	45	1.59E+00	201289.4297	1.24E+04	4.03E+05
23	10	46	1.66E+00	219787.1214	1.30E+04	4.40E+05
24	10	47	1.73E+00	239531.3411	1.35E+04	4.79E+05
25	10	42	1.39E+00	152745.3774	1.08E+04	3.05E+05
26	10	41	1.32E+00	138709.5431	1.03E+04	2.77E+05
27	10	23.45	4.32E-01	14843.70458	3.37E+03	2.97E+04
28	10	22.61	4.02E-01	12828.41981	3.13E+03	2.57E+04
29	10	24.32	4.65E-01	17172.17069	3.62E+03	3.43E+04
30	30.1	25.11	4.95E-01	19514.51514	3.86E+03	3.90E+04
31	17.27	26.78	5.63E-01	25247.1991	4.39E+03	5.05E+04
32	30.1	25.11	4.95E-01	19514.51514	3.86E+03	3.90E+04
33	12.73	56.78	2.53E+00	510214.1125	1.98E+04	1.02E+06
34	8.26	69.28	3.77E+00	1130843.303	2.94E+04	2.26E+06
35	8.26	68.33	3.67E+00	1070080.863	2.86E+04	2.14E+06
Length	437.67					
Weight	10.1Kg					
E	1.96E+11					
Density	7905Kg/m^3					

Table 9.6 HPT rotor geometric data

This case was applied on the H.P.T rotor by using seven planes balancing (influence coefficient procedure), and two unbalance masses of 100 g were added to the rotor at the balancing planes (planes 1&7). Also in this test several other significant factors were applied. We found that some of the results were giving the similar results, so we decided to present only one case of the significant factor (0.01,0.02,0.1).

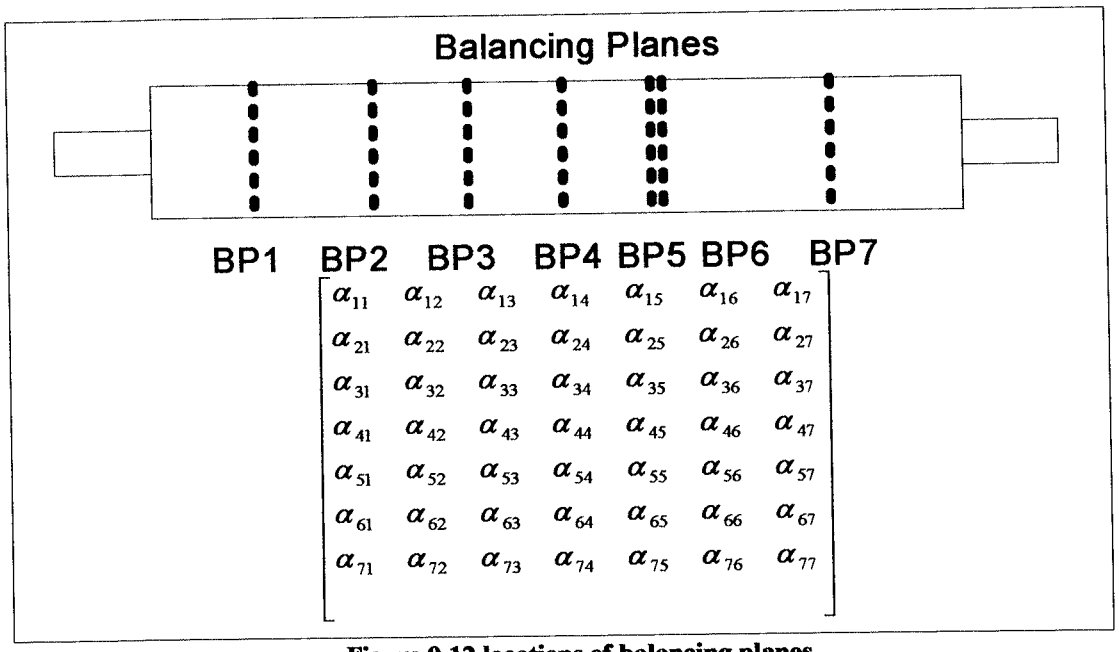

Figure 9.12 locations of balancing planes

The influence coefficient matrix $[a]$ for the test

$$1.0e\text{-}008 * \begin{bmatrix} 0.2157 & 0.3222 & 0.3597 & 0.3657 & 0.3571 & 0.2983 & 0.1401 \\ 0.2148 & 0.3420 & 0.3924 & 0.4049 & 0.3982 & 0.3366 & 0.1592 \\ 0.2398 & 0.3738 & 0.4643 & 0.4890 & 0.4855 & 0.4166 & 0.1989 \\ 0.2438 & 0.4049 & 0.4890 & 0.5295 & 0.5337 & 0.4692 & 0.2271 \\ 0.2414 & 0.4024 & 0.4884 & 0.5331 & 0.5409 & 0.4803 & 0.2338 \\ 0.1989 & 0.3365 & 0.4166 & 0.4692 & 0.4895 & 0.4704 & 0.2424 \\ 0.1401 & 0.2388 & 0.2983 & 0.3406 & 0.3596 & 0.3635 & 0.2173 \end{bmatrix}$$

Matrix condition number= 9.0436e+003

Results of the correction masses calculated by a different method **(Least square, QR and SVD)** after elimination of the influence coefficient matrix columns of the new ordered matrix using QR pivoting.

Least square solution = QR solution = SVD solution =1.0e+003 *

$$\begin{bmatrix} -1.2906 \\ 0.2609 \\ 2.7781 \\ -4.1803 \\ 1.9894 \\ 0.4187 \\ -0.5443 \end{bmatrix}$$

9.4.2.1 Case 1 elimination by using significant factor (0.01)

Influence coefficient matrix Columns Significant factor =

[1.0000 0.0427 0.0280 0.0131 0.0030 0.0054 0.0120]

Matrix Columns order after elimination =
The $[a]$ matrix after Column elimination

1.0e-008 *

$$\begin{bmatrix} 0.2157 & 0.3222 & 0.3597 & 0.3657 & 0.1401 \\ 0.2148 & 0.3420 & 0.3924 & 0.4049 & 0.1592 \\ 0.2398 & 0.3738 & 0.4643 & 0.4890 & 0.1989 \\ 0.2438 & 0.4049 & 0.4890 & 0.5295 & 0.2271 \\ 0.2414 & 0.4024 & 0.4884 & 0.5331 & 0.2338 \\ 0.1989 & 0.3365 & 0.4166 & 0.4692 & 0.2424 \\ 0.1401 & 0.2388 & 0.2983 & 0.3406 & 0.2173 \end{bmatrix}$$

Matrix condition number = 1458.6323

Results of the correction masses calculated by a different method **(Least square, QR and SVD)** after elimination of the influence coefficient matrix columns of the new ordered matrix using QR pivoting.

Least square solution = QR solution = SVD solution =
$$\begin{bmatrix} -726.5142 \\ 175.0789 \\ 477.8031 \\ -41.6392 \\ -138.0995 \end{bmatrix}$$

Elimination by using rank (QR)

New Matrix columns order = $[5 \quad 2 \quad 7 \quad 3 \quad 1 \quad 6 \quad 4]$

Least square solution = QR solution = SVD solution = 1.0e+003 *
$$\begin{bmatrix} 1.9894 \\ 0.2609 \\ -0.5443 \\ 2.7781 \\ -1.2906 \\ 0.4187 \\ -4.1803 \end{bmatrix}$$

Significant factor after pivoting=
$[1.0000 \quad 0.0883 \quad 0.0808 \quad 0.0131 \quad 0.0169 \quad 0.0057 \quad 0.0003]$
Matrix Columns order after elimination $= [1 \quad 2 \quad 3 \quad 4 \quad 5]$

The $[a]$ matrix after Column elimination=

1.0e-008 *
$$\begin{bmatrix} 0.3571 & 0.3222 & 0.1401 & 0.3597 & 0.2157 \\ 0.3982 & 0.3420 & 0.1592 & 0.3924 & 0.2148 \\ 0.4855 & 0.3738 & 0.1989 & 0.4643 & 0.2398 \\ 0.5337 & 0.4049 & 0.2271 & 0.4890 & 0.2438 \\ 0.5409 & 0.4024 & 0.2338 & 0.4884 & 0.2414 \\ 0.4895 & 0.3365 & 0.2424 & 0.4166 & 0.1989 \\ 0.3596 & 0.2388 & 0.2173 & 0.2983 & 0.1401 \end{bmatrix}$$

Matrix condition number $= 316.0066$

Results of the correction masses calculated by a different method **(Least square, QR and SVD)** after elimination of the influence coefficient matrix columns of the new ordered matrix using QR pivoting.

Least square solution = QR solution = SVD solution =

$$\begin{bmatrix} 91.1329 \\ 130.7726 \\ -184.7864 \\ 327.3508 \\ -597.9465 \end{bmatrix}$$

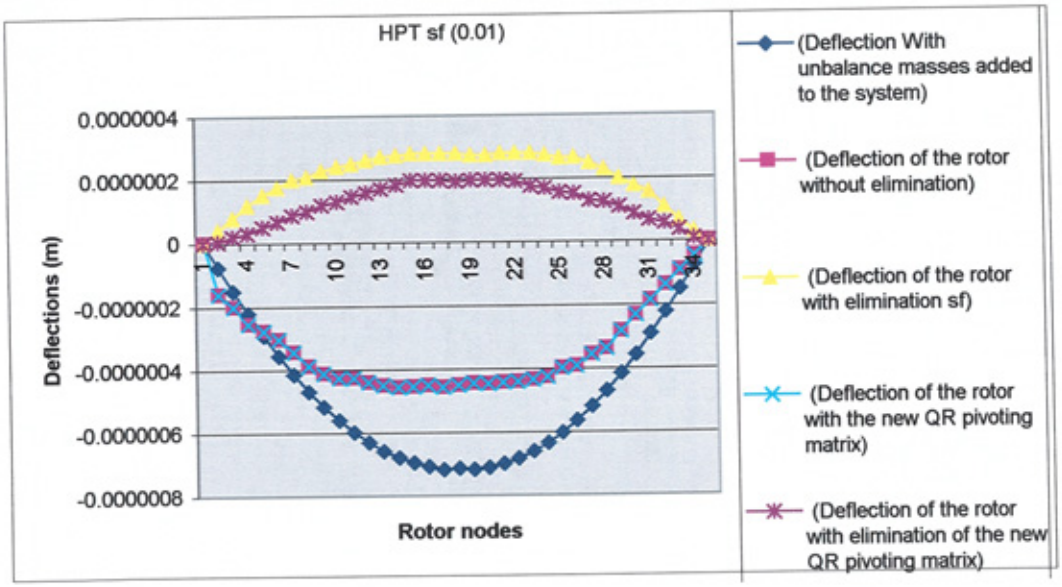

Figure 9.13 Results of HPT rotor after adding correction masses with S_f (0.01)

9.4.2.2 Case 2 elimination by using significant factor (0.02)

Influence coefficient matrix Columns Significant factor =
$[1.0000 \quad 0.0427 \quad 0.0280 \quad 0.0131 \quad 0.0030 \quad 0.0054 \quad 0.0120]$

Matrix Columns order after elimination = $[1 \quad 2 \quad 3]$

The $[a]$ matrix after Column elimination = 1.0e-008 *

$$\begin{bmatrix} 0.2157 & 0.3222 & 0.3597 \\ 0.2148 & 0.3420 & 0.3924 \\ 0.2398 & 0.3738 & 0.4643 \\ 0.2438 & 0.4049 & 0.4890 \\ 0.2414 & 0.4024 & 0.4884 \\ 0.1989 & 0.3365 & 0.4166 \\ 0.1401 & 0.2388 & 0.2983 \end{bmatrix}$$

Matrix condition number = 52.2965

Results of the correction masses calculated by a different method **(Least square, QR and SVD)** after elimination of the influence coefficient matrix columns of the new ordered matrix using QR pivoting.

$$\textbf{Least square solution = QR solution = SVD solution} = \begin{bmatrix} -360.2163 \\ 62.2804 \\ 272.5605 \end{bmatrix}$$

New Matrix columns order = [5 2 7 3 1 6 4]

Results of the correction masses calculated by different method **(Least square, QR and SVD)** after elimination the influence coefficient matrix columns of the new ordered matrix using QR pivoting.

$$\textbf{Least square solution = QR solution = SVD solution} = 1.0e{+}003 * \begin{bmatrix} 1.9894 \\ 0.2609 \\ -0.5443 \\ 2.7781 \\ -1.2906 \\ 0.4187 \\ -4.1803 \end{bmatrix}$$

Influence coefficient matrix Columns Significant factor =
[1.0000 0.0883 0.0808 0.0131 0.0169 0.0057 0.0003]

Matrix Columns order after elimination = [1 2 3]

$$\textbf{The } [a] \textbf{ matrix after Column elimination} = 1.0e{-}008 * \begin{bmatrix} 0.3571 & 0.3222 & 0.1401 \\ 0.3982 & 0.3420 & 0.1592 \\ 0.4855 & 0.3738 & 0.1989 \\ 0.5337 & 0.4049 & 0.2271 \\ 0.5409 & 0.4024 & 0.2338 \\ 0.4895 & 0.3365 & 0.2424 \\ 0.3596 & 0.2388 & 0.2173 \end{bmatrix}$$

Matrix condition number = 59.8005

Results of the correction masses calculated by a different method **(Least square, QR and SVD)** after elimination of the influence coefficient matrix columns of the new ordered matrix using QR pivoting.

Least square solution = QR solution = SVD solution $= \begin{bmatrix} 421.3117 \\ -212.6607 \\ -293.8371 \end{bmatrix}$

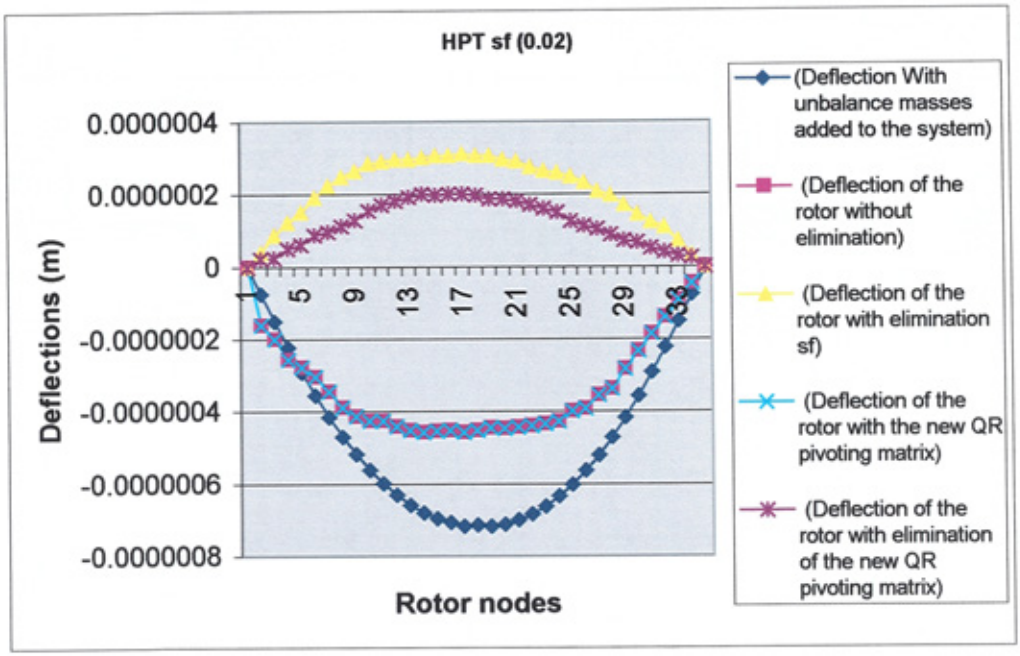

Figure 9.14 Results of HPT rotor after adding correction masses with S_f (0.02)

9.4.2.3 Case 3 elimination by using significant factor (0.1)

Influence coefficient matrix Columns Significant factor
$= \begin{bmatrix} 1.0000 & 0.0427 & 0.0280 & 0.0131 & 0.0030 & 0.0054 & 0.0120 \end{bmatrix}$

Matrix Columns order after elimination = 1

The $[a]$ matrix after Column elimination = 1.0e-008 * $\begin{bmatrix} 0.2157 \\ 0.2148 \\ 0.2398 \\ 0.2438 \\ 0.2414 \\ 0.1989 \\ 0.1401 \end{bmatrix}$

Matrix Rank= 1

Matrix condition number = 1

Results of the correction masses calculated by a different method **(Least square, QR and SVD)** after elimination of the influence coefficient matrix columns of the new ordered matrix using QR pivoting.

Least square solution = QR solution = SVD solution = 269.6633
Elimination by using rank (QR)

New Matrix columns order = [5 2 7 3 1 6 4]

Results of the correction masses calculated by a different method **(Least square, QR and SVD)** after elimination of the influence coefficient matrix columns of the new ordered matrix using QR pivoting.

Least square solution = QR solution = SVD solution = 1.0e+003 * $\begin{bmatrix} 1.9894 \\ 0.2609 \\ -0.5443 \\ 2.7781 \\ -1.2906 \\ 0.4187 \\ -4.1803 \end{bmatrix}$

Influence coefficient matrix Columns Significant factor =

[1.0000 0.0883 0.0808 0.0131 0.0169 0.0057 0.0003]

Matrix Columns order after elimination = 1

The $[a]$ matrix after Column elimination = 1.0e-008 * $\begin{bmatrix} 0.3571 \\ 0.3982 \\ 0.4855 \\ 0.5337 \\ 0.5409 \\ 0.4895 \\ 0.3596 \end{bmatrix}$

Matrix condition number = 1

Results of the correction masses calculated by a different method **(Least square, QR and SVD)** after elimination of the influence coefficient matrix columns of the new ordered matrix using QR pivoting.

Least square solution = QR solution = SVD solution =128.5290

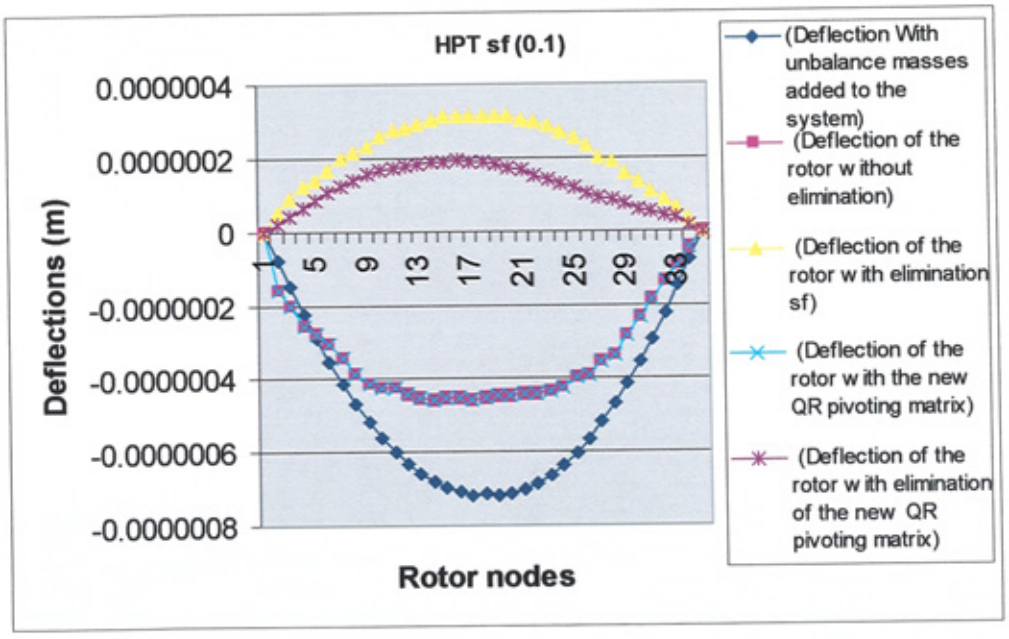

Figure 9.15 Results of HPT rotor after adding correction masses with S_f (0.1)

9.5 Results of using plane elimination of the pivoted matrix

Tables 9.7 and 9.8 shows the results of the amount of the correction masses achieved after using the new influence coefficient matrix which was based on the new order of the columns using QR pivoting procedure.

	No. Of planes (HPT rotor)						
Actual planes	5	2	7	3	1	6	4
	1	2	3	4	5	6	7
Correction masses							Matrix is close to singular or badly scaled. Results may be inaccurate. RCOND = 2.303820e-020 1.0e+020 *
Correction mass (1)	128.5290	138.6016	421.3117	442.1574	91.1329	-1686.6	-0.0000
Correction mass (2)		-13.2381	-212.6607	-191.8892	130.7726	307.6	-0.0000
Correction mass (3)			-293.8371	-303.0998	-184.7864	-764.2	-0.0000
Correction mass (4)				-35.4608	327.3508	1421.1	-0.0000
Correction mass (5)					-597.9465	-1194.5	1.0307
Correction mass (6)						1315.8	-1.0307
Correction mass (7)							-0.0000

Table 9.7 Results of correction masses of the HPT rotor (after plane elimination of the pivoting matrix)

	No. Of planes					
Actual plane	4	2	6	1	5	3
Correction masses	1	2	3	4	5	6
				1.0e+003 *	1.0e+003 *	1.0e+003 *
Correction mass (1)	150.3298	117.3121	737.9302	0.2956	-1.5923	-1.4665
Correction mass (2)		44.4290	-323.6241	1.0930	2.1805	2.2716
Correction mass (3)			-559.6382	-0.3652	-1.3114	-1.2964
Correction mass (4)				-1.5127	-2.3291	-2.3830
Correction mass (5)					2.2394	2.1753
Correction mass (6)						-0.1210

Table 9.8 Results of correction masses of the symmetrical rotor (after plane elimination of the pivoting matrix)

9.6 Results Discussion

For the first and second test cases, where a 2 plane balancing technique was used, the influence coefficient matrices were fairly well conditioned as we can see from the matrix condition number in the whole subcases. Where the significant factor changed between 0.01 and 0.5. The values of the calculated correction masses for the first and second sets of the results agree with seems with the unbalance masses introduced to the system in both cases.

For the third and fourth test cases, where 6 and 7 plane respectively balancing was used, the influence coefficient matrices were not well conditioned as indicated by the value of the

Matrix condition number in the whole subcases, where the tolerance number changed between 0.01 and 0.5 the corresponding value of the calculated correction masses for the third and forth sets of the results seems to be large and tending to cancel.

The results of case 3 and 4 illustrate that, the outcome of the results using significant factor amount above 0.05 will give the same results. As we can see from the results of significant factor range of 0.05 to 0.5 all give the same condition number (i.e. case 3 was 1 and correction mass was 305.0215).

Figures 9.8-9.15 and tables A8.28-A8.33 illustrate the deflection of the rotor for each case applied in the series of the above tests, in comparison to the plots of the deflection after elimination using the QR significant number and elimination using the same method but applied to the new pivoting matrix (using QR). There is an improvement of the results, as the amount of the correction masses is much smaller than before. Also the deflection is less as shown in the plots.

Tables 9.7 and 9.8 illustrate the results of the amount of the correction masses achieved after using the new influence coefficient matrix, which was based on the new order of the columns using QR pivoting procedure. As far as the amounts of the correction masses were concerned, most of planes calculated gave quite a big amount compared to the unbalance masses added. If the results obtained by using 2 plane balancing, are considered it can be seen that this method is the closest method to identifying the unbalance mass, ie, in table 9.8 the amount of correction masses were (117.3121 and 44.4290) respectively which was the closest results compared with the other planes results.

9.7 Conclusion

The results of the first 2 sets shows that the significant number does not play a big role in the case of well conditioned influence coefficient matrix, but in the case of an ill conditioned matrices (cases 3 and 4) the results shows that the higher the significant number the more matrix columns should be eliminated.

The results of case 3 and 4 the column elimination of the original matrix did not seem acceptable in term of practical application, which surely will leave some issues to be answered regarding the practical application of the optimization of the balancing planes procedure. Particularly the questions concern the effect on real rotor balancing test data, depending on the acceptable level of the significant factor and whether this acceptable factor should be related to the influence coefficient matrix condition.

To sum up the conclusion, the results shows that with the use of 2 plane balancing we achieved better results (as expected), whereas all other results failed to give the desired results. So generally speaking, it is recommended use 2 plane balancing, which will cut the use of the number of instruments (vibration amplitude measurement) and less manpower. Also in the case of using a multi plane procedure, it is suggested to use the new pivoting matrix (using QR) after elimination.

9.8 Results Discussion of the optimum locations of the balancing planes

A set of benchmark Tests on elastic beam (pin – pin rotor) analysis were carried out using the commercially available finite element analysis packages ANSYS and are presented to validate techniques for optimizing the balancing planes. Results (table 9.12) in general show agreement with those previously obtained using the Theoretical analysis. The main thrust of the present study has been to compare the ANSYS results with those obtained by analytical results.

9.8.1 the effect of changing the balancing planes locations (e.g. adding the correction mass in a different plane of the trial mass plane).

In summary, the finite element method provides a powerful numerical technique for solving boundary-value problems over a complex domain. The finite element method has been used to analyze the mechanical deformations of a rotor. The results of this analysis are presented in this thesis.

The results tables and Figures show that:

- The Young's Modulus of the rotor does not have any effect on the balancing planes locations, and the amount of the trial mass. As we can see in Figures 9.3, 9.4 and tables 9.4, 9.5.
- In the case of using 10%, 15% and 20% of the total mass as a trial mass the results were good as they identify the amount of unbalance mass, which added to the system in order to create imbalance rotor. (See Figure 9.2 and table 9.3)
- Figures 9.6-9.7 show the results of where to place the correction mass showed that the correction mass should be inserted in the same plane as the trial mass but in case of some difficulties it is recommended to place the correction mass as close as possible to the trial mass plane.

Further test cases (i.e third and fourth sets of results), where 6 and 7 planes balancing were used, the influence coefficient matrices were not well conditioned. The calculated correction masses for these sets of the results seem to be too large and not practical.

Obviously the condition number of the influence coefficient matrix (after eliminating the matrix columns) shows substantial improvement over the condition number of the original influence coefficient matrix. The results of case 3 and 4 illustrate that, the outcome of the results using a significant factor amount above 0.05 will give the same results, as seen from the results of significant factor range of 0.05 to 0.5 all give the same condition number (i.e. case 3 was 1 and correction masses was 305.0215).

Chapter 10

CONCLUSIONS

10.1 General Conclusion

The objective of this chapter is to clarify the contribution of the project towards the development of a method for rotor balancing discussed in detail in Chapter 1. The aim of the project was to develop a balancing procedure to correct the vibration within the operating range of the machine. The proposed balancing methods, which are described in Chapter 6, 7, 8 and 9, were conceived for application to multi-rotor multi-bearing systems, in order to provide more efficient procedures leading to higher balance and alignment quality.

The experience obtained during the application of the methods included in this thesis allowed the author to draw the conclusions listed herein.

- Vibration levels can be influenced by many factors other than strictly rotor unbalance. Such factors as resonance, shaft misalignment, mechanical looseness, defective bearings, rotor loose on the shaft and cracks in the rotor can all contribute to high vibration.
- The influence coefficient method has great flexibility not only for solving balancing problems, but also as a tool for understanding rotor behaviour.
- Experimental tests conducted further demonstrate the ability of the influence coefficient method to achieve precise balance of flexible rotors for virtually any design or operation through virtually any speed range.
- Several reasons can affect the accuracy of the results; the influence coefficient method uses equations which are not entirely independent, the structural system may be non-linear with respect to resonance, other root causes of vibration exist, the system may be unstable, bearings may be worn, shafts may be distorted, or test weights may be ill-placed.

10.2 Measurement Uncertainty

Due to the flow of new instrumentation and component developments there has been rapid growth of balancing technology in recent years. Equally important has been the practical adaptation of procedures for general flexible-rotor balancing, their industrial verification, and the development of balancing standards and criteria. Balancing should be done in several successive steps because of the limited accuracy of measurements and because of the possible non-linearity of the influence coefficient matrix.

All machines are subject to random vibration as well as periodic vibration. Therefore, it is advisable to acquire several sets of data and average them to eliminate spurious signals. Averaging also improves the repeatability of the data, and must reduce the effects of random errors because only the continuous signals are retained. So now the question to be answered is how many data sets have to be averaged to obtain an accurate representation of the shape of the data? Obviously the more the better but, as can be seen from the test data (see 6.1), a point of diminishing returns is reached relatively quickly. Typically, a minimum of three samples should be collected for an average. However, the factor that determines the sample count is time. Specifically, steps taken to minimize vibration, and an average of five scans produce acceptable average results. This keeps the time spent measuring within the DAQ systems ability to increase data-acquisition speed.

Because of experimental measurement uncertainty, it is recommended that whenever a balancing test is run, the measurements (vibration amplitudes and the phase angle) should be taken at several times (more than 3 times) and averaged; it is also necessary to consider the standard deviation at any calculations which follow the test.

Uncertainty is an unavoidable part of any measurement and starts to matter when results are close to a specified limit. A proper evaluation of uncertainty is good practice and can provide valuable information. It is recommended that one understands the workings of each instrument, and also each measurement is taken carefully, and rechecked to make sure that

precision is achieved. Without accuracy and precise measurements, calculation even if done correctly is quite useless.

10.3 Trim Balancing Techniques

It is difficult to make relevant contributions to a subject that has been so extensively studied over the years. The modal balancing theory, as it is applied to rotor balancing, reached its present state of development after several important contributions by Bishop, Gladwell, Parkinson and others back in the 1960's, and it has not undergone major modifications since then.

One of the subjects analyzed during this project was the influence coefficient method. Careful analysis of this method allowed modifying the procedure for the determination of the influence coefficient matrix for the trim balancing procedure, which was previously restricted to the use of new vibration data for the new influence coefficient matrix.

This modification is presented here because, with the exception of a couple of papers by Dresser in (1976) and (1980), no publications were found in this respect, even when there are indications that similar procedures have been used in practice. This and the fact that Dresser did not consider some practical aspects of the method motivated the presentation of a methodology for the determination of the influence matrix.

Ideally, it would be useful to eliminate the unbalance completely. In practice it is usually not possible to completely remove all unbalance. Some residual unbalance will always remain. It is very rare that the desired results are produced by one step balancing because there are errors in vibration parameter measurements, differences in parameters of attached masses in comparison with the calculated ones, influences of mechanical machine properties and non-inertial forces.

Trim balancing can be carried out as many times as desired. After each successive iteration, the rotation should become smoother. If it does not, perhaps the limits of balancing improvements have been achieved (probably in relation to the measurements

accuracy), or the physical response of the rotor is nonlinear, and a new problem must be started with fresh original data.

In conclusion, the results achieved from the tests of balancing for both HP & LP turbine rotors achieved best balancing condition. The main purpose of the test was to verify the new trim balancing approach, described in the calculation section (Method C). Something worth mentioning is that the calculation in method C gives better results as far as the amount of the correction masses and the balancing quality grade were concerned in all of the tests compared with the previous method (see Tables A8.1-8.3 and figures 6.5-6.8).

It is expensive to carry out balancing runs especially for large rotating machines. The use of trim balancing reduces the number of runs from 3 to 2. Hence it is cheaper to use the trim balancing procedure.

If the mass must be located at the same location as a previous mass, both masses (previous balance mass and trim balance mass) should be combined into a single mass by making a larger mass or using a material of greater density.

After finishing the test, we now try to improve the rotor condition, by applying the trim balancing runs. The main purpose of the test was to verify the new trim balancing approach, which as mentioned in the calculation section (Method C)

10.4 Least Square, QR Factorization and SVD Aided Solving Influence Coefficient Matrix

The question to be answered is what is the fastest and most accurate algorithm for solving least squares problems? Solving the normal equations is fastest, followed by QR and the SVD. If the matrix is quite well conditioned, then the normal equations are as accurate as the other methods. When the matrix is not well conditioned but far from rank deficient, the author recommends to use of the QR factorization method. Since the design of fast algorithms for rank-deficient least squares problems is a current research area, it is difficult to recommend a single algorithm to use. The author summarizes a recent study that

compared the performance of several algorithms, comparing them to the fastest stable algorithm for the non-rank deficient case.

The methods of normal equations: This is the fastest method but it has two disadvantages; it only works for non-degenerate, over determined systems and it is numerically unstable. Solving the normal equations is the cheapest. However, it is apparent that it is much less well conditioned than the other two methods, i.e. there can be instabilities (accumulation of round-off errors). The normal equation method can lose twice as many digits of accuracy as the methods based on QR and SVD. However, since the normal equation method is the fast way to solve the least square problem, it is the method of choice when the problem is well conditioned.

It is useful to understand that the solution of a least squares problem directly from the normal equations is rather susceptible to round-off errors. An alternative, and preferred technique, involves QR decomposition and the singular value decomposition of the matrix.

The mathematical definition of stability is a measure of the effect of errors in coefficient of a posed problem or in the solving process on the solution. The degree of stability of a problem is typically indicated in terms of condition. The stable system is a system of linear equations and is said to be well conditioned if small errors in the coefficients or in the solving process have only a small effect on the solution. The unstable system is a system of linear equations and is said to be ill-conditioned if small errors in the coefficients or in the solving process have large effects on the solution. From the stability viewpoint, one can show that both QR and SVD methods properly implemented are numerically stable. On the other hand the normal equation methods are not necessarily stable.

QR factorization: This method is recommended for most cases. It can handle all cases and is usually stable. It takes about twice as much computer time as methods of normal equation. QR is cheaper than SVD. It is the method of choice as long as the matrix is not too close to being rank deficient.

SVD should be used for cases where QR factorization fails: It takes five to ten times more computer time than the normal equations, but it is extremely stable. It can also be used for

other purposes, for example when Gaussian elimination fails. SVD costs about as much as QR when m > *n* (which is often the case). It is also the method of choice if the matrix is close to being rank-deficient (all data are not independent).

Additional information given by the (SVD) can be used to verify the reliability of influence coefficients and then the optimal correction masses can be selected. The effectiveness of the (SVD) algorithm for influence coefficient balancing is established through numerical analysis and a balancing example. By using this method the minimum number of balance planes, as well as minimum balance weights, can be used to balance a rotor in the most cost effective and accurate manner. The method may also be used to predict the worst unbalance response in a flexible rotor.

The benefit of solving least square problems by using QR and SVD methods is that the final solution is much more tolerant to ill-conditioned systems, i.e. less sensitive to the inevitable round-off errors of the computation.

10.5 Shaft-to- Shaft Alignment

An experimental investigation on the effect of shaft alignment on the balanced rotors reveals that.

- When a single rotor is supported by more than two radial bearings, or when two or more rotating shafts (e.g. a multi-stage pump or compressor) are coupled, the alignment of the several bearings becomes an important consideration. Ideally all bearings should be centered on a single straight-line axis of rotation.
- Misalignment places undesirable loads on the rotor and the bearings and may cause undesirable vibrations. Misalignment may be due to faulty positioning of the bearings during installation, or due to subsequent displacement of the bearings because of foundation settlement or thermal expansion.

Detecting shaft misalignment can be difficult if not impossible on operating rotating machines. Even for severe misalignment conditions, sometimes only slight changes in vibration or temperature occur making it difficult to identify the severity of the problem.

Not until mechanical degradation actually occurs, can the root cause of misalignment be suspected but by then, the damage has already taken its charge on the equipment. Correcting a known misalignment condition can be one of the most frustrating tasks you could undertake.

Misalignment of machinery shafts causes the rotor mass to be distributed away from the axis of the rotation. Hence the rotor unbalance forces and the reaction forces will increase. Consequently the vibration amplitude will increase. This is often a major cause of machinery vibration. The effect that misalignment has on the machines is a function of the radius of the shaft movement, which consequently will increase the centrifugal force, which leads to an unbalanced system.

The ideal rotor excites minimal vibration as a result of pure alignment errors, because no rotating force exists. In practice, however there is no ideal rotor and no sure alignment error. There is always a mixture of various alignment and coupling error, errors in unbalance, bearing failure. Therefore you will always find vibration in rotating machines. Alignment is a subject too vast ranging to allow a comprehensive coverage of all of the areas associated with this field. Structural errors and machine errors often compound alignments. These defects can turn a simple job into an all day affair and also unsatisfactory results despite a conscientious effort and a considerable investment in manpower and downtime

The results in this research, which estimate the adverse impact that misalignment has on system vibration, should be considered a minimum estimate. Therefore, according to the series of tests which have been carried out in this study it is suggest that after any balancing procedure it is essential to make sure that the system is well aligned as well, because the results of this thesis showed that the higher misalignment shafts will cause higher vibration and subsequently may increase the unbalance of the rotors. Also it is recommended to check the vibration condition of the machine after finishing the balancing test, and as the alignment test will not take longer time due to the introduction the modern laser alignment techniques. It is recommended to check the system alignment after the balancing test.

10.6 Finite Element Method

The finite element method provides a powerful numerical technique for solving boundary-value problems over a complex domain. The finite element method has been used to analyze the mechanical deformations of a rotor. The results of this analysis are presented in this thesis.

For some rotors, especially those of irregular shapes, the balancing problem is different from the usual rotor balancing problem, in that the corrections are conveniently made in completely selected locations instead of in the ordinary way in which transverse planes are selected, but the angular position of the correction is left for determination Baker (1939).

In order to balance flexible rotors effectively, the selection of the correction planes is very important. Because ill-selection of the correction planes occasionally results in excess of correction mass which may not be permissible for that rotor. Any balancing process requires the formulation of systematic methods for selecting and positioning a suitable correction mass.

From the results tables and the previous discussion, it is clear there are some definitive guidelines that should always be considered on complex rotors. Specifically, the following items are summarized for future reference:

- Mass correction locations should be modally effective. If a mass change produces an unexpected result, the presumed mode shape may be incorrect.
- When adding (or removing) trial masses, check the response vector. Small vector changes indicate a lack of sensitivity to the mass.

Vibration sensor location(s) must be the same for all (trial) runs during a given balance operation. Moving the sensor mounting location, even slightly, will alter the test conditions and readings (vibration phase and amplitude) unnecessarily. It is also a good practice to locate sensors in the same locations for future balance operations, once good results are obtained. Sensor locations on a machine may be marked by ink, paint or a shallow drill-point indentation.

To sum up the conclusion, the results shows that for the particular cases studied, 2 plane balancing achieved better results (as expected), whereas all other results were not as accurate so generally speaking it is recommended to use 2 plane balancing, which will cut the number of instruments (vibration amplitude measurement) and require less man power. In the case of using a multi plane procedure it is suggested to use the new eliminated pivoted matrix.

10.6.1 Practical Considerations for Trial and Correction Mass Location

1. Mount the trial and the correction masses at the same radial distance from the shaft, or else a (simple) correction factor must be applied.
2. Mount the correction masses in the same plane as the trial masses (plane perpendicular to the shaft longitudinal, main, axis).
3. If the desired correction mass position is not convenient or practical, there is a way to divide or split the required amount of mass into two or more parts. This enables mounting of masses at convenient locations such as blades, vanes, existing holes, etc.
4. Masses should be mounted axially as close as possible to the (rotor) imbalance source.
5. A correction plane is any plane perpendicular to the shaft axis where balance corrections are made. Whenever possible correction planes should be selected in places where mass is concentrated. This provides the best chance for corrections to be in the plane of unbalance.
6. Any balancing process requires the formulation of a systematic method for selecting and positioning a suitable correction mass.

Chapter 11

RECOMMENDATIONS FOR FUTURE WORK

Future lines of research in this area may be proposed directly from the above conclusions and from the experience gained during the development of the project. These are listed in the following points.

1. This suggests that some of the practical difficulties still need to be overcome, which keeps the door open for further research in this area. Consequently, high-speed rotors often deform significantly under the action of these unbalanced forces. Rotors, which exhibit such behavior, are generally referred to as flexible rotors.
2. Several authors have published studies concerning the minimization of the correction masses and complete elimination of balancing planes, but a literature search revealed no reports of systematic application of these procedures to flexible rotors. This suggested that some practical difficulties had still to be overcome, opening the possibility for further research in this area.
3. It is suggested that the available finite element software packages may be used to develop a computational model of multi-rotor multi-bearing system to study the influence of misaligned rotors on the dynamic behaviour of the rotor system, with different condition such as speed, bearing, types of shafts and types of coupling
4. Use of neutral networks in rotor balancing and shaft alignment combined with SVD. A neural net can be difficult to associate experimentally with the measured vibration response and the imbalance and alignment causing them. The net can indicate the location of the imbalance and the amount of shaft alignment. This could speed-up the balancing and alignment process.
5. There is considerable scope for further application of expert systems and other computer-based systems in machine health monitoring. Their use is not widespread, but they are becoming more popular. They are able to help diagnose many faults but further work needs to be carried out to establish more reliable algorithms for diagnostic purpose for various types of rotating machine faults.

6. By applying genetic algorithms (GA), it should be possible to find the unbalance masses based upon the measurements of the original vibration in the bearing sections at one or several operating speeds. An obvious superiority of this method is that no further prior knowledge about the bearing parameters is required. Furthermore, this method could simultaneously evaluate the bearing parameters and their working situation in the different service environments of large rotating machinery.

REFERENCES:

1. Badgley, R.H., Modren Influence coefficient Techniques for Multiplane Rotor Balancing in the Factory, Vibrations in Rotating Machinery, Institute of Mechanical Engineers Conference Publications1976, pp 201-207.
2. Baker J.G., Methods of rotor unbalance determination, Trans American Society of Mechanical Engineers, Journal Applied Mechanics 1939 (61), pp AI-A6.
3. Balda M., Balancing flexible rotors as a problem of mathematical program, Proceedings of the Institution of Mechanical Engineers 1980, pp 253-257.
4. Barry M. Wise and Neal B. Gallagher. An Introduction to Linear Algebra. The MathWorks,Inc 1999.
5. Bigret, Roland, Curami, Andrea, Frigeri, Claudio, and Macchi, Nagelo, Use of In-Field Computer for Balancing High Power Turbomachinery, American Society of Mechanical Engineers (September) 1977 Paper No. 77DET-II.
6. Bishop R.E.D. and Mahalingam, Some experiments in the vibrations of a rotating shaft, Proc. Royal Society London, Series A: Mathematical and Physical Sciences 1966.Vol 292, No (1431), pp 537-561.
7. Bishop, R.E.D., and Parkinson, A.G., On the Use of Balancing Machines for Flexible Rotors, Transactions of the American Society of Mechanical Engineers, Journal of Engineering for Industry, 1972 (94).
8. Bishop, R.E.D., On the Possibility of Balancing Rotating Flexible Shafts, Journal of Mechanical Engineering Science, 1982,Vol. 24, pp 215-220.
9. Bishop. R.E.D. and Gladwell. G.M.L., The vibration and balancing of an unbalanced flexible rotor, J. Mechanical Engineering science 19591,Vol (1), pp 66-77.
10. Bishop. R.E.D. and Parkinson. A.G., On the isolation of modes in the balancing of flexible shafts, Proc. institute of Mechanical Engineers 1963,Vol 177,No.16,pp 407-423.

11. Bishop. R.E.D., The vibration of rotating shafts, J. Mechanical engineering Science 1959,Vol 1,No. (1), pp 50-65.
12. Black .H., A linearized model using transfer matrix to study the forced whirling of centrifugal pumps rotor systems. Journal of Engineering for Industry 1974.
13. Bloch H. P., Hydrocarbon Processing. How to upgrade turbomachinery by optimized coupling selection. 1976 Vol 55,No. (1), pp 87-90.
14. Chen L.W. and Ku D.M. Finite element analysis of natural whirl speeds of rotating shafts. Computers and Structures 1991,No.40, pp741-747.
15. Chen, W. J., A Note on Computational Rotor Dynamics, ASME Transactions, Journal of Vibration and Acoustics, 1998,Vol. 120, pp 228-233.
16. Church, A.H., and Plunkett, R., Balancing Flexible Rotors, Transactions of the American Society of Mechanical Engineers, Journal of Engineering for Industry, (November) 1961,Vol. 83, No.4. pp 383-389.
17. DAQ 6023E/6024E/6025E User Manual December 2000 Edition
18. Darlow M.S, Balancing of high-speed machinery: Theory., Methods and experimental results. Mechanical Systems one Signal Processing 1987, Vol 1,No. (1) pp 105-134.
19. Darlow, M.S., and Smalley, A.J., Application of the Principle of Reciprocity to Flexible Rotor Balancing, Transactions of the American Society of Mechanical Engineers, Journal of Mechanical Design, 1982,Vol. 104, No.2, pp 329-333.
20. Darlow, M.S., Smalley, A.J., and Fleming, D.P., Demonstration of a Supercritical Power Transmission Shaft, published in the Proceedings of the National Conference on Power Transmission, Chicago, Illinois, (November 7-9) 1978.
21. Darlow M.S., Balancing of High-Speed Machinery, Mechanical Engineeril1& Series, Springer-Verlag, New York, 1989.

22. Darlow, M.S., Smalley, A.J., and Parkinson, A.G., A Unified Approach to Flexible Rotor Balancing: Outline and Experimental Verification, presented at the Institute of Mechanical Engineers' Conference on Vibrations in Rotating Machinery, Cambridge, England, (September) 1980.

23. Darlow, M.S., Smalley, A.J., and Parkinson, A.G., Demonstration of a Unified Approach to the Balancing of Flexible Rotors, Transactions of the American Society of Mechanical Engineers, Journal of Engineering for Power, 1980.

24. Darlow, M.S., The Identification and Elimination of Non-Independent Balance Planes in Influence Coefficient Balancing. Presented at the American Society of Mechanical Engineers International Gas Turbine Conference, (April) 1982.

25. Den Hartog, J.P., Mechanical Vibrations, New York, McGraw-Hill. 1934.

26. Den Hartog J.P., The balancing of flexible rotors in air space, and instruments, McGraw-Hill, 1963,pp165-182.

27. Dimarogonas A. D. and Paipeties S. A. Analytical Methods in Rotor Dynamics. New York: Applied Science Publishers. 1983.

28. Dimentberg. F.M., Flexural Vibrations of Rotating Shafts. London: Butterworth 1961.

29. Drechslen, J. Systematic combination of experiments and data processing in balancing of flexible rotors, in: Proc. 1st Int. Conf. on Vibrations in Rotating Machinery, Cambridge, England, Institute of Mechanical Engineers, 1976, pp 129-132.

30. Drechslen 15. Processing surplus information in computer aided balancing of large flexible rotors, in: Conf. Vibrations in Rotating Machinery, Cambridge, U.K., Institute of Mechanical Engineers, 1980, pp. 65-70.

31. Ding J., Computation of Multi-Plane Imbalance For A Multi-Bearing Rotor System, Journal of Sound And Vibration, Aug 1997,Vol. 205, No 3, pp 364-371.

32. Enrich F. F., Handbook of Rotordynamics. New York: McGraw-Hill. 1992

33. Eisenmann.R.C, Machinery Malfunction diagnosis and correction, Prentice Hall PRT, newjersy 1998.

34. Eshleman R. L., Flexible Rotor Bearing Systems Dynamics. 1978 New York: ASME Publications.

35. Fawzy, I., and Bishop, R.E.D., A Strategy for Investigating the Linear Dynamics of a Rotor in Bearings, Vibrations in Rotating Machinery, Institute of Mechanical Engineers' Conference Publications 1976, pp. 239-244.

36. Federn, I.K., Looking to the Future in Balancing, presented at the Avery Symposium on Dynamic Balancing, (March) 1964.

37. Feng, N.S. Using Vibration Analysis Software to balance turbomachinery, Trans. Of Institution Of Engineers, Australia Mechanical Engineering, 1996 Vol (21), No. (3), pp 147-155.

38. Foiles W C, P.E Allaire, and E J Gunter, Min-max optimum flexible rotor balancing compared to weighted least squares, Proceedings of the Institution of Mechanical Engineers 2000, pp141-149.

39. Foiles.W.C, Allaire P.E and Gunter.E. Review: Rotor Balancing, Journal Shock And Vibration 1998, Vol 5, No. (5-6) pp325-336.

40. Gaberson, H.A., and R Cappillino, "Rotating Machinery Energy Loss Due to Shaft Misalignment", Proceedings of the Society for Machinery Failure Preventive Technology, Virginia Beach, VA, 1998,pp. 519-428.

41. Gibbons B. Coupling misalignment forces. Proceedings of the Fifth Turbomachinery Symposium, Gas Turbine Laboratories, Texas A & M University, College Station, Texas 1976, pp 111-116.

42. Gladwell. G.M.L. and Bishop. R.E.D., The vibration of rotating shafts supported in flexible bearings, J. Mechanical Engineering Science 1959,Vol 1,No.3, pp 195-206.

43. Gilbert Strang. Linear Algebra and Its Applications. Harcourt College Publishers, 3 rd Edition, 1988.

44. Glasgow. D. A. and Nelson. H. D. Stability analysis of rotor-bearing system using component mode synthesis. ASME Journal Machine Design1980 Vol.102, pp185-193.

45. Gmlir. T. C. and rodrigues. J. D. Shaft finite elements for rotor dynamic analysis. ASME Journal of Vibration and Acoustics 1991,Vol 113, pp 482-493.

46. Goodwin.M.J, Dynamics of rotor bearing systems, London. Unwin Hyman 1989.

47. Goodman T.P, A least-squares method for computing balances corrections, Trans. American Society of Mechanical Engineers, J. Engineering for Industry 1964, Vol 86,No.3, pp 273-279.

48. Goseiwski, Z., journal of sound and vibration. An automatic balancing of flexible rotors part 1: syntheses of system. 1985,Vol. 220, No.(4), pp 551-567.

49. Gosiewski, Z., Automatic Balancing of Flexible Rotors, Part 2, Synthesis of System, Journal of Sound and Vibration, 1987,Vol. 114, pp 103-119.

50. Grobel, L.P., "Balancing Turbine-Generator Rotors," General Electric Review, 1953 Vol. 56, No.4.

51. Gu H, H.Ren and J.yang, An improved least squares method for calculating balancing correction masses, Institution of Mechanical Engineers, 1988,PP 499-507.

52. Howard Anton. Elementary Linear Algebra. John Wiley & Sons, 7th edition, December 1993.

53. Hopkirk K.R., Notes on methods of balancing, The Engineer 1940,Vol 170, pp 38-39.

54. Iwatsubo, T. Error Analysis of Vibration of Rotor/Bearing System, Proceedings of the Institution of Mechanical Engineers - Vibrations in Rotating Machinery, 1976, pp 87-92.

55. Jeffcott H.H., The lateral vibration of loaded shafts in the Neighborhood of a whirling speed - the effect of want of balance, Philosophical Magazine 1919, Vol 37, pp 304-314.

56. Jhon H. Mathews and Kurtis D. Fink, numerical methods using matlab, 3rd edition, 1999.

57. Kang Y., Shim Y. P. and Lee A. C. Investigation on the steady-state response of asymmetric rotor ASME Journal of Vibration and Acoustics 1992-No.114, pp 194-208.

58. Kang, Y. C., P. Liu, G.J Sheen, A Modified Influence Coefficient Method For Balancing Unsymmetrical Rotor-Bearing Systems Journal Of Sound And Vibration, 1996,Vol. 194, No. 2, pp 199-218.

59. Kellenberger, W. and Rihak P., Bimodal (complex) balancing of large turbogenerator rotors having large or small unbalance. Proc. Institution of Mechanical Engineers. Conf. Vibrations in Rotating Machinery. Heriot-Watt Univ. September 1988, Paper C292/88,pp 479-486.

60. Kellenberger, W. Should a flexible rotor be balanced in N or N+ 2 planes? Journal. Eng. Ind. 1972 No. 2,pp 548-560.

61. Kramer E., Dynamics of Rotors and Foundations. Berlin: Springer. 1993

62. Kreuzinger-Janik T and H Lrretier, Unbalance identification of flexible rotors based on experimental modal analysis, Proceedings of the Institution of Mechanical Engineers 2000, pp335-349.

63. Krodkiewski J.M., Identification of unbalance change using a non-linear mathematical model for rotor bearing systems, Journal Sound and Vibration 1994, No.169, pp 685-689.

64. Kennedy C.C. and Pancu D.D.P., Use of factors. in vibration measurements and analysis, J. aeronautical science 1947 Vol 14, No.11, pp 603-625.

65. Lalanne M. and Ferraris G. Rotordynamics Prediction in Engineering New York. 1990.

66. Larson Lars-Ove, On the determination of the influence coefficients in rotor balancing using linear regression analysis, in: Proc. on Vibrations in Rotating Machinery, Cambridge, England, Institute of Mechanical Engineers, 1976, pp. 93-97.

67. Lay, David C. Linear Algebra and Its Applications. Addison Wesley Longman, Inc., 1997.

68. Lee A. -C., Kang Y. and Shim Y. P. A modified transfer matrix method for linear rotor-bearing systems. ASME Journal of Applied Mechanics 1991,No.58, pp776-783.

69. LeGrow, J. V., Multiplane Balancing of Flexible Rotors--A Method of Calculating Correction Weights," American Society of Mechanical Engineers Third Vibration Conference (September) 1971,Paper No. 71-Vibr-52, Toronto, Canada.

70. Leung P S. An investigation of the dynamic behavior of floating rings bearing systems and their application to turbogenerator, PhD thesis Northumbria University 1988.

71. Leon, Steven. Linear Algebra with Applications. Prentice Hall, Inc., 1998.

72. Lindley A.L.G. and Bishop R.E.D., Some recent research of the balancing of large flexible rotors, Proc. Institute of Mechanical Engineers (1963), Vol 177 No. 30. pp 811-825.

73. Ling-J Cao-Y Improving Traditional Balancing Methods For High Speed Rotors, Journal Of Gas Turbine And Power, Transaction Of The American Society of Mechanical Engineers. 1996 Vol 118,No 1, pp 95-99.

74. Little, R.M., The Application of Linear Programming Techniques to Balancing Flexible Rotors, Ph.D. Thesis, University of Virginia, 1971.

75. Little, R.M., and W.D. Pilkey. A Linear Programming Approach for Balancing Flexible Rotors, Transactions of the American Society of Mechanical Engineers, Journal of Engineering for Industry, 1976.Vol. 98, No.3, pp 1030-1035.

76. Ludeca,Inc. Maintenance study, Evaluating energy consumption on misaligned machines 1994.

77. Lund I.W. and J. Tonnesen, Analysis and experiments on multi-plane balancing of a flexible rotor, Trans. American Society of Mechanical Engineers, J. Engineering for Industry 1972,Vol 1, pp 233-242.

78. Lund, J. W., Stability and Damped Critical Speeds of a Flexible Rotor in Fluid-Film Bearings, ASME Transactions, Journal of Engineering for Industry, 1974,Vol. 96, pp 509-517.

79. Lund, J. W., and Orcutt, F. K., Calculations and Experiments on the Unbalance Response of a Flexible Rotor, ASME Transactions, Journal of Engineering for Industry, 1967,Vol. 89, pp 785-796.

80. MATLAB User manual "Revisions 5.2, 5.3 and 6" .matworks

81. ANSYS User manual "Revision 5.4" Swanson Analysis systems. Houston, USA.

82. Modal analysis "ANSYS User manual Revision 5.4" Swanson Analysis systems. Houston, USA.

83. Meacham, W.L., Talbert, P.B., Nelson, H.D., and Cooperrider, N.K., Complex Modal Balancing of Flexible Rotors Including Residual Bow, Journal of Propulsion and Power, 1988Vol. 4,No.3, pp 245-251.

84. Moore L.S. and Dodd E.G., Mass balancing of large flexible rotors, General Electric Review Journal, 1964,Vol. 31, No.2.

85. Nakai, Takafumi and Miwa, Shuzo, Balancing of a Flexible Rotor, Bulletin of the Japanese Society of Mechanical Engineers, 1980 Vol. 23, No. 176, pp. 280-285.

86. Nelson H. D. A finite rotating shaft element using Timoshenko beam theory. Journal of Mechanical Design 1980 No.102, pp 793-803

87. Nelson, H. D., and Chen, W. J., Undamped Critical Speeds of Rotor Systems Using Assumed Modes," ASME Transactions, Journal of Vibration and Acoustics, 1993,Vol. 115, pp 367-369.

88. Nelson, H. D., and McVaugh, J. M., The Dynamics of Rotor-Bearing Systems Using Finite Elements, ASME Transactions, Journal of Engineering for Industry, May1976, pp 593-600.

89. Parkinson A.G. and Bishop R.E.D., Residual vibration in modal balancing, J. Mechanical Engineering Science 1965, Vol 7,No. (1).

90. Parkinson A.G. and McGuire P.M., Rotordynamics standards: New developments and the need for involvement, Proc. Institution of Mechanical Engineers, Part C: Journal. Mechanical Engineering Science 1995, Vol 209 No (5), pp315-322.

91. Parkinson A.G., An introduction to the vibration of rotating flexible shafts, Bulletin of Mechanical Engineering Education 1967, pp 47-66.

92. Parkinson A.G., Balancing of rotating machinery, Proc. Institution of Mechanical Engineers 1991,Vol 205, pp 53-66.

93. Parkinson A.G., Jackson K.L. and Bishop R.E.D., Some experiments on the balancing of small flexible rotors: Part I, theory, Journal Mechanical Engineering Science 1963, Vol 5,No. 1, pp114-128.

94. Parkinson A.G., Jackson K.L. and Bishop R.E.D., Some experiments on the balancing of small flexible rotors: Part II -experiments, J. Mechanical Engineering Science 1963, Vol 5,No.2, pp133-145.

95. Parkinson A.G., Darlow M.S., Smalley A.J. and Badgley R.H., A theoretical introduction to the development of a unified approach to flexible rotor balancing, J. Sound and Vibration 1980,Vol 68, No.4, pp 489-506.

96. Parkinson, A.G., The Modal Interpretation of the Vibration of a Damped Rotating Shaft, Vibrations in Rotating Machinery, Institution of Mechanical Engineers Conference Publications 1976.

97. Parkinson A.G. and R.E.D. Bishop, Vibration and balancing of rotating continuous shafts, J. Mechanical Engineering Science 1961,Vol 3,No.200.

98. Parkinson A.G., Balancing of rotating machinery, Proc. Institution of Mechanical Engineers 1991,Vol 205, pp 53-66.

99. Parkinson, A.G., The Vibration and Balancing of Shafts Rotating in Asymmetric Bearings, Journal of Sound and Vibration, 1965, Vol. 2, No.4, p. 477.

100. Pilkey W.D. and Bailey J.T., Constrained balancing techniques for flexible rotors, J. Mechanical Design, Trans. American Society, of mechanical Engineers, 1979, Vol 101,No. 2, pp 304-308.

101. Pilkey, W.D. J. Bailey and P.D. Smith, A computational technique for optimizing correction weights and axial locations of balance planes of rotating shafts, American Society of Mechanical Engineers, Journal Vibration. Acoustics, Stress and Reliability in Design 1983, Vol 105,No. 1, pp 90-93.

102. Piotrowski J. Shaft Alignment Handbook. New York and Basel: Marcel Dekker, Inc1986.

103. Piotrowski, John, Shaft Alignment Handbook, 2-nd edition. Marcel Dekker Inc, New York, NY, 1995.

104. Prabhu. B. An experimental investigation on the misalignment effects in journal bearings. Tribology Transactions 1997,Vol 40, pp 235-242.

105. Preciado E., Bannister R.H. and Aguirre J.E., Influence coefficient method for rotor balancing using multiple trial mass sets, The Institution of Mechanical Engineers, London, Mechanical Engineering 1996. pp 491-501.

106. Rao, J. S. Rotor dynamics. New Delhi: Wiley Eastern. 1983.

107. Rao, J. S. Rotor dynamics. New Delhi: Wiley Eastern. 1991.

108. Rathbone TC. Discussion: Methods of rotor unbalance determination J. Applied Mechanics 1939, pp 131-133.

109. Rieger N.F., Balancing of rigid and flexible rotors. The Shock and Vibration Information Center, Naval Research Laboratory, Washington, DC, 1986.

110. Rieger N.F., flexible rotors bearing system dynamics, American Society, of mechanical engineers, 1973, pp 2-29.

111. Rieger, N.F., Computer Program for Balancing of Flexible Rotors, Mechanical Technology Incorporated Report 67TR68, (September) 1967.

112. Rieger, N.F., Vibrations of rotating machinery part 1: rotor-bearing dynamics. Clarendon Hills: Vibration Inst. Illinois. 1982.

113. Rouch K. E. and Rao J. S. A tapered beam finite element for rotor dynamic analysis. Journal of Sound and Vibration 1979, No.66, pp119-140.

114. Ruhl. R. L. and Booker. J. F. A finite element model for distributed parameter turborotor systems. ASME Journal of Engineering for Industry 1972, No 94, pp126-132.

115. Saito S. and T. Azurna, Balancing of flexible by complex modal method (3rd report, first method of revising correction weight - part 1), Trans. Japan Society of Mechanical Engineers 1984,Vol 50,No.455, pp 1133-1139.

116. Sanderson A.F.P., Turbine generator trim balancing using optimized least square method, Proceedings of the Institution of Mechanical Engineers 1988, pp 491-497

117. Sekhar, A.S., and Prabhu, B.S., Effects of Coupling Misalignment on Vibrations of Rotating Machinery, Journal of Sound and Vibration, 1995, Vol. 185,No.4, pp 655-671.

118. Shiau, T. N., and Hwang, J. L., A New Approach to the Dynamic Characteristic of Undamped Rotor-Bearing Systems," ASME Transactions, Journal of Vibration, Acoustics, Stress, and Reliability in Design, 1989,Vol. 111, pp 379-385.

119. Shiohata, K., and Fujisawa, F., Balancing Method of Multi-span, Multi-bearings Rotor System Bulletin of the Japanese Society of Mechanical Engineers, (November) 1980,Vol. 23, No. 185, pp 1894-1898.

120. Simon .G. Prediction of vibration of large turbo-machinery on elastic foundation due to unbalance and coupling misalignment. Proceedings of the Institution of Mechanical Engineers, 1992,Vol. 206, pp29-39.

121. Strang, Gilbert. Introduction to Linear Algebra Wellesley-Canbridge Press,1998

122. Tan, S.G., and Wang, X.X., A Theoretical Introduction to Low-Speed Balancing of Flexible Rotors - Unification and Development of the Modal Balancing and Influence Coefficient Techniques, Journal of Sound and Vibration, 1993, Vol. 168,No.3, pp. 385-394.

123. Tessarzik, J.M., and Badgley, R.H., Experimental Evaluation of the Exact Point-Speed and Least-Squares Procedures for Flexible Rotor Balancing by the Influence Coefficient Method, Transactions of the American Society of Mechanical Engineers, Journal of Engineering for Industry, (May) 1974,Vol. 96, No.2, pp. 633-643.

124. Tessarzik, J.M., Badgley, R.H., and Anderson, W.J., Flexible Rotor Balancing by the Exact Point-Speed Influence Coefficient Method, Transactions of the American Society of Mechanical Engineers, Journal of Engineering for Industry, (February) 1972 Vol. 94, No1. pp 148-158.

125. Tessarzik, J.M., Badgley, R.H., and Fleming, D.P., Experimental Evaluation of Multiplane-Multispeed Rotor Balancing through Multiple Critical Speeds, Transactions of the American Society of Mechanical Engineers, Journal of Engineering for Industry, (August) 1976.

126. Thearle E.L., Dynamic balancing of rotating machinery in the field, American Society of Mechanical Engineers, Journal Applied Mechanics 1934, No.56 pp 745-753.

127. Tonnesen J and J.W. Lund, Impact excitation tests to determine the influence coefficients for balancing lightly damped rotors, Trans. American Society of Mechanical Engineers, Engineering for Gas Turbines and Power 1988 Vol 110, No. (4), pp 600-604.

128. Tonneson, J., Further Experiments on Balancing of a High-Speed Flexible Rotor, Transactions of the American Society of Mechanical Engineers, Journal of Engineering for Industry, (May) 1974 Vol. 96, No.2, pp. 431-440.

129. Van de Vegte, J. and Lake, R. T., Balancing of Rotating Systems During Operation, Journal of Sound and Vibration, 1978 Vol. 57, No.2, pp. 225-235.

130. Woomer, E. and Pilkey, W., The Balancing of Rotating Shafts by Quadratic Programming, Journal of Mechanical Design, 1981,Vol. 103. pp 831-834.

131. Wowk V., Machinery Vibration, Balancing, McGraw-Hill, 1995.

132. Zu J.W. and Han R. P. S. Natural frequencies and normal modes of a spinning Timoshenko beam with general boundary conditions ASME Journal of Applied Mechanics 1992 No.59, pp197-204.

APPENDIXES

Appendix 1. Mechanical vibration and Rotor balancing standards

- ISO 1925:1990 Mechanical vibration - Balancing – Vocabulary.
- ISO 1940-1:1986 Mechanical vibration - Balance quality requirements of rigid rotors -- Part 1: Determination of permissible residual unbalance.
- ISO 1940-2:1997 Mechanical vibration - Balance quality requirements of rigid rotors -- Part 2: Balance errors.
- ISO 2017:1982 Vibration and shock - Isolators - Procedure for specifying characteristics.
- ISO 2041:1990 Vibration and shock – Vocabulary.
- ISO 2247:2000 Packaging - Complete, filled transport packages and unit loads - Vibration tests at fixed low frequency.
- ISO 2631-1:1997 Mechanical vibration and shock - Evaluation of human exposure to whole-body vibration - Part 1: General requirements.
- ISO 2631-2:1989 Evaluation of human exposure to whole-body vibration - Part 2: Continuous and shock-induced vibrations in buildings (1 to 80 Hz).
- ISO 2671:1982 Environmental tests for aircraft equipment - Part 3: Acoustic vibration.
- ISO 2953:1999 Mechanical vibration - Balancing machines - Description and evaluation.
- ISO 2954:1975 Mechanical vibrations of rotating and reciprocating machinery - Requirements for instruments for measuring vibration severity.
- ISO 3719:1994 Mechanical vibrations - Symbols for balancing machines and associated instrumentation.
- ISO 5348:1998 Mechanical vibration and shock - Mechanical mounting of accelerometers.
- ISO 6070:1981 Auxiliary tables for vibration generators - Methods of describing equipment characteristics.

- ISO 6721-3:1994 Plastics - Determination of dynamic mechanical properties - Part 3: Flexural vibration - Resonance-curve method.
- ISO 6721-4:1994 Plastics - Determination of dynamic mechanical properties - Part 4: Tensile vibration - Non-resonance method.
- ISO 6721-5:1996 Plastics - Determination of dynamic mechanical properties - Part 5: Flexural vibration - Non-resonance method.
- ISO 6721-6:1996 Plastics - Determination of dynamic mechanical properties - Part 6: Shear vibration - Non-resonance method.
- ISO 6721-7:1996 Plastics - Determination of dynamic mechanical properties - Part 7: Torsional vibration - Non-resonance method.
- ISO 6721-8:1997 Plastics - Determination of dynamic mechanical properties - Part 8: Longitudinal and shear vibration - Wave-propagation method.
- ISO 6721-9:1997 Plastics - Determination of dynamic mechanical properties - Part 9: Tensile vibration - Sonic-pulse propagation method.
- ISO 6954:2000 Mechanical vibration - Guidelines for the measurement, reporting and evaluation of vibration with regard to habitability on passenger and merchant ships.
- ISO 7626-5:1994 Vibration and shock - Experimental determination of mechanical mobility - Part 5: Measurements using impact excitation with an exciter, which is not attached to the structure.
- ISO 7919-1:1996 Mechanical vibration of non-reciprocating machines - Measurements on rotating shafts and evaluation criteria - Part 1: General guidelines.
- ISO 7919-2:1996 Mechanical vibration of non-reciprocating machines - Measurements on rotating shafts and evaluation criteria - Part 2: Large land-based steam turbine generator sets.
- ISO 7919-3:1996 Mechanical vibration of non-reciprocating machines - Measurements on rotating shafts and evaluation criteria - Part 3: Coupled industrial machines.
- ISO 7919-4:1996 Mechanical vibration of non-reciprocating machines - Measurements on rotating shafts and evaluation criteria - Part 4: Gas turbine sets.

- ISO 7919-5:1997 Mechanical vibration of non-reciprocating machines - Measurements on rotating shafts and evaluation criteria - Part 5: Machine sets in hydraulic power generating and pumping plants.
- ISO 8821:1989 Mechanical vibration- Balancing - Shaft and fitment key convention.
- ISO 10814:1996 Mechanical vibrations - Susceptibility and sensitivity of machines to unbalance.
- ISO 10815:1996 Mechanical vibrations - Measurement of vibration generated internally in railway tunnels by the passage of trains.
- ISO 10816-1:1995 Mechanical vibration - Evaluation of machine vibration by measurements on non-rotating parts - Part 1: General guidelines.
- ISO 10816-2:1996 Mechanical vibration - Evaluation of machine vibration by measurements on non-rotating parts - Part 2: Large land-based steam turbine generator sets in excess of 50 MW.
- ISO 10816-3:1998 Mechanical vibration - Evaluation of machine vibration by measurements on non-rotating parts - Part 3: Industrial machines with nominal power above 15 kW and nominal speeds between 120 r/min and 15 000 r/min when measured in situ.
- ISO 10816-4:1998 Mechanical vibration - Evaluation of machine vibration by measurements on non-rotating parts - Part 4: Gas turbine driven sets excluding aircraft derivatives.
- ISO 10816-5:2000 Mechanical vibration - Evaluation of machine vibration by measurements on non-rotating parts - Part 5: Machine sets in hydraulic power generating and pumping plants.
- ISO 10816-6:1995 Mechanical vibration - Evaluation of machine vibration by measurements on non-rotating parts - Part 6: Reciprocating machines with power ratings above 100 kW.
- ISO 10817-1:1998 Rotating shaft vibration measuring systems - Part 1: Relative and absolute sensing of radial vibration.
- ISO 11342:1998 Mechanical vibrations - Methods and criteria for the mechanical balancing of flexible rotors.

- ISO 13090-1:1998 Mechanical vibration and shock - Guidance on safety aspects of tests and experiments with people - Part 1: Exposure to whole-body mechanical vibration and repeated shock.
- ISO 13753:1998 Mechanical vibration and shock - Hand-arm vibration - Method for measuring the vibration transmissibility of resilient materials when loaded by the hand-arm system.
- ISO 14964:2000 Mechanical vibration and shock - Vibration of stationary structures - Specific requirements for quality management in measurement and evaluation of vibration.
- ANSI S2.5-1962 (R1997) - American National Standard Recommendations for Specifying the Performance of Vibration Machines.
- ANSI S2.7-1982 (R1997) -American National Standard Balancing Terminology.
- ANSI S2.13-1996/Part 1 - American National Standard Mechanical Vibration of Non-Reciprocating Machines - Measurements on Rotating Shafts and Evaluation - Part 1: General Guidelines.
- ANSI S2.17-1980 (R1997) - American National Standard Techniques of Machinery Vibration Measurement.
- ANSI S2.19-1989 (R1997) - American National Standard Mechanical Vibration - Balance Quality Requirements of Rigid Rotors - Part 1: Determination of Permissible Residual Unbalance.
- ANSI S2.38-1982 (R1997) - American National Standard Field Balancing Equipment - Description and Evaluation.
- ANSI S2.40-1984 (R1997) - American National Standard Mechanical Vibration of Rotating and Reciprocating Machinery-Requirements for Instruments for Measuring Vibration Severity.
- ANSI S2.41-1985 (R1997) - American National Standard Mechanical Vibration of Large Rotating Machines with Speed Range from 10 to 200 rev/s - Measurement and Evaluation of Vibration Severity in Situ.
- ANSI S2.42-1982 (R1997) - American National Standard Procedures for Balancing Flexible Rotors.

- ANSI S2.43-1984 (R1997) - American National Standard Criteria for Evaluating Flexible Rotor Balance.
- ANSI S2.60-1987 (1997) - American National Standard Balancing Machines - Enclosures and Other Safety Measures.
- ANSI S2.61-1989 (R1997) - American National Standard Guide to the Mechanical Mounting of Accelerometers.

Appendix 2. Glossary of Terms for Rotor Balancing and Shaft Alignment

Alignment: A condition where the axis or centerlines of two shafts are in line or coaxial.

Angular Misalignment: A condition where two shafts are not parallel. The axis or centerlines of two shafts intersect at angles to each other.

Axial Expansion: This is a lengthening of a shaft. It could be caused by thermal changes in environment or induced through the use of a sliding coupling.

Axial misalignment: It is a condition where shafts could be in angular and parallel alignment. However, the shafts move in and out relative to each other.

Balanced Condition: For rotating machinery, a condition where the shaft geometric centerline coincides with the mass centerline.

Balancing Mass Plane (Balancing Plane): Rotor axial position where balancing mass corrections applied.

Balancing Resonance Speed(s): A rotative speed that corresponds to a natural resonance frequency.

Balancing: A procedure for adjusting the radial mass distribution of a rotor so that the mass centerline approaches the rotor geometric centerline.

Check Balance: Data taken at the balancing speed after the addition of a correction mass set. If the improvement in the balance is not sufficient, an additional correction mass set may be calculated using the check balance data.

Correction Mass: A mass which is added to, or removed from, a rotor at a specified axial, ¿radial and angular position; intended to modify the location of the center of mass of the rotor in such a way as to reduce the rotor's unbalance response.

Critical Speed: Synchronous natural frequency of a rotor.

Field Balancing: In-situ balancing of a rotor (rigid or flexible), which is fully installed, and operating.

Finite Element Modeling: A computer aided design technique for predicting the dynamic behavior of a mechanical system prior to construction. Modeling can be used, for example, to predict the natural frequencies of a flexible rotor.

Flexible (High-Speed) Rotor Balancing: The balancing of rotors, which operate in the vicinity of, or above, one or more flexural critical speeds. Thus, the shape of the rotor, and consequently of the mass centroidal axis, changes with speed.

Flexural Critical Speed: A critical speed at which the rotor exhibits significant flexural deformation.

Fluid-Film Bearing: A bearing which supports the shaft on a thin film of oil. The fluid-film layer may be generated by journal rotation (hydrodynamic bearing), or by externally applied pressure (hydrostatic bearing).

Forced Vibration: The oscillation of a system under the action of a forcing function. Typically forced vibration occurs at the frequency of the exciting force.

Free Vibration: Vibration of a mechanical system following an initial force—typically at one or more natural frequencies.

Individual Trial Mass: A single trial mass used to generate influence coefficients for individual balance mass planes; used for influence coefficient balancing, or for calculating modal trial mass

Influence Coefficient Balancing: An entirely empirical, flexible rotor balancing method, which uses known trial masses to experimentally determine the sensitivity of a rotor; and subsequently uses this sensitivity information to determine a set of discrete correction masses that will minimize synchronous vibrational amplitudes.

Influence Coefficient: A complex value representing the effect of the addition of a unit trial mass in a specific balancing plane on the rotor response at a particular measurement plane.

Measurement Error: Random or biased variations in empirical vibration measurements, which are due to mechanical and/or electrical noise and other uncontrollable, variable physical parameters.

Measurement Plane: Rotor axial position where unbalance response measurements may be made.

Modal Balancing: Any of a group of flexible rotor balancing methods, which assume orthogonal modes of vibrational deformation and strive to compensate for them individually.

Mode Number: Generally, the order in which critical speeds occur when the speed of the rotor-bearing system is increased. For generally rigid bearings, this number refers to the number of anti-nodes in the mode shape. For generally flexible bearings with distinctly separate rigid body modes, this number will be one for the first rigid body mode and one greater than the number of rigid body modes.

Mode Shape: The resultant deflected shape of a rotor at a specific rotational speed to an applied forcing function. A three-dimensional presentation of rotor lateral deflection along the shaft axis.

Parallel Misalignment: A condition where the shaft axis or centerlines of two shafts are parallel but offset from each other

Phase Angle: A measurement used to identify the circumferential location of a trial or correction mass, or unbalance response peak amplitude, relative to a specific angular reference position on the rotor.

Radial Vibration: Shaft dynamic motion or casing vibration which is in a direction perpendicular to the shaft centerline.

Repeatability: The ability of a transducer or readout instrument to reproduce readings when the same input is applied repeatedly.

Residual (Unbalance) Response: The unbalance response of a rotor remaining after the completion of one or more balancing operations.

Rotor Balancing: The application of any of a variety of methods for reducing the unbalance response of a rotor through the addition of correction masses to adjust the rotor's mass centroidal axis.

Rigid Rotor: A rotor which operates substantially below its first bending critical speed. A rigid rotor can be brought into, and will remain in, a state of satisfactory balance at all operating speeds when balanced on any two arbitrarily selected correction planes.

Supercritical Rotor: A rotor that operates above one or more critical speeds.

Torsional Vibration: Amplitude modulation of torque measured in degrees peak-to-peak referenced to the axis of shaft rotation.

Trial Mass: A single mass, of known magnitude installed in a rotor at a specific balancing plane and angle, to generate data used for calculating influence coefficients of the rotor-bearing system for this balancing mass location at speeds and measurement planes at which data are taken.

Unbalance Response: Synchronous response of a rotor due to a lack of concentricity of its mass centroidal axis, with respect to the center of rotation.

Unbalance: The generally accepted term for the eccentricity of the center of mass of a rotor relative to its center of rotation (although the proper term is imbalance).

Appendix 3. Summary of Theoretical and Numerical Linear Algebra.

Introduction

Theoretically perfect algorithms could be very unstable numerically. Errors pop up unavoidably, and they can get amplified enormously, especially for real-life applications, when big matrices are considered.

Orthogonal matrices are the best for numerical stability (their condition number is should be used all the times. The theoretical and numerical linear algebra are summarized based on references [Howard (1993), Barry, The MathWorks (1999), Lay David (1997), Leon Steven, (1998), Strang Gilbert (1998)].

Linear algebra has two fundamental problems:

i. Solving $A*x=b$
ii. Diagonalizing a matrix $[A]$.

Methods for $A*x=b$

- ***Theoretical methods for*** $A*x=b$.

The most common method is the **Gauss elimination**, which is equivalent to the **LU decomposition**.

Advantages of L U:

i. Applicable for any matrix
ii. Finds all solutions
iii. Easy to program
iv. Fast

Disadvantages of L U.

i. Could easily be unstable
ii. Does not find approximate solutions (least square)

A more advanced method is the **QR-decomposition**. Suppose first that we already have an exact QR-decomposition. Then $A*x=b$ is reduced to $Rx=Q^{'}b$ which is easy to backsolve.

Advantages of QR over L U:

i. If you have a QR-decomposition, then solving $A*x=b$ via $Rx=Q^{'}b$ is as well-conditioned as the original problem.
ii. Finds least square solutions as well (when no exact solution exists). When there are exact solutions, it finds all of them.

Disadvantages of QR over L U:

It usually takes a more complicated algorithm to find the QR-decomposition than LU.

It is slower than LU (mainly because it has to compute lots of norms, square roots etc.)

But in general **QR-decomposition is always superior to the LU-decomposition**.

This raises the question: **How to find the QR-decomposition**? Theoretically, the QR - decomposition is obtained via **Gram-Schmidt procedure**

Advantages of finding QR with Gram-Schmidt:

i. Applicable for any matrix
ii. Easy to program
iii. Fast

Disadvantages of finding QR with Gram-Schmidt:

i. Can be unstable, especially for matrices with (almost) linearly dependent columns.

❖ **Numerical methods for $A * x = b$.**

LU-decomposition (=Gauss elimination) can be improved by **partial pivoting**

Advantages of partial pivoting

i. Can improve the stability of LU quite a bit
ii. Easy to program, it almost takes no extra effort and running time

❖ **Disadvantages of partial pivoting**

i. Only reduces instability, but in many cases still far from the optimal stability.

Given the advantages of solving $A * x = b$ with QR, it is of primary importance to find the QR-decomposition in a numerically stable way. The way to do it is via orthogonal matrices, i.e. **by Householder reflections or Givens rotations.** The performances of the two methods are similar. Givens is easier to program, but performs slower.

❖ **Advantages of Householder or Givens over Gram-Schmidt**

ii. They are stable
iii. They also can be applied for any matrix, as Gram-Schmidt (though we just learned them for square matrices).

Disadvantages of Householder or Givens over Gram-Schmidt:

NONE

Finally, certain equations $A * x = b$ can be solved iteratively. We learned the **Jacobi and Gauss-Seidel iterations** (only for square matrices, but there are versions for general matrices). In general **Gauss-Seidel is better than Jacobi** for speed, memory requirement and programming.

❖ **Advantages of Jacobi or Gauss Seidel over the exact methods: L U and QR**

i. Stable (QR is also stable, LU is not)

ii. They are fast for special matrices.

❖ **Disadvantages of Jacobi or Gauss Seidel over the exact methods: L U and QR**

i. For many matrices they don't converge. There are many tricks to improve this feature, but in general these methods are applicable only for special matrices - something like "strong diagonal". But for numerical solutions of differential equations such matrices arise very often.

ii. Even if they converge, they find only one solution. Usually they perform badly for degenerate matrices (we just learned them for regular square matrices, but again, there are generalizations)

Methods for diagonalizing a square matrix $[A]$

Theoretical methods for diagonalizing $[A]$, finding eigenvalues, -vectors

Remember, that in general there is no exact method, only iterative ones.

The basic strategy is first finding the characteristic polynomial $\rho(\lambda)$ (by computing a determinant), and then finding the roots of $\rho(\lambda)$ (usually by Newton's method - this is the iterative part of the method), finally finding the eigenvectors by solving several linear equations (one for each eigenvalue). This last problem is the one discussed in the previous section.

Advantages of diagonalizing via charateristic polynomial:

i. Applicable for any diagonalizable matrix

ii. Conceptually clear

Newton's method is stable and there are methods in the previous section to solve $(A-\lambda)x=0$ in a stable way.

Disadvantages of diagonalizing via charateristic polynomial:

i. Computing large determinants (especially with a variable symbol λ) can be unstable.
ii. Newton's method works only if there are some a-priori guesses on the solutions. In addition, it requires modifications to deal with complex eigenvalues.
iii. The program is quite complicated altogether, it has many steps and takes a long time.

Numerical methods for diagonalizing A, finding eigenvalues, -vectors

The Power method:

Advantages of the power method:

i. Fast and simple for individual eigenvalues-vectors.
ii. Can be modified (shift, inversion) to find all eigenvalues (including complex ones), but need some guess on the location of the eigenvalues (as in Newton)
iii. Stable.

Disadvantages of the power method:

i. There are complications for multiple eigenvalues.
ii. Needs some initial guess on the eigenvalues
iii. One has to find each eigenvalue-eigenvector separately, i.e. not very fast for full diagonalization.

The Jacobi iteration:

Advantages of the Jacobi iteration

i. Fully diagonalizes a symmetric matrix in one iteration

ii. Easy to program
iii. Stable.

Disadvantages of the Jacobi iteration

i. Works only for symmetric matrices *(but this is what one needs for SVD)*
ii. Slow

The **QR-iteration: This is the best and most commonly used method** for eigenvalues (with its several variants and improvements)

Advantages of the QR-iteration:

i. Gives eigenvalues for general matrices and also eigenvectors for symmetric ones.
ii. Gives everything in one iteration
iii. Faster than Jacobi, if one has a good QR-decomposition algorithm
iv. Stable

Disadvantages of the QR-iteration:

Cannot deal with complex or multiple eigenvalues, unless modified. Modifications exist but they are not so simple (*use SVD*).

The Singular Value Decomposition (SVD)

Readers familiar with matrix eigenvalues should note that the matrices AA^T and A^TA. have the same nonzero eigenvalues and that the singular values of α are the positive square roots of these eigenvalues. Moreover, the left and right singular vectors are particular choices of the eigenvectors of AA^T and A^TA, respectively.

Advantages of the SVD:

The great advantage of the use of the SVD in determining the rank of a matrix is that decisions need be made only about the negligibility of single numbers-the small singular values-rather than vectors or sets of vectors.

The singular values are the positive square roots of the eigenvalues of $A^T A$.

The SVD can be used to solve linear sets of equations, including those involving least squares, even when the $[A]$ matrix is rank deficient.

In practical problems, $[A]$ is not typically "singular" but rather "ill-conditioned"

The QR factorization can be used when $[A]$ is of full rank $m \geq n$ and the singular value decomposition can be used without restriction on $[A]$

Summary

A singular value decomposition of an m-by-n real matrix $[A]$ is any factorization of the form

$$A = USV^T$$

Where U is an m-by-m orthogonal matrix, V is an n-by-n orthogonal matrix, and S is an m-by-n

diagonal matrix with $\sigma_{ij} = 0$ if $i \neq j$ and $\alpha_{ii} = \alpha_i \geq 0$. The quantities α_i are called the singular values of $[A]$, and the columns of U and V are called the left and right singular vectors.

The rank of $[A]$ is the number of nonzero singular values of α.

The condition number of a matrix $[A]$ of full rank is

$$cond(A) = \frac{\alpha_{man}}{\alpha_{\min}},$$

where $\alpha_{\max}$ and $\alpha_{\min}$ are the largest and smallest singular values of α

The columns of U and V are respectively eigenvectors of AA^T and $A^T A$. These sets of columns are called the left singular vectors (for U) and the right singular vectors (for V).

The singular values are the positive square roots of the eigenvalues of $A^T A$.

If $[A]$ is symmetric and positive semidefinite, then the singular values of $[A]$ are the eigenvalues of $[A]$, and the SVD is a spectral decomposition of$[A]$. If $[A]$ is an autocorrelation matrix, it satisfies this condition.

Numerical example of i11-conditioned Least Squares Problem

The Least Squares procedure will fail, when A is rank deficient. The best we can do is to find x+. When A is nearly rank deficient, small change in the b vector will produce wildly different regression vectors. x. In this case the pseudoinverse gives more stable solution. So let us consider the following Example

$$A = \begin{bmatrix} 1 & 2 \\ 2 & 4 \\ 3 & 6 \\ 4 & 8.0001 \end{bmatrix} \text{ and } b = \begin{bmatrix} 2 \\ 4 \\ 6 \\ 8 \end{bmatrix} \qquad (12)$$

The second column of A is almost first column multiplied by 2, A is close to being singular. The Least Squares solution is:

$$x = (A^T A)^{-1} A^T b = \begin{bmatrix} 2 \\ 0 \end{bmatrix}$$

If the third element in vector b changes from 6 to 5.9999 and 6.0001, Least Squares give the following solutions:

$$x=\begin{bmatrix}0.2857\\0.8571\end{bmatrix} \text{ for } b(3)=5.9999 \text{ and } x=\begin{bmatrix}0.3.7143\\-0.8571\end{bmatrix} \text{ for } b(3)=6.0001$$

It can be seen that regression vector changes from

$$x=\begin{bmatrix}0.2857\\0.8571\end{bmatrix} \text{to } x=\begin{bmatrix}3.7143\\-0.8571\end{bmatrix}$$

given this very small change in the vector b. The pseudoinverse results the following solution of the system

$$x^{+}=A^{+}b=\begin{bmatrix}0.4000\\0.8000\end{bmatrix}$$

Changes in the b would no longer change the result significantly:

$$x=\begin{bmatrix}0.4000\\0.8000\end{bmatrix} \text{ for } b(3)=5.9999 \text{ and } x=\begin{bmatrix}0.4000\\0.8000\end{bmatrix} \text{for } b(3)=6.0001$$

This example illustrates that the use of a pseudoinverse can enhance the stability of our calculations.

Appendix 4. Influence coefficient Method Flow chart

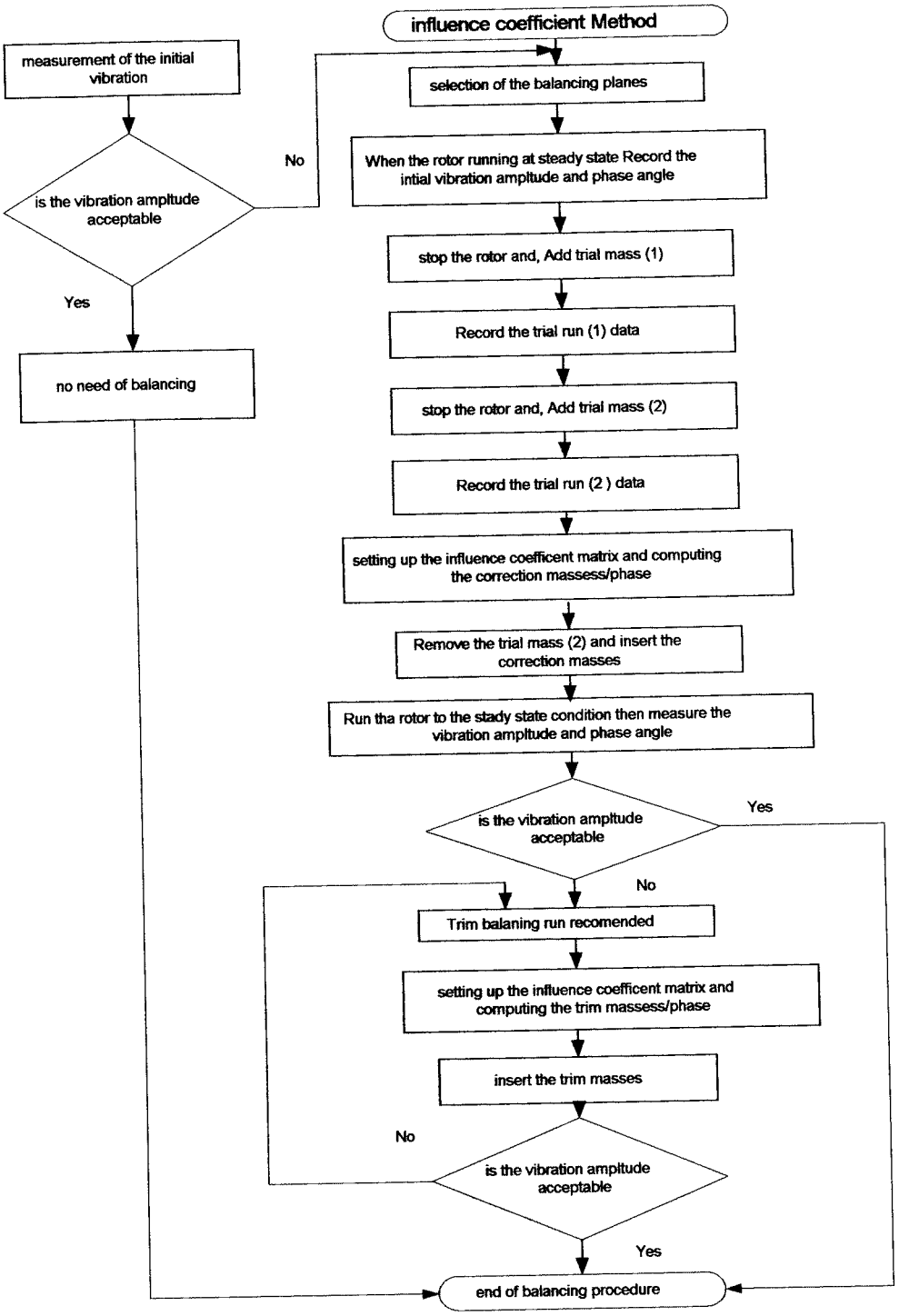

Appendix 5. Published papers

Experimental Investigation into The Behavior of Misaligned Shafts on Balanced Rotors

G Hanish, Dr P S Leung, Prof P K Datta

[1,2,3]School of Engineering and Technology, Northumbria University, Newcastle upon Tyne, NEI 8ST- UK

[1]Phone: +44 -191-2273674,Fax: +44 -191-2273646, E-mail: g.hanish@unn.ac.uk

Abstract

Rotor unbalance and shaft misalignment are the two main sources of vibration in rotating machinery such as gas turbine. The vibration caused by unbalance and misalignment may destroy critical parts of the machine, such as bearings, seals and couplings.

Experimentally, the effect of parallel, angular and parallel-angular misalignment shafts on the balanced rotors investigated by using the system of High pressure, Low pressure and generator rotors. The second objective is to study the effect of unbalanced rotors on the well-aligned rotors.

Key words:

Rotor balancing, laser alignment, vibration amplitude, shaft-to-shaft

Published at International Gas Turbine Congress 2003 Tokyo 8th Congress in Japan November 2-7, 2003, paper No. TS-015

A theoretical study on the optimum locations of the balancing planes

[1]G Hanish, [2] Dr P S Leung, [3]Prof P K Datta

[1,2,3]School of Engineering and Technology, Northumbria University, Newcastle upon Tyne, NEI 8ST- UK

[1]Phone: +44 -191-2273674,Fax: +44 -191-2273646, E-mail: g.hanish@unn.ac.uk

Abstract

Balancing the rotors involves the selection of appropriate locations of the balancing planes. There are still some questions with regard to the practical selection of these balance planes. If the balancing planes are chosen incorrectly, the accuracy of the balancing condition will be affected. In this study, the desirability of using "optimum" locations for balance planes have been investigated by using some case studies. However in most machines, constraints exist which inhibit the use of the optimum locations, and a means to evaluate "non-ideal" locations is clearly necessary. At the same time, other "non-ideal" aspects of "real" balancing requirements must be recognized.

The answer to the above question and to provide criteria for establishing ideal balance plane locations, analysis was performed, which will give guidelines to the selection of balancing planes.

Key words:

Balancing planes, computer methods, vibration amplitude, finite element, correction – trial mass

Published at ISROMAC - 10th International Symposium on Rotating Machinery Honolulu, Hawaii, USA March 07 - 11, 2004

Experimental Investigation on The Effectiveness of Measurement Uncertainty to Rotor Balancing

[1]G Hanish, [2] Dr P S Leung, [3]Prof P K Datta

[1,2,3]School of Engineering and Technology, Northumbria University, Newcastle upon Tyne, NEI 8ST- UK

[1]Phone: +44 -191-2273674,Fax: +44 -191-2273646, E-mail: g.hanish@unn.ac.uk

Abstract

A measurement result is complete only when accompanied by a quantitative statement of its uncertainty. The uncertainty is required in order to decide if the result is adequate for its intended purpose and to determine if it is consistent with the results of similar measurements.

This paper is concerned with the error, analysis of the balancing of rotors. The effects of the measurement errors on the Influence Coefficients matrix are experimentally investigated for several balance tests. Many different measures are used to characterize measurement error; often making it difficult to determine which interpretation should be associated with the uncertainty. However, there is a growing consensus among engineering societies and among instrumentation engineers. Uncertainty is an unavoidable part of any measurement and it starts to matter when results are close to a specified limit. A proper evaluation of uncertainty is good professional practice and can provide us valuable information about the quality and reliability of the result.

Key Words:

Errors; Measuring Instrument; Vibration; Accuracy; Uncertainty; Rotor Balancing; Influence Coefficient Matrix,

Published at 18th international congress on acoustics ICA 2004, 4-9 April Kyoto, Japan

A new balancing procedure for flexible rotors based on modified QR and SVD techniques with least square optimization

[1]G Hanish, [2] Dr P S Leung, [3]Prof P K Datta

[1,2,3]School of Engineering and Technology, Northumbria University, Newcastle upon Tyne, NEI 8ST- UK

[1]Phone: +44 -191-2273674,Fax: +44 -191-2273646, E-mail: g.hanish@unn.ac.uk

Abstract

This paper presents a new balancing method for the identification of rotor unbalance in rotating machines. This method is based on the combined use of the QR factorization, singular value decomposition (SVD) technique, and the least square optimization technique.

In this paper, the QR factorization technique is used to solve the system influenced coefficient matrix, due to its orthogonal properties and numerical stability. In order to eliminate other sources of errors, the least square optimization technique is also integrated to the method of solution.

The work has been carried theoretically by using computer program writing by Matlab software to validate the new proposed method to measure the unbalance motions of uniform slender shaft

Key words:

Rotor balancing, computer methods, influence coefficient, least square optimization, QR factorization, SVD

Published at ISMA2004 International Conference on Noise and Vibration Engineering, September 20 - 22, 2004 Belgium

Experimental Investigation into the effect of Misaligned Shafts on Balanced Rotors

G Hanish, Dr P S Leung, Prof P K Datta

[1,2,3]School of Engineering and Technology, Northumbria University, Newcastle upon Tyne, NEI 8ST- UK

[1]Phone: +44 -191-2273674,Fax: +44 -191-2273646, E-mail: g.hanish@unn.ac.uk

Abstract

Rotor unbalance and shaft misalignment are the two main sources of vibration in rotating machinery such as gas turbine. The vibration caused by unbalance and misalignment may destroy critical parts of the machine, such as bearings, seals and couplings.

Due to current trends in the design of rotating machinery towards higher speeds, manufacturers tend to produce machines, which operate closer to their lateral critical speeds than has previously been necessary. Consequently, the effect of coupling upon the critical speeds and its misalignment on vibration amplitudes of such machines is becoming an increasingly important consideration for rotor-bearing systems.

Experimentally, the effect of parallel, angular and parallel-angular misalignment shafts on the balanced rotors investigated by using the system of High pressure, Low pressure and generator rotors. The second objective is to study the effect of unbalanced rotors on the well-aligned rotors.

Key words:

Rotor balancing, laser alignment, vibration amplitude, shaft-to-shaft

Paper submitted to the MAINTENANCE JOURNAL and waiting for referee comments on the full paper

Experimental Investigation Into The Validation of New Technique For Rotor Balancing Using Trim-Balance Procedure

G Hanish, Dr P S Leung, Prof P K Datta

[1,2,3]School of Engineering and Technology, Northumbria University, Newcastle upon Tyne, NEI 8ST- UK

[1]Phone: +44 -191-2273674,Fax: +44 -191-2273646, E-mail: g.hanish@unn.ac.uk

Abstract

The vibration of rotating shafts is a source of much trouble in the operation of a wide range of machinery in many various industries such as compressors, steam and gas turbines and multi-stages pumps. The mass balancing of rotating machines (referred to more briefly as rotor balancing) has been an important consideration in machinery design and manufacture for more than forty years.

The "trim" balancing run is defined by that any correction balance run after the first attempted balance correction; usually any mass adjustment due to the trim balancing mass amount should be significantly less than the initial balance correction mass; the trim is usually a fine-tuning of the initial balance correction, because usually further reduction of the vibration level is necessary.

This paper presents a new balancing method for trim balancing mass calculation. This method is based on the combined use of the original influence coefficient matrix and the new data obtained after adding the correction mass to the system.

Key words:

Rotor balancing, computer methods, vibration amplitude, phase angle, trim mass, influence coefficient matrix

Paper submitted to the MAINTENANCE JOURNAL and waiting for referee comments on the full paper

Appendix 6. Computer programs

```
% Simulation of a slender uniform shaft under rotating unbalance
%
% Details of the model
%
% Assume pin-pin support at either end
clear all
%
dia1=0.05
len1=1
ee1=196e9;
den1=7905;
%
ii1=pi*(dia1^4)/64;
vol1=pi*(dia1^2)/4;
totmass1=vol1*den1
masperln=totmass1/len1;
%
wn1=pi*pi*sqrt(ee1*ii1/(masperln*len1^4));
cnv=pi/180;
cv1=60/(2*pi);
rpm1=wn1*cv1
%
% specify unbalance quantity
%
% G40 -> 125 gmm/kg
%
%ttunba=(125*totmass1)/1000/1000
ttunba=0.002
% in kg*m
%
% Dividing the shaft
%
% no of sections
nuofsec=12
dl=len1/nuofsec;
% no of useful nodes
nuofnode=nuofsec-1;
%
% no of orginal unbalance
nofunp=2
apum=ttunba/nofunp
%
% no of trial mass plane
untmp=nofunp
tmass=500*0.10197
%
%set speed
%
dww=1000;
for iw=1:1;
   rw=iw*dww
   ww=rw/cv1;
% set initial forces first
%
for ii=1:nuofnode;
   fs(ii)=0+0i;
   yyo(ii)=0+0i;
   for jj=1:nuofnode;
```

```
      yy(ii,jj)=0+0i;
   end;
end;
%
doj=(nuofnode+1)/(nofunp+1);
for jj=1:nofunp;
      doldj(jj)=round(doj*jj);
%
fs(doldj(jj))=apum*(cos(0)+i*sin(0))+fs(doldj(jj));
%
end
%Generate initial unbalance measurements
%
for jj=1:nuofnode;
   aa=jj*dl;
   bb=len1-aa;
      for ii=1:nuofnode;
      lxx=ii*dl;
      yyo(ii)=yyo(ii)+(ww^2*fs(jj)*bb*lxx*(len1^2-lxx^2-
bb^2)/(6*ee1*ii1*len1));
   end;
end;
maxyyo=max(yyo)
% trial mass measurements
%
dj=(nuofnode+1)/(untmp+1);
for jj=1:untmp;
      ddj(jj)=round(dj*jj);
   ttmass(jj)=tmass*(cos(0)+i*sin(0));
   fs(ddj(jj))=ttmass(jj)+fs(ddj(jj));
   for nj=1:nuofnode;
   aa=nj*dl;
   bb=len1-aa;
   for ii=1:nuofnode;
      lxx=ii*dl;
      yy(ii,jj)=yy(ii,jj)+(ww^2*fs(nj)*bb*lxx*(len1^2-lxx^2-
bb^2)/(6*ee1*ii1*len1));
   end;
   end;
   fs(ddj(jj))=-ttmass(jj)+fs(ddj(jj));
end
%set up A matrix
%
for jj=1:untmp;
   for ii=1:nuofnode;
      A(ii,jj)=(yy(ii,jj)-yyo(ii))/ttmass(jj);
   end;
end;
%
for ii=1:nuofnode;
   x(ii)=-yyo(ii);
end;
%
if(iw < 2);
AA=(A);
xx=(x');
else
   AA=(AA ; A)
   xx=(xx ; x')
end
% end speed
end
```

```
% least square
wo=AA\xx
woabs=abs(wo)
abs(sum(woabs)-ttunba)/ttunba
stdo=sqrt(sum((woabs-apum).^2))/nofunp
%
wo1=pinv(AA)*xx
wo1abs=abs(wo1)
abs(sum(wo1abs)-ttunba)/ttunba
stdo1=sqrt(sum((wo1abs-apum).^2))/nofunp
%
display('least square')
w1=inv(AA'*AA)*AA'*xx;
w1abs=abs(w1)
abs(sum(w1abs)-ttunba)/ttunba
stdw1=sqrt(sum((w1abs-apum).^2))/nofunp
%QR Algorithm
display('Q R')
(Q,R)=qr(AA);
w2=pinv(R)*Q'*xx;
w2abs=abs(w2)
abs(sum(w2abs)-ttunba)/ttunba
stdw2=sqrt(sum((w2abs-apum).^2))/nofunp
%SVD
display('SVD')
(U,S,V)=svd(AA);
w3=V*pinv(S)*U'*xx;
w3abs=abs(w3)
abs(sum(w3abs)-ttunba)/ttunba
stdw3=sqrt(sum((w3abs-apum).^2))/nofunp
%QR+SVD
display('QR+SVD')
(uu,ss,vv)=svd(R);
w4=vv*pinv(ss)*uu'*Q'*xx;
w4abs=abs(w4)
abs(sum(w4abs)-ttunba)/ttunba
stdw4=sqrt(sum((w4abs-apum).^2))/nofunp

%XXXX
```

```
T1=cond(A)
%a=(mc1;mc2);
%a=inv(A)*b;
%CM=abs(a)

% LSQ
Rank(A)
cond(A)
w0=inv(A'*A)*A'*b;
n0=abs(w0)
w1=pinv(A)*b
n1=abs(w1)
%%%%%%%%%%%%%%%%%%%%%%%%%
%svd
(U,S,V)=svd(A);
U*S*V';
w2=V*Pinv(S)*U'*b;                          %(1)
n2=abs(w2)
w22=V*inv(S)*U'*b ;                         %(2)
n22=abs(w22)
%%%%%%%%%%%%%%%%%%%%%%%%%
%QR
(Q,R)=qr(A);
w3=pinv(R)*Q'*b;                            %(1)
n3=abs(w3)
%%%%%%%%%%%%%%%%%%%%%%%%
%QR&SVD
(uu,ss,vv)=svd(R);
w4=vv*pinv(ss)*uu'*Q'*b;                    %(2)
n4=abs(w4)

XXXX
```

```
mu =rho*A

%deflection of the shaft
%x<=(L-b)
x=a
F=100:100:500
for j=1:5
y=((F(j)*b*x*(L^2-x^2-b^2))/(6*E*L*I))
end
XXXX
```

```
      ylabel('amplitude')
      xlabel('time')
      title('daq')
      zoom on
      subplot(2,2,3);
      plot(data(:,7)),axis((0,500,-10,10));
      grid on
      ylabel('amplitude')
      xlabel('time')
      title('daq')
      zoom on
      pause(10) % 10 sec for saving the plot
      mx= max(data(:,cc))
      mn= min(data(:,cc))
      z(tt,ss,cc)=abs((mx-mn)/2)
      uplimit=-1;

      if mx>uplimit
         input('max too high, check the transducer rotor gab')
      end

      x1(1)=0;
      x1(2)=0;
      for i=1:50000-1
         if (data(i+1,7)-data(i,7)>2)
            if x1(1)==0
               x1(1)=i+1
            elseif x1(2)==0
               x1(2)=i+1
            end
         end
      end

      biger=-10.0;
      for ki= x1(1):1:x1(2)
         if(biger<data(ki,cc))
            biger=data(ki,cc);
         end
      end

      for kj= x1(1):x1(2)
         if(biger==data(kj,cc))
            pp=kj
         end
      end

      q(tt,ss,cc)=(pp-x1(1))/(x1(2)-x1(1))*360                    %
phase angle reading
      v(tt,ss,cc)=
(z(tt,ss,cc)*cos(q(tt,ss,cc)*cv)+z(tt,ss,cc)*sin(q(tt,ss,cc)*cv)*j)*L
VDT       % vibration amplitude reading
   end
   input('change operation speed')

   end
   %second run with trial mass1
if (tt<n+1)
      m=input('stop the rotor and Enter trial mass by the gram to one
plane,(press enter)')
      theta=input('location of trial mass angle in degree,(press
enter)')
```

```
      mt(tt+1)= m*cos(theta*cv)+m*sin(theta*cv)*j    %  trial mass
equestion
      input('run the rotor again to the same orginal rpm and record
the amplitude and phase angle in the planes,(press enter)')

   end
end

save ('rotor','q')
save ('rotor1','v')
save ('rotor2','mt')
save ('rotor3','z')
save ('rotor4','R')

m(1)=mt(1)*Rd(1);
m(2)=mt(1)*Rd(2);

% calculation fot the influence coefficient Matrix

               for ss=1:n+1;
                 for jj=1:n;
                    for ii=1:5;
                       B(ii,jj,ss)=(v(jj+1,ss,ii)-v(1,ss,ii))/m(jj)
                    end
                 end
  % calculation fot the itiial amplitude matrix


                    for ii=1:5;
                       c(ii,ss)=-v(1,ss,ii);
                    end
               end


               A=(B(:,:,1);B(:,:,2);B(:,:,3))
               x=(c(:,1);c(:,2);c(:,3))
               % LSQ
              ww=inv(A'*A)*A'*x
              www=abs(ww)
              gg(1)=www(1)/Rd(1)
              gg(2)=www(2)/Rd(2)
              phase=(1/cv)*atan2(imag(ww),real(ww))

              %QR
              (Q,R)=qr(A)
              w2=pinv(R)*Q*x
              ww2=abs(w2)
              gg(1)=ww2(1)/Rd(1)
              gg(2)=ww2(2)/Rd(2)
              phase=(1/cv)*atan2(imag(w2),real(w2))

              %SVD
              (U,S,V)=svd(A);
              w3=V*pinv(S)*U'*x
              ww3=abs(w3)
              gg(1)=ww3(1)/Rd(1)
              gg(2)=ww3(2)/Rd(2)
              phase=(1/cv)*atan2(imag(w3),real(w3))

              %QR+SVD
              (uu,ss,vv)=svd(R);
              w4=vv*pinv(ss)*uu'*Q'*x
```

```
            ww4=abs(w4)
            gg(1)=ww4(1)/Rd(1)
            gg(2)=ww4(2)/Rd(2)
            phase=(1/cv)*atan2(imag(w4),real(w4))

input('(CM) is the amounts of the balancing masses must be added on
the  planes, phase is the  amounts of the phase angle of the
balancing mass must be added on the  planes,(press enter)')
input('stop the rotor and add the correction weights and remove the
trial weight,(press enter)')
input('run the rotor at normal speed and measure the vibration
amplitude to check an improvement if further improvement desired do
the same procedure starting from last step,(press enter)')

% Calculation for trim balancing
br=0;
while br==0
   NOS=n+1;
   for kk=1:n-1
      for ff=1:NOS
         for hh=1:n
            start(AI);
            data =getdata(AI);
      subplot(2,2,1);
      plot(data(:,plane(hh))),axis((0,500,-10,0));
      grid on;
      ylabel('ampltiude')
      xlabel('time')
      title('daq')
      zoom on
      subplot(2,2,3);
      plot(data(:,7)),axis((0,500,-10,10));
      grid on
      ylabel('ampltiude')
      xlabel('time')
      title('daq')
      zoom on
      pause(10) % 10 sec for saving the plot
      mx= max(data(:,hh))
      mn= min(data(:,hh))
      z=abs((mx-mn)/2)
      uplimit=-1;

      if mx>uplimit
         input('max too high,check the transducer rotor gab')
      end

      x1(1)=0;
      x1(2)=0;
      for i=1:50000-1
         if (data(i+1,7)-data(i,7)>2)
            if x1(1)==0
               x1(1)=i+1
            elseif x1(2)==0
               x1(2)=i+1
            end
         end
      end

      biger=-10.0;
      for ki= x1(1):1:x1(2)
         if(biger<data(ki,hh))
```

```
            biger=data(ki,hh);
         end
      end

      for kj= x1(1):x1(2)
         if(biger==data(kj,hh))
            pp=kj
         end
      end

      Txx(kk,ff,hh)=(pp-x1(1))/(x1(2)-x1(1))*360                    %
phase angle for the trim balancing
      xuu(kk,ff,hh)=
(z*cos(Txx(kk,ff,hh)*cv)+z*sin(Txx(kk,ff,hh)*cv)*j)*LVDT % vibration
amplitude reading for the trim balancing
   end
   input('change operation speed')
end
end
save ('rotor5','xuu')
save ('rotor6','Txx')

 for ss=1:n+1;
                  for jj=1:n;
                     for ii=1:5;
                        F(ii,jj,ss)=(v(jj+1,ss,ii)-v(1,ss,ii))/m(jj)
                     end
                  end
  % Calculation for the initial amplitude matrix


                  for ii=1:5;
                     c(ii,ss)=-v(1,ss,ii);
                  end
               end


               A=(F(:,:,1);F(:,:,2);F(:,:,3))
               x=(c(:,1);c(:,2);c(:,3))
               % LSQ% trim balancing correction mass

              ww=inv(A'*A)*A'*x
              www=abs(ww)
              gg(1)=www(1)/Rd(1)
              gg(2)=www(2)/Rd(2)
              phase=(1/cv)*atan2(imag(ww),real(ww))


   br=input('enter 0 to carry on ,any other number to finish the
program')
   end

%XXXX
```

```
set(chans,'InputRange',(-10 10));  % specified the range of the
analog input (sensors)
set(chans,'SensorRange',(-10 10)); % specified the range of data from
thw sensors
set(chans,'UnitsRange',(-10 10));  % specified the linear scaling of
the data extracted form the sensors
set(AI,'SampleRate',5000);
ActualRate = get(AI, 'SampleRate'); %specified the channels rate at
which the analoge data converted to digital data.
set(AI,'SamplesPerTrigger',duration*ActualRate);

LVDT=0.127            % mm/volt calibration factor

plane(1)=(1) % vibration amplitude at channel 0
plane(2)=(2) % vibration amplitude at channel 1
plane(3)=(3) % vibration amplitude at channel 2
plane(4)=(4) % vibration amplitude at channel 3
plane(5)=(5) % vibration amplitude at channel 4
plane(6)=(6) % vibration amplitude at channel 5
plane(7)=(7) % vibration amplitude at channel 6
plane(8)=(8) % vibration amplitude at channel 8
plane(9)=(9) % vibration amplitude at channel 9
plane(10)=(10) % vibration amplitude at channel 10
plane(11)=(11) % vibration amplitude at channel 11
plane(12)=(12) % vibration amplitude at channel 12
%phase angle=channel(7)

NOP=n   % NOP is the number of plots required
cv=pi/180
for ww=1:5
for tt=1:NOP
for cc=1:12
    start(AI);
    data =getdata(AI);
      subplot(2,2,1);
      plot(data(:,plane(cc))),axis((0,500,-10,0));
      grid on;
      ylabel('ampltiude')
      xlabel('time')
      title('daq')
      zoom on
      subplot(2,2,3);
      plot(data(:,7)),axis((0,500,-10,10));
      grid on
      ylabel('ampltiude')
      xlabel('time')
      title('daq')
      zoom on
      pause(10) % 10 sec for saving the plot
      mx= max(data(:,cc))
      mn= min(data(:,cc))
      z(tt,cc)=abs((mx-mn)/2)

      x1(1)=0;
      x1(2)=0;
      for i=1:50000-1
         if (data(i+1,7)-data(i,7)>2)
            if x1(1)==0
               x1(1)=i+1
            elseif x1(2)==0
               x1(2)=i+1
            end
```

```
        end
    end

    biger=-10.0;
    for ki= x1(1):1:x1(2)
        if(biger<data(ki,cc))
            biger=data(ki,cc);
        end
    end

    for kj= x1(1):x1(2)
        if(biger==data(kj,cc))
            pp=kj
        end
    end

    q(tt,cc)=(pp-x1(1))/(x1(2)-x1(1))*360                    %
phase angle reading
    v(tt,cc)=
(z(tt,cc)*cos(q(tt,cc)*cv)+z(tt,cc)*sin(q(tt,cc)*cv)*j)      %
vibration amplitude reading
   end
end

for cc=1:12
   ff1=mean(q(:,cc))          %is the mean value of the phase angle
reading
   ff2=std(q(:,cc))           %is the standard deviation of the
phase angle reading
   rr1=mean(z(:,cc))          %is the mean value of the vibration
amplitude reading
   rr2=std(z(:,cc))           %is the standard deviation of the
vibration amplitude reading
   qq(tt,cc)=ff1
   zz(tt,cc)=rr1

end
z
q
v

input('hold on for few seconds')
end
%%%%%%%%%%%%%%%%%%%%%%%%%%%%%%%%%%%%%%%%%%%%%%%%%%%%%%%%%%%%%%%%


function [qq,rr,aam,oom,sff]=grams22(w19);
[m,n]=size(w19);
% compute qr using Gram-schmidt
% eliminate planes less than tol
%
tol=0.5;
cnd=cond(w19)
%
for j=1:n
    v=w19(:,j);
    vn(j)=norm(v);
    for i=1:j-1
        rr(i,j)=qq(:,i)'*w19(:,j);
        v=v-rr(i,j)*qq(:,i);
    end
    rr(j,j)=norm(v);
```

```
    qq(:,j)=v/rr(j,j);
%    en(j)=(r(j,j));
    sff(j)=rr(j,j)/vn(j)
end
%
% Plane elimination
%
jm=1;
for j=1:n
    if sff(j)>tol
        %e=[sff(1) sff(7)]
        oom(jm)=j
        aam(:,jm)=w19(:,j)
        %aam=[w19(:,1) w19(:,7)]
        jm=jm+1;
    end
end
%

%%%%%%%%%%%%%%%%%%%%%%%%%%%%%%%%%%%%%%%%%%%%%%%%%%%%%%%%%%%%%%%%%%%%%%%%%%%%
function [q,r,am,om,sf]=grams2(a);
[m,n]=size(a);
% compute qr using Gram-schmidt
% eliminate planes less than tol
%
tol=0.5;
cnd=cond(a)
%
for j=1:n
    v=a(:,j);
    vn(j)=norm(v);
    for i=1:j-1
        r(i,j)=q(:,i)'*a(:,j);
        v=v-r(i,j)*q(:,i);
    end
    r(j,j)=norm(v);
    q(:,j)=v/r(j,j);
%    en(j)=(r(j,j));
    sf(j)=r(j,j)/vn(j)
end
%
% Plane elimination
%
jm=1;
for j=1:n
    if sf(j)>tol
        om(jm)=j
        %am=[a(:,1) a(:,7)]
        am(:,jm)=a(:,j)
        jm=jm+1;
    end
end
%e=[sf(1) sf(7)]
%%%%%%%%%%%%%%%%%%%%%%%%%%%%%%%%%%%%%%%%%%%%%%%%%%%%%%%%%%%%%%%%%%%%%%%%%%%%

%2 plane HPT

%v=[-.48634E-06  -.48864E-06;
%   .38011E-06  .10399E-06;
%   .10624E-06  .38469E-06]

%2 plane regular rotor
```

```
%v=[-.92117E-05 -.11975E-04;
    .55270E-05 .92117E-06;
    .36847E-05 .11054E-04]


%6 plane regular rotor
v=[ -.92117E-05 -.13809E-04 -.17714E-04  -.18250E-04   -.17070E-04        -.11975E-04;
    .55270E-05 .71476E-05   .66678E-05   .51539E-05    .32817E-05         .92117E-06;
    .47594E-05 .70879E-05   .75005E-05   .62190E-05    .43489E-05         .16718E-05;
    .67553E-05 .10756E-04   .13646E-04   .12782E-04    .10409E-04         .56976E-05;
    .63906E-05 .10660E-04   .15448E-04   .16294E-04    .14573E-04         .89217E-05;
    .43564E-05 .76103E-05   .11900E-04   .13394E-04    .13021E-04         .85976E-05;
    .36847E-05 .66614E-05   .11047E-04   .13096E-04   .13789E-04         .11054E-04];

 %7 plane HPT
v=[-.35579E-06 -.56098E-06 -.65800E-06 -.70627E-06 -.71679E-06 -.66183E-06 -.35739E-6;
    .29131E-06 .40562E-06  .42110E-06  .39069E-06  .35465E-06  .23308E-06 .62888E-07;
   .28861E-06 .46512E-06  .51915E-06   .50838E-06  .47794E-06  .34783E-06 .12018E-06;
   .36361E-06  .56033E-06 .73490E-06   .76071E-06  .73969E-06  .58803E-06 .23922E-06;
   .37552E-06 .65367E-06  .80898E-06   .88228E-06  .88444E-06  .74565E-06 .32385E-06;
   .36844E-06 .64629E-06  .80717E-06   .89292E-06  .90578E-06  .77920E-06 .34415E-06;
   .24081E-06 .44867E-06  .59186E-06   .70120E-06  .75167E-06  .74943E-06 .36966E-06;
   .64481E-07 .15536E-06  .23691E-06   .31558E-06  .36214E-06  .42874E-06 .29450E-06];

Rd=[0.05];
mt=300;
m=mt*Rd;

n=6;
for ii=1:n;
   for jj=1:n;
      a(ii,jj)=(v(ii+1,jj)-v(1,jj))/mt;
   end
end
for ii=1:n;
   b(ii)=-v(1,ii);
end

rnk=rank(a)
cnd=cond(a)
%('display normal solution')
%w0=inv(a)*b % normal solution
%('display least square solution')
w2=inv(a'*a)*a'*b'; %least square solution
%('display QR solution')
[Q,R]=qr(a); % QR solution
w3=R\(Q'*b');
%('display SVD')
[U,S,V]=svd(a);% SVD solution
w4=V*[S\(U'*b')]
('display elemination by using Significant factor (0.5)')
[q,r,am,om,sf]=grams2(a);% elemination by using Significant number
rk=rank(am);
cd=cond(am);
%('display least square solution')
w5=inv(am'*am)*am'*b';
%('display QR solution')
[Q,R]=qr(am);
w6=R\Q'*b';
%('display SVD')
[U,S,V]=svd(am);
w7=V*[S\(U'*b')]
%%%%%%%%%%%%%%%%%%%%%%%%%%%%%%%%
('display elemination by using rank (QR)')
```

```
[Q4,R4,h4]=qr(a,0);                    % elemination by using rank (QR)
h4
w19=a(:,h4)
rk=rank(w19);
cd=cond(w19);
[qq,rr,aam,oom,sff]=grams22(w19);% elemination by using Significant
number
rk=rank(aam)
cd=cond(aam)


w55=inv(aam'*aam)*aam'*b';
%('display QR solution')
[Q,R]=qr(aam);
w66=R\Q'*b';
%('display SVD')
[U,S,V]=svd(aam);
w77=V*[S\(U'*b')]

%('display least square solution')
a1m=w19(:,1);
w155=inv(a1m'*a1m)*a1m'*b';
[Q,R]=qr(a1m);
w166=R\Q'*b';
[U,S,V]=svd(a1m);
w177=V*[S\(U'*b')]
a2m=[w19(:,1)w19(:,2)];
w255=inv(a2m'*a2m)*a2m'*b';
[Q,R]=qr(a2m);
w266=R\Q'*b';
[U,S,V]=svd(a2m);
w277=V*[S\(U'*b')]
a3m=[w19(:,1)w19(:,2)w19(:,3)];
w355=inv(a3m'*a3m)*a3m'*b';
[Q,R]=qr(a3m);
w366=R\Q'*b';
[U,S,V]=svd(a3m);
w377=V*[S\(U'*b')]
a4m=[w19(:,1)w19(:,2)w19(:,3)w19(:,4)];
w45=inv(a4m'*a4m)*a4m'*b';
[Q,R]=qr(a4m);
w46=R\Q'*b';
[U,S,V]=svd(a4m);
w47=V*[S\(U'*b')]

a5m=[w19(:,1)w19(:,2)w19(:,3)w19(:,4)w19(:,5)];
w55=inv(a5m'*a5m)*a5m'*b';
[Q,R]=qr(a5m);
w56=R\Q'*b';
[U,S,V]=svd(a5m);
w57=V*[S\(U'*b')]
a6m=[w19(:,1)w19(:,2)w19(:,3)w19(:,4)w19(:,5)w19(:,6)];
w65=inv(a6m'*a6m)*a6m'*b';
[Q,R]=qr(a6m);
w66=R\Q'*b';
[U,S,V]=svd(a6m);
w67=V*[S\(U'*b')]
%a7m=[w19(:,1)w19(:,2)w19(:,3)w19(:,4)w19(:,6)w19(:,6)w19(:,7)];
%w75=inv(a7m'*a7m)*a7m'*b';
%[Q,R]=qr(a7m);
%w766=R\Q'*b';
%[U,S,V]=svd(a7m);
```

```
%w777=V*[S\(U'*b')]
%%%
```

```
%a=[1 1;2.05 -1;3.06 1;-1.02 2;4.08 -1]
%b=[1.98;0.95;3.98;0.92;2.90]
%%%%%%%%%%%%%%%%%%%%%%%%%%%%%%%%%%
%Example (9)
%a=[0.9355 0.8936 0.8132;0.9169 0.0579 0.0099;0.8798 -1.6136 -1.5967]
%b=[0.2028;0.1987;0.6038]
%Example (9)
%a=[0.99 1;1 1]
%b=[1;1]
%Example (9)
%a=[1.2969 0.8642;0.2161 0.1441]
%b=[08642;0.1440]

%a=[0.0300 0.0100;0.0050 0.0300]
%b=[0.0400;0.0350]

%a=[1 1 1;1 1 2;1 1 3;1 1 4]
%b=[1;0;1;0]


%a=[1.05 1.05;0.95 1.01]
%b=[2;2]


%m=100; n=15;
%t=(0:m-1)'/(m-1);
%a=[];
%for i=1:n,
    %a=[a t.^(i-1)];
    %end
%b=exp(sin(4*t));
%b=b/2006.787453080206;
b=b'

rnk=rank(a);
cnd=cond(a);
('display normal solution')
w0=inv(a)*b % normal solution
('display least square solution')
w2=inv(a'*a)*a'*b'; %least square solution
('display QR solution')
[Q,R]=qr(a); % QR solution
w3=R\(Q'*b');
('display SVD')
[U,S,V]=svd(a);% SVD solution
w4=V*[S\(U'*b')];
('display elemination by using Significant factor (0.0)')
[q,r,am,om,sf]=grams2(a);% elemination by using Significant number
rk=rank(am);
cd=cond(am);
('display least square solution')
w6=inv(am'*am)*am'*b';
('display QR solution')
[Q,R]=qr(am);
x2x=R\Q'*b';
('display SVD')
[U,S,V]=svd(am);
w8w8=V*[S\(U'*b')]
%%%%%%%%%%%%%%%%%%%%%%%%%%%%%%%%%%
('display elemination by using rank (QR)')
[Q4,R4,h4]=qr(a,0);              % elemination by using rank (QR)
h4;
```

```
w19=a(:,h4);
rk=rank(w19);
cd=cond(w19);
[q,r,aam,oom,sf]=grams2(w19);% elemination by using Significant
number
rk=rank(aam)
cd=cond(aam)
('display least square solution')
w6=inv(aam'*aam)*aam'*b'
('display QR solution')
[Q,R]=qr(aam);
xx=R\Q'*b'
('display SVD')
[U,S,V]=svd(aam);
ww8=V*[S\(U'*b')]
```

Appendix 7. Instrument Specifications

Appendix 7.1 Vibration Amplitude Measurements

Eddy-current displacement probes. Bently Nevada 3300 RAM proximity transducers type.

Input	Accepts one non- contacting 3300-series 5 mm
Power:	Requires -17.5 Vdc to -26 Vdc without barriers at 12 mA maximum consumption
Linear range	2 mm linear range begins at approximately 0.25 mm from target and is from 0.25 to 2.3 mm (Approximately -1 to -17 Vdc).
Output resistance	50 ohms
Recommended gap setting	1.27 mm
Minimum target size	15.2 mm diameter (flat target)
Weight	246 g

Appendix 7.2 Phase Angle Instrument

The OMRAN E3M-VG Colour Mark Sensor (an optical switch)

Part number	E3M-VG21
Method of detection	Diffuse type
Supply voltage	10 to 30 VDC, 10% ripple max. (p-- p)
Current consumption	100 mA max
Sensing distance	10 ±3 mm
Spot size (W x H)	1 x4 mm
Light source (wavelength)	Green LED, 525 nm
Output	NPN open collector
	Residual voltage: 1.2 V max
	100 mA load, 30 VDC max.
	Light-ON/Dark-ON switch selectable
	Short-circuit protected
Circuit protection	Protection from reversed polarity connection and load short-circuit
Insulation resistance	20 M Ωmin. (at 500 VDC)
Dielectric strength	1,000 VAC, 50/60Hz, 1 min.
Vibration resistance	10 to 55 Hz, 1-mm double amplitude or 150 m/s^2 for 2 hrs each in X, Y, and Z axes With bracket attached: 0.75-mm double amplitude or 100 m/s^2
Shock resistance	500 m/s^2 3 times each in X, Y, and Z-axes. With bracket attached: 300 m/s^2
Connection method	Quick-disconnect M12
Weight	100 g (with carton)

Appendix 7.3 Shaft Alignment Equipment

An OPTALIGN PLUS laser equipment

Transducer	
Laser, visible	Ga-AI-As semiconductor laser
Safety class	Class 2; FDA 21 CFR 1000 & 1040
Beam power	< 1 mW
Safety precautions	Do not look into laser beam
Detector meas. area	Unlimited, dynamically extendible
Resolution	1 µm
Environmental protection	IP 67 (submersible, dustproof)
Dimensions	Approx. 107 x 70 x 49 mm
Weight	Only about 177g
Reflector	
Type	90° roof prism
Environmental protection	IP 67 (submersible, dustproof)
Dimensions	Approx. 100 x 41 x 35 mm
Weight	Approx. 65g
Control Unit	
Environmental protection	IP 65 (water spray resistant, dustproof except for sealed Battery compartment); fully electrically insulated
Interfaces	1 x sensor; 1 x printer/PC (serial)
Dimensions	Approx. 145 x 290 x 67 mm
Weight, complete kit	Only about 6.8 kg

Appendix 7.4 DAQ Card 6024E

Voltage Output

Range	± 10 V
Output coupling	DC
Output impedance	0.1 max
Current drive	±5 mA max
Protection	Short-circuit to ground
Power-on state (steady state)	±200 mV

Digital Trigger

Compatibility	TTL
Response	Rising or falling edge
Pulse width	10 ns min
RTSI	
Trigger lines	7

Analog Input

Number of channels	16 single-ended or 8 differential
(Software-selectable per channel)	Successive approximation
Type of ADC	
Resolution	12 bits, 1 in 4,096
Sampling rate	200 kS/s guaranteed
Input signal ranges	Bipolar only
Input coupling	DC
Max working voltage	
(Signal + common mode)	Each input should remain within ±11 V of ground
Over voltage protection	
FIFO buffer size	2048 S
Data transfers	Interrupts, programmed I/O
Configuration memory size	512 words

Analog Output

Number of channels	2 voltage
Resolution	12 bits, 1 in 4,096
Max update rate	
Interrupts	1 kHz, system dependent
Type of DAC	Double buffered, multiplying
FIFO buffer size	None
Data transfers	Interrupts, programmed I/O

Triggers (Digital Trigger)

Compatibility	TTL
Response	Rising or falling edge
Pulse width	10 ns min

Calibration

Recommended warm-up time	30 min
Interval	1 year
External calibration reference	> 6 and < 10 V
Onboard calibration reference	
Level	5.000 V (±3.5 mV) (actual value stored in EEPROM)
Temperature coefficient	±5 ppm/°C max
Long-term stability	±15 ppm/

Power Requirement

+5 VDC (±5%)	270 mA
Power available at I/O connector	+4.65 to +5.25 VDC at 0.75 A

Physical

PC card type	Type II
I/O connector	68-position VHDCI female connector

Environment

Operating temperature	0 to 40 °C with a maximum internal device temperature of 70 °C as measured by onboard temperature sensor.
Storage temperature	–20 to 70 °C
Relative humidity	10 to 95% non-condensing

Appendix 8. Results Tables

A8.1 Conclusion of the tests results (vibration amplitude and phase angle) of the balancing HPT & LPT rotors (Trim Balancing)

Conclusion of the tests results (vibration amplitude and phase angle)								
Test speed	Initial vibration amplitude (mm)/Phase angle (degree)				Method A Vibration amplitude (mm)/Phase angle (degree) after balancing			
	Plane (1)	Plane (2)	Plane (3)	Plane (4)	Plane (1)	Plane (2)	Plane (3)	Plane (4)
Conclusion of tests results of 2 plane balancing of turbine rotor (HPT) (1080&3000&3500 rpm)								
1080	0.651@ 10.285	0.394@ 252.692			0.112@ 13.382	0.110@ 11.955		
3000	0.758@ 310.258	0.328@ 23.225			0.227@ 293.195	0.203@ 97.500		
3500	0.236@ -13.125	0.334@ 222.012			0.192@ 308.135	0.280@ 247.228		
Conclusion of tests results of 3 plane balancing of turbine rotor (HPT) (1080&3000&3500 rpm)								
1080	0.675@ -21.801	0.263@ 32.787	0.357@ -59.987		0.627@ 131.296	0.122@ 117.469	0.229@ 115.821	
3000	0.748@ 320.053	0.338@ 208.800	0.336@ 352.800		0.316@ 181.855	0.326@ 181.855	0.306@ 178.144	
3500	0.784@ 344.347	0.323@ 11.612	0.345@ -63.254		0.640@ 109.714	0.309@ 125.783	0.310@ 138.795	
Conclusion of tests results of 2 plane balancing of turbine rotor (LPT) (1080&3000&3500 rpm)								
1080	0.297@ 333.125	0.143@ 355.035			0.175@ 25.239	0.117@ 201.918		
3000	0.985@ 25.714	0.249@ 128.955			0.419@ 96.494	0.223@ 103.917		
3500	0.707@ 308.002	0.245@ 144.025			0.297@ 303.614	0.188@ 295.714		

Table A8.1 Results of the balancing HPT & LPT rotors

Conclusion of the tests results (vibration amplitude and phase angle)								
Test speed	**Initial vibration amplitude (mm)/Phase angle (degree)**				**Method A**			
					Vibration amplitude (mm)/Phase angle (degree) after balancing			
	Plane (1)	**Plane (2)**	**Plane (3)**	**Plane (4)**	**Plane (1)**	**Plane (2)**	**Plane (3)**	**Plane (4)**
Conclusion of tests results of 3 plane balancing of turbine rotor (LPT) (1080&3000&3500 rpm)								
1080	0.305@ 45.000	0.825@ 5.032	0.157@ 72.078		0.265@ 62.205	0.277@ 53.136	0.133@ 53.136	
3000	0.935@ 225.712	0.177@ 35.334	0.266@ 180.000		0.284@ 137.319	0.145@ 126.185	0.256@ 152.164	
3500	0.722@ 192.245	0.124@ 64.615	0.193@ -3.258		0.165@ 158.571	0.107@ 162.857	0.188@ 188.571	
Conclusion of tests results of 4 plane balancing of turbine rotor (LPT) (1080&3000&3500 rpm)								
1080	0.276@ 292.500	0.882@ 91.914	0.228@ 330.000	0.142@ 42.352	0.183@ 326.831	0.384@ 341.161	0.183@ 336.101	0.096@ 306.931
3000	0.935@ 342.524	0.177@ 320.052	0.745@ 315.052	0.245@ 74.226	0.645@ 47.755	0.103@ 33.402	0.355@ 24.489	0.124@ 238.087
3500	0.825@ 260.000	0.124@ 180.000	0.534@ 195.000	0.156@ 326.000	0.417@ 27.169	0.106@ 35.122	0.506@ 40.645	0.112@ 23.225
Conclusion of tests results of 2 plane balancing of turbine rotor (HPT) by using Least Square Method (1080&3000&3500)								
1080	0.520@ 82.974	0.298@ 205.333			0.441@ 102.666	0.111@ 179.335		
3000	0.612@ 121.090	0.244@ 181.855			0.491@ 90.000	0.201@ 181.855		
3500	0.598@ 125.783	0.256@ 99.759			0.491@ 82.409	0.161@ 184.285		
Conclusion of tests results of 3 plane balancing of turbine rotor (HPT) by using Least Square Method (1080&3000&3500)								
1080	0.517@ 87.675	0.224@ 101.333	0.278@ 182.666		0.397@ 96.974	0.136@ 41.180	0.106@ 185.333	
3000	0.605@ 111.341	0.251@ 81.649	0.224@ 185.567		0.493@ 116.470	0.337@ 40.824	0.180@ 180.356	
3500	0.588@ 128.570	0.263@ 60.722	0.239@ 182.168		0.298@ 117.108	0.115@ 69.397	0.202@ 98.571	

Table A8.1 (continue) Results of the balancing HPT & LPT rotors

Conclusion of the tests results (vibration amplitude and phase angle)								
Test speed	**Initial vibration amplitude (mm)/Phase angle (degree)**				**Method A**			
					Vibration amplitude (mm)/Phase angle (degree) after balancing			
	Plane (1)	**Plane (2)**	**Plane (3)**	**Plane (4)**	**Plane (1)**	**Plane (2)**	**Plane (3)**	**Plane (4)**
Conclusion of tests results of 2 plane balancing of turbine rotor (LPT) by using Least Square Method (1080&3000&3500))								
1080	0.214@ 328.118	0.114@ 243.099			0.111@ 328.118	0.085@ 338.745		
3000	0.713@ 70.515	0.195@ 89.072			0.127@ 141.030	0.154@ 74.226		
3500	0.544@ 78.072	0.149@ 132.857			0.504@ 182.168	0.109@ 145.714		
Conclusion of tests results of 3 plane balancing of turbine rotor (LPT) by using Least Square Method (1080&3000&3500)								
1080	0.210@ 297.564	0.239@ 289.594	0.117@ 215.203		0.185@ 333.333	0.194@ 298.893	0.105@ 284.558	
3000	0.705@ 37.113	0.664@ 3.711	0.178@ 51.428		0.157@ 122.474	0.281@ 13.750	0.125@ 93.750	
3500	0.566@ 42.857	0.503@ 43.373	0.141@ 108.433		0.282@ 225.542	0.277@ 145.714	0.135@ 173.494	
Conclusion of tests results of 4 plane balancing of turbine rotor (LPT) by using Least Square Method (1080&3000&3500)								
1080	0.205@ 346.666	0.649@ 296.000	0.232@ 358.671	0.958@ 245.333	0.199@ 101.125	0.625@ 310.667	0.199@ 346.764	0.135@ 326.789
3000	0.649@ 81.649	1.399@ 48.247	0.674@ 18.556	0.205@ 100.206	0.163@ 162.352	0.640@ 111.340	0.214@ 77.938	0.118@ 113.877
3500	0.647@ 85.714	0.840@ 77.142	0.473@ 68.571	0.131@ 134.457	0.152@ 188.571	0.207@ 125.783	0.365@ 90.000	0.101@ 321.428

Table A8.1 (continue) Results of the balancing HPT & LPT rotors

A8.2 Test results of correction masses and their phase angles of the balancing HPT & LPT rotors (Trim Balancing)

Table A8.2 show the correction masses results of methods (B&C) and vibration amplitudes methods (B&C) of tests held on HPT and LPT rotors, by using different planes (2,3&4), and using least square method (more measurement locations than balancing planes) and using different calculation methods (B&C).

Conclusion of tests results of 2 plane balancing of (HPT&LPT) rotor (1080&3000&3500 rpm)																
	Method B				Method C				Method B				Method C			
Test Speed	Correction Mass (gram)/Phase Angle (degree) after trim balancing				Correction Mass (gram)/Phase Angle (degree) after trim balancing				Vibration amplitude (mm)/Phase angle (degree) after trim balancing				Vibration amplitude (mm)/Phase angle (degree) after trim balancing			
	Plane (1)	Plane (2)	Plane (3)	Plane (4)	Plane (1)	Plane (2)	Plane (3)	Plane (4)	Plane (1)	Plane (2)	Plane (3)	Plane (4)	Plane (1)	Plane (2)	Plane (3)	Plane (4)
Conclusion of tests results of 2 plane balancing of (HPT) rotor (1080&3000&3500 rpm)																
1080	35.90 @ 46.959	17.625@ -102.623			30.201@ 42.128	13.665@ 10.325			0.111@ 9.298	0.101@ 30.666			0.088@ 46.558	0.078@ 158.687		
3000	4.908 @ -51.292	13.415@ -56.698			4.058 @ 156.514	10.541@ 45.681			0.220@ 181.855	0.198@ 289.484			0.200@ 44.413	0.105@ 312.268		
3500	27.729 @ 26.953	20.410@ -104.723			25.689@ 78.668	16.936@ -155.368			0.184@ 245.853	0.184@ 240.000			0.165@ 145.235	0.174@ 134.285		
Conclusion of tests results of 3 plane balancing of turbine rotor (HPT) rotor (1080&3000&3500)																
1080	16.969@ 132.185	15.115@ 80.177	31.841@ 56.552		11.983@ -102.126	11.998@ 25.714	30.125@ 225.550		0.235@ 46.388	0.132@ 41.137	0.215@ 71.059		0.222@ -79.472	0.101@ -102.623	0.200@ 174.66	
3000	6.833@ 124.553	13.222@ -51.482	2.605@ 174.66		4.256@ -45.444	13.222@ -51.482	2.605@ 174.66		0.315@ 181.855	0.322@ 178.144	0.305@ 185.567		0.221@ 78.668	0.251@ 166.122	0.301@ 115.525	
3500	3.783@ 33.345	6.947@ -160.233	2.782@ -46.777		3.299@ 153. 546	6.002@ 155.235	2.028@ 256.227		0.650@ 124.285	0.312@ 121.445	0.302@ 137.142		0.553@ 111.340	0.298@ 107.628	0.182@ 155.235	
Conclusion of tests results of 2 plane balancing of (LPT) rotor (1080&3000&3500 rpm)																
1080	36.951@ 9.120	32.661@ -61.284			28.125@ 125.356	24.225@ -281.445			0.1952@ 346.7159	0.125@ 44.000			0.176@ 132.822	0.109@ 102.857		
3000	4.633@ 156.010	9.953@ -79.47			4.235@ -110.225	7.369@ 312.268			0.4252@ 111.3402	0.232@ 107.628			0.410@ 66.761	0.201@ -46.777		
3500	8.848@ -44.413	19.778@ 33.725			8.235@ -44.413	12.228@ 155.816			0.1889@ 300.000	0.200@ 216.867			0.155@ 245.853	0.101@ 236.004		

Table A8.2 Results of the balancing HPT & LPT rotors (Trim Balancing)

Conclusion of tests results of 2 plane balancing of (HPT&LPT) rotor (1080&3000&3500 rpm)																
	Method B				Method C				Method B				Method C			
Test Speed	Correction Mass (gram)/Phase Angle (degree) after trim balancing				Correction Mass (gram)/Phase Angle (degree) after trim balancing				Vibration amplitude (mm)/Phase angle (degree) after trim balancing				Vibration amplitude (mm)/Phase angle (degree) after trim balancing			
	Plane (1)	Plane (2)	Plane (3)	Plane (4)	Plane (1)	Plane (2)	Plane (3)	Plane (4)	Plane (1)	Plane (2)	Plane (3)	Plane (4)	Plane (1)	Plane (2)	Plane (3)	Plane (4)
Conclusion of tests results of 3 plane balancing of (LPT) rotor (1080&3000&3500 rpm)																
1080	20.163@ -77.548	17.903@ -115.601	24.633@ 162.684		14.225@ 162.336	13.557@ 255.001	22.553@ -23.215		0.264@ 47.647	0.257@ 49.333	0.114@ 53.136		0.195@ 333.399	0.194@ 292.893	0.089@ 284.558	
3000	4.330@ -122.404	1.536@ 31.861	11.227@ -120.568		4.021@ 312.223	1.522@ 225.364	9.358@ 66.522		0.254@ 155.876	0.155@ 141.030	0.205@ 133.608		0.187@ 126.474	0.150@ 223.750	0.185@ 93.750	
3500	9.550@ -11.306	2.174@ 66.761	24.952@ -113.391		5.221@ -103.325	2.003@ -295.325	20.534@ 61.364		0.150@ 203.855	0.101@ 190.843	0.181@ 173.494		0.170@ 112.562	0.177@ 145.714	0.135@ 25.717	
Conclusion of tests results of 4 plane balancing of (LPT) rotor (1080&3000&3500 rpm)																
1080	19.394@ -138.983	19.606@ -18.985	45.717@ -60.038	21.262@ 45.561	17.553@ 284. 384	15.622@ -103.109	41.312@ -210.184	18.365@ 350.255	0.192@ 303.088	0.197@ 324.132	0.148@ 344.059	0.083@ 325.461	0.175@ 10.125	0.175@ 310.666	0.126@ 346.764	0.071@ 326.789
3000	3.957@ 162.861	12.274@ 99.533	10.162@ 78.096	10.164@ -97.741	3.097@ 162.861	11.228@ 102.857	8.235@ 132.822	9.336@ -335.554	0.623@ 47.605	0.091@ 33.321	0.344@ 23.544	0.119@ -23.690	0.463@ 162.352	0.044@ 111.340	0.214@ 77.938	0.104@ 113.877
3500	5.112@ 11.260	4.680@ 86.770	11.560@ 100.384	6.002@ -42.750	5.001@ 96.571	4.021@ 246.723	10.500@ 215.300	5.532@ -133.211	0.471@ 27.155	0.111@ 35.079	0.520@ 40.589	0.101@ 23.257	0.352@ 188.571	0.058@ 125.783	0.365@ 90.000	0.085@ 321.428
Conclusion of tests results of 2 plane balancing of (HPT) rotor by using Least Square Method (1080&3000&3500)																
1080	4.460@ 2.376	3.651@ 94.344			3.5464@ 98.571	3.211@ 333.321			0.356@ 91.084	0.102@ 180.000			0.235@ 46.3228	0.101@ 41.137		
3000									0.405@ 102.857	0.174@ 183.750			0.483@ 132.822	0.156@ 27.155		
3500									0.484@ 98.571	0.104@ 184.285			0.481@ 246.723	0.102@ 184.285		
Conclusion of tests results of 3 plane balancing of (HPT) rotor by using Least Square Method (1080&3000&3500)																
1080	11.640@ -157.447	16.874@ 41.458	10.169@ -149.361		8.996@ 55.312	12.334@ 102.807	9.134@ 127.108		0.356@ 107.142	0.129@ 98.571	0.087@ 98.571		0.222@ 297.564	0.109@ 289.594	0.086@ 215.203	
3000									0.366@ 117.108	0.112@ 98.571	0.155@ 95.421		0.331@ 181.855	0.110@ 178.144	0.123@ 185.567	
3500									0.205@ 112.771	0.108@ 60.722	0.184@ 99.759		0.195@ 124.285	0.099@ 121.445	0.122@ 137.142	
Conclusion of tests results of 2 plane balancing of (LPT) rotor by using Least Square Method (1080&3000&3500)																
1080	9.400@ -42.814	16.259@ -175.954			8.125@ -117.128	13.333@ -100.235			0.066@ 313.33	0.081@ 204.000			0.055@ 102.857	0.080@ 96.571		
3000									0.129@ 91.836	0.165@ 40.824			0.111@ 162.352	0.150@ -42.750		
3500									0.498@ 154.285	0.103@ 117.108			0.456@ 78.096	0.104@ 102.857		

Conclusion of tests results of 3 plane balancing of (HPT&LPT) rotor (1080&3000&3500 rpm)																
Test Speed	Method B Correction Mass (gram)/Phase Angle (degree) after trim balancing				Method C Correction Mass (gram)/Phase Angle (degree) after trim balancing				Method B Vibration amplitude (mm)/Phase angle (degree) after trim balancing				Method C Vibration amplitude (mm)/Phase angle (degree) after trim balancing			
	Plane (1)	Plane (2)	Plane (3)	Plane (4)	Plane (1)	Plane (2)	Plane (3)	Plane (4)	Plane (1)	Plane (2)	Plane (3)	Plane (4)	Plane (1)	Plane (2)	Plane (3)	Plane (4)
Conclusion of tests results of 3 plane balancing of (LPT) rotor by using Least Square Method (1080&3000&3500)																
1080	8.893@ 0.166	11.784@ -13.517	36.502@ 142.667		6.995@ 350.108	9.402@ 303.356	30.628@ 225.522		0.169@ 4.000	0.202@ 357.333	0.095@ 48.000		0.175@ 46.388	0.182@ 41.137	0.086@ 71.059	
3000									0.149@ 11.020	0.223@ 345.000	0.122@ 208.800		0.120@ 161.340	0.134@ 77.938	0.114@ 113.877	
3500									0.182@ 225.542	0.197@ 145.714	0.119@ 173.494		0.131@ 35.079	0.130@ 40.589	0.121@ 23.257	
Conclusion of tests results of 4 plane balancing of turbine rotor (LPT) by using Least Square Method (1080&3000&3500)																
1080	6.41@ -127.518	7.212@ 20.819	14.042@ 77.951	21.062@ -127.143	6.236@ -254.001	6.995@ 342.365	10.354@ 154.285	18.368@ -312.771	0.155@ 304.329	0.126@ 200.412	0.100@ 14.845	0.115@ 174.433	0.117@ 237.155	0.099@ -35.079	0.097@ 40.589	0.111@ -23.257
3000									0.153@ 148.453	0.442@ 96.494	0.223@ 189.278	0.109@ 185.567	0.130@ -78.668	0.311@ 266.122	0.111@ -115.525	0.098@ 40.824
3500									0.144@ 311.752	0.205@ 345.154	0.274@ 356.288	0.089@ 348.750	0.108@ -181.855	0.202@ 178.144	0.225@ -185.567	0.083@ 348.750

Table A8.2 (continue) Results of the balancing HPT & LPT rotors (Trim Balancing)

Conclusion of the tests results (vibration amplitude and phase angle)												
Speeds RPM	**Vibration amplitude (mm) improvement % Method B&C**				**Vibration amplitude (mm) improvement % Method B**				**Vibration amplitude (mm) improvement % Method C**			
	Plane (1)	**Plane (2)**	**Plane (3)**	**Plane (4)**	**Plane (1)**	**Plan (2)**	**Plan (3)**	**Plane (4)**	**Plane (1)**	**Plane (2)**	**Plane (3)**	**Plane (4)**
Results of 2 plane balancing of turbine rotor (HPT) (1080&3000&3500 rpm)												
1080	82.796	72.081			0.893	8.182			21.429	29.091		
3000	70.053	38.110			3.084	2.463			11.894	48.276		
3500	18.644	16.168			4.167	34.286			14.063	37.857		
Results of 3 plane balancing of turbine rotor (HPT) (1080&3000&3500 rpm)												
1080	7.111	53.612	35.854		27.273	1.639	6.114		64.593	17.213	12.664	
3000	57.754	3.550	8.929		0.316	1.227	0.327		30.063	23.006	1.634	
3500	18.367	4.334	10.145		8.125	-0.971	2.581		13.594	3.560	41.290	
Results of 2 plane balancing of turbine rotor (LPT) (1080&3000&3500 rpm)												
1080	41.077	18.182			5.714	-0.855			28.000	6.838		
3000	57.462	10.442			-1.480	-4.036			2.148	9.865		
3500	57.992	23.265			36.397	14.362			47.811	46.277		
Results of 3 plane balancing of turbine rotor (LPT) (1080&3000&3500 rpm)												
1080	13.115	66.424	15.287		0.377	7.220	14.286		26.415	29.964	33.083	
3000	69.626	18.079	3.759		10.563	-6.897	19.922		34.155	30.345	27.734	
3500	77.147	13.710	2.591		9.091	5.607	3.723		32.727	17.757	28.191	
Results of 4 plane balancing of turbine rotor (LPT) (1080&3000&3500 rpm)												
1080	33.696	56.463	19.737	32.394	-4.918	48.698	19.126	13.542	4.372	54.427	31.148	26.042
3000	31.016	41.808	52.349	49.388	3.411	11.650	3.099	4.032	28.217	57.282	39.718	16.129
3500	49.455	14.516	5.243	28.205	4.077	-4.717	-2.767	9.821	15.588	45.283	27.866	24.107
Results of 2 plane balancing of turbine rotor (HPT) by using Least Square Method (1080&3000&3500)												
1080	15.192	62.752			19.274	8.108			46.712	9.009		
3000	19.771	17.623			17.515	13.433			1.629	22.388		
3500	17.893	37.109			1.426	35.404			2.037	36.646		
Results of 3 plane balancing of turbine rotor (HPT) by using Least Square Method (1080&3000&3500)												
1080	23.211	39.286	61.871		10.327	5.147	17.925		44.081	19.853	18.868	
3000	18.512	31.076	19.643		25.761	35.260	13.889		32.860	36.416	31.667	
3500	49.320	56.274	15.481		31.208	6.087	8.911		34.564	13.913	39.604	
Results of 2 plane balancing of turbine rotor (LPT) by using Least Square Method (1080&3000&3500))												
1080	48.131	25.439			40.541	4.706			50.450	5.882		
3000	82.188	21.026			-1.575	-1.299			12.598	2.597		
3500	7.353	26.846			1.190	5.505			7.738	4.587		
Results of 3 plane balancing of turbine rotor (LPT) by using Least Square Method (1080&3000&3500)												
1080	11.905	18.828	10.256		8.649	-4.124	9.524		5.405	6.186	18.095	
3000	77.730	57.681	29.775		5.096	20.641	2.400		23.567	52.313	8.800	
3500	50.177	44.930	4.255		35.461	28.881	11.852		53.546	53.069	10.370	
Results of 4 plane balancing of turbine rotor (LPT) by using Least Square Method (1080&3000&3500)												
1080	2.927	3.698	14.224	85.908	22.111	79.840	49.749	14.815	41.206	84.160	51.256	17.778
3000	74.884	54.253	68.249	42.439	6.135	30.938	-4.206	7.627	20.245	51.406	48.131	16.949
3500	76.507	75.357	22.833	22.901	22.111	79.840	49.749	14.815	41.206	84.160	51.256	17.778

Table A8.3 general results conclusion

A8.2 New balancing procedures based on modified QR and SVD techniques with least square optimization

A8.2.1 High Pressure Turbine Rotor

Table A8.4 shows the initial balancing results achieved for the HPT (Figure A8.1) rotor by using traditional Influence Coefficient Method (two plane, two measurements locations and one speed).

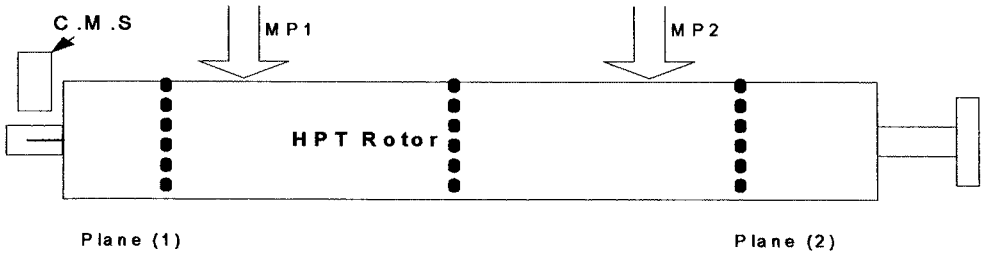

Figure A8.1 schematic diagram of HPT rotor test set up (2 measurements points)

Results of the balancing HPT rotor									
Run	T. Mass	Vibration amplitudes (mm)		Phase angle (Deg)		Calculated Correction Masses/Phase Angle		Actual Correction Masses/Phase Angle	
		Plane (1) Radius 29.3mm	Plane (2) Radius 37.05mm	Plane (1) Radius 29.3mm	Plane (2) Radius 37.05mm	Plane (1) Radius 29.3mm	Plane (2) Radius 37.05mm	Plane (1) Radius 29.3mm	Plane (2) Radius 37.05mm
0		0.595	0.315	113.87	196.363	18.938@ -63.690	9.163@ 62.855	18.2@ -60	9.9 @ 60
1	33.6@60	1.123	0.385	154.285	155.876				
2	33.6@60	0.642	0.637	115.051	320.400				
		Vibration amplitude data after adding C. Masses		Phase angle data after adding C. Masses					
		0.315	0.201	216.717	122.128				

Table A8.4 Results of the test (HPT rotor)

Test results of validation of the combination of least square optimization, QR factorization, singular value decomposition (SVD) and the QR combined with SVD (LSQ+QR+SVD) on High Pressure Turbine Rotor Figure A8.2 by using (3 plane balancing, 5 measurement locations and 4 operation speeds 840,1080,2040,3000 rpm) and the total weight was 10.1 Kg), the known masses added to the system were 50.1

@0° (plane 1), 36.1 g @0° (plane 2). According to the results Tables the introduced masses are added in plane 1&3. Table A8.5 demonstrates that vibration amplitude and phase angle for the above test.

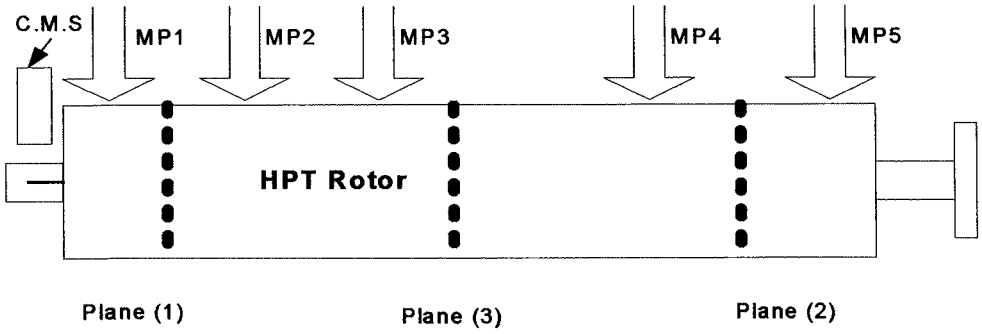

Figure A8.2 schematic diagram of HPT rotor test set up (5 measurements points)

3 plane 5 MP and 3 speeds											
Run	Speeds	Trial Mass	Vibration amplitude (mm)					Phase angle (degree)				
			MP1	MP2	MP3	MP4	MP5	MP1	MP2	MP3	MP4	MP5
0	840 rpm		0.249	0.246	0.102	0.173	0.363	341.138	234.830	227.076	194.953	85.555
	1080 rpm		0.278	0.288	0.168	0.219	0.427	254.666	238.666	202.666	200.590	88.000
	2040 rpm		1.213	0.940	0.874	0.808	0.598	226.923	221.342	208.800	201.600	110.400
	3000 rpm		1.396	1.286	1.418	1.382	1.769	281.612	243.871	219.512	222.439	193.170
1	840 rpm	33.6 @60	0.380	0.341	0.166	0.197	0.391	334.054	238.918	194.119	201.686	82.994
	1080 rpm		0.227	0.149	0.241	0.207	0.464	224.090	233.181	184.867	199.545	85.584
	2040 rpm		0.857	0.739	0.923	0.869	0.884	223.373	219.036	188.674	182.168	142.275
	3000 rpm		1.457	1.594	1.919	1.700	1.658	225.365	232.258	181.463	193.170	197.419
2	840 rpm	33.6 @60	0.244	0.254	0.141	0.162	0.359	348.454	247.696	192.070	205.263	85.263
	1080 rpm		0.424	0.312	0.244	0.260	0.527	221.845	240.000	192.619	201.918	84.000
	2040 rpm		0.884	0.710	0.637	0.637	0.647	255.238	242.526	212.210	192.381	144.761
	3000 rpm		1.443	1.440	1.697	1.826	1.355	274.029	280.000	216.000	224.000	204.666
3	840 rpm	33.6 @60	0.290	0.261	0.102	0.188	0.327	336.851	255.868	201.224	221.046	86.064
	1080 rpm		0.329	0.295	0.141	0.195	0.415	255.645	238.064	244.337	205.301	88.192
	2040 rpm		0.910	0.656	0.405	0.560	0.599	264.444	262.822	228.198	202.222	139.888
	3000 rpm		1.404	1.206	1.094	2.071	1.644	261.538	242.181	214.678	211.376	195.321

Table A8.5 Data of the test (HPT rotor)

A8.2.1.1 High Pressure Turbine Rotor Results For 3 plane balancing

Table A8.6 shows the results of High Pressure Turbine Rotor For 3 plane balancing with 4 different operation speeds. Table A8.7 shows the influence coefficient Matrix properties for each test.

Correction Masses (gram)/Phase Angle (degree								
Speeds Test	Plane (1) Radius 29.3mm				Plane (3) Radius 27.35 mm			
	Targeted amount 50.1 @0°				Targeted amount 0 g @0°			
	LSQ	QR	SVD	QR+SVD	LSQ	QR	SVD	QR+SVD
All speeds	45.995@ -17.339	45.995@ -17.339	45.995@ -17.339	45.995@ -17.339	55.787@ 121.573	55.787@ 121.573	55.787@ 121.573	55.787@ 121.573
840 rpm	87.708@ -90.349	87.708@ -90.349	87.708@ -90.349	87.708@ -90.349	26.873@ 74.222	26.873@ 74.222	26.873@ 74.222	26.873@ 74.222
1080 pm	67.217@ 58.274	67.217@ 58.274	67.217@ 58.274	67.217@ 58.274	59.301@ -94.858	59.301@ -94.858	59.301@ -94.858	59.301@ -94.858
2040rpm	43.500@ -106.744	43.500@ -106.744	43.500@ -106.744	43.500@ -106.744	36.620@ 66.984	36.620@ 66.984	36.620@ 66.984	36.620@ 66.984
3000rpm	47.743@ -10.351	47.743@ -10.351	47.743@ -10.351	47.743@ -10.351	62.008@ 115.280	62.008@ 115.280	62.008@ 115.280	62.008@ 115.280

Correction Masses (gram)/Phase Angle (degree				
Speeds Test	Plane (2) Radius 37.05mm			
	Targeted amount 36.1 g @0°			
	LSQ	QR	SVD	QR+SVD
All speeds	6.104 @ 42.483	6.104 @ 42.483	6.104 @ 42.483	6.104 @ 42.483
840 rpm	69.063@ 94.741	69.063@ 94.741	69.063@ 94.741	69.063@ 94.741
1080 pm	79.491@ 60.650	79.491@ 60.650	79.491@ 60.650	79.491@ 60.650
2040rpm	51.536@ 124.011	51.536@ 124.011	51.536@ 124.011	51.536@ 124.011
3000rpm	15.388@ -55.251	15.388@ -55.251	15.388@ -55.251	15.388@ -55.251

Table A8.6 Results of the test (HPT rotor)

Influence coefficient matrix properties		
	Rank	Condition Number
All speeds	3	3.105
840 rpm	3	3.429
1080 pm	3	4.658
2040rpm	3	14.624
3000rpm	3	3.750

Table A8.7 Results Matrixes properties (HPT rotor)

A8.2.1.2 High Pressure Turbine Rotor Results For 2 plane balancing

Table A8.8 shows the results of High Pressure Turbine Rotor For 2 plane balancing with 4 different operation speeds. Table A8.9 shows the influence coefficient Matrix properties for each test.

Correction Masses (gram)/Phase Angle (degree								
Speeds Test	Plane (1)				Plane (2)			
	Targeted amount 50.1 @0°				Targeted amount 36.1 g @0°			
	LSQ	QR	SVD	QR+SVD	LSQ	QR	SVD	QR+SVD
All speeds	47.581@ -16.368	47.581@ -16.368	47.581@ -16.368	47.581@ -16.368	56.713@ 117.639	56.713@ 117.639	56.713@ 117.639	56.713@ 117.639
840 rpm	78.982@ -93.813	78.982@ -93.813	78.982@ -93.813	78.982@ -93.813	80.881@ 76.555	80.881@ 76.555	80.881@ 76.555	80.881@ 76.555
1080 pm	46.949@ 69.833	46.949@ 69.833	46.949@ 69.833	46.949@ 69.833	61.874@ -100.462	61.874@ -100.462	61.874@ -100.462	61.874@ -100.462
2040rpm	52.683@ -78.635	52.683@ -78.635	52.683@ -78.635	52.683@ -78.635	94.224@ 110.452	94.224@ 110.452	94.224@ 110.452	94.224@ 110.452
3000rpm	51.091@ -13.604	51.091@ -13.604	51.091@ -13.604	51.091@ -13.604	59.127@ 113.643	59.127@ 113.643	59.127@ 113.643	59.127@ 113.643

Table A8.8 Results of the test (HPT rotor)

Influence coefficient matrix properties		
	Rank	Condition Number
All speeds	2	2.048
840 rpm	2	2.780
1080 pm	2	2.183
2040rpm	2	2.311
3000rpm	2	2.630

Table A8.9 Results Matrixes properties (HPT rotor)

A8.2.2 Low Pressure Turbine Rotor

Table A8.10 shows the initial balancing results achieved for the Low Pressure Turbine Rotor (Figure A8.3) rotor by using traditional Influence Coefficient Method (two plane, two measurements locations and one speed).

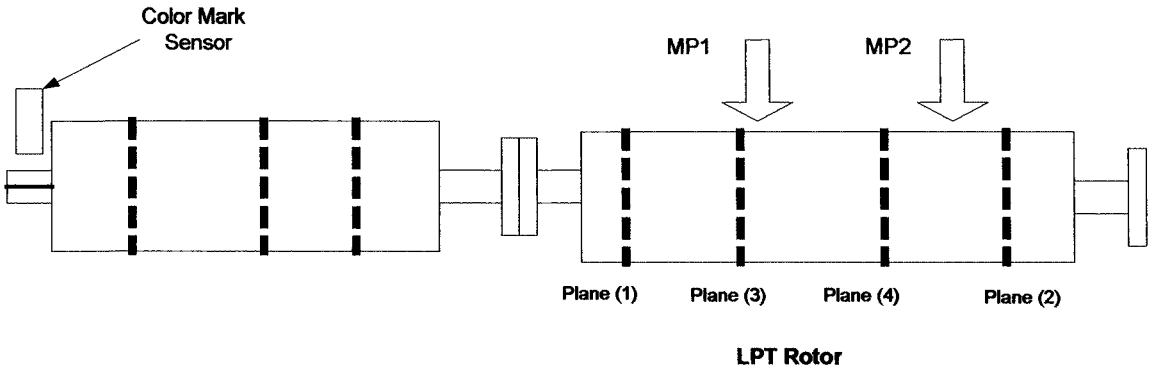

Figure A8.3 schematic diagram of HPT connected to LPT rotor test set up

Results of the balancing LPT rotor									
Run	T. Mass	Vibration amplitudes (mm)		Phase angle (Deg)		Calculated Correction Masses/Phase Angle		Actual Correction Masses/Phase Angle	
		Plane (1) Radius (48.6) mm	Plane (2) Radius (48.6) mm	Plane (1) Radius (48.6) mm	Plane (2) Radius (48.6) mm	Plane (1) Radius (48.6) mm	Plane (2) Radius (48.6) mm	Plane (1) Radius (48.6) mm	Plane (2) Radius (48.6) mm
0	33.6@60	0.801	0.532	307.500	100.206	43.034@ -52.149	30.297@ 1.286	44.1@ -60	32.3@ 30
1		0.964	1.711	18.556	196.701				
2		0.698	1.423	15.000	159.587				
		Residual unbalance after adding C. Masses		Phase angle after adding C. Masses					
		0.502	0.305	290.727	155.129				

Table A8.10 Results of the test (LPT rotor)

Test results of validation of the combination of least square optimization, QR factorization, singular value decomposition (SVD) and the QR combined with SVD (LSQ+QR+SVD) on L.P.T rotor Figure A8.3 by using (4 plane balancing, 5 measurements locations and 4 operation speeds 1500,2040,3000,3600 rpm and the total weight was 43.922 Kg), the known Masses added to the system were 86.7 @0 (plane 1), 96.3 g @0 (plane 2). According to the results Tables the introduced masses are

added in plane 1&4 Table A8.11 demonstrates that vibration amplitude and phase angle for the above test.

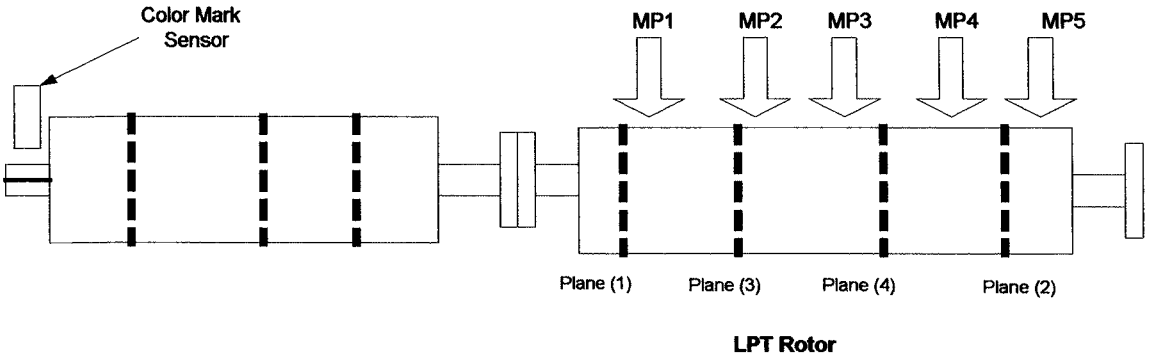

Figure A8.4 schematic diagram of HPT connected to LPT rotor test set up

4 plane 5 MP and 4 speeds												
Run	Speeds	Trial Mass	Vibration amplitude (mm)					Phase angle (degree)				
			MP1	MP2	MP3	MP4	MP5	MP1	MP2	MP3	MP4	MP5
0	1500 rpm		0.153	0.295	0.595	0.561	0.161	333.116	130.485	135.145	148.645	146.796
	2040 rpm		0.327	0.500	0.693	0.742	0.297	306.087	221.538	221.538	205.961	237.115
	3000 rpm		0.710	1.282	1.252	1.284	0.578	282.222	271.111	268.888	247.362	206.666
	3600 rpm		1.306	1.978	2.300	2.034	1.431	312.923	217.674	244.379	302.189	260.146
1	1500 rpm	33.6 @60	0.185	0.280	0.586	0.539	0.192	310.670	120.348	132.244	129.473	141.052
	2040 rpm		0.498	0.696	0.725	0.871	0.420	322.574	257.142	246.502	235.862	178.217
	3000 rpm		0.996	1.623	1.538	1.572	0.749	284.705	271.111	288.888	280.000	206.666
	3600 rpm		0.190	1.199	1.291	1.255	0.739	331.153	326.315	328.421	309.473	328.421
2	1500 rpm	33.6 @60	0.715	0.307	0.688	0.525	0.170	345.263	121.276	127.384	130.000	104.767
	2040 rpm		0.246	0.351	0.510	0.620	0.210	333.157	183.157	187.136	202.995	150.000
	3000 rpm		0.713	1.206	1.282	1.255	0.710	338.947	326.315	322.105	307.058	334.736
	3600 rpm		1.062	1.628	1.687	1.826	0.932	285.000	281.095	286.027	256.438	234.246
3	1500 rpm	33.6 @60	0.144	0.317	0.739	0.556	0.170	326.213	121.558	128.571	133.680	125.825
	2040 rpm		0.151	0.234	0.522	0.503	0.131	317.213	140.740	147.541	160.000	143.114
	3000 rpm		0.410	0.442	0.532	0.429	0.288	321.428	321.428	252.857	157.365	327.664
	3600 rpm		0.424	0.468	0.652	0.363	0.420	352.394	344.000	296.055	201.398	322.237
4	1500 rpm	33.6 @60	0.141	0.385	0.659	0.603	0.192	80.122	128.414	125.454	146.181	147.720
	2040 rpm		0.161	0.410	0.666	0.713	0.205	303.934	154.918	154.074	164.444	201.481
	3000 rpm		0.576	0.954	1.042	1.186	0.486	304.285	289.704	279.053	234.319	272.142
	3600 rpm		0.840	1.531	1.523	1.775	0.788	274.736	246.315	246.315	232.105	225.000

Table A8.11 Data of the test (LPT rotor)

Correction Masses (gram)/Phase Angle (degree								
Speeds Test	**Plane (1) Radius (48.6) mm**				**Plane (2) Radius (45.2) mm**			
	Targeted amount 86.7 g@0				**Targeted amount 0g @0**			
	LSQ	**QR**	**SVD**	**QR+SVD**	**LSQ**	**QR**	**SVD**	**QR+SVD**
All speeds	4.671@ 115.146	4.671@ 115.146	4.671@ 115.146	4.671@ 115.146	13.581@ 126.174	13.581@ 126.174	13.581@ 126.174	13.581@ 126.174
1500 rpm	82.734@ 29.252	82.734@ 29.252	82.734@ 29.252	82.734@ 29.252	25.048@ -169.462	25.048@ -169.462	25.048@ -169.462	25.048@ -169.462
2040 rpm	19.563@ -106.215	19.563@ -106.215	19.563@ -106.215	19.563@ -106.215	39.697@ 131.010	39.697@ 131.010	39.697@ 131.010	39.697@ 131.010
3000 rpm	34.848@ 8.084	34.848@ 8.084	34.848@ 8.084	34.848@ 8.084	46.608@ 179.321	46.608@ 179.321	46.608@ 179.321	46.608@ 179.321
3600 rpm	19.571@ 92.985	19.571@ 92.985	19.571@ 92.985	19.571@ 92.985	9.137@ 162.625	9.137@ 162.625	9.137@ 162.625	9.137@ 162.625

Correction Masses (gram)/Phase Angle (degree								
Speeds Test	**Plane (3) Radius (48.6) mm**				**Plane (4) Radius (48.6) mm**			
	Targeted amount 0 g@0				**Targeted amount 96.3 g @0**			
	LSQ	**QR**	**SVD**	**QR+SVD**	**LSQ**	**QR**	**SVD**	**QR+SVD**
All speeds	20.395@ 72.881	20.395@ 72.881	20.395@ 72.881	20.395@ 72.881	22.326@ -28.383	22.326@ -28.383	22.326@ -28.383	22.326@ -28.383
1500 rpm	95.141@ -62.815	95.141@ -62.815	95.141@ -62.815	95.141@ -62.815	44.055@ -107.601	44.055@ -107.601	44.055@ -107.601	44.055@ -107.601
2040 rpm	48.544@ 40.700	48.544@ 40.700	48.544@ 40.700	48.544@ 40.700	44.463@ -86.341	44.463@ -86.341	44.463@ -86.341	44.463@ -86.341
3000 rpm	44.271@ -14.584	44.271@ -14.584	44.271@ -14.584	44.271@ -14.584	61.733@ 71.836	61.733@ 71.836	61.733@ 71.836	61.733@ 71.836
3600 rpm	5.917@ 88.185	5.917@ 88.185	5.917@ 88.185	5.917@ 88.185	26.944@ -4.677	26.944@ -4.677	26.944@ -4.677	26.944@ -4.677

Table A8.12 Results of the test (LPT rotor)

Influence coefficient matrix properties		
	Rank	**Condition Number**
All speeds	4	9.418
840 rpm	4	14.956
1080 pm	4	19.400
2040rpm	4	20.565
3000rpm	4	21.741

Table A8.13 Results Matrixes properties (LPT rotor)

A8.2.2.1 Low Pressure Turbine Rotor Results For 3 plane balancing

Table A8.14 shows the results of Low Pressure Turbine Rotor For 3 plane balancing with 4 different operation speeds. Table A8.15 shows the influence coefficient Matrix properties for each test.

Correction Masses (gram)/Phase Angle (degree)								
Speeds Test	Plane (1)				Plane (3)			
	Targeted amount 86.7 g@0				Targeted amount 0 g @0°			
	LSQ	QR	SVD	QR+SVD	LSQ	QR	SVD	QR+SVD
All speeds	12.311@ 86.746	12.311@ 86.746	12.311@ 86.746	12.311@ 86.746	43.079@ -0.708	43.079@ -0.708	43.079@ -0.708	43.079@ -0.708
840 rpm	89.657@ -10.687	89.657@ -10.687	89.657@ -10.687	89.657@ -10.687	91.684@ -49.002	91.684@ -49.002	91.684@ -49.002	91.684@ -49.002
1080 pm	23.275@ -93.616	23.275@ -93.616	23.275@ -93.616	23.275@ -93.616	56.241@ -33.810	56.241@ -33.810	56.241@ -33.810	56.241@ -33.810
2040rpm	10.731@ 50.543	10.731@ 50.543	10.731@ 50.543	10.731@ 50.543	32.220@ 29.116	32.220@ 29.116	32.220@ 29.116	32.220@ 29.116
3000rpm	22.175@ 90.517	22.175@ 90.517	22.175@ 90.517	22.175@ 90.517	34.999@ 4.531	34.999@ 4.531	34.999@ 4.531	34.999@ 4.531

Correction Masses (gram)/Phase Angle (degree				
Speeds Test	Plane (2)			
	Targeted amount 36.1 g @0°			
	LSQ	QR	SVD	QR+SVD
All speeds	29.822@ 145.062	29.822@ 145.062	29.822@ 145.062	29.822@ 145.062
840 rpm	35.025@ -104.656	35.025@ -104.656	35.025@ -104.656	35.025@ -104.656
1080 pm	47.577@ 113.197	47.577@ 113.197	47.577@ 113.197	47.577@ 113.197
2040rpm	32.342@ 135.234	32.342@ 135.234	32.342@ 135.234	32.342@ 135.234
3000rpm	16.472@ 171.356	16.472@ 171.356	16.472@ 171.356	16.472@ 171.356

Table A8.14 Results of the test

Influence coefficient matrix properties		
	Rank	Condition Number
All speeds	3	3.536
840 rpm	3	4.618
1080 pm	3	7.943
2040rpm	3	14.172
3000rpm	3	11.621

Table A8.15 Results Matrixes properties (LPT rotor)

A8.2.2.2 Low Pressure Turbine Rotor Results For 2 plane balancing

Table A8.16 shows the results of Low Pressure Turbine Rotor For 2 plane balancing with 4 different operation speeds. Table A8.17 shows the influence coefficient Matrix properties for each test.

Correction Masses (gram)/Phase Angle (degree								
Speeds Test	Plane (1)				Plane (2)			
	Targeted amount 86.7 g@0				Targeted amount 96.3 g @0			
	LSQ	QR	SVD	QR+SVD	LSQ	QR	SVD	QR+SVD
All speeds	22.322@ 105.313	22.322@ 105.313	22.322@ 105.313	22.322@ 105.313	23.606@ 22.802	23.606@ 22.802	23.606@ 22.802	23.606@ 22.802
1500 rpm	116.454@ -20.855	116.454@ -20.855	116.454@ -20.855	116.454@ -20.855	38.378@ -51.107	38.378@ -51.107	38.378@ -51.107	38.378@ -51.107
2040 rpm	1.050@ -160.761	1.050@ -160.761	1.050@ -160.761	1.050@ -160.761	35.759@ 5.063	35.759@ 5.063	35.759@ 5.063	35.759@ 5.063
3000 rpm	60.487@ 148.407	60.487@ 148.407	60.487@ 148.407	60.487@ 148.407	61.291@ 134.493	61.291@ 134.493	61.291@ 134.493	61.291@ 134.493
3600 rpm	28.475@ 100.557	28.475@ 100.557	28.475@ 100.557	28.475@ 100.557	21.90@ -4.158	21.90@ -4.158	21.90@ -4.158	21.90@ -4.158

Table A8.16 Results of the test (LPT rotor)

Influence coefficient matrix properties		
	Rank	Condition Number
All speeds	2	1.862
840 rpm	2	1.416
1080 pm	2	2.715
2040rpm	2	2.197
3000rpm	2	2.243

Table A8.17 Results Matrixes properties (LPT rotor)

A8.2.3 Generator Rotor

Table A8.18 shows the initial balancing results achieved for the G. rotor (Figure A8.5) rotor by using traditional Influence Coefficient Method (two plane, two measurements locations and one speed).

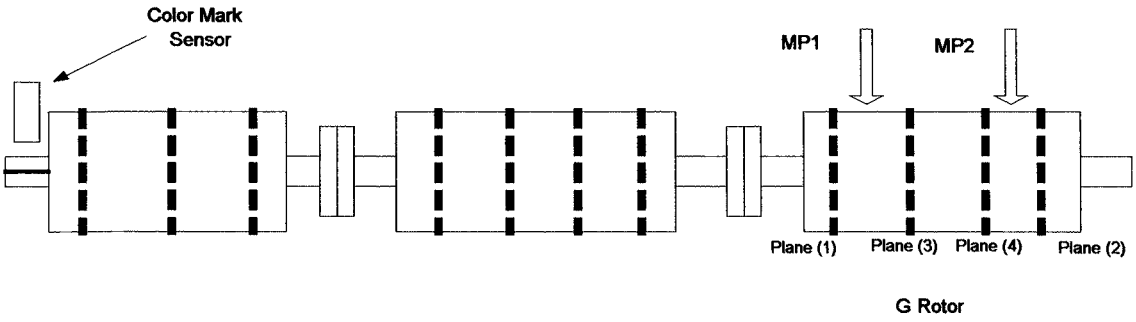

Figure A8.5 schematic diagram of HPT, LPT and G. rotor test set up

Results of the balancing G rotor									
Run	T. Mass	Vibration amplitude (mm)		Phase angle (Deg)		Calculated Correction Masses/Phase Angle		Actual Correction Masses/Phase Angle	
		Plane (1) Radius (29.7) mm	Plane (2) Radius (29.7) mm	Plane (1) Radius (29.7) mm	Plane (2) Radius (29.7) mm	Plane (1) Radius (29.7) mm	Plane (2) Radius (29.7) mm	Plane (1) Radius (29.7) mm	Plane (2) Radius (29.7) mm
0	33.6@60	0.975	0.278	136.544	-61.971	50.078@ -178.226	58.460@ -173.449	50.2@ -180	56.7@ -180
1		0.943	0.319	149.889	-61.446				
2		1.012	0.268	144.1827	-27.919				
		Vibration amplitude data after adding C. Masses		Phase angle data after adding C. Masses					
		0.526	0.183	120.368	187.135				

Table A8.18 Results of the test (G rotor)

Test results of validation of the combination of least square optimization, QR factorization, singular value decomposition (SVD) and the QR combined with SVD

(LSQ+QR+SVD) on Generator rotor Figure A8.6 by using (4 plane balancing, 5 measurements locations and 4 operation speeds 2040,3000,3500,4000 rpm and the total weight was 71.610 Kg), the known Masses added to the system were 96.4 @0° (plane 1), 91.3 g @0° (plane 2) According to the results Table A8s the introduced masses are added in plane 1&4. Table A8.19 demonstrates the vibration amplitude and phase angle for the above test. Table A8.20-A8.22 displays the correction masses and phase angle for the above test.

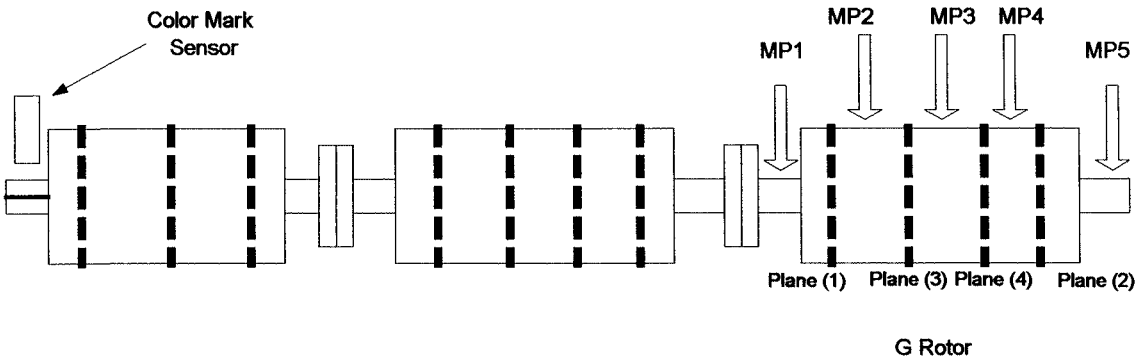

Figure A8.6 schematic diagram of HPT, LPT and G rotor test set up

2 plane 5 MP and 3 speeds known masses added at the same phase												
Run	Speeds	Trial Mass	Vibration amplitude (mm)					Phase angle (degree)				
			MP1	MP2	MP3	MP4	MP5	MP1	MP2	MP3	MP4	MP5
0	2040 rpm		1.047	1.413	1.614	0.866	0.402	153.529	325.588	329.670	311.441	332.205
	3000 rpm		0.957	1.621	1.934	1.125	0.507	148.520	326.098	330.810	348.699	325.945
	3500 rpm		0.747	1.873	2.349	1.440	0.608	155.106	308.021	321.723	343.475	282.994
	4000 rpm		0.644	2.092	2.705	1.587	0.698	148.965	310.344	291.400	262.971	285.517
1	2040 rpm	33.6 @60	1.108	1.316	1.443	0.739	0.349	151.322	334.372	329.387	330.711	301.224
	3000 rpm		1.113	1.330	1.477	0.840	0.383	143.720	324.980	330.697	347.393	324.843
	3500 rpm		1.064	1.406	1.655	1.018	0.473	151.493	312.545	333.698	351.818	325.636
	4000 rpm		0.932	1.599	1.982	1.199	0.583	147.096	305.806	285.645	267.741	278.709
2	2040 rpm	33.6 @60	1.037	1.465	1.682	0.893	0.446	151.972	322.629	321.250	336.250	317.500
	3000 rpm		0.971	1.592	1.907	1.084	0.503	156.705	326.117	324.705	344.470	328.941
	3500 rpm		0.827	1.794	2.239	1.313	0.559	151.748	317.837	322.702	350.270	344.529
	4000 rpm		0.630	2.068	2.776	1.660	0.717	148.571	304.468	301.000	283.829	278.095
3	2040 rpm	33.6 @60	1.101	1.350	1.450	0.783	0.427	156.521	324.123	322.886	337.732	321.649
	3000 rpm		1.035	1.396	1.599	0.871	0.449	147.907	317.976	329.182	341.789	329.182
	3500 rpm		0.969	1.501	1.831	1.028	0.512	153.122	312.760	327.272	342.081	333.818
	4000 rpm		0.769	1.824	2.337	1.355	0.661	149.032	305.513	294.193	274.378	282.580

4	2040 rpm	33.6 @60	1.084	1.357	1.501	0.774	0.393	140.487	321.115	326.132	336.250	321.115
	3000 rpm		1.040	1.418	1.604	0.852	0.422	154.488	325.984	331.764	345.826	279.212
	3500 rpm		0.942	1.567	1.917	1.116	0.461	156.746	320.571	334.285	339.330	295.598
	4000 rpm		0.739	1.851	2.332	1.321	0.647	140.439	314.754	292.747	281.147	280.879

Table A8.19 Data of the test (G rotor)

Correction Masses/Phase Angle								
Speeds Test	Plane (1) Radius (29.7) mm				Plane (2) Radius (29.7) mm			
	Targeted amount 96.4g @0°				Targeted amount 0 @0°			
	LSQ	QR	SVD	QR+SVD	LSQ	QR	SVD	QR+SVD
All speeds	12.226@ -15.667	12.226@ -15.667	12.226@ -15.667	12.226@ -15.667	37.041@ 167.123	37.041@ 167.123	37.041@ 167.123	37.041@ 167.123
2040 rpm	22.803@ 15.551	22.803@ 15.551	22.803@ 15.551	22.803@ 15.551	121.613@ -160.225	121.613@ -160.225	121.613@ -160.225	121.613@ -160.225
3000 rpm	127.548@ -63.379	127.548@ -63.379	127.548@ -63.379	127.548@ -63.379	129.951@ 45.315	129.951@ 45.315	129.951@ 45.315	129.951@ 45.315
3500 rpm	47.457@ 102.803	47.457@ 102.803	47.457@ 102.803	47.457@ 102.803	59.652@ 88.090	59.652@ 88.090	59.652@ 88.090	59.652@ 88.090
4000 rpm	219.466@ -127.932	219.466@ -127.932	219.466@ -127.932	219.466@ -127.932	200.361@ -127.107	200.361@ -127.107	200.361@ -127.107	200.361@ -127.107

Table A8.20 Balancing planes radius (G rotor)

Correction Masses/Phase Angle								
Speeds Test	Plane (3) Radius (29.7) mm				Plane (4) Radius (29.7) mm			
	Targeted amount 0g @0°				Targeted amount 91.3 g @0°			
	LSQ	QR	SVD	QR+SVD	LSQ	QR	SVD	QR+SVD
All speeds	51.7027@ -2.167	51.7027@ -2.167	51.7027@ -2.167	51.7027@ -2.167	10.654@ 19.892	10.654@ 19.892	10.654@ 19.892	10.654@ 19.892
2040 rpm	121.690@ 53.904	121.690@ 53.904	121.690@ 53.904	121.690@ 53.904	87.067@ -55.235	87.067@ -55.235	87.067@ -55.235	87.067@ -55.235
3000 rpm	59.867@ 49.263	59.867@ 49.263	59.867@ 49.263	59.867@ 49.263	40.2723@ 61.732	40.2723@ 61.732	40.2723@ 61.732	40.2723@ 61.732
3500 rpm	130.553@ -78.582	130.553@ -78.582	130.553@ -78.582	130.553@ -78.582	69.0175@ 84.861	69.0175@ 84.861	69.0175@ 84.861	69.0175@ 84.861
4000 rpm	466.396@ 48.328	466.396@ 48.328	466.396@ 48.328	466.396@ 48.328	61.183@ 6.744	61.183@ 6.744	61.183@ 6.744	61.183@ 6.744

Table A8.21 Results of the test (G rotor)

Influence coefficient matrix properties		
	Rank	Condition Number
All speeds	4	8.735
840 rpm	4	6.084
1080 pm	4	10.383
2040rpm	4	16.128
3000rpm	4	38.918

Table A8.22 Results Matrixes properties (G rotor)

A8.2.3.1 Generator rotor Results For 3 plane balancing

Table A8.23 shows the results of generator rotor For 3 plane balancing with 4 different operation speeds. Table A8.24 shows the influence coefficient Matrix properties for each test.

Correction Masses (gram)/Phase Angle (degree								
Speeds Test	Plane (1)				Plane (3)			
	Targeted amount 96.4g @0°				Targeted amount 0 g @0°			
	LSQ	QR	SVD	QR+SVD	LSQ	QR	SVD	QR+SVD
All speeds	38.181@ 0.344	38.181@ 0.344	38.181@ 0.344	38.181@ 0.344	18.509@ 16.642	18.509@ 16.642	18.509@ 16.642	18.509@ 16.642
840 rpm	71.323@ 61.553	71.323@ 61.553	71.323@ 61.553	71.323@ 61.553	71.273@ -50.341	71.273@ -50.341	71.273@ -50.341	71.273@ -50.341
1080 pm	105.646@ -36.348	105.646@ -36.348	105.646@ -36.348	105.646@ -36.348	35.848@ 71.345	35.848@ 71.345	35.848@ 71.345	35.848@ 71.345
2040rpm	31.523@ -26.010	31.523@ -26.010	31.523@ -26.010	31.523@ -26.010	39.438@ 76.998	39.438@ 76.998	39.438@ 76.998	39.438@ 76.998
3000rpm	55.145@ -27.880	55.145@ -27.880	55.145@ -27.880	55.145@ -27.880	21.066@ 109.049	21.066@ 109.049	21.066@ 109.049	21.066@ 109.049

Correction Masses (gram)/Phase Angle (degree				
Speeds Test	Plane (2)			
	Targeted amount 91.3 g @0°			
	LSQ	QR	SVD	QR+SVD

All speeds	16.066@ 160.891	16.066@ 160.891	16.066@ 160.891	16.066@ 160.891
840 rpm	55.810@ -177.064	55.810@ -177.064	55.810@ -177.064	55.810@ -177.064
1080 pm	122.399@ 53.787	122.399@ 53.787	122.399@ 53.787	122.399@ 53.787
2040rpm	11.759@ 102.750	11.759@ 102.750	11.759@ 102.750	11.759@ 102.750
3000rpm	7.936@ 132.794	7.936@ 132.794	7.936@ 132.794	7.936@ 132.794

Table A8.23 Results of the test (HPT rotor)

Influence coefficient matrix properties		
	Rank	**Condition Number**
All speeds	3	3.691
840 rpm	3	3.088
1080 pm	3	5.581
2040rpm	3	5.731
3000rpm	3	5.891

Table A8.24 Results Matrixes properties (HPT rotor)

A8.2.3.2 Generator rotor Results For 2 plane balancing

Table A8.25 shows the results of generator rotor For 2 plane balancing with 4 different operation speeds. Table A8.26 shows the influence coefficient Matrix properties for each test.

Correction Masses (gram)/Phase Angle (degree								
Speeds Test	**Plane (1)**				**Plane (2)**			
	Targeted amount 96.4g @0°				**Targeted amount 91.3 g @0°**			
	LSQ	**QR**	**SVD**	**QR+SVD**	**LSQ**	**QR**	**SVD**	**QR+SVD**
All speeds	39.250@ 1.090	39.250@ 1.090	39.250@ 1.090	39.250@ 1.090	15.616@ 44.554	15.616@ 44.554	15.616@ 44.554	15.616@ 44.554
2040 rpm	149.322@ 119.982	149.322@ 119.982	149.322@ 119.982	149.322@ 119.982	115.963@ -26.480	115.963@ -26.480	115.963@ -26.480	115.963@ -26.480
3000 rpm	128.125@ 30.347	128.125@ 30.347	128.125@ 30.347	128.125@ 30.347	68.842@ 123.375	68.842@ 123.375	68.842@ 123.375	68.842@ 123.375
3500 rpm	51.583@ 42.981	51.583@ 42.981	51.583@ 42.981	51.583@ 42.981	80.200@ 127.663	80.200@ 127.663	80.200@ 127.663	80.200@ 127.663
4000 rpm	113.684@ 29.489	113.684@ 29.489	113.684@ 29.489	113.684@ 29.489	59.895@ 166.472	59.895@ 166.472	59.895@ 166.472	59.895@ 166.472

Table A8.25 Results of the test (G rotor)

Influence coefficient matrix properties		
	Rank	Condition Number
All speeds	2	3.292
840 rpm	2	2.056
1080 pm	2	2.993
2040rpm	2	4.697
3000rpm	2	4.622

Table A8.26 Results Matrixes properties (G rotor)

Due to the stability of the experimental system (HPT, LPT and G rotors) we used in the above experimental results, the results achieved shows no different between all methods (normal solution, least square, QR factorization and SVD) used to calculate the final correction masses.

In the next subsection in this chapter, the author will try some artificial data to demonstrate the proposed methods and the use of plane elimination by using the influence coefficient matrix rank.

A8.3 List of Numerical Examples

The following list of examples, which will demonstrate the use of linear algebra to solve ill conditions matrixes, the solutions will include matrix elimination by using significant factor (Darlow 1982 method) and proposed method by using the rand of the matrix.

- **Example 1**

$$a = \begin{bmatrix} 0.0300 & 0.0100 \\ 0.0050 & 0.0300 \end{bmatrix} \quad b = \begin{bmatrix} 0.0400 \\ 0.0350 \end{bmatrix}$$

Matrix condition number = 1.66359976082907

Least square solution = QR solution = SVD solution $= \begin{bmatrix} 1.00000000000000 \\ 1.00000000000000 \end{bmatrix}$

Elimination by using significant number

The $[a]$ **matrix after Column elimination**

$$a = \begin{bmatrix} 0.0100 \\ 0.0300 \end{bmatrix}$$

Influence coefficient matrix Columns Significant factor = 1.00000000000000

0.88378791634706

Least square solution = QR solution = SVD solution = $\begin{bmatrix} 1.00000000000000 \\ 1.00000000000000 \end{bmatrix}$

Elimination by using Rank
Column order after pivoting = 2 1

Least square solution = QR solution = SVD solution = $\begin{bmatrix} 1.00000000000000 \\ 1.00000000000000 \end{bmatrix}$

Elimination by using singular value

Least square solution = QR solution = SVD solution = $\begin{bmatrix} 1.00000000000000 \\ 1.00000000000000 \end{bmatrix}$

- **Example 2**

$$a = \begin{bmatrix} 1 & 1 \\ 1 & 1.01 \end{bmatrix} \quad b = \begin{bmatrix} 2 \\ 2.01 \end{bmatrix}$$

Matrix condition number = 402.0075

Least square solution = QR solution = SVD solution = $\begin{bmatrix} 1.00000000000000 \\ 1.00000000000000 \end{bmatrix}$

Elimination by using significant number

The $[a]$ **matrix after Column elimination**

$$a = \begin{bmatrix} 1 \\ 1 \end{bmatrix}$$

Influence coefficient matrix Columns Significant factor = $\begin{bmatrix} 1.0000 & 0.0050 \end{bmatrix}$

Least square solution = QR solution = SVD solution = 2.0050

Elimination by using Rank

Column order after pivoting = 2 1

Least square solution = QR solution = SVD solution = 2.0050

Elimination by using singular value

Least square solution = QR solution = SVD solution = 2.0050

- **Example3**

$$A=\begin{bmatrix}1000 & 999\\ 999 & 998\end{bmatrix},\ b=\begin{bmatrix}1999\\ 1997\end{bmatrix}$$

Matrix condition number = 3.992005999708306e+006

Normal solution= $\begin{bmatrix}1.0000\\ 1.0000\end{bmatrix}$

Gaussian elimination= $\begin{bmatrix}1.0000\\ 1.0000\end{bmatrix}$

Least square solution = $\begin{bmatrix}1.00117206573486\\ 0.99987149238586\end{bmatrix}$

QR solution = $\begin{bmatrix}1.00000000023283\\ 0.99999999976717\end{bmatrix}$

SVD solution = $\begin{bmatrix}0.99999999976717\\ 1.00000000023283\end{bmatrix}$

Elimination by using significant number

Column left after elimination

$$A=\begin{bmatrix}1000\\ 999\end{bmatrix}$$

Influence coefficient matrix Columns Significant factor

= $\begin{bmatrix}1.00000000000000 & 0.00000050100150\end{bmatrix}$

Least square solution = QR solution = SVD solution = 1.99899950000025

Elimination by using Rank

Column order after pivoting = $\begin{bmatrix}1 & 2\end{bmatrix}$

QR solution = $\begin{bmatrix}1.0000\\ 1.0000\end{bmatrix}$

SVD solution = $\begin{bmatrix}0.99999999962754\\ 1.00000000037284\end{bmatrix}$

Elimination by using singular value

Least square solution = QR solution = SVD solution = $\begin{bmatrix} 1.0000 \\ 1.0000 \end{bmatrix}$

- **Example4**

Definition of the a and b matrix, (due the largeness of the matrix size, it was not able to display it)

```
m=100; n=15;
t=(0:m-1)'/(m-1);
a=[];
for i=1:n,
a=[a t.^(i-1)];
end
b=exp(sin(4*t));
b=b/2006.787453080206;
```

Matrix condition number = 2.271777264691908e+010

Rank = 15
Normal solution
x(15) = 0.393 390 698 702 83
Least square

[Q , R]
x(15) = 1.000 000 056 533 99

[Q , R] = mgs (A)
x(15) ans = 1.029 265 945 326 72

Matlab via Householder triangularization: using the built-in \ operator.
x(15) = 0.999 999 943 110 87

(i.e., QR factorization via Householder triangularization)
[Q,R] = gr(A,0) ;
x(15)=1.000 000 315 287 23

SVD
x(15) = 0.999 999 982 304 71

Elimination by using significant number=$\begin{bmatrix} 1 & 2 & 3 \end{bmatrix}$

Influence coefficient matrix Columns Significant factor =

$$\begin{bmatrix} 1.0000 & 0.5038 & 0.1687 & 0.0509 & 0.0146 & 0.0041 & 0.0011 & 0.0003 & 0.0001 & 0.0000 \\ 0.0000 & 0.0003 & 0.0016 & 0.0047 & 0.0105 & & & & & \end{bmatrix}$$

Least square solution = QR solution = SVD solution =
$$\begin{bmatrix} 0.00055165937508 \\ 0.00308099829295 \\ -0.00373205477864 \end{bmatrix}$$

Elimination by using Rank

Column order after pivoting

$$\begin{bmatrix} 1 & 3 & 15 & 2 & 7 & 5 & 11 & 4 & 13 & 9 & 6 & 14 & 8 & 12 & 10 \end{bmatrix}$$

QR solution =
$$\begin{bmatrix} 0.00049831516854 \\ 0.00421287054480 \\ 1.00000036294035 \\ 0.00198998442623 \\ 4.38580732062201 \\ 0.07434879044758 \\ 84.72882647899131 \\ -0.00623696979898 \\ 30.63117857785431 \\ 42.44668742206861 \\ -0.81841996000552 \\ -8.38142526823229 \\ -16.41702291249669 \\ -64.10938968635196 \\ -73.54082154139000 \end{bmatrix}$$

$$\text{SVD solution} = \begin{bmatrix} 0.00049831516855 \\ 0.00421287054478 \\ 1.00000036293642 \\ 0.00198998442623 \\ 4.38580732062116 \\ 0.07434879044775 \\ 84.72882647886173 \\ -0.00623696979901 \\ 30.63117857778008 \\ 42.44668742202926 \\ -0.81841996000587 \\ -8.38142526820650 \\ -16.41702291248666 \\ -64.10938968622877 \\ -73.54082154130087 \end{bmatrix}$$

- **Example 5**

$$a = \begin{bmatrix} 1 & 1 \\ 1 & 1 \end{bmatrix} \quad b = \begin{bmatrix} 1 \\ 1 \end{bmatrix}$$

Matrix condition number = Inf

Normal solution=Inf

Least square solution = Inf

$$\text{QR solution} = \text{SVD solution} = \begin{bmatrix} 0.5000 \\ 0.5000 \end{bmatrix}$$

Elimination by using significant number

The $[a]$ matrix after Column elimination

$$a = \begin{bmatrix} 1 \\ 1 \end{bmatrix}$$

Influence coefficient matrix Columns Significant factor = $\begin{bmatrix} 1.0000 & 0.0000 \end{bmatrix}$

Least square solution = QR solution = SVD solution = 1.0000

Elimination by using Rank
Column order after pivoting = 1 2

Least square solution = QR solution = SVD solution = $\begin{bmatrix} 0.5000 \\ 0.5000 \end{bmatrix}$

Elimination by using singular value

Least square solution = QR solution = SVD solution = $\begin{bmatrix} 0.5000 \\ 0.5000 \end{bmatrix}$

- **Example 6**

$$a = \begin{bmatrix} 1 & 0.99 \\ 0.99 & 1.01 \end{bmatrix} \quad b = \begin{bmatrix} 2 \\ 2 \end{bmatrix}$$

Matrix condition number = 1.331128889172591e+002

Least square solution = QR solution = SVD solution = $\begin{bmatrix} 1.33779264214047 \\ 0.66889632107024 \end{bmatrix}$

The $[a]$ **matrix after Column elimination**

$$a = \begin{bmatrix} 1 \\ 0.99 \end{bmatrix}$$

Influence coefficient matrix Columns Significant factor = $\begin{bmatrix} 1.00000000000000 & 0.01502418473488 \end{bmatrix}$

Least square solution = QR solution = SVD solution = 2.00999949497500

Column order after pivoting = $\begin{bmatrix} 2 & 1 \end{bmatrix}$

Least square solution = QR solution = SVD solution = $\begin{bmatrix} 0.66889632107023 \\ 1.33779264214047 \end{bmatrix}$

- **Example 7**

$$A=\begin{bmatrix}10 & 7 & 8 & 6.999\\ 7 & 6 & 6 & 5\\ 8 & 5 & 10 & 9\\ 7 & 5 & 9 & 10\end{bmatrix}, b=\begin{bmatrix}32\\ 23\\ 33\\ 31\end{bmatrix}$$

Matrix condition number = 2.965934399575547e+003

Least square solution = QR solution = SVD solution = $\begin{bmatrix}1.02485089463227\\ 0.95924453280276\\ 1.00994035785307\\ 0.99403578528822\end{bmatrix}$

The $[a]$ matrix after Column elimination

$$a=\begin{bmatrix}8\\ 6\\ 10\\ 9\end{bmatrix}$$

Significant factor =

$[1.00000000000000 \quad 0.02711247372095 \quad 0.14280825098985 \quad 0.00516115233285]$

Least square solution = QR solution = SVD solution = $\begin{bmatrix}1.33264645275244\\ 2.31262879010891\end{bmatrix}$

Column order after pivoting = $[3 \quad 1 \quad 4 \quad 2]$

Least square solution = QR solution = SVD solution = $\begin{bmatrix}1.00994035785285\\ 1.02485089463213\\ 0.99403578528829\\ 0.95924453280330\end{bmatrix}$

- **Example 8**

$$a=\begin{bmatrix}1 & 2\\ 2 & 4\\ 3 & 6\\ 4 & 8\end{bmatrix} \quad b=\begin{bmatrix}2\\ 4\\ 6\\ 8\end{bmatrix}$$

Matrix condition number = 1.258794363780394e+016

Warning: Matrix is singular to working precision.

Least square solution = $\begin{bmatrix}\text{Inf}\\ \text{Inf}\end{bmatrix}$

Warning: Rank deficient, Rank = 1 tol = 9.7295e-015.

QR solution = $\begin{bmatrix} 0.00000000000000 \\ 1.00000000000000 \end{bmatrix}$

Warning: Rank deficient, Rank = 1 tol = 1.0878e-014.

SVD solution = $\begin{bmatrix} 0.40000000000000 \\ 0.80000000000000 \end{bmatrix}$

The $[a]$ **matrix after Column elimination** $a = \begin{bmatrix} 1 \\ 2 \\ 3 \\ 4 \end{bmatrix}$

Influence coefficient matrix Columns Significant factor =
$[1.00000000000000 \quad 0.00000000000000]$

Least square solution = QR solution = SVD solution = 2.00000000000000

Column order after pivoting = $[2 \quad 1]$

Warning: Rank deficient, Rank = 1 tol = 9.7295e-015.

QR solution = $\begin{bmatrix} 1.00000000000000 \\ 0.00000000000000 \end{bmatrix}$

Warning: Rank deficient, Rank = 1 tol = 1.0878e-014.

SVD solution = $\begin{bmatrix} 0.80000000000000 \\ 0.40000000000000 \end{bmatrix}$

- **Example 9**

$$a = \begin{bmatrix} 3.021 & 2.714 & 6.913 \\ 1.031 & 4.273 & 1.121 \\ 5.084 & -5.832 & 9.155 \end{bmatrix} \quad b = \begin{bmatrix} 12.648 \\ -2.121 \\ 8.407 \end{bmatrix}$$

Matrix condition number = 3.726860520732594e+004

Least square solution = $\begin{bmatrix} 0.99999999188367 \\ 0.99999999384886 \\ 1.00000001860462 \end{bmatrix}$

QR solution = $\begin{bmatrix} 1.00000000000489 \\ 1.00000000000056 \\ 0.99999999999764 \end{bmatrix}$

$$\textbf{SVD solution} = \begin{bmatrix} 1.00000000000904 \\ 1.00000000000104 \\ 0.99999999999564 \end{bmatrix}$$

The $[a]$ matrix after Column elimination

$$a = \begin{bmatrix} 2.714 \\ -4.273 \\ -5.832 \end{bmatrix}$$

Influence coefficient matrix Columns Significant factor

$$= [1.00000000000000 \quad 0.83000860533635 \quad 0.00007346247849]$$

$$\textbf{Least square solution = QR solution = SVD solution} = \begin{bmatrix} 3.07414306351634 \\ 1.23827120713092 \end{bmatrix}$$

Column order after pivoting $= [3 \quad 2 \quad 1]$

$$\textbf{Least square solution = QR solution = SVD solution} = \begin{bmatrix} 0.99999999999764 \\ 1.00000000000056 \\ 1.00000000000490 \end{bmatrix}$$

- **Example 10**

$$a = \begin{bmatrix} 1 & 1 & 1 \\ 1 & 1 & 2 \\ 1 & 1 & 3 \\ 1 & 1 & 4 \end{bmatrix} \quad b = \begin{bmatrix} 1 \\ 1 \\ 1 \\ 1 \end{bmatrix}$$

Matrix condition number = 2.7786e+016

$$\textbf{Least square solution} = \begin{bmatrix} \text{NaN} \\ \text{NaN} \\ \text{NaN} \end{bmatrix}$$

$$\textbf{QR solution} = \begin{bmatrix} 1.0000 \\ 0.0000 \\ -0.2000 \end{bmatrix}$$

Warning: Rank deficient, Rank = 2 tol = 5.3965e-015.

$$\textbf{SVD solution} = \begin{bmatrix} 0.5000 \\ 0.5000 \\ -0.2000 \end{bmatrix}$$

Condition number = 2.7786e+016

Influence coefficient matrix Columns Significant factor = $\begin{bmatrix} 1 & 0 & \text{NaN} \end{bmatrix}$

The $[a]$ **matrix after Column elimination**

$$a = \begin{bmatrix} 1 \\ 1 \\ 1 \\ 1 \end{bmatrix}$$

Least square solution = QR solution = SVD solution =
0.5000

Column order after pivoting = $\begin{bmatrix} 3 & 2 & 1 \end{bmatrix}$

Warning: Rank deficient, Rank = 2 tol = 4.8648e-015.

$$\textbf{QR solution} = \begin{bmatrix} -0.2000 \\ 1.0000 \\ 0.0000 \end{bmatrix}$$

Warning: Rank deficient, Rank = 2 tol = 5.3965e-015.

$$\textbf{SVD solution} = \begin{bmatrix} -0.2000 \\ 0.5000 \\ 0.5000 \end{bmatrix}$$

- **Example 11**

$$a = \begin{bmatrix} 1 \\ 1 \end{bmatrix} \quad b = \begin{bmatrix} 2 \\ 2 \end{bmatrix}$$

Matrix condition number =Inf

Warning: Matrix is singular to working precision.

Least square solution = QR solution = SVD solution = $\begin{bmatrix} \text{Inf} \\ \text{Inf} \end{bmatrix}$

Influence coefficient matrix Columns Significant = 1

The $[a]$ **matrix after Column elimination**

$$a = \begin{bmatrix} 1 \\ 1 \end{bmatrix}$$

Least square solution = QR solution = SVD solution = 2.0000

Warning: Matrix is singular to working precision.

QR solution $= \begin{bmatrix} \text{Inf} \\ \text{Inf} \end{bmatrix}$

Warning: Matrix is singular to working precision.

SVD solution $= \begin{bmatrix} -\text{Inf} \\ \text{NaN} \end{bmatrix}$

- **Example 12**

$$a = \begin{bmatrix} 1 \\ 1 \end{bmatrix} \quad b = \begin{bmatrix} 2 \\ 2 \end{bmatrix}$$

Matrix condition number = 1

Least square solution = QR solution = SVD solution = 2.0000

The $[a]$ matrix after Column elimination

$$a = \begin{bmatrix} 1 \\ 1 \end{bmatrix}$$

Least square solution = QR solution = SVD solution = 2.0000

Column order after pivoting = 1

Least square solution = QR solution = SVD solution = 2.0000

- **Example 13**

$$a = \begin{bmatrix} 1.01 & 0.99 \\ 0.99 & 1.05 \end{bmatrix} \quad b = \begin{bmatrix} 2 \\ 2 \end{bmatrix}$$

Matrix condition number = 50.7614

Least square solution = QR solution = SVD solution $= \begin{bmatrix} 1.4925 \\ 0.4975 \end{bmatrix}$

Influence coefficient matrix Columns Significant= 0.0394

The $[a]$ matrix after Column elimination

$$a = \begin{bmatrix} 1.01 \\ 0.99 \end{bmatrix}$$

Least square solution = QR solution = SVD solution = 1.9998

Column order after pivoting = $\begin{bmatrix}2 & 1\end{bmatrix}$

Least square solution = QR solution = SVD solution = $\begin{bmatrix}0.4975\\1.4925\end{bmatrix}$

- **Example 14**

$$a=\begin{bmatrix}1.05 & 1.05\\0.95 & 1.01\end{bmatrix} \quad b=\begin{bmatrix}2\\2\end{bmatrix}$$

Matrix condition number = 65.5022

Least square solution = QR solution = SVD solution = $\begin{bmatrix}-1.2698\\3.1746\end{bmatrix}$

Influence coefficient matrix Columns Significant factor = 1.0000 0.0305

The $[a]$ **matrix after Column elimination**

$$a=\begin{bmatrix}1.05\\0.95\end{bmatrix}$$

Least square solution = QR solution = SVD solution = 1.9950

Column order after pivoting = $\begin{bmatrix}2 & 1\end{bmatrix}$

Least square solution = QR solution = SVD solution = $\begin{bmatrix}3.1746\\-1.2698\end{bmatrix}$

Numerical cases		Matrix inverse solution	Gaussian elimination	Least square	QR	SVD	Plane Elimination by using Significant factor					Matrix Elimination by using rank		Matrix Elimination by using singular value	
Examples	State						Normal	Gaussian elimination	Least square	QR	SVD	QR	SVD	QR	SVD
EX1	Well- cond.	✓	✓	✓	✓	✓	✓	✓	✓	✓	✓	✓	✓	✓	✓
EX2	Ill-cond.	✓	✓	✗	✓	✓	✓	✓	✓	✓	✓	✓	✓	✓	✓
EX3	Ill-cond.	✗	✗	✗	✓	✓✓	‖ ✓	‖ ✓	‖ ✓	‖ ✓	‖ ✓	✓	✓	✓	✓
EX4	Ill-cond.	✓	✓	✓	✓	✓	‖ ✓	‖ ✓	‖ ✓	‖ ✓	‖ ✓	✓	✓	✓	✓
EX5	Ill-cond.	✓	✓	✓	✓	✓	‖ ✓	‖ ✓	‖ ✓	‖ ✓	‖ ✓	✓	✓	✓	✓
EX6	Ill-cond.	✓	✓	✓	✓	✓	‖ ✓	‖ ✓	‖ ✓	‖ ✓	‖ ✓	✓	✓	✓	✓
EX7	Ill-cond.	✗	✗	✗	✗	✓	‖ ✓	‖ ✓	‖ ✓	‖ ✓	‖ ✓	✗	✓	✓	✓
EX8	Ill-cond.	✓	✓	✓	✓	✓	‖ ✓	‖ ✓	‖ ✓	‖ ✓	‖ ✓	✓	✓	✓	✓
EX9	Ill-cond.	✗	✗	✗	✗	✗	‖ ✓	‖ ✓	‖ ✓	‖ ✓	‖ ✓	✗	✗	✗	✗
EX10	Ill-cond.	✗	✗	✗	✗	✗	‖ ✓	‖ ✓	‖ ✓	‖ ✓	‖ ✓	✗	✓	✓	✓
EX11	Ill-cond.	✓	✓	✓	✓	✓	‖ ✓	‖ ✓	‖ ✓	‖ ✓	‖ ✓	✓	✓	✓	✓
EX12	Ill-cond.	✓	✓	✓	✓	✓	‖ ✓	‖ ✓	‖ ✓	‖ ✓	‖ ✓	✓	✓	✓	✓
EX13	Ill-cond.	✓	✓	✓	✓	✓	‖ ✓	‖ ✓	‖ ✓	‖ ✓	‖ ✓	✓	✓	✓	✓
EX14	Ill-cond.	✓	✓	✓	✓	✓	‖ ✓	‖ ✓	‖ ✓	‖ ✓	‖ ✓	✓	✓	✓	✓

Table A8 27 summarized Results Matrixes properties and solutions

Symmetrical rotor significant factor = 0.01				
(Deflection With unbalance masses added to the system)	(Deflection of the rotor without elimination)	(Deflection of the rotor with elimination sf)	(Deflection of the rotor with the new QR pivoting matrix)	(Deflection of the rotor with elimination of the new QR pivoting matrix)
0	0	0	0	0
-1.09E-05	-3.54E-05	8.87E-06	-7.07E-06	3.99E-06
-2.17E-05	-7.06E-05	1.77E-05	-1.41E-05	7.98E-06
-4.30E-05	-1.40E-04	3.52E-05	-2.80E-05	1.60E-05
-5.34E-05	-1.74E-04	4.37E-05	-3.47E-05	2.01E-05
-7.34E-05	-2.38E-04	6.03E-05	-4.77E-05	2.84E-05
-8.30E-05	-2.69E-04	6.82E-05	-5.39E-05	3.26E-05
-1.01E-04	-3.26E-04	8.32E-05	-6.54E-05	4.13E-05
-1.09E-04	-3.52E-04	9.03E-05	-7.07E-05	4.57E-05
-1.25E-04	-3.99E-04	1.03E-04	-8.08E-05	5.44E-05
-1.32E-04	-4.20E-04	1.09E-04	-8.56E-05	5.85E-05
-1.44E-04	-4.56E-04	1.19E-04	-9.47E-05	6.63E-05
-1.50E-04	-4.71E-04	1.23E-04	-9.91E-05	6.98E-05
-1.60E-04	-4.95E-04	1.30E-04	-1.07E-04	7.60E-05
-1.64E-04	-5.05E-04	1.33E-04	-1.11E-04	7.86E-05
-1.72E-04	-5.18E-04	1.37E-04	-1.16E-04	8.31E-05
-1.75E-04	-5.23E-04	1.38E-04	-1.18E-04	8.49E-05
-1.79E-04	-5.26E-04	1.39E-04	-1.21E-04	8.76E-05
-1.81E-04	-5.25E-04	1.39E-04	-1.21E-04	8.85E-05
-1.83E-04	-5.19E-04	1.37E-04	-1.20E-04	8.94E-05
-1.83E-04	-5.14E-04	1.36E-04	-1.19E-04	8.95E-05
-1.82E-04	-4.99E-04	1.32E-04	-1.14E-04	8.88E-05
-1.81E-04	-4.90E-04	1.29E-04	-1.11E-04	8.80E-05
-1.77E-04	-4.68E-04	1.23E-04	-1.04E-04	8.57E-05
-1.74E-04	-4.55E-04	1.19E-04	-9.97E-05	8.42E-05
-1.67E-04	-4.27E-04	1.11E-04	-9.14E-05	8.05E-05
-1.63E-04	-4.12E-04	1.07E-04	-8.72E-05	7.82E-05
-1.53E-04	-3.79E-04	9.72E-05	-7.86E-05	7.31E-05
-1.47E-04	-3.61E-04	9.21E-05	-7.43E-05	7.02E-05
-1.35E-04	-3.24E-04	8.16E-05	-6.55E-05	6.37E-05
-1.27E-04	-3.05E-04	7.61E-05	-6.10E-05	6.01E-05
-1.12E-04	-2.63E-04	6.49E-05	-5.20E-05	5.23E-05
-9.20E-05	-2.41E-04	5.92E-05	-4.74E-05	4.82E-05
-8.44E-05	-1.96E-04	4.77E-05	-3.81E-05	3.93E-05
-7.46E-05	-1.72E-04	4.18E-05	-3.34E-05	3.47E-05
-5.41E-05	-1.24E-04	3.00E-05	-2.39E-05	2.51E-05
-4.36E-05	-9.99E-05	2.40E-05	-1.92E-05	2.02E-05
0	0	0	0	0

Table A8.28 results of Symmetrical rotor significant factor = 0.01

Symmetrical rotor significant factor = 0.02				
(Deflection With unbalance masses added to the system)	(Deflection of the rotor without elimination)	(Deflection of the rotor with elimination sf)	(Deflection of the rotor with the new QR pivoting matrix)	(Deflection of the rotor with elimination of the new QR pivoting matrix)
0	0	0	0	0
-1.09E-05	-3.54E-05	8.87E-06	-7.07E-06	8.59E-07
-2.17E-05	-7.06E-05	1.77E-05	-1.41E-05	1.72E-06
-4.30E-05	-1.40E-04	3.52E-05	-2.80E-05	3.46E-06
-5.34E-05	-1.74E-04	4.37E-05	-3.47E-05	4.34E-06
-7.34E-05	-2.38E-04	6.03E-05	-4.77E-05	6.13E-06
-8.30E-05	-2.69E-04	6.82E-05	-5.39E-05	7.04E-06
-1.01E-04	-3.26E-04	8.32E-05	-6.54E-05	8.93E-06
-1.09E-04	-3.52E-04	9.03E-05	-7.07E-05	9.89E-06
-1.25E-04	-3.99E-04	1.03E-04	-8.08E-05	1.19E-05
-1.32E-04	-4.20E-04	1.09E-04	-8.56E-05	1.29E-05
-1.44E-04	-4.56E-04	1.19E-04	-9.47E-05	1.49E-05
-1.50E-04	-4.71E-04	1.23E-04	-9.91E-05	1.59E-05
-1.60E-04	-4.95E-04	1.30E-04	-1.07E-04	1.78E-05
-1.64E-04	-5.05E-04	1.33E-04	-1.11E-04	1.87E-05
-1.72E-04	-5.18E-04	1.37E-04	-1.16E-04	2.03E-05
-1.75E-04	-5.23E-04	1.38E-04	-1.18E-04	2.10E-05
-1.79E-04	-5.26E-04	1.39E-04	-1.21E-04	2.20E-05
-1.81E-04	-5.25E-04	1.39E-04	-1.21E-04	2.23E-05
-1.83E-04	-5.19E-04	1.37E-04	-1.20E-04	2.26E-05
-1.83E-04	-5.14E-04	1.36E-04	-1.19E-04	2.24E-05
-1.82E-04	-4.99E-04	1.32E-04	-1.14E-04	2.16E-05
-1.81E-04	-4.90E-04	1.29E-04	-1.11E-04	2.10E-05
-1.77E-04	-4.68E-04	1.23E-04	-1.04E-04	1.93E-05
-1.74E-04	-4.55E-04	1.19E-04	-9.97E-05	1.82E-05
-1.67E-04	-4.27E-04	1.11E-04	-9.14E-05	1.59E-05
-1.63E-04	-4.12E-04	1.07E-04	-8.72E-05	1.46E-05
-1.53E-04	-3.79E-04	9.72E-05	-7.86E-05	1.21E-05
-1.47E-04	-3.61E-04	9.21E-05	-7.43E-05	1.08E-05
-1.35E-04	-3.24E-04	8.16E-05	-6.55E-05	8.36E-06
-1.27E-04	-3.05E-04	7.61E-05	-6.10E-05	7.24E-06
-1.12E-04	-2.63E-04	6.49E-05	-5.20E-05	5.30E-06
-9.20E-05	-2.41E-04	5.92E-05	-4.74E-05	4.49E-06
-8.44E-05	-1.96E-04	4.77E-05	-3.81E-05	3.14E-06
-7.46E-05	-1.72E-04	4.18E-05	-3.34E-05	2.58E-06
-5.41E-05	-1.24E-04	3.00E-05	-2.39E-05	1.66E-06
-4.36E-05	-9.99E-05	2.40E-05	-1.92E-05	1.27E-06
0	0	0	0	0

Table A8.29 results of Symmetrical rotor significant factor = 0.02

Symmetrical rotor significant factor = 0.1				
(Deflection With unbalance masses added to the system)	(Deflection of the rotor without elimination)	(Deflection of the rotor with elimination sf)	(Deflection of the rotor with the new QR pivoting matrix)	(Deflection of the rotor with elimination of the new QR pivoting matrix)
0	0	0	0	0
-1.09E-05	-3.54E-05	1.64E-06	-7.07E-06	3.22E-07
-2.17E-05	-7.06E-05	3.29E-06	-1.41E-05	6.44E-07
-4.30E-05	-1.40E-04	6.56E-06	-2.80E-05	1.29E-06
-5.34E-05	-1.74E-04	8.18E-06	-3.47E-05	1.62E-06
-7.34E-05	-2.38E-04	1.14E-05	-4.77E-05	2.30E-06
-8.30E-05	-2.69E-04	1.30E-05	-5.39E-05	2.64E-06
-1.01E-04	-3.26E-04	1.61E-05	-6.54E-05	3.35E-06
-1.09E-04	-3.52E-04	1.77E-05	-7.07E-05	3.71E-06
-1.25E-04	-3.99E-04	2.07E-05	-8.08E-05	4.42E-06
-1.32E-04	-4.20E-04	2.21E-05	-8.56E-05	4.77E-06
-1.44E-04	-4.56E-04	2.48E-05	-9.47E-05	5.42E-06
-1.50E-04	-4.71E-04	2.61E-05	-9.91E-05	5.73E-06
-1.60E-04	-4.95E-04	2.85E-05	-1.07E-04	6.28E-06
-1.64E-04	-5.05E-04	2.95E-05	-1.11E-04	6.52E-06
-1.72E-04	-5.18E-04	3.14E-05	-1.16E-04	6.93E-06
-1.75E-04	-5.23E-04	3.22E-05	-1.18E-04	7.10E-06
-1.79E-04	-5.26E-04	3.34E-05	-1.21E-04	7.34E-06
-1.81E-04	-5.25E-04	3.39E-05	-1.21E-04	7.41E-06
-1.83E-04	-5.19E-04	3.44E-05	-1.20E-04	7.45E-06
-1.83E-04	-5.14E-04	3.45E-05	-1.19E-04	7.42E-06
-1.82E-04	-4.99E-04	3.42E-05	-1.14E-04	7.23E-06
-1.81E-04	-4.90E-04	3.39E-05	-1.11E-04	7.07E-06
-1.77E-04	-4.68E-04	3.28E-05	-1.04E-04	6.67E-06
-1.74E-04	-4.55E-04	3.20E-05	-9.97E-05	6.42E-06
-1.67E-04	-4.27E-04	3.02E-05	-9.14E-05	5.86E-06
-1.63E-04	-4.12E-04	2.92E-05	-8.72E-05	5.56E-06
-1.53E-04	-3.79E-04	2.69E-05	-7.86E-05	4.91E-06
-1.47E-04	-3.61E-04	2.56E-05	-7.43E-05	4.58E-06
-1.35E-04	-3.24E-04	2.28E-05	-6.55E-05	3.91E-06
-1.27E-04	-3.05E-04	2.14E-05	-6.10E-05	3.57E-06
-1.12E-04	-2.63E-04	1.84E-05	-5.20E-05	2.94E-06
-9.20E-05	-2.41E-04	1.68E-05	-4.74E-05	2.64E-06
-8.44E-05	-1.96E-04	1.36E-05	-3.81E-05	2.06E-06
-7.46E-05	-1.72E-04	1.19E-05	-3.34E-05	1.79E-06
-5.41E-05	-1.24E-04	8.58E-06	-2.39E-05	1.26E-06
-4.36E-05	-9.99E-05	6.88E-06	-1.92E-05	1.00E-06
0	0	0	0	0

Table A8.30 results of Symmetrical rotor significant factor = 0.1

H.P.T rotor significant factor = 0.02				
(Deflection With unbalance masses added to the system)	(Deflection of the rotor without elimination)	(Deflection of the rotor with elimination sf)	(Deflection of the rotor with the new QR pivoting matrix)	(Deflection of the rotor with elimination of the new QR pivoting matrix)
0	0	0	0	0
-7.55E-08	-1.60E-07	4.00E-08	-1.60E-07	5.61E-09
-1.50E-07	-2.00E-07	8.00E-08	-2.00E-07	2.15E-08
-2.22E-07	-2.56E-07	1.20E-07	-2.56E-07	3.10E-08
-2.91E-07	-2.79E-07	1.51E-07	-2.79E-07	5.20E-08
-3.56E-07	-3.04E-07	1.77E-07	-3.04E-07	6.80E-08
-4.15E-07	-3.44E-07	2.00E-07	-3.44E-07	8.80E-08
-4.69E-07	-3.89E-07	2.08E-07	-3.89E-07	9.90E-08
-5.18E-07	-4.13E-07	2.29E-07	-4.13E-07	1.20E-07
-5.61E-07	-4.26E-07	2.40E-07	-4.26E-07	1.30E-07
-5.99E-07	-4.26E-07	2.49E-07	-4.26E-07	1.45E-07
-6.31E-07	-4.42E-07	2.60E-07	-4.42E-07	1.58E-07
-6.58E-07	-4.52E-07	2.70E-07	-4.52E-07	1.71E-07
-6.80E-07	-4.57E-07	2.75E-07	-4.57E-07	1.82E-07
-6.96E-07	-4.55E-07	2.80E-07	-4.55E-07	1.97E-07
-7.06E-07	-4.52E-07	2.80E-07	-4.52E-07	1.97E-07
-7.17E-07	-4.57E-07	2.80E-07	-4.57E-07	1.97E-07
-7.13E-07	-4.52E-07	2.80E-07	-4.52E-07	1.92E-07
-7.17E-07	-4.46E-07	2.75E-07	-4.46E-07	1.97E-07
-7.11E-07	-4.47E-07	2.75E-07	-4.47E-07	1.97E-07
-7.00E-07	-4.44E-07	2.80E-07	-4.44E-07	1.97E-07
-6.84E-07	-4.40E-07	2.80E-07	-4.40E-07	1.92E-07
-6.62E-07	-4.34E-07	2.80E-07	-4.34E-07	1.77E-07
-6.35E-07	-4.27E-07	2.75E-07	-4.27E-07	1.71E-07
-6.02E-07	-3.99E-07	2.65E-07	-3.99E-07	1.56E-07
-5.64E-07	-3.93E-07	2.67E-07	-3.93E-07	1.51E-07
-5.20E-07	-3.56E-07	2.49E-07	-3.56E-07	1.30E-07
-4.71E-07	-3.38E-07	2.29E-07	-3.38E-07	1.25E-07
-4.17E-07	-2.83E-07	2.00E-07	-2.83E-07	1.09E-07
-3.57E-07	-2.34E-07	1.77E-07	-2.34E-07	8.80E-08
-2.92E-07	-1.86E-07	1.56E-07	-1.86E-07	6.80E-08
-2.23E-07	-1.39E-07	1.09E-07	-1.39E-07	5.70E-08
-1.51E-07	-9.26E-08	6.80E-08	-9.26E-08	3.60E-08
-7.58E-08	-4.62E-08	3.10E-08	-4.62E-08	9.37E-09
0	0	0	0	0

Table A8.31 results of HPT rotor significant factor = 0.02

H.P.T rotor significant factor = 0.01				
(Deflection With unbalance masses added to the system)	(Deflection of the rotor without elimination)	(Deflection of the rotor with elimination sf)	(Deflection of the rotor with the new QR pivoting matrix)	(Deflection of the rotor with elimination of the new QR pivoting matrix)
0	0	0	0	0
-7.55E-08	-1.60E-07	4.00E-08	-1.60E-07	2.24E-08
-1.50E-07	-2.00E-07	8.70E-08	-2.00E-07	2.40E-08
-2.22E-07	-2.56E-07	1.23E-07	-2.56E-07	5.00E-08
-2.91E-07	-2.79E-07	1.51E-07	-2.79E-07	6.10E-08
-3.56E-07	-3.04E-07	1.91E-07	-3.04E-07	8.70E-08
-4.15E-07	-3.44E-07	2.23E-07	-3.44E-07	9.70E-08
-4.69E-07	-3.89E-07	2.49E-07	-3.89E-07	1.13E-07
-5.18E-07	-4.13E-07	2.64E-07	-4.13E-07	1.29E-07
-5.61E-07	-4.26E-07	2.85E-07	-4.26E-07	1.55E-07
-5.99E-07	-4.26E-07	2.90E-07	-4.26E-07	1.70E-07
-6.31E-07	-4.42E-07	2.96E-07	-4.42E-07	1.81E-07
-6.58E-07	-4.52E-07	2.96E-07	-4.52E-07	1.91E-07
-6.80E-07	-4.57E-07	3.01E-07	-4.57E-07	2.00E-07
-6.96E-07	-4.55E-07	3.06E-07	-4.55E-07	1.97E-07
-7.06E-07	-4.52E-07	3.06E-07	-4.52E-07	2.00E-07
-7.17E-07	-4.57E-07	3.11E-07	-4.57E-07	2.00E-07
-7.13E-07	-4.52E-07	3.06E-07	-4.52E-07	1.97E-07
-7.17E-07	-4.46E-07	3.06E-07	-4.46E-07	1.86E-07
-7.11E-07	-4.47E-07	2.96E-07	-4.47E-07	1.86E-07
-7.00E-07	-4.44E-07	2.90E-07	-4.44E-07	1.81E-07
-6.84E-07	-4.40E-07	2.75E-07	-4.40E-07	1.70E-07
-6.62E-07	-4.34E-07	2.64E-07	-4.34E-07	1.60E-07
-6.35E-07	-4.27E-07	2.59E-07	-4.27E-07	1.50E-07
-6.02E-07	-3.99E-07	2.49E-07	-3.99E-07	1.24E-07
-5.64E-07	-3.93E-07	2.33E-07	-3.93E-07	1.13E-07
-5.20E-07	-3.56E-07	2.07E-07	-3.56E-07	1.03E-07
-4.71E-07	-3.38E-07	1.97E-07	-3.38E-07	8.70E-08
-4.17E-07	-2.83E-07	1.70E-07	-2.83E-07	7.10E-08
-3.57E-07	-2.34E-07	1.44E-07	-2.34E-07	6.60E-08
-2.92E-07	-1.86E-07	1.23E-07	-1.86E-07	5.00E-08
-2.23E-07	-1.39E-07	1.09E-07	-1.39E-07	4.00E-08
-1.51E-07	-9.26E-08	7.10E-08	-9.26E-08	3.00E-08
-7.58E-08	-4.62E-08	3.10E-08	-4.62E-08	2.40E-08
0	0	0	0	0

Table A8.32 results of HPT rotor significant factor = 0.01

H.P.T rotor significant factor = 0.1				
(Deflection With unbalance masses added to the system)	(Deflection of the rotor without elimination)	(Deflection of the rotor with elimination sf)	(Deflection of the rotor with the new QR pivoting matrix)	(Deflection of the rotor with elimination of the new QR pivoting matrix)
0	0	0	0	0
-7.55E-08	-1.60E-07	5.30E-08	-1.60E-07	2.01E-08
-1.50E-07	-2.00E-07	9.30E-08	-2.00E-07	4.06E-08
-2.22E-07	-2.56E-07	1.21E-07	-2.56E-07	6.18E-08
-2.91E-07	-2.79E-07	1.39E-07	-2.79E-07	8.41E-08
-3.56E-07	-3.04E-07	1.67E-07	-3.04E-07	1.08E-07
-4.15E-07	-3.44E-07	1.99E-07	-3.44E-07	1.23E-07
-4.69E-07	-3.89E-07	2.14E-07	-3.89E-07	1.42E-07
-5.18E-07	-4.13E-07	2.34E-07	-4.13E-07	1.57E-07
-5.61E-07	-4.26E-07	2.59E-07	-4.26E-07	1.65E-07
-5.99E-07	-4.26E-07	2.75E-07	-4.26E-07	1.71E-07
-6.31E-07	-4.42E-07	2.79E-07	-4.42E-07	1.77E-07
-6.58E-07	-4.52E-07	2.90E-07	-4.52E-07	1.83E-07
-6.80E-07	-4.57E-07	3.01E-07	-4.57E-07	1.86E-07
-6.96E-07	-4.55E-07	3.11E-07	-4.55E-07	1.89E-07
-7.06E-07	-4.52E-07	3.11E-07	-4.52E-07	1.91E-07
-7.17E-07	-4.57E-07	3.11E-07	-4.57E-07	1.89E-07
-7.13E-07	-4.52E-07	3.11E-07	-4.52E-07	1.87E-07
-7.17E-07	-4.46E-07	3.11E-07	-4.46E-07	1.82E-07
-7.11E-07	-4.47E-07	3.11E-07	-4.47E-07	1.73E-07
-7.00E-07	-4.44E-07	3.01E-07	-4.44E-07	1.64E-07
-6.84E-07	-4.40E-07	2.96E-07	-4.40E-07	1.51E-07
-6.62E-07	-4.34E-07	2.85E-07	-4.34E-07	1.38E-07
-6.35E-07	-4.27E-07	2.70E-07	-4.27E-07	1.30E-07
-6.02E-07	-3.99E-07	2.54E-07	-3.99E-07	1.19E-07
-5.64E-07	-3.93E-07	2.33E-07	-3.93E-07	1.03E-07
-5.20E-07	-3.56E-07	1.97E-07	-3.56E-07	9.30E-08
-4.71E-07	-3.38E-07	1.86E-07	-3.38E-07	8.30E-08
-4.17E-07	-2.83E-07	1.55E-07	-2.83E-07	7.20E-08
-3.57E-07	-2.34E-07	1.34E-07	-2.34E-07	6.00E-08
-2.92E-07	-1.86E-07	1.08E-07	-1.86E-07	5.10E-08
-2.23E-07	-1.39E-07	8.70E-08	-1.39E-07	4.10E-08
-1.51E-07	-9.26E-08	6.60E-08	-9.26E-08	3.36E-08
-7.58E-08	-4.62E-08	2.99E-08	-4.62E-08	1.66E-08
0	0	0	0	0

Table A8.33 results of HPT rotor significant factor = 0.1